Flocculants from wastewater

Victor Olusola Ajao

2020

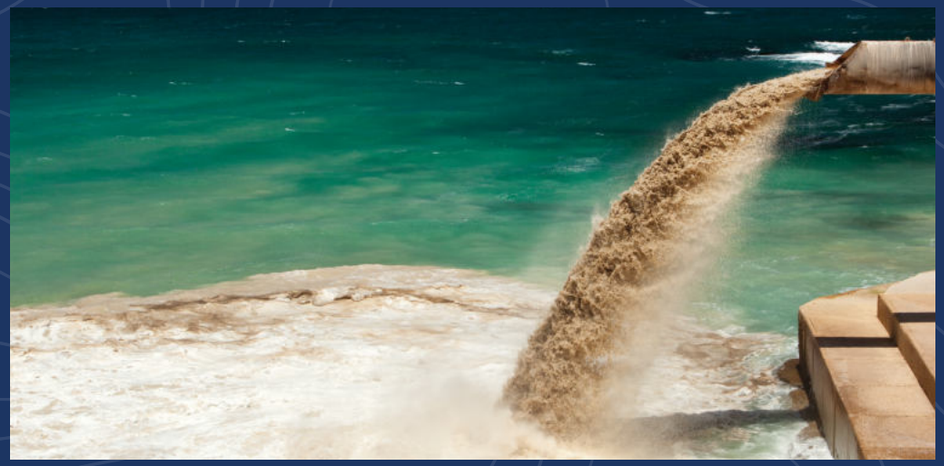

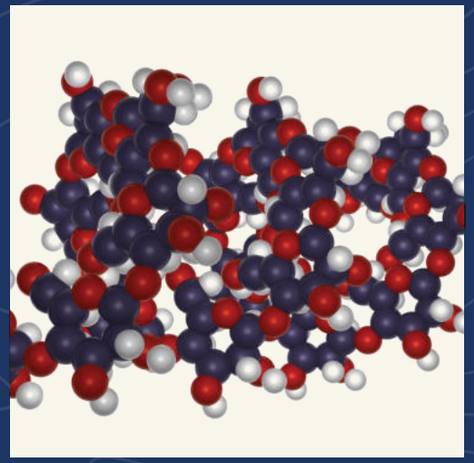

Flocculants from wastewater

Victor Olusola Ajao

Propositions

1. Nitrogen concentration in wastewater steers the quantity and quality of produced extracellular polymeric substances (EPS) as flocculants.
   (this thesis)

2. The so-called soluble and bound EPS fractions are chemically similar fractions.
   (this thesis)

3. Scientific research findings only become societally relevant when combined with popular science communication.

4. Innovation in any educational system will flourish by abandoning authoritarian hierarchy.

5. The best way to better understand a subject is to teach what you already know about it.

6. Financial aid is the reason developing countries will never develop.

Propositions belonging to the thesis, entitled
''Flocculants from wastewater''

Victor Olusola Ajao

Leeuwarden, 11 September 2020.

Flocculants from wastewater

Victor Olusola Ajao

Thesis committee

Promotor

Prof. Dr H.H.M. Rijnaarts

Professor of Environmental Technology

Wageningen University & Research

Co-promotors

Dr B.G. Temmink

Associate Professor, Environmental Technology

Wageningen University & Research

Dr H. Bruning

Assistant Professor, Environmental Technology

Wageningen University & Research

Other members

Prof. Dr A.J.M. Stams, Wageningen University & Research

Prof. Dr G.J.W. Euverink, University of Groningen

Dr R. Kleerebezem, Delft University of Technology

Dr C. Chassagne, Delft University of Technology

This research was conducted under the auspices of the Graduate School for Socio-Economic and Natural Sciences of the Environment (SENSE)

Flocculants from wastewater

Victor Olusola Ajao

Thesis

submitted in fulfilment of the requirements for the degree of doctor

at Wageningen University

by the authority of the Rector Magnificus,

Prof. Dr A.P.J. Mol,

in the presence of the

Thesis Committee appointed by the Academic Board

to be defended in public

on Friday 11 September 2020

at 3:30 p.m. in De Harmonie, Leeuwarden.

Victor Olusola Ajao

Flocculants from wastewater

224 pages.

PhD thesis, Wageningen University, Wageningen, the Netherlands (2020)

With references, with summary in English

ISBN: 978-94-6395-471-6

DOI: https://doi.org/10.18174/527116

Table of Contents

Chapter 1

General Introduction

1. Wastewater treatment and resource recovery

Every year, close to 1000 km^3 (10^9 m^3) of wastewater is generated around the world, with over 30% being municipal wastewater and more than 60% coming from various industries [1]. Since the discharge of untreated water is harmful to humans and the environment, wastewater treatment is imperative. Coupled with the growing global population and freshwater shortage, water reuse becomes equally important.

The conventional aerobic wastewater treatment process (also known as the activated sludge process), is the oldest (106 years [2]) and most common treatment technology for municipal wastewater because of its robustness and ability to meet effluent discharge quality. During this process, heterotrophic microorganisms oxidise (in the presence of oxygen) typically 50 - 60 % of the biodegradable organic pollutants to products such as CO_2 and water while using oxygen as the electron acceptor. Organics in wastewater supply microorganisms the energy they need to grow and the remaining 40 - 50 % (biodegradable) organics are converted to new biomass. The mixture of biomass, wastewater and any other substance produced in the process is referred to as sludge or mixed liquor. Under proper conditions, this sludge forms settleable flocs that can be separated by sedimentation or (membrane) filtration, after which the treated water can be discharged to surface water if it meets the discharge guidelines. The separated sludge is partly recycled to the biological treatment process (referred to as return activated sludge) and partly wasted (called the surplus or waste activated sludge).

With about 50 - 60 % of the wastewater organics being destroyed, there is a room for improvement as regards sustainability. Not only is the potential chemical energy of the organic pollutants wasted, energy is also consumed for the aeration process. Typically, aeration alone accounts for 40 - 60 % of the overall energy consumption of a WWTP [1]. Only a minor fraction (20 - 30 %) of the potential chemical energy is recovered when the waste activated sludge is digested anaerobically to biogas [3]. This is one of the reasons wastewater treatment plants (WWTPs) have been recognised as one of the largest greenhouse gas (GHG) emitters [1]. It was estimated that the organic degradation process during wastewater treatment contributed about 0.77 Gt CO_2-equivalent GHG emissions in 2010, making up about 1.57% of global GHG emissions (49 Gt CO_2-equivalent) [1].

Considering the abundant resources in wastewater (carbon, nitrogen, phosphorus and other resources), the destruction of some of these resources during the conventional wastewater treatment process and the high cost (~ 45 billion annually) to treat only a fraction of the material considered waste [4], a paradigm shift is underway in wastewater treatment [1]. Gradually, although slowly, WWTPs are being transformed into resource recovery factories for the recovery of carbon (in the form of energy, biopolymers, or chemicals) and nutrients (nitrogen and phosphorus) [5]. With respect to biopolymer recovery, cellulose [6], polyhydroxyalkanoates (bioplastics) [2,7] and microbial extracellular polymers (specifically the Kaumera Nerada® gum from the aerobic granular sludge process) [8,9] are three biopolymers that are close to commercialisation. These biopolymers have valuable and sometimes unique properties, which broaden their range of applications – as both commodity and speciality products [2,8].

2. Extracellular polymers from wastewater

Microorganisms responsible for biological degradation of organics in wastewater also excrete biopolymers, generally referred to as extracellular polymeric substances (EPS). EPS are products of biochemical secretions [10]. They are the major component of biofilms (up to 90% of the total dry mass) and interconnect in a three-dimensional polymeric network (Fig. 1) to provide mechanical stability to biofilms. In sludge, they constitute 40 - 70 % of the organic fraction and are responsible for sludge bioflocculation [11–13]. EPS are composed of different biomacromolecules: polysaccharides, proteins, nucleic acids, lipids, humic acids or their combinations such as glycoproteins, which make them high molecular weight compounds [14]. The charged components give them a net negative charge due to the predominant presence of anionic functional groups like carboxyl and phosphoryl groups, which outweigh the positive charges such as amino groups present in lower numbers.

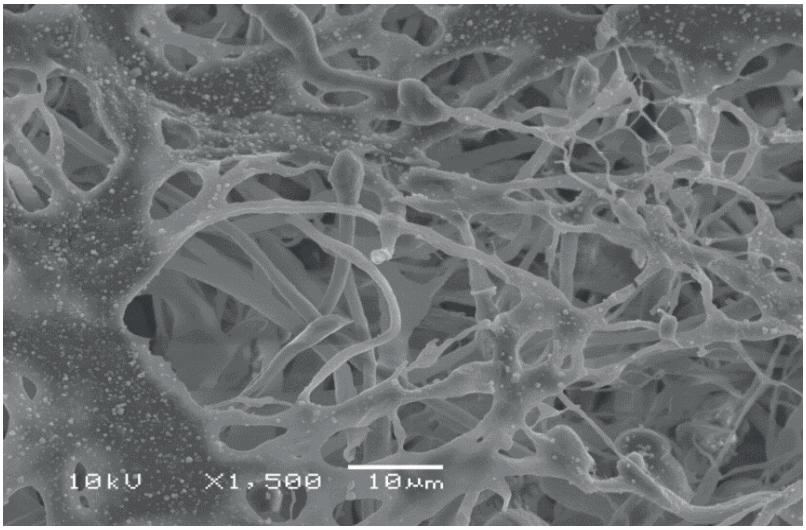

Fig. 1. Scanning electron microscopy (SEM) micrograph of freeze-dried soluble EPS.

EPS can be broadly classified as soluble and bound fractions based on the nature of their association with cells and the method used to separate them from cells [14] (Fig. 2). The bound EPS are closely attached to microbial cells or flocs, while the soluble EPS are weakly attached to cells or dissolved in the bulk liquid [15]. Both fractions are generally separated by centrifugation: the supernatant contains the soluble EPS while the bound EPS remain attached to the pellets. The bound EPS can be extracted from the cells by physical methods (e.g., sonication and heating) or via the use of chemicals such as inorganic acids, alkalis, ethylenediaminetetraacetic acid (EDTA) or cation exchange resins (CER). A CER was used in this thesis to extract the bound EPS due to its reported high extraction efficiency and low cell lysis [14].

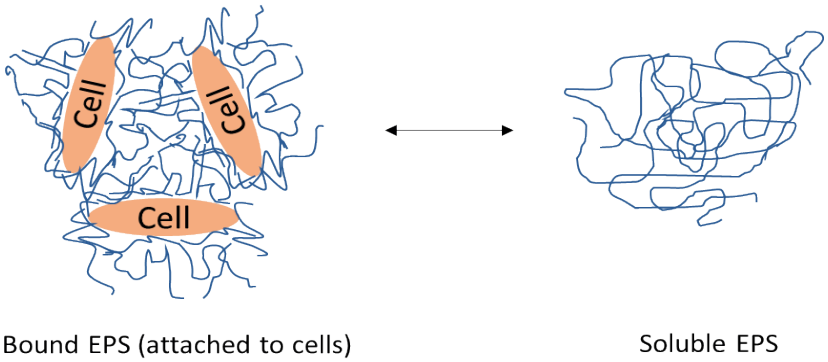

Fig. 2. Schematic depiction of soluble and bound EPS (proposed by Nielsen and Jahn [16]).

2.1. Factors affecting EPS production and concentrations in sludge systems

The production of EPS depends on several factors, such as the reactor's redox condition (aerobic or anaerobic), the wastewater composition (substrate type and carbon/nitrogen ratio) and operational parameters such as solids retention time and dissolved oxygen (DO) concentration. Quite consistently in literature, **aerobic** systems have been reported to favour EPS production compared to anaerobic systems [12,14,17], probably due to a higher energy gain in the presence of oxygen; hence, more energy is available to invest in EPS synthesis. The production of most commercial exopolysaccharides occurs under aerobic conditions, either under microaerophilic conditions (e.g. bacterial alginates) or maximal aeration (e.g. xanthan gum) [17]. Faust *et al*. [18] also observed increased EPS production from municipal wastewater at a high DO concentration (4 mg/L) compared to a low DO concentration (1 mg/L).

Although studies regarding the effect of **solids retention time** (**SRT** – the average time sludge solids are in a reactor) on EPS production is largely controversial, perhaps due to the wide range of SRTs investigated [13], Faust *et al*. [18] conclusively reported that EPS concentration first increases with increasing SRT (typically 0.125 - ~ 1 d), after which it declines as the SRT is further increased (> 5 d). With increasing sludge retention (SRT > 5 d), a significant fraction of the wastewater-COD (COD – chemical oxygen demand) is mineralised instead of being converted to EPS. On the other hand, at very low SRTs, there is also a risk of poor wastewater-COD removal. Hence, there exists an optimum SRT that ensures maximum wastewater-COD removal and maximum EPS production (i.e., minimum degree of COD mineralisation).

Wastewater composition also has a major influence on EPS production. Although this effect has been largely studied on pure bacterial strains [14,19,20], the effect of wastewater composition on EPS produced from mixed culture is understudied and the obtained results are inconsistent. For instance, in activated sludge systems fed with glucose and acetate, it was found that the sludge fed with glucose produced more EPS than the sludge fed with acetate [21]. However, Ye *et al*. [22] reported the opposite i.e., acetate-fed sludge had more EPS than the glucose-fed sludge. Clearly, the effect of carbon source on EPS production requires a more extensive study, including their influence on the EPS characteristics and sludge microbial population.

Perhaps even more crucial for EPS production is the **wastewater carbon/nitrogen (C/N) ratio or chemical oxygen demand/nitrogen (COD/N) ratio**. A few studies have investigated this effect on EPS production and composition, but the results are also largely contradictory. Durmaz & Sanin [23], Miqueleto *et al*. [24] and Feng *et al*. [25] reported higher EPS concentrations at increased COD/N ratio while Ye *et al*. [26] and Wang *et al*. [27] observed EPS production to be independent on the COD/N ratio. In another study, the total EPS concentration was found to decrease at higher COD/N ratios [28]. However, for most of these studies, there was no clear distinction between operating at an excess or a limited nitrogen condition (tested COD/N ratios were 3.9 – 55.6); hence it is difficult to draw conclusions on the effect of either condition on EPS production. Moreover, at the long SRTs (> 15 d) reported in some of these studies [25,27,28], the effect of COD/N ratio can hardly be established because most of the wastewater-COD would have been oxidised. Hence, there is still a need to establish the effect of excess and limited wastewater nitrogen on the valorisation of wastewater to EPS.

2.2. Applications of extracellular polymers

The occurrence or production of EPS in some systems (e.g., membrane-based water treatment processes) are unwanted and poses a serious issue, namely fouling, which leads to increased chemical and energy cost [29,30]. Although EPS are considered a nuisance in such systems, their potential applications are still unfathomable. Their high molecular weight (typically > 10 kDa), anionic charge (> 0.5 meq/g EPS), a general non-toxic property [14,19], biodegradability and amphiphilicity (hydrophilicity/hydrophobicity) make them interesting biopolymers for different applications such as particle flocculation [14,19], heavy metal adsorption [31], toxic organic chemical removal [32,33] and dye decolourisation [14,34]. The use of EPS for a specific application is contingent on the characteristics (composition, molecular weight, charge density, etc.) of the produced EPS, which in turn depends on the factors discussed in Section 2.1. For instance, EPS with a high hydrophobic/hydrophilic ratio are more beneficial for organic pollutant adsorption [32], while hydrophilic EPS with a high molecular weight would be more interesting for particle flocculation, and hydrophilic EPS with a very high charge density would be more favourable for heavy metal adsorption.

2.2.1. Extracellular polymers as sustainable and biodegradable flocculants

This thesis, for the most part, focuses on the use of wastewater-produced EPS as bioflocculants and as an add-on application, they were also tested as heavy metal adsorbents. The presence of high molecular weight (MW) components (mainly polysaccharides and proteins) coupled with their net (anionic) charge make EPS potential polyelectrolytes for particle flocculation.

Flocculation involves the use of an organic polymer to agglomerate particles suspended in water. This process may either take place unaided or after coagulation – the use of multivalent metal salts (such as $CaCl_2$, $FeCl_3$, $AlCl_3$) to destabilise particles in solution. The coagulation/flocculation process has been employed for centuries as a simple and effective way to remove particles from water and wastewater. During this process, fine particles are destabilised (coagulation) and agglomerated (flocculation) to facilitate their removal by sedimentation, (membrane) filtration or (dissolved air)

flotation. Currently, the flocculation process is widely achieved with the use of fossil-based organic flocculants, which are efficient at low dosages and able to form dense and strong flocs [35]. However, most of these synthetic flocculants biodegrade poorly and some generate toxic degradation products/monomer residues (e.g., acrylamide from polyacrylamide, ethyleneimine from polyethyleneimine) that cause neurotoxic or carcinogenic effects in humans and death of aquatic animals [35–37]. Besides, unreacted toxic chemicals used to synthesise the monomer units, such as formaldehyde, epichlorohydrin and dimethylamine have been found as sources of contaminants in treated water and concentrates [35,37]. Countries such as Germany, France, Spain, Switzerland, the UK, and the USA have either forbidden or placed restrictions on the use of some synthetic flocculants, such as polyacrylamide, for drinking water applications [38,39]. For instance, in the USA, polyacrylamide dosage for drinking water application is limited to 1 mg/L and in Europe, it is restricted to 0.5 mg/L with an acrylamide concentration of 0.02% [37]. Hence, the use of synthetic flocculants can hardly be considered a sustainable (waste) water treatment approach, especially in open system applications such as surface water treatment, dredging and land reclamation, tunnelling, and mining.

Microbial EPS can be potential alternatives to synthetic fossil-based flocculants [14,19,40,41]. Aside from their functional properties (molecular weight, charge density, hydrophilicity), their environmental properties (biodegradable and generally non-toxic) also make them attractive for open systems and their concentrates may be reused, for instance, in agriculture (if the concentrate is of organic nature and free of heavy metals and pathogens) to improve soil fertility. Commercially available exopolysaccharides such as alginate, dextran, xanthan gum, levan (each having a specific monomer composition) are in the high MW range (500 - 2000 kDa) and can be employed as effective and environmentally friendly flocculants. However, the high cost of these polymers limits their use to speciality applications such as food, feed, medicine and cosmetics [42], and are not applied in the flocculant sector. This high cost is due to the production of these polymers from pure microbial strains, which require sterile conditions, utilisation of expensive substrates such as glucose, and downstream extraction and purification processes. In the same vein, although not available on the market, somewhat mixed EPS (comprising non-specific monomer composition) produced from isolated bacterial strains have been explored as biodegradable flocculants [14,19,41]. However, their production strategy, which is similar to the aforementioned approach is unsustainable and also results in polymers too expensive for the flocculant market. For these reasons, the recovery of EPS from wastewater (as studied in this thesis) seems to be a much better strategy to produce cost-effective flocculants that can be commercialised. The use of non-sterile mixed cultures and the utilisation of wastewater as feedstock make them economically attractive. And like commercial exopolysaccharides, they are also biodegradable and generally pose no toxic risk. Moreover, their production from wastewater contributes to a circular economy and may result in a lower CO_2 footprint compared to synthetic flocculant production.

EPS, being anionic polyelectrolytes, have a similar flocculation mechanism as synthetic anionic flocculants such as polyacrylamide. In activated sludges, EPS have been reported to cause bioflocculation via the divalent cationic bridging (DCB) mechanism, whereby divalent cations such

as Ca^{2+} and Mg^{2+} form 'bridges' between anionic groups of EPS and the negatively charged particles in sludge (schematised in Fig. 3) [43]. These cations also reduce the electrostatic repulsion between the particles due to the compressed double layer (according to the DLVO theory). A similar mechanism of DCB has also been reported for anionic polyacrylamide flocculation of particles [36,44]. However, in addition to the DCB theory, other particle binding mechanisms (e.g., hydrogen bonding) are also possible under certain conditions such as high ionic strength or high sodium concentrations [45].

2.2.2. Extracellular polymers as heavy metal adsorbents

Heavy metal pollution is a critical environmental concern today due to the hazard caused on human health and the environment. Heavy metals are toxic to exposed organisms and can accumulate in soil and water bodies [46,47]. They are found in high concentrations in wastes discharged into the environment by various industries such as metallurgy, mining and smelting, iron and steel, electroplating, electrolysis, and electric appliance manufacturing [48]. At the same time, the provision of these metals (which are essential and critical elements for our lifestyles) to many industries and economies is at risk, due to depleting natural reserves and their concentration in a few nations, and is thus subjected to geopolitical risks [49]. The recovery of metals from waste streams is, therefore, of increasing economic interest. Hence, treating heavy metal waste streams has two important objectives: removal to environmental standards and recovery to economic standards.

Conventional methods for removing metal ions from aqueous solution, such as chemical precipitation and filtration, are ineffective to remove low metal concentrations (< 1 – 50 mg/L) and produce large quantities of sludge (because they co-precipitate/filter impurities as well) which are expensive to dispose of [48,50]. On the other hand, technologies that do not generate such secondary waste streams and are efficient for metal removal and recovery, are costly. Examples of these are ion exchange, reverse osmosis, adsorption on activated carbon, and evaporation [50].

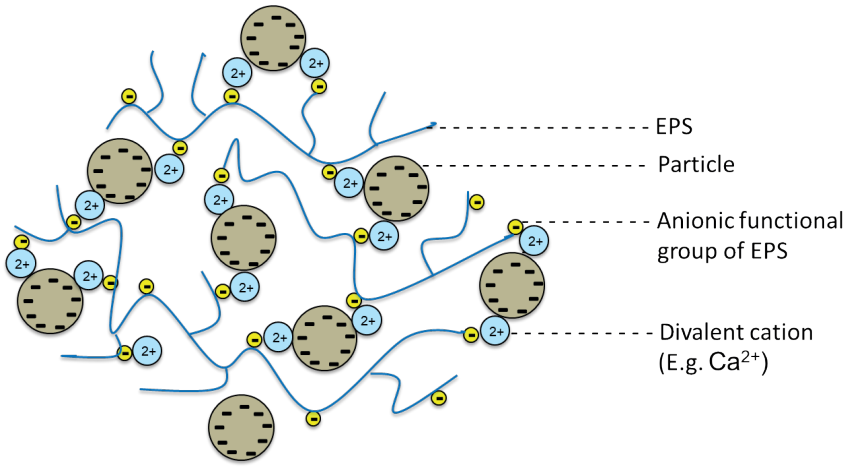

Fig. 3. Schematic illustration of the divalent cationic bridging mechanism of EPS (not drawn to scale).

EPS can be low-cost adsorbents for heavy metal removal [31], especially when produced from wastewater using mixed cultures. The EPS' functional groups (such as carboxyl, hydroxyl and amine groups) can bind to heavy metals either via ion exchange (where the COOH groups are involved) or complexation mechanism (where COOH, OH and NH_2 groups may be involved) [51–53].

Although there are various reports on the use of EPS for heavy metal adsorption [14], most are still far from an economically feasible application in practice due to various limitations: the use of pure-cultured EPS [31], a focus on adsorption only and not on recovery, the use of unrealistically high EPS concentrations in batch studies without practical significance in an industrial or environmental context [53], and the lack of information on the possibility to regenerate and reuse the sorbent.

3. Can wastewater be valorised to EPS? An open research field to explore

As explained in Section 2.2.1, EPS production for different applications has been focused on using pure cultures [14,19,41,54]. Prior to this study, there was no work performed on dedicated EPS production from (waste)water, be it fresh or saline water. Aside from the advantage of non-sterility from employing such a mixed-culture approach, wastewater treatment can be simultaneously combined with EPS production, since wastewater can serve as both carbon and nutrient source for bacteria. Previous reports on EPS production have only studied it as a factor that affects biological wastewater treatment processes such as sludge bioflocculation [26,55] and dewaterability [26,56]). This has led to conflicting results and prevented clear conclusions on the key factors needed to valorise wastewater to EPS (Section 2.1). Hence, a systematic research on the crucial parameters for high EPS yields from wastewater is necessary. As described by More *et al*. [14], many factors (and some may be interrelated) affect EPS yields in sludge systems, but among these factors, the operational SRT and wastewater composition (including the COD/N ratio) may play the major roles (Section 2.1). The SRT of the reactor system determines the rate of EPS' production and degradation, as well as the fraction of wastewater-COD that is mineralised (Section 2.1). Secondly, the type of wastewater substrate influences the microbial community, the substrate incorporation into the cells [17,57], and the metabolic pathway to produce secondary metabolites such as EPS. Beside studying the effect of substrates, it is even more important to investigate the effect of excess or limited wastewater nitrogen content on EPS production.

4. How effective are wastewater-produced EPS as flocculants?

As described in Section 2.2.1, molecular weight (MW) and charge density (CD) are two vital properties that determine the flocculation ability of polyelectrolytes [36], including EPS. Flocculation performance generally increases with MW, and for anionic flocculants, there is an optimum CD value [36,58], which is typically between 2 – 5 meq/g. Hence, the primary goal of this research is to investigate strategies that will ensure the production of high EPS yields combined with the highest possible MW and optimum CD range of EPS. Therefore, it will be vital to investigate the relationship between EPS production strategies and their influence on MW and CD. Since the CD of EPS is contingent on the chemical composition of the produced EPS, which in turn may be influenced by the substrate composition and developed microbial community, it will be essential to further study

the main EPS monomers and key EPS producers under different substrates. Furthermore, the mechanism(s) of flocculation of such mixed EPS produced from mixed cultures should be elucidated.

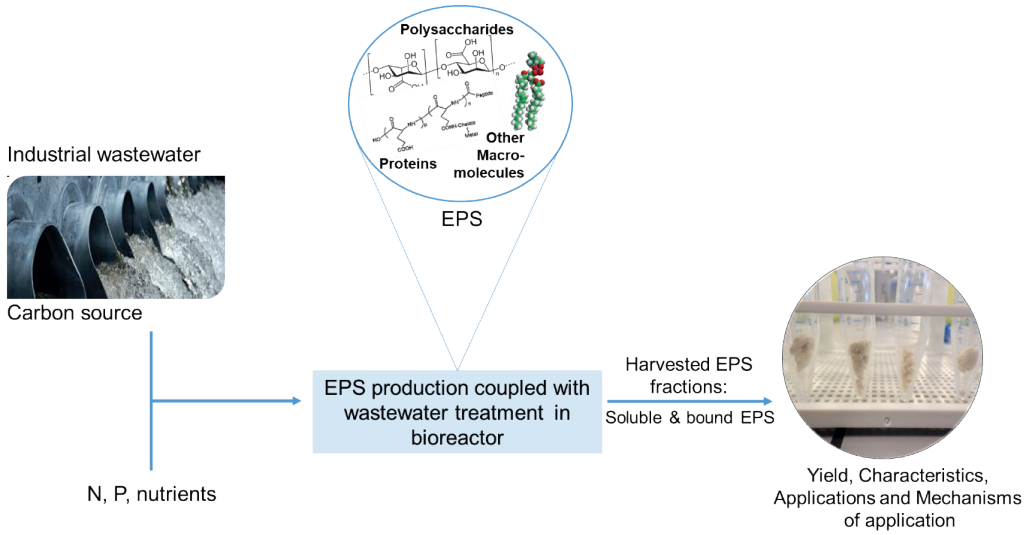

Fig 4. A general scheme of the thesis.

5. Aim and thesis outline

This thesis aimed to valorise selected industrial wastewaters to extracellular polymeric substances (EPS) that can be employed as bioflocculants, heavy metal adsorbents and other applications. To achieve this aim, it was important to study three aspects of the technology value chain: the **production** of EPS, their **characteristics**, and their **applications** as flocculants and heavy metal adsorbents (Fig. 4).

Chapter 2 of this thesis sets the stage on the possibility to use EPS produced from fresh and saline glycerol/ethanol-rich synthetic wastewater as flocculants to remove (clay) particles in both saline and non-saline environments. The hypothesis was that EPS produced from saline (waste)water would better flocculate particles under saline condition than freshwater-produced EPS, and vice versa. Soluble and bound EPS fractions were extracted from the freshwater and saline bioreactors, purified and characterised for their functionalities, basic composition, molecular weights and charge densities. The relationship between the EPS' characteristics and flocculation performances are discussed, and the flocculation performances of the different EPS fractions are compared with a commercial anionic polyacrylamide. Under the tested saline and non-saline flocculation environments, EPS flocculation mechanisms are proposed.

In **Chapter 3**, the underlying research question is to resolve the effects of solids retention time (in comparison to Chapter 2) and COD/N ratios (excess and limited nitrogen regimes) of the feed on

the recovery, characteristics, and flocculation performances of the produced EPS. This Chapter focuses on valorising wastewater to obtain high EPS yield and is the first its kind to dedicate a reactor system for much EPS production while concurrently treating the wastewater.

In **Chapter 4**, selected industrial wastewater types are tested for their suitability to produce EPS in high yields. Additionally, the effects of the different carbon substrates on the produced EPS characteristics and microbial communities are discussed. Since the biopolymer fraction of the produced EPS was mainly composed of polysaccharides, further characterisation was done on the sugar composition. The relationship between the EPS' monosaccharides, charge density, molecular weights, and different applications of EPS are discussed.

Chapter 5 is about investigating the flocculation mechanism involved when wastewater-produced EPS are used as flocculants. Wastewater-produced EPS, being heterodispersed in nature (referred to as 'mixed EPS'), were size-fractionated and each fraction was characterised and investigated for its role in the overall flocculation mechanism of mixed EPS in single and dual particle systems. The hypothesis was that mixed EPS would better flocculate a mixture of particles compared to the use of the high MW EPS fraction for the same purpose. Optical reflectometry was used to observe the *in-situ* adsorption of EPS on a silica surface. Coupled with systematic flocculation tests, the mechanism on how the various molecular weight EPS fractions adsorb to particles is elucidated.

In **Chapter 6**, the fundamental research question was to study if EPS, based on its properties, could be harnessed as a heavy metal adsorbent. Here, we show the possibility to immobilise EPS on a column for continuous flow-through adsorption and recovery of heavy metals (Cu^{2+}, Pb^{2+} and Au^{3+}). The possibility to regenerate and reuse the immobilised EPS after successive adsorption-desorption cycles were studied and the adsorption mechanisms are discussed.

In **Chapter 7**, a general discussion on the production, characteristics and applications of EPS is provided. The experimental findings, (practical) implications, opportunities and limitations originating from the five experimental chapters are discussed. Finally, suggestions for follow-up research and future recommendations are given.

References

[1] L. Lu, J.S. Guest, C.A. Peters, X. Zhu, G.H. Rau, Z.J. Ren, Wastewater treatment for carbon capture and utilization, Nat. Sustain. 1 (2018) 750–758. doi:10.1038/s41893-018-0187-9.

[2] D. Puyol, D.J. Batstone, T. Hülsen, S. Astals, M. Peces, O. Jens, Resource recovery from wastewater by biological technologies: opportunities, challenges and prospects, Front. Microbiol. 7 (2016) 1–23. doi:10.3389/fmicb.2016.02106.

[3] W. Rulkens, Sewage sludge as a biomass resource for the production of energy: Overview and assessment of the various options, Energy and Fuels. 22 (2008) 9–15. doi:10.1021/ef700267m.

[4] Z. Jason Ren, Editorial Perspectives: The value proposition of resource recovery, Environ. Sci. Water Res. Technol. 5 (2019) 196–197. doi:10.1039/c9ew90004g.

[5] W.-W. Li, H.-Q. Yu, B.E. Rittmann, Reuse water pollutants, Nature. 528 (2015) 29–31. doi:10.1038/528029a.

[6] C.J. Ruiken, G. Breuer, E. Klaversma, T. Santiago, M.C.M. van Loosdrecht, Sieving wastewater - Cellulose recovery, economic and energy evaluation, Water Res. 47 (2013) 43–48. doi:10.1016/j.watres.2012.08.023.

[7] R. Kleerebezem, M.C. van Loosdrecht, Mixed culture biotechnology for bioenergy production, Curr. Opin. Biotechnol. 18 (2007) 207–212. doi:10.1016/j.copbio.2007.05.001.

[8] Y.M. Lin, K.G.J. Nierop, E. Girbal-Neuhauser, M. Adriaanse, M.C.M. van Loosdrecht, Sustainable polysaccharide-based biomaterial recovered from waste aerobic granular sludge as a surface coating material, Sustain. Mater. Technol. 4 (2015) 24–29. doi:10.1016/j.susmat.2015.06.002.

[9] Y. Lin, M. de Kreuk, M.C.M. van Loosdrecht, A. Adin, Characterization of alginate-like exopolysaccharides isolated from aerobic granular sludge in pilot-plant, Water Res. 44 (2010) 3355–3364. doi:10.1016/j.watres.2010.03.019.

[10] H.-C. Flemming, J. Wingender, The biofilm matrix, Nat. Publ. Gr. 8 (2010) 623–633. doi:10.1038/nrmicro2415.

[11] B. Frølund, R. Palmgren, K. Keiding, P.H. Nielsen, Extraction of extracellular polymers from activated sludge using a cation exchange resin, Water Res. 30 (1996) 1749–1758. doi:10.1016/0043-1354(95)00323-1.

[12] P.H. Nielsen, B. Frølund, K. Keiding, Changes in the composition of extracellular polymeric substances in activated sludge during anaerobic storage, Appl. Microbiol. Biotechnol. 44 (1996) 823–830. doi:10.1007/BF00178625.

[13] L. Faust, Bioflocculation of wastewater organic matter at short retention times, 2014. http://edepot.wur.nl/321026.

[14] T.T. More, J.S.S. Yadav, S. Yan, R.D. Tyagi, R.Y. Surampalli, Extracellular polymeric substances of bacteria and their potential environmental applications, J. Environ. Manage. 144 (2014) 1–25. doi:10.1016/j.jenvman.2014.05.010.

[15] G. Sheng, H. Yu, X. Li, Extracellular polymeric substances (EPS) of microbial aggregates in biological wastewater treatment systems: A review, Biotechnol. Adv. 28 (2010) 882–894. doi:10.1016/j.biotechadv.2010.08.001.

[16] J.A. Nielsen PH, Extraction of EPS. In: Microbial extracellular polymeric substances: characterization, structure, and function., in: Springer, 1999: pp. 49–72.

[17] F. Freitas, V.D. Alves, M.A.M. Reis, Advances in bacterial exopolysaccharides: From production to biotechnological applications, Trends Biotechnol. 29 (2011) 388–398. doi:10.1016/j.tibtech.2011.03.008.

[18] L. Faust, H. Temmink, A. Zwijnenburg, A.J.B. Kemperman, H.H.M. Rijnaarts, Effect of dissolved oxygen concentration on the bioflocculation process in high loaded MBRs, Water Res. 66 (2014) 199–207. doi:10.1016/j.watres.2014.08.022.

[19] H. Salehizadeh, N. Yan, Recent advances in extracellular biopolymer flocculants, Biotechnol. Adv. 32 (2014) 1506–1522. doi:10.1016/j.biotechadv.2014.10.004.

[20] M. Khani, A. Bahrami, A. Chegeni, M.D. Ghafari, A.M. Zadeh, Optimization of carbon and nitrogen sources for extracellular polymeric substances production by chryseobacterium indologenes MUT.2, Iran. J. Biotechnol. 14 (2016) 13–18. doi:10.15171/ijb.1266.

[21] X.Y. Li, S.F. Yang, Influence of loosely bound extracellular polymeric substances (EPS) on the flocculation, sedimentation and dewaterability of activated sludge, Water Res. 41 (2007) 1022–1030. doi:10.1016/j.watres.2006.06.037.

[22] F. Ye, G. Peng, Y. Li, Influences of influent carbon source on extracellular polymeric substances (EPS) and physicochemical properties of activated sludge, Chemosphere. 84 (2011) 1250–1255. doi:10.1016/j.chemosphere.2011.05.004.

[23] B. Durmaz, F.D. Sanin, Effect of carbon to nitrogen ratio on the physical and chemical properties of activated sludge, Environ. Technol. 24 (2003) 1331–1340. doi:10.1080/09593330309385677.

[24] A.P. Miqueleto, C.C. Dolosic, E. Pozzi, E. Foresti, M. Zaiat, Influence of carbon sources and C/N ratio on EPS production in anaerobic sequencing batch biofilm reactors for wastewater treatment, Bioresour. Technol. 101 (2010) 1324–1330. doi:10.1016/j.biortech.2009.09.026.

[25] S. Feng, N. Zhang, H. Liu, X. Du, Y. Liu, H. Lin, The effect of COD/N ratio on process performance and membrane fouling in a submerged bioreactor, Desalination. 285 (2012) 232–238. doi:10.1016/j.desal.2011.10.008.

[26] F. Ye, Y. Ye, Y. Li, Effect of C/N ratio on extracellular polymeric substances (EPS) and

physicochemical properties of activated sludge flocs, J. Hazard. Mater. 188 (2011) 37–43. doi:10.1016/j.jhazmat.2011.01.043.

[27] Z. Wang, M. Gao, S. Wang, Y. Xin, D. Ma, Z. She, Z. Wang, Q. Chang, Y. Ren, Effect of C/N ratio on extracellular polymeric substances of activated sludge from an anoxic–aerobic sequencing batch reactor treating saline wastewater, Environ. Technol. 35 (2014) 2821–2828. doi:10.1080/09593330.2014.924563.

[28] L. Hao, S.N. Liss, B.Q. Liao, Influence of COD:N ratio on sludge properties and their role in membrane fouling of a submerged membrane bioreactor, Water Res. 89 (2015) 132–141. doi:10.1016/j.watres.2015.11.052.

[29] F. Meng, S.R. Chae, A. Drews, M. Kraume, H.S. Shin, F. Yang, Recent advances in membrane bioreactors (MBRs): Membrane fouling and membrane material, Water Res. 43 (2009) 1489–1512. doi:10.1016/j.watres.2008.12.044.

[30] Z. Wang, Z. Wu, X. Yin, L. Tian, Membrane fouling in a submerged membrane bioreactor (MBR) under sub-critical flux operation: Membrane foulant and gel layer characterization, J. Memb. Sci. 325 (2008) 238–244. doi:10.1016/j.memsci.2008.07.035.

[31] K. Raj, U.R. Sardar, E. Bhargavi, I. Devi, B. Bhunia, O.N. Tiwari, Advances in exopolysaccharides based bioremediation of heavy metals in soil and water: A critical review, Carbohydr. Polym. 199 (2018) 353–364. doi:10.1016/j.carbpol.2018.07.037.

[32] R. Späth, H.-C. Flemming, S. Wuertz, Sorption properties of biofilms, Water Sci. Technol. 37 (1998) 207–210.

[33] C. Jia, P. Li, X. Li, P. Tai, W. Liu, Z. Gong, Degradation of pyrene in soils by extracellular polymeric substances (EPS) extracted from liquid cultures, Process Biochem. 46 (2011) 1627–1631. doi:10.1016/j.procbio.2011.05.005.

[34] M. Solís, A. Solís, H.I. Pérez, N. Manjarrez, M. Flores, Microbial decolouration of azo dyes: A review, Process Biochem. 47 (2012) 1723–1748. doi:10.1016/j.procbio.2012.08.014.

[35] C.S. Lee, J. Robinson, M.F. Chong, A review on application of flocculants in wastewater treatment, Process Saf. Environ. Prot. 92 (2014) 489–508. doi:10.1016/j.psep.2014.04.010.

[36] B. Bolto, J. Gregory, Organic polyelectrolytes in water treatment, Water Res. 41 (2007) 2301–2324. doi:10.1016/j.watres.2007.03.012.

[37] M. Lapointe, B. Barbeau, Dual starch–polyacrylamide polymer system for improved flocculation, Water Res. 124 (2017) 202–209. doi:10.1016/j.watres.2017.07.044.

[38] R.D. Letterman, R.W. Pero, Contaminants in polyelectrolytes used in water treatment, J. / Am. Water Work. Assoc. 82 (1990) 87–97. doi:10.1002/j.1551-8833.1990.tb07056.x.

[39] WHO, WHO guidelines for drinking water quality, in: 2000.

[40] K. Okaiyeto, U.U. Nwodo, S.A. Okoli, L. V. Mabinya, A.I. Okoh, Implications for public health

demands alternatives to inorganic and synthetic flocculants: Bioflocculants as important candidates, Microbiologyopen. 5 (2016) 177–211. doi:10.1002/mbo3.334.

[41] M. Shahadat, T.T. Teng, M. Rafatullah, Z.A. Shaikh, T.R. Sreekrishnan, S.W. Ali, Bacterial bioflocculants: A review of recent advances and perspectives, Chem. Eng. J. 328 (2017) 1139–1152. doi:10.1016/j.cej.2017.07.105.

[42] J. Schmid, V. Sieber, B. Rehm, Bacterial exopolysaccharides: Biosynthesis pathways and engineering strategies, Front. Microbiol. 6 (2015) 1–24. doi:10.3389/fmicb.2015.00496.

[43] D.C. Sobeck, M.J. Higgins, Examination of three theories for mechanisms of cation-induced bioflocculation, Water Res. 36 (2002) 527–538. doi:10.1016/S0043-1354(01)00254-8.

[44] M.S. Nasser, A.E. James, The effect of polyacrylamide charge density and molecular weight on the flocculation and sedimentation behaviour of kaolinite suspensions, Sep. Purif. Technol. 52 (2006) 241–252. doi:10.1016/j.seppur.2006.04.005.

[45] Y. Ji, Q. Lu, Q. Liu, H. Zeng, Effect of solution salinity on settling of mineral tailings by polymer flocculants, Colloids Surfaces A Physicochem. Eng. Asp. 430 (2013) 29–38. doi:10.1016/j.colsurfa.2013.04.006.

[46] W. Liu, J. Zhang, Y. Jin, X. Zhao, Z. Cai, Adsorption of Pb(II), Cd(II) and Zn(II) by extracellular polymeric substances extracted from aerobic granular sludge: Efficiency of protein, J. Environ. Chem. Eng. 3 (2015) 1223–1232. doi:10.1016/j.jece.2015.04.009.

[47] J.J. Gray, The interaction of proteins with solid surfaces, Curr. Opin. Struct. Biol. 14 (2004) 110–115. doi:10.1016/j.sbi.2003.12.001.

[48] J. Wang, C. Chen, Biosorbents for heavy metals removal and their future, Biotechnol. Adv. 27 (2009) 195–226. doi:10.1016/j.biotechadv.2008.11.002.

[49] J.R. Dodson, H.L. Parker, A. Muñoz García, A. Hicken, K. Asemave, T.J. Farmer, H. He, J.H. Clark, A.J. Hunt, Bio-derived materials as a green route for precious & critical metal recovery and re-use, Green Chem. 17 (2015) 1951–1965. doi:10.1039/C4GC02483D.

[50] B. Volesky, Detoxification of metal-bearing effluents: Biosorption for the next century, Hydrometallurgy. 59 (2001) 203–216. doi:10.1016/S0304-386X(00)00160-2.

[51] H. Liu, H.H.P. Fang, Characterization of electrostatic binding sites of extracellular polymers by linear programming analysis of titration data, Biotechnol. Bioeng. 80 (2002) 806–811. doi:10.1002/bit.10432.

[52] W.W. Li, H.Q. Yu, Insight into the roles of microbial extracellular polymer substances in metal biosorption, Bioresour. Technol. 160 (2014) 15–23. doi:10.1016/j.biortech.2013.11.074.

[53] G.M. Gadd, Biosorption: Critical review of scientific rationale, environmental importance and significance for pollution treatment, J. Chem. Technol. Biotechnol. 84 (2009) 13–28. doi:10.1002/jctb.1999.

[54] D.J. Lee, Y.R. Chang, Bioflocculants from isolated stains: A research update, J. Taiwan Inst. Chem. Eng. 87 (2018) 211–215. doi:10.1016/j.jtice.2018.03.037.

[55] L. Faust, H. Temmink, A. Zwijnenburg, A.J.B. Kemperman, H.H.M. Rijnaarts, High loaded MBRs for organic matter recovery from sewage: effect of solids retention time on bioflocculation and on the role of extracellular polymers., Water Res. 56 (2014) 258–66. doi:10.1016/j.watres.2014.03.006.

[56] C. Hong, Y. Xing, X. Hua, Y. Si, G. Qiao, Z. Wang, Dewaterability of sludge conditioned with surfactant DDBAC pretreatment by acid/alkali, Appl. Microbiol. Biotechnol. 99 (2015) 6103–6111. doi:10.1007/s00253-015-6451-2.

[57] G.P. da Silva, M. Mack, J. Contiero, Glycerol: A promising and abundant carbon source for industrial microbiology, Biotechnol. Adv. 27 (2009) 30–39. doi:10.1016/j.biotechadv.2008.07.006.

[58] J. Gregory, S. Barany, Adsorption and flocculation by polymers and polymer mixtures, Adv. Colloid Interface Sci. 169 (2011) 1–12. doi:10.1016/j.cis.2011.06.004.

Chapter 2

Natural flocculants from fresh and saline wastewater: comparative properties and flocculation performances

A modified version of this Chapter has been published as:

V. Ajao, H. Bruning, H. Rijnaarts, H. Temmink, Natural flocculants from fresh and saline wastewater: Comparative properties and flocculation performances, Chem. Eng. J. 349 (2018) 622–632. doi:10.1016/j.cej.2018.05.123.

Abstract

Natural flocculants, due to their eco-friendliness, have gained increasing attention for (waste) water treatment and are promising alternatives to fossil-based synthetic flocculants. We systematically investigated simultaneous industrial wastewater treatment with the production of microbial extracellular polymeric substances (EPS) as natural flocculants. EPS were produced in two membrane bioreactors, respectively treating fresh and saline synthetic wastewater from biodiesel and (bio)ethanol industries. From each reactor, soluble and bound EPS fractions were extracted, purified and characterised for their functionalities, molecular weights and charge densities using Fourier transform infrared (FTIR), size exclusion chromatography and colloid titration, respectively. High removal of chemical oxygen demand (COD) was achieved in both reactors (93 - 95 %), with 5.8 - 7.6 % of the influent COD recovered as EPS. FTIR spectroscopy reveals these EPS as a mixture predominantly composed of proteins and polysaccharides, possessing carboxyl, hydroxyl and amine groups. These functional groups, which provided a net anionic charge density (1.5 - 2.9 meq/g at neutral pH), coupled with EPS mixed molecular weight (MW) distribution: high (> 1000 kDa), medium (1000 - 100 kDa) and low (< 100 kDa) MW fractions, make them promising flocculants. Extracted EPS showed good flocculation of non-saline kaolin suspension (74 - 89 % turbidity reduction) and excellent flocculation of saline kaolin suspension (88 - 97 %), with performances comparable to anionic polyacrylamide. The results show the possibility for wastewater treatment plants to combine wastewater treatment with the production of valuable flocculants.

1. Introduction

Fields such as water and wastewater treatment, dredging, mining, food processing, textile and paper making, petroleum and chemical industries face the challenge of particle removal from saline/non-saline (waste) water. These fine suspended and colloidal particles may have adverse effects on water potability and aquatic life when discharged into the environment untreated [1]. The challenge is to aggregate these particles into heavier mass by coagulation/flocculation, which facilitates their removal by settling, (membrane) filtration or flotation.

Currently, coagulation/flocculation is widely achieved with the use of inorganic coagulants (such as alum, aluminium chloride, and other multivalent metal salts), and/or fossil-based organic flocculants, such as polyacrylamide and polyethyleneimine [2]. Inorganic coagulants are cheap and easy to use. However, they do not coagulate efficiently at a low dosage, and at high concentrations may leave residual metal particles in treated water, e.g., aluminium, which is linked to Alzheimer's disease [3]. Also, they produce toxic (metal hydroxide) sludges which are difficult to dewater, expensive to dispose of [2], and not reusable in agriculture for soil improvement. Synthetic organic flocculants, on the other hand, have higher flocculating efficiency, lower dosage requirements, form strong and dense flocs and can dewater sludge more efficiently [2]. Nonetheless, some suffer significant drawbacks of slow biodegradability and generation of toxic degradation products/monomer residues (e.g., acrylamide from polyacrylamide, ethyleneimine from polyethyleneimine), that may enter the food chain and cause neurotoxic or carcinogenic effects [2,4]. Besides, unreacted toxic chemicals used to synthesise the monomer units, such as formaldehyde, epichlorohydrin, and dimethylamine, have been found as sources of contaminants in treated water [2]. Hence, the use of some synthetic flocculants can hardly be considered a sustainable (waste) water treatment approach, especially in open systems such as in dredging and mining applications.

Natural flocculants, due to their environmental friendliness, have gained increasing attention for water treatment and are promising alternatives to synthetic fossil-based flocculants [5–8]. They are of great interest because most are considered safe and biodegradable, fairly resistant to shear, and produced sludges of organic nature can be degraded by microbes and reused in agriculture to improve soil fertility [2,9]. One of the natural flocculants yet to be fully explored are microbial extracellular polymeric substances (EPS). These are products of biochemical secretions and can make up as much as 50 - 90 % of the organic matter content of microbial aggregates [10,11]. EPS include high molecular weight substances like polysaccharides, proteins, lipids, and sometimes their derivatives, such as glycoproteins, liposaccharides, and lipoproteins. Most EPS possess at neutral pH a net negative charge due to the predominant presence of anionic functional groups like carboxyl, hydroxyl and phosphoryl groups, outweighing positive charges such as amino groups present in lower numbers. EPS are often referred to as 'slimy', 'capsular', 'soluble' or 'bound' (loosely- and tightly- bound) depending on how they are extracted or associated with the cells [10]. These EPS fractions have been shown to have different properties (composition, content, molecular weight), which gives each fraction a distinctive characteristic that can be harnessed for its flocculating ability [12–14].

More often than not, EPS production strategy consists of the identification and isolation of EPS-producing microbial strains, their enrichment and feeding with single organic substrates to obtain a single type of EPS, usually polysaccharides [9,15–17]. Although this strategy yields biodegradable polymers, the disadvantage is that the pure cultures need to be fed with expensive and unsustainable carbon sources as well as with valuable nutrients. As a more sustainable alternative, we establish a mixed-culture approach that requires non-sterile cultures and feedstocks, e.g., organic wastewater as a carbon and nutrient source. Here one uses the potential of cooperative growth and symbiotic relationships in mixed cultures of EPS-producing and non-EPS producing bacterial strains as found in activated sludge. This mixed-culture approach may increase EPS yield and produce higher molecular weight biopolymers that can enhance flocculation, compared to pure-cultured EPS [10,18]. By using industrial wastewater as carbon source, wastewater treatment plants can combine biological wastewater treatment with the production of natural flocculants, saving (energy) costs.

EPS, being anionic polyelectrolytes, have a similar flocculation mechanism with synthetic anionic flocculants such as polyacrylamide. In sludges, EPS have been reported to cause bioflocculation via the divalent cation bridging (DCB) mechanism, whereby divalent cations such as Ca^{2+} and Mg^{2+} form bridges between anionic groups of EPS and negatively charged particles in sludge [19]. These cations also reduce the electrostatic repulsion between the particles due to the compressed double layer (according to the DLVO theory) [19]. A similar mechanism of DCB has also been reported for anionic polyacrylamide flocculation of (kaolin) particles [4,20].

This study is not aimed to maximise EPS production but to explore wastewater-derived polyelectrolytes as attractive and alternative flocculants to synthetic organic flocculants, under saline and non-saline conditions. We produced and extracted various EPS fractions from a mixed microbial population treating synthetic industrial wastewater – fresh and saline, to investigate mixed EPS production, characteristics, and flocculation behaviour under saline and non-saline environments. We hypothesised that EPS produced from saline (waste)water would better flocculate particles under saline condition than freshwater-produced EPS, and vice versa. To test the flocculation performance of such polymers, we used kaolin clay suspension as a model. To the best of our knowledge, this is the first time mixed EPS have been systematically investigated as potential flocculants for (waste) water treatment, more importantly, the use of mixed EPS produced under saline condition for saline (waste) water flocculation is novel.

2. Materials and methods

2.1. Reactor system and operation

Two lab-scale membrane bioreactors (MBRs, 3.3 L effective volume) were operated in parallel, with the aim of combining wastewater treatment with EPS production. MBR was employed to retain biomass and EPS, and avoid sedimentation problems often encountered at high salt concentration [1,21]. The MBRs were operated under similar reactor conditions and parameters (Table 1), but with different wastewater salinities and sources of inocula. One MBR was operated under freshwater condition (FW-MBR) and the other under saline condition (Sal-MBR). The FW-MBR was inoculated

with aerobic sludge from a municipal WWTP (located in Leeuwarden, Netherlands) having low sodium concentration (182 ± 62 mg Na^+/L). The Sal-MBR was inoculated with aerobic sludge obtained from a saline wastewater treatment plant (located in Delfzijl, Netherlands) that treats wastewater from local chemical industries. The sludge had been adapted to a salinity of 8 - 14 g Na^+/L for more than seven years. We fed both MBRs with nutrients and readily biodegradable substrates – glycerol and ethanol, simulating biodiesel and (bio)ethanol wastewater (Table 2). These substrates also make up more than 50% of the wastewater-COD of Delfzijl WWTP.

Detailed reactor design has been previously described by Akanyeti *et al*. [22]. Briefly, each MBR comprised one submerged flat sheet membrane (Kubota membrane cartridge 203) made from polyvinylidene fluoride (PVDF) with a surface area of 0.1 m^2 and nominal pore size of 0.2 µm. Perforated PVC sheets were placed underneath the membrane module to provide coarse air bubbles that scoured the membrane surface to reduce fouling. The permeate pumps (Masterflex L/S, Cole-Parmer) were operated in cycles with 15 min permeation followed by a 5-min relaxation.

Table 1. Reactor set-up and operational parameters.

Parameter	Freshwater & saline reactors
Reactor type	submerged MBR
Effective volume (L)[a]	3.3
Temperature (°C)[b]	20 ± 1
pH[c]	7.5 ± 0.1
Solids retention time, SRT (d)	15
Hydraulic retention time, HRT (h)	5 (freshwater MBR); 5.5 (saline MBR)
Dissolved O_2 concentration (mg/L)	4.0 ± 1.0
Operation time (d)	50
Influent COD[d] (mg/L)	520 ± 20 mg/L
Influent TN[e] (mg/L)	32 ± 2 mg/L
Carbon/nitrogen ratio (g COD/ g TN)	16 ± 1

[a] Controlled with a level controller (ifm LR7000); [b] Ambient temperature; [c] controlled with doses of 0.1 M NaOH solution; [d] COD: chemical oxygen demand; [e] TN: total nitrogen - sum of all NH_3-N, NO_3^--N, NO_2^--N, organic N.

2.2. EPS extraction

EPS were extracted from sludge using a cation exchange resin (CER – Sigma-Aldrich's DOWEX Marathon C, sodium form, 20 - 50 mesh size) as described by Frølund *et al*. [23] and Faust *et al*. [21], with slight modifications: 100 mL sludge was centrifuged (using Avanti J-26 XP centrifuge) at 12000 *g* for 10 min at 4°C. The supernatant was collected as crude soluble-EPS (S-EPS) after being passed

through a 0.22 µm filter. Sludge pellet was washed and homogenised in a 1x phosphate buffer saline (PBS) solution (10x Dulbecco's PBS: 0.2 g/L KCl, 0.2 g/L KH_2PO_4, 8 g/L NaCl, Na_2HPO_4) at pH 7.4, at 300 rpm using a stirring plate. The homogenised pellet was added to a flask containing 70g CER/g VSS and extracted in PBS for 2 h at 600 rpm (using Heidolph MR Hei-Max L stirring plate). CER was prewashed in PBS for 1 h before use. After the 2-hour extraction, centrifugation was carried out at 12000 *g* for 15 min at 4 ^oC, and the supernatant filtered (as described above). The filtrate was collected as crude bound-EPS (B-EPS). Both the crude S-EPS and B-EPS were dialysed using tubular dialysis membranes with a 12 - 14 kDa molecular weight cut-off (Spectra/Por 2) against Milli-Q water for 2 h first, then 4 h, and finally for 48 h, with a change of Milli-Q water after each period. Dialysis was necessary to concentrate and purify the EPS by removing low molecular weight metabolites and salts. Purified EPS were lyophilised at -84 ^oC and 0.001 mbar.

2.3. Analyses

2.3.1. Chemical Oxygen Demand (COD)

COD was measured using Hach Lange test kits (LCK, Hach Lange, UK), heated in a thermostat (HT 200S, Hach Lange) to 170 ^oC and analysed in a spectrophotometer (DR 3900 VIS spectral photometer, wavelength range 320 – 750 nm).

Table 2. Composition of synthetic wastewater in both reactors. The main COD sources were glycerol and ethanol. The main nitrogen source was NH_4Cl. Yeast extract also contributed 10.5% of the total nitrogen.

Compound	Concentration (mg/L)	Nutrient solution	Concentration (mg/L)
Glycerol	205	$FeCl_3 \cdot 6H_2O$	1500
Ethanol	120	H_3BO_3	150
NH_4Cl	100	$CoCl_2 \cdot 6H_2O$	150
Yeast extract	60	$ZnSO_4 \cdot 7H_2O$	120
K_2HPO_4	7.5	$MnCl_2 \cdot 2H_2O$	120
KH_2PO_4	12.5	$Na_2MoO_4 \cdot 2H_2O$	60
$MgCl_2 \cdot 6H_2O$	100	$CuSO_4 \cdot 5H_2O$	60
$CaCl_2 \cdot 2H_2O$	150	KI	30
NaCl*	30000		
Nutrient solution	2 mL/L		

* NaCl was fed only to the saline MBR.

2.3.2. Total Suspended Solids (TSS) and Volatile Suspended Solids (VSS)

TSS and VSS were analysed according to the Standard Methods for the Examination of Water and Waste water [24].

2.3.3. Functional group determination

Fourier transform infrared spectroscopy (FTIR) was carried out on the purified and lyophilised EPS samples using Shimadzu FTIR-8400S spectrometer, with a scanning range of 4000 - 650 cm^{-1} for 40 scans at a spectral resolution of 2 cm^{-1}.

2.3.4. Total proteins and polysaccharides quantification

Total protein content in EPS samples were determined using the Total Protein Kit – Peterson's modification of micro Lowry (Sigma Aldrich). Dilutions were prepared in PBS (pH 7.4) and bovine serum albumin (BSA) was used as a standard. Absorbance was measured at 570 nm in a spectrophotometer (Victor3 1420 Multilabel Counter, Perkin Elmer). Polysaccharides were quantified using the phenol-sulphuric acid method described by DuBois *et al*. [25] using glucose as a standard. Absorbance was measured at 490 nm in the spectrophotometer mentioned above.

2.3.5. Dissolved organic carbon and nitrogen (DOC and DON), and molecular weight

Purified samples were sent for analysis at DOC-Labor Dr Huber, Germany. Sample solution was first passed through 0.45 µm polyethersulfone filter before DOC and DON analysis using a liquid chromatography-organic carbon detection-organic nitrogen detection (LC-OCD-OND – model 7, DOC-Labor) with built-in Siemens Ultramat 6^E non-dispersive infrared detector (NDIR), coupled with a proprietary organic nitrogen detector (UV 220 nm) and UV detector (254 nm). The column used was a tandem setup with TSK HW65S followed by TSKHW50S (250mm x 20 mm each), and it separated each sample into five fractions: biopolymers, humic substances, building blocks, low molecular weight (LMW) acids, and LMW neutrals. The mobile phase was a phosphate buffer (28 mmol, pH 6.58). Data analysis was performed with DOC-Labor software (ChromLog).

2.3.6. Charge density

The surface charge of the flocculants was determined by colloid titration using a Mütek Particle Charge Detector (PCD03) described by Tan *et al*. [26]. Each sample was titrated against a complexing agent of opposite charge (0.01 mN poly-diallyldimethylammonium chloride, pDADMAC), using an automatic titrator (Metrohm Titrando 888). The titrant was added in steps of 0.02 mL to 10 mL sample solution (1 mg/L) in the PCD measuring cell. The streaming potentials (mV) were recorded simultaneously. Titrant consumption in mL formed the basis for further calculations using the formula:

$$q = \frac{c*V}{m} \qquad (1)$$

where q is the specific charge quantity (eq/g), c is the titrant concentration (eq/L), V is the consumed titrant volume (L), and m is the mass of the sample (g).

CD was determined at the initial pH of sample solution (~ 5), pH 7 and pH 10, using 0.1 M NaOH/HCl for pH adjustment.

2.3.7. Morphology

Scanning Electron Microscopy (SEM) was performed on freeze-dried EPS samples and kaolin flocs using a JEOL-6480LV (JEOL Ltd, Tokyo, Japan). Floc samples were taken from the settled fraction obtained after flocculation in jar tests and allowed to air dry. Both EPS and floc samples were coated with a gold layer and analysed under a high vacuum (6 kV or 15 kV). Micrographs can be found in the supplementary information (Fig. S4 and S5).

2.4. Flocculation tests

Kaolin clay (Sigma Aldrich's natural kaolinite, $Al_2O_3 \cdot 2SiO_2 \cdot 2H_2O$, full composition in Fig. S1) was used to model wastewater particles. Like wastewater particles, kaolin clay possesses a net negative surface charge and has been employed to determine the flocculation activity of flocculants [17,27,28]. In our study, we investigated the potential of the different EPS fractions in comparison with a commercially available synthetic flocculant (Superfloc A120V provided by Kemira, Netherlands. Superfloc A120V is an anionic polyacrylamide with high molecular weight and medium charge density – two important properties known to favour particle flocculation [4]), to flocculate kaolin particles under saline and non-saline conditions. For this purpose, two model suspensions were prepared: (i) saline kaolin suspension: 5 g kaolin/L and 30 g NaCl/L (to mimic saline water) (ii) non-saline kaolin suspension comprising only 5 g kaolin/L. Both were prepared with Milli-Q water. Flocculant solutions were made by dissolving lyophilised EPS powder/synthetic PE in Milli-Q water at a concentration of 1 g/L.

First, we determined for each flocculant the optimum concentration required to best flocculate the saline kaolin clay particles at pH 6.7 (initial pH of suspension). Second, we further investigated the flocculation performances after the addition of 50 mg Ca^{2+}/L ($CaCl_2 \cdot 2H_2O$) to the saline kaolin suspension. Lastly, we examined the flocculation performances of the various flocculants on the non-saline kaolin suspension (pH 6.7) using 100 mg Ca^{2+}/L as a coagulant. All tests were carried out at room temperature (21 ± 1 °C) and in duplicates.

Flocculation tests were carried out on a jar test flocculation unit (Lovibond® ET 740). The tests were performed on a 100-mL scale with 1 min rapid mixing (250 rpm) of the kaolin suspension (after Ca^{2+} addition), followed by a 10-min slow mixing (25 rpm) after flocculant addition. In each experiment, controls (kaolin suspension without the flocculant) were examined simultaneously. After the flocculation program was completed, stirrers stopped and settling was allowed for 5 min. Subsequently, 30 mL samples were taken from the supernatant (approximately 1 cm below the surface) for immediate turbidity determination as Nephelometric Turbidity Units (NTU), using a turbidimeter (2100N IS, Hach). Flocculation efficiency of the PE was calculated as follows:

$$Flocculation\ efficiency\ (\%) = \frac{NTU_{control} - NTU_{test}}{NTU_{control}} \qquad (2)$$

3. Results and discussion

3.1. Wastewater treatment performance

The total COD removal (efficiencies) in both the FW and Sal MBRs is shown in Fig. 1A, with average efficiencies of 95(±2) % and 93(±2) %, respectively. This performance is comparable to the performance of the industrial WWTP in Delfzijl (93%, at 30 d SRT), treating similar wastewater composition. This implies that the carbon-oxidizing bacteria were not inhibited at the 3% salinity. Effluent COD concentrations from the FW-MBR were steady and ranged from 15 - 45 mg/L throughout the operation period, while the Sal-MBR achieved steady effluent COD concentrations (21 - 45 mg/L) after 10 days. Soluble COD concentrations were 60 mg/L in the FW-MBR and 66 mg/L in the Sal-MBR. These values were higher than the average effluent concentrations (27 and 35 mg/L respectively), signifying that the 0.2 µm membrane retained approximately 55% of the freshwater soluble COD and 47% of the saline soluble COD. This large retention of soluble COD was probably caused by higher retention of the fouling layer on the membrane surface compared to the clean membrane [22]. Overall, soluble influent COD removal by microbial degradation was approximately 88%, and 6% removal was achieved by the membranes, indicating that biological degradation was the predominant treatment process in both reactors.

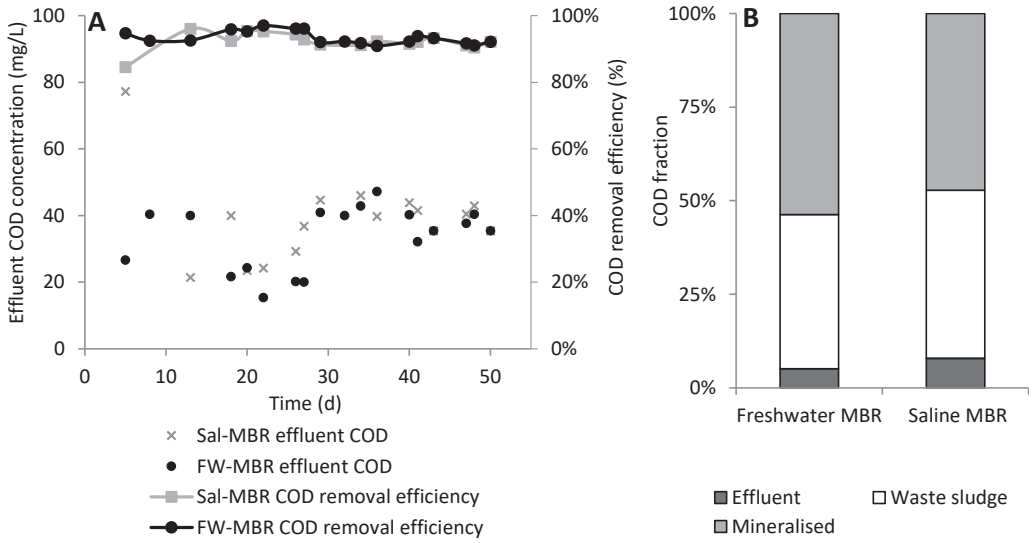

Fig. 1. (**A**) COD removal by both freshwater and saline membrane bioreactors, (**B**) COD distribution as a fraction of influent COD in both bioreactors.

Fig. 1B shows the approximated COD mass balance of each reactor. Mineralisation was estimated as the closure of the mass-balance. In both reactors, about half the influent COD fraction was mineralised, which was expected due to the relatively long SRT, which resulted in the loss of a significant amount of COD via oxidation (by the way, a 15-day SRT was utilised to ensure high COD conversion). However, the degree of mineralisation may have been slightly overestimated because substantial amounts of COD were occasionally removed from the membrane surface to decrease

fouling. The waste sludge consisting of biomass and EPS contributed approximately 41% and 45% (FW- and Sal-MBR, respectively) to the COD mass balance.

3.2. EPS production

After 50 days reactor operation, two EPS fractions were extracted from the MBR sludges: soluble-EPS (S-EPS) and bound-EPS (B-EPS) – Fig. 2B. The former refers to EPS secreted from the microbial cells into the bulk liquid, while the latter are attached to the flocs [29]. Extracted EPS concentrations and recoveries are based on the weight of solids obtained after lyophilisation (Fig. 2). EPS recovery was based on the influent COD using the formula:

$$EPS\ recovery\ (\%) = \frac{Q_{was} * C_{EPS}}{Q_{inf} * COD_{inf}} * COD_{EPS} \qquad (3)$$

where Q_{was} and Q_{inf} are the flow rates (L/d) of the waste sludge and influent feed respectively, C_{EPS} is the concentration of EPS (g/L), COD_{inf} is the influent COD (g/L), COD_{EPS} is the COD of extracted EPS (g COD/g EPS).

The total EPS concentrations in each MBR were ~1 g/L, fractionated into 0.43 g/L freshwater S-EPS and 0.54 g/L freshwater B-EPS (Fig. 2A). In the same vein, the saline S-EPS and B-EPS concentrations were 0.34 g/L and 0.62 g/L. Bound-EPS concentrations were found to be higher than the corresponding soluble-EPS, which is also consistent with many reports [21,30]. This distribution of soluble and bound EPS fractions can vary and may be a function of the applied shear in the reactor [10,29]. In perspective, a total of 5.8% of the influent COD was recovered as FW EPS (2.1 and 3.7 % for soluble and bound FW EPS, respectively), and 7.6 % of the influent COD was recovered as Sal EPS (4.1 and 3.5 % for soluble and bound Sal EPS, respectively). These correspond to 14 and 17 % EPS-COD going into the waste sludge line while the remaining fraction (27 and 28 % for FW-MBR and Sal-MBR, respectively) consists of biomass (see Fig. 1B). However, these EPS recovery values do not take into account the EPS that were removed from the membrane during the cleaning process.

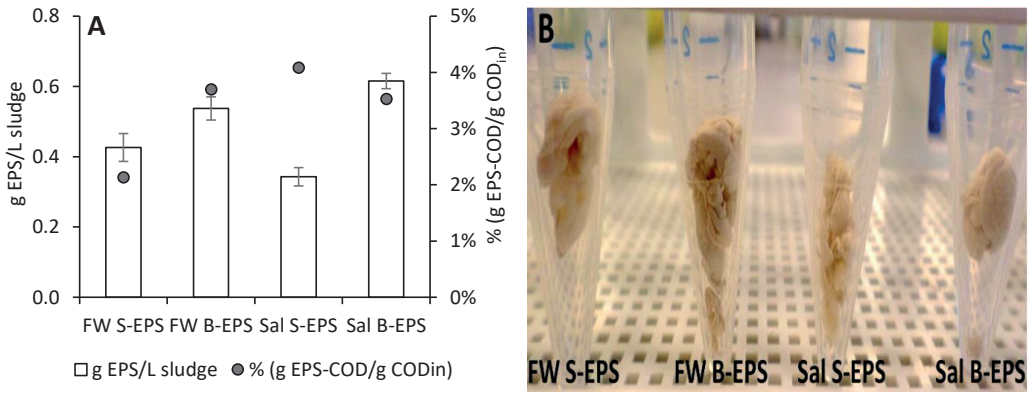

Fig. 2. (**A**) EPS concentration (g EPS/L sludge) and recovery with respect to influent COD, % (g EPS-COD/COD_{inf}) after extraction; (**B**) Images of the dried EPS. FW S-EPS: freshwater soluble-EPS, FW B-EPS: freshwater bound-EPS, Sal S-EPS: saline soluble-EPS, Sal B-EPS: saline bound-EPS. Data expressed as mean ± standard deviation of duplicate extractions.

3.3. EPS functionality and composition

EPS, being a mixture of compounds, provide different functional groups. FTIR analysis reveals similar vibration bands and functionality of the 4 EPS fractions (Fig. 3A). The broad absorption bands at 3280 cm^{-1} are formed by the stretching vibration of both hydroxyl (of polysaccharides) and amino group (of proteins) [31,32]. The sharper peak at 2910 is attributed to C–H stretching vibration. Amide I (1700 - 1600 cm^{-1}), amide II (1600 - 1500 cm^{-1}), and amide III (1450 - 1200 cm^{-1}) are peculiar to proteins [32], while bands at 1250 - 1000 cm^{-1} are associated with polysaccharides [31]. The amide I band at 1632 cm^{-1} is predominantly assigned to C=O stretching vibration of β-sheets in secondary protein structure, which have been shown to favour sludge flocculation [31,32]. The amide II band at 1534 cm^{-1} originates from the out-of-phase N–H bending and C–N stretching vibrations in –CO–NH of proteins. The small band at 1448 cm^{-1} is representative of the amide III band, which is assigned to the in-phase N–H bending and C–N stretch in proteins. Also, some of the bands attributed to proteins are possible with amino-sugars [27]. The band at 1376 cm^{-1} is ascribed to C=O symmetric stretching of $–COO^-$ groups [27]. The bands near 1220 cm^{-1} are associated with the C–O stretching of ether or alcohol and the bands near 1042 cm^{-1} are attributed to the asymmetrical stretching vibration of the C–O–C ester linkage of polysaccharides. Overall, these findings suggest that both saline and freshwater EPS possess similar functional groups such as carboxyl, hydroxyl and amino groups. Hence, they are amphoteric polyelectrolytes (PE) and can be anionic, cationic or zwitterionic, depending on pH.

Detailed quantification of the total protein (PN) and polysaccharide (PS) content of each EPS fraction is given in Fig. 3B. The freshwater biopolymer (PN and PS) fraction accounts for 82% w/w of the total extracted EPS (soluble and bound). The remaining 18% is composed of biopolymer building blocks, LMW acids and neutrals (see Fig. 4A and S2). Of the 82% freshwater biopolymeric fraction, the bound-EPS (57% w/w) contains at least twice the PN and PS content compared to the soluble-EPS (25% w/w). The saline MBR produced a higher percentage of biopolymers (soluble and bound: 91% w/w) than the freshwater EPS (82 % w/w), perhaps due to the protective response of bacteria to salt stress [12,33]. This increase was majorly expressed in the EPS fraction that ended up in the bulk liquid (Sal S-EPS: 34% w/w compared to 25% w/w in FW S-EPS), indicating that salinity had more influence on the soluble-EPS content than the bound fraction. A similar outcome was reported by Zhang *et al*. [34], who observed a positive correlation between salinity and EPS content in the bulk solution but no apparent correlation between salinity and (tightly) bound-EPS. De Temmerman *et al*. [35] also demonstrated that a 2 g/L NaCl shock had a more palpable effect on S-EPS content than B-EPS.

Fig. 3B further reveals a higher fraction of PN than PS in the four EPS fractions (freshwater soluble-EPS, freshwater bound- EPS, saline soluble-EPS, saline bound-EPS), which is consistent with several studies [21,23,30]. This can be related to higher PN production at such a relatively long SRT. Nielsen *et al*. [36] reported that with an increasing biofilm age, the relative PN content of the biofilm in a biofilter also increased, most likely due to preferential hydrolysis of other fractions such as PS.

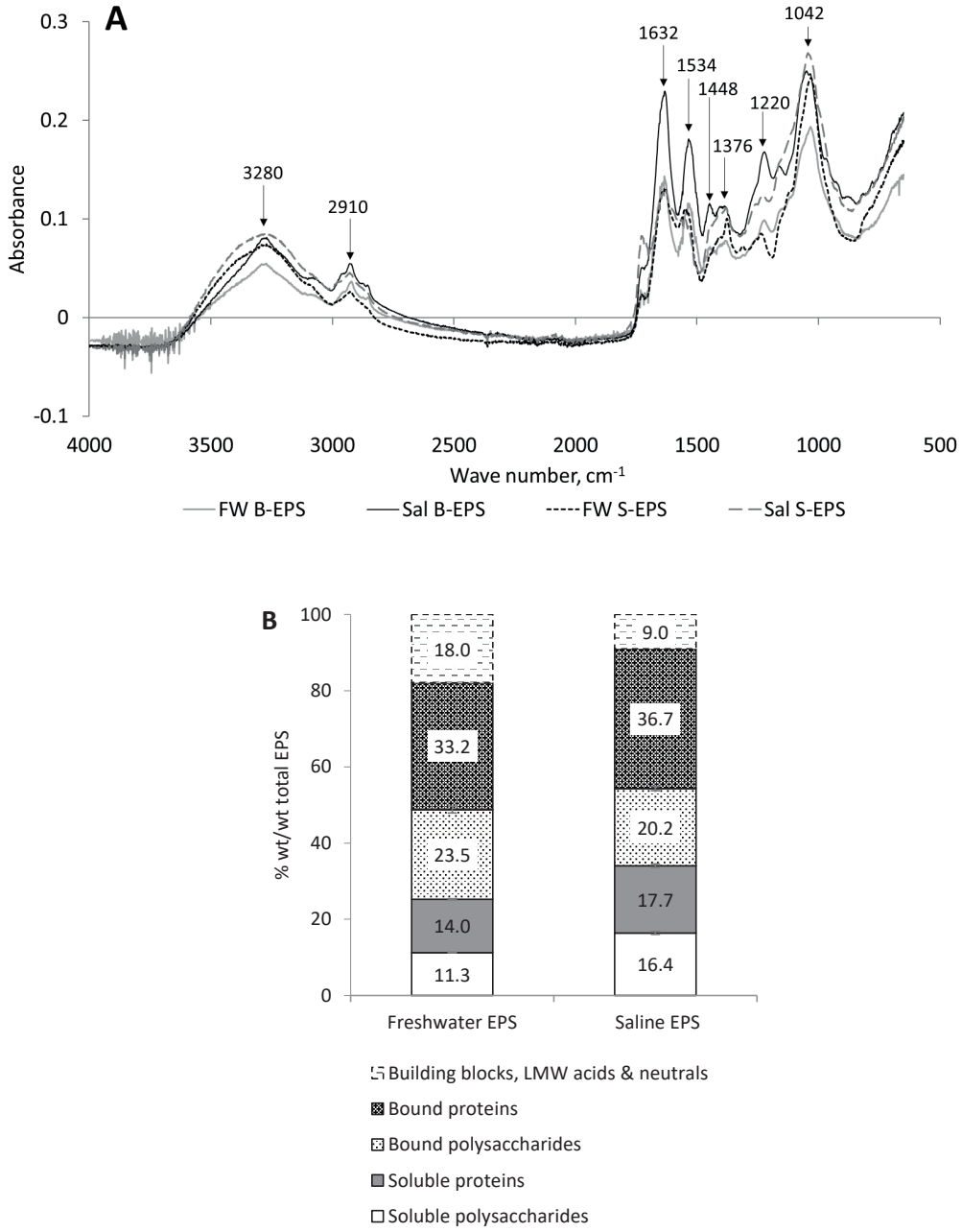

Fig. 3. EPS functionality and composition. (**A**) FTIR spectra of the extracted EPS fractions: freshwater bound-EPS (FW B-EPS), saline bound-EPS (Sal B-EPS), freshwater soluble-EPS (FW S-EPS), saline soluble-EPS (Sal S-EPS). (**B**) Polysaccharide and protein content of freshwater and saline EPS fractions. The fraction of building blocks, LMW acids and neutrals was estimated as closure of EPS content based on LC-OCD results.

3.4. EPS chemical fractions, molecular weight, and charge density

3.4.1. EPS fractions

From the LC-OCD-OND analysis (Fig. 4A), four distinct EPS fractions were observed and quantified based on MW: biopolymers (polysaccharides and proteins, or their combination), biopolymer building blocks, low molecular weight (LMW) neutrals (such as alcohols, aldehydes, ketones) and LMW acids (e.g., monoprotic organic acids). Humic substances were absent in the EPS samples since they were not in the synthetic wastewater. As seen in Fig. 4A, the biopolymer fraction of the FW B-EPS and Sal B-EPS represented 80.9 and 85.1 % DOC, respectively; while the building blocks, LMW neutrals and acids corresponded to 6.6/4.1, 10.8/9.4 and 1.4/1.4 % of total DOC. In comparison to the bound EPS, soluble EPS fractions showed lower biopolymer fractions (FW S-EPS: 50%, Sal S-EPS: 55.7%) and higher fractions of building blocks (FW S-EPS: 36.4%, Sal S-EPS: 35.1%). A possible explanation is that the centrifugation extraction process sheared off low MW biopolymer fractions (< 100 kDa).

The essential polymer properties from the viewpoint of flocculation are the molecular weight (MW), and in the case of polyelectrolytes, the charge density (CD) [37].

3.4.2. Molecular weight (MW) distribution

Fig. 4B and 4C show the broad MW distribution of EPS biopolymer fractions. Surprisingly, a similar trend was observed for the FW S-EPS and Sal S-EPS; and for the FW B-EPS and Sal B-EPS. However, their concentrations differ: in all the MW fractions, higher biopolymer concentrations were found in the Sal S-EPS (DOC: 154.6 mg/g EPS, DON: 11.8 mg/g EPS) than the FW S-EPS (DOC: 52.1 mg/g EPS, DON: 5.6 mg/g EPS). A different trend was noticed for bound EPS concentrations: at higher MW fractions (> 2000 – 1000 kDa), concentrations of FW B-EPS (DOC: 19.4 mg/g EPS, DON: 2.9 mg/g EPS) were slightly higher than Sal B-EPS (DOC: 13.5 mg/g EPS, DON: 1.7 mg/g EPS); but at lower MW fractions (500 – <10 kDa), the reverse was the case (Sal B-EPS – DOC: 102.3 mg/g EPS, DON: 20.9 mg/g EPS; FW B-EPS – DOC: 72.7 mg/g EPS, DON: 8.2 mg/g EPS) see Fig. S2.

These findings show that salinity does not influence the MW distribution of wastewater-produced EPS but does play a role in the concentration. The Sal-MBR had a 66% higher concentration of soluble biopolymer DOC and 29% higher bound biopolymer DOC concentration than the corresponding FW fractions. Likewise, the DON concentration (originated from EPS-proteins and amino sugars) [38] of the Sal-EPS were also higher in both the soluble (53%) and bound (50%) EPS than their corresponding FW-EPS. These results confirm that microorganisms under saline conditions produce higher concentrations of EPS polysaccharides and proteins [39].

Furthermore, compared to the bound-EPS, soluble-EPS (FW and Sal) had higher biopolymer concentrations of the highest MW fraction (> 2000 kDa). A likely explanation for this is the occurrence of polymer-polymer interactions in the bulk liquid. From the model by Tielen *et al*. [40], there is a possible electrostatic interaction between the positively charged amino acid chain of proteins and the negatively charged carboxyl groups of polysaccharides. Although this model was applied for biofilms, a similar mechanism has been reported for MBRs [41].

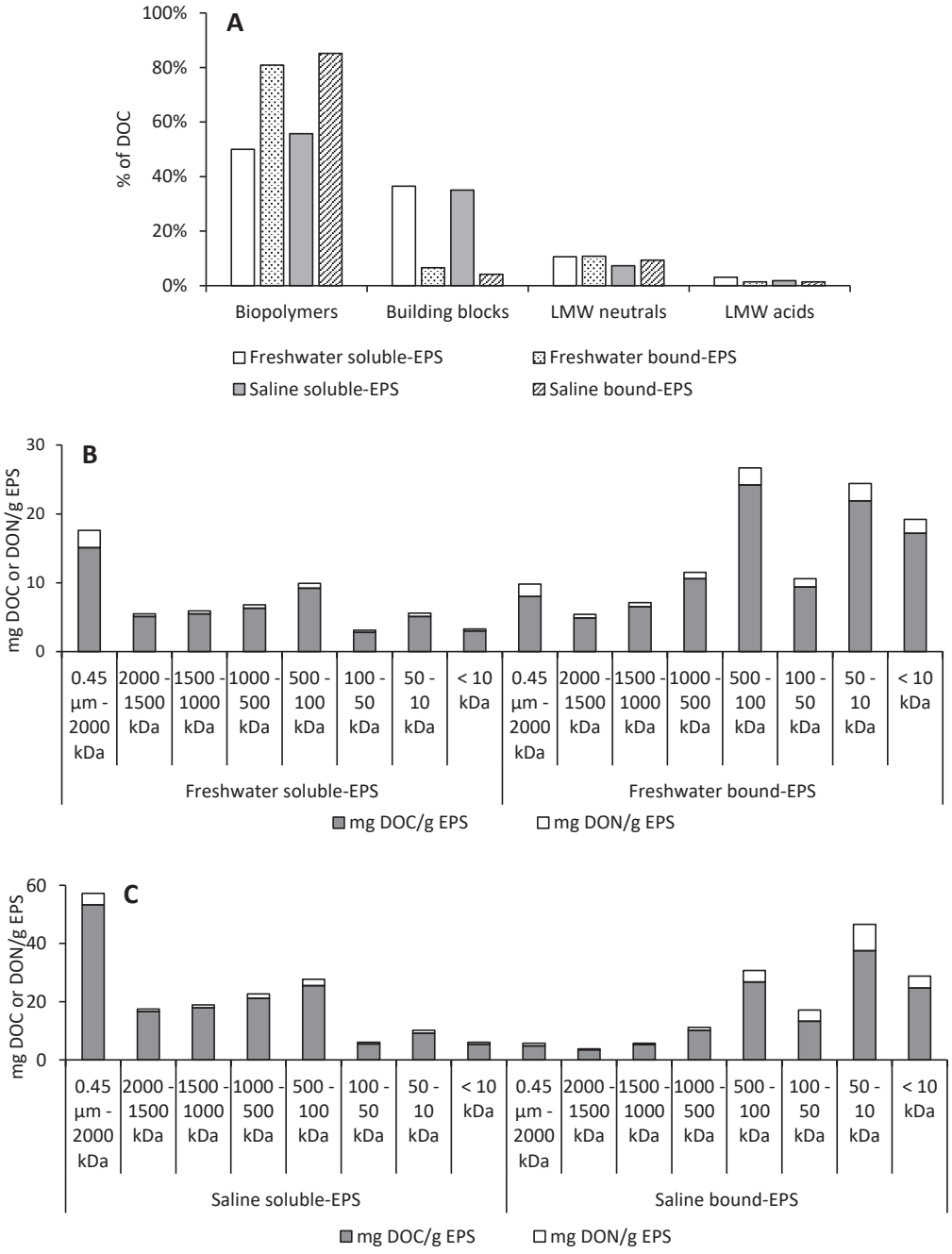

Fig. 4. (**A**) Organic carbon (OC) fractions of extracted freshwater and saline EPS samples. The molecular weight distribution of soluble and bound EPS from freshwater (**B**), and saline (**C**) bioreactors. DOC: dissolved organic carbon, DON: dissolved organic nitrogen.

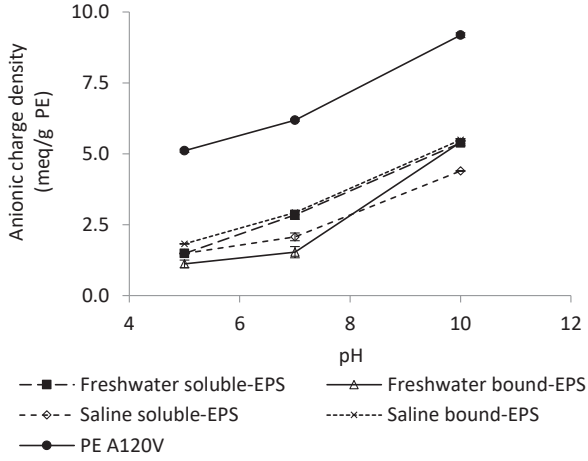

Fig. 5. Anionic charge densities of extracted EPS fractions and commercial anionic polyacrylamide (PE A120V) as a function of pH.

3.4.3. Charge density (CD)

EPS possess surface charge due to the presence of charged functional groups with counter ions (Fig. S3). Fig. 5 shows the CDs of the four EPS fractions and synthetic PE A120V at the initial pH of each sample solution (~5), neutral pH (7) and alkaline pH (10). They all showed a similar trend of increasing anionic CD with rising pH. Under acidic conditions, the carboxyl and amino groups are protonated (–COOH, $–NH_3^+$), decreasing the net anionic CD. At an elevated pH of 10, both groups occur in the deprotonated form ($–COO^-$, $–NH_2$), resulting in a higher anionic CD.

The four EPS samples showed similar anionic CDs at each pH: 1.1 - 1.8 meq/g at pH ~5, 1.5 - 2.9 meq/g at neutral pH and 4.4 - 5.5 meq/g at pH 10. The EPS CD values at neutrality are within the range reported by Mikkelsen [42], (1 - 3 meq/g) for most EPS. However, these values are lower than the CD of PE A120V (5.1, 6.2 and 9.2 meq/g at pH 5, 7 and 10 respectively).

3.5. EPS flocculation performances and the effect of MW and CD

The high molecular weight of these EPS, coupled with their surface charge, make them potential polyelectrolytes to flocculate suspended and colloidal particles (e.g., kaolin clay).

The flocculation performances of the four EPS fractions and synthetic PE A120V toward saline kaolin suspension is given in Fig. 6A. The synthetic PE A120V showed maximum flocculation efficiency (98.6 ± 0.1%) at a concentration of 0.1 mg/g kaolin (corresponding to 0.5 mg/L kaolin suspension), but a reduced efficiency at higher concentrations. This was probably caused by the restabilisation of kaolin particles at higher concentrations [4,27]. On the other hand, no conspicuous optimum dosage was observed for the EPS fractions. This is likely due to the lower CD of EPS compared to the commercial PE. The advantage is that excess EPS dosage will have little or no effect on the flocculation performance.

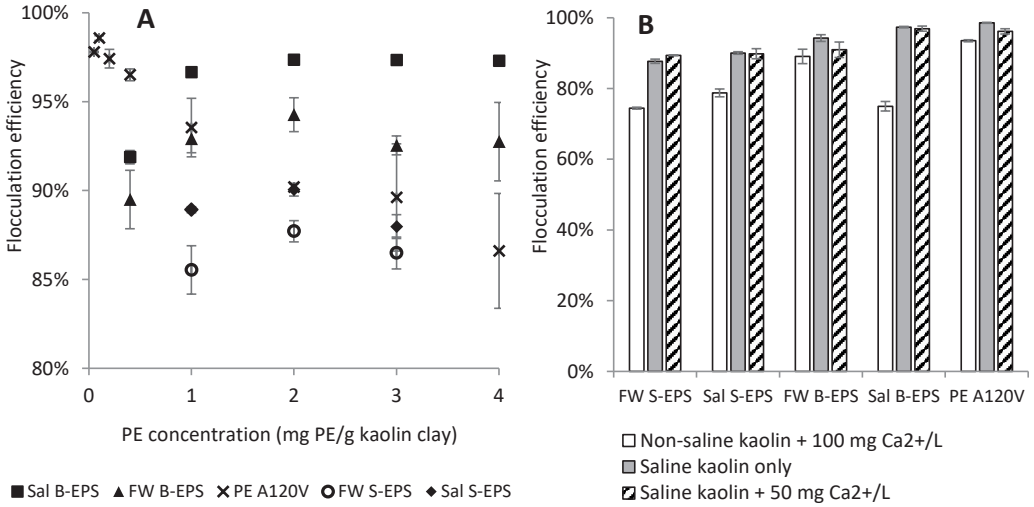

Fig. 6. Flocculation efficiencies of extracted EPS fractions and a commercial anionic polyacrylamide (PE A120V) at (**A**) different polymer concentrations on saline kaolin suspension (5 g kaolin/L and 11.7g Na^{+}/L), (**B**) optimum polymer dosage on saline and non-saline kaolin suspension (5 g kaolin/L), with and without Ca^{2+} addition as a coagulant.

At a concentration of 2 mg/g kaolin (corresponding to 10 mg/L kaolin suspension), each EPS fraction achieved maximum performance in the tested concentrations. Of the four EPS fractions, the Sal B-EPS performed best for flocculating saline kaolin suspension, with an efficiency of 97.4 ± 0.2 %, a value close to the performance of the commercial PE. The FW B-EPS, Sal S-EPS, and FW S-EPS had efficiencies of 94.3 ± 1.0 %, 90.0 ± 0.4 % and 87.7 ± 0.7 %, respectively. The EPS dosage employed in our study is similar to that reported by Liu *et al*. [17] (maximum flocculation efficiency: 95.3% at pH 6.5) but lower than reports from some other authors (Sam *et al*. [28] – 400 mg EPS/g kaolin, Cosa *et al*. [43] – 50 mg/g kaolin, Li *et al*. [44] – 10 mg/g kaolin), who all used bioflocculants from isolated bacterial strains. This suggests that mixed-culture EPS could be more effective flocculants than certain pure-cultured EPS [45], although the mechanistic reason still needs to be further investigated.

Using the best-tested dosage of each flocculant, further addition of divalent cation (50 mg Ca^{2+}/L) to the saline kaolin suspension had little or no effect on the flocculation performances (Fig. 6B). The slightly lower flocculation efficiencies noticed for some flocculants (FW B-EPS and PE A120V) when compared to the non-Ca dosed saline kaolin suspension was most likely caused by charge reversal because of the cationic charge overdose, which probably led to restabilisation of the clay particles. Lee *et al*. [46] reported the dual effect of divalent cation dosage, which either causes particle-binding cationic bridging that leads to flocculation, or polymer-binding cationic bridging that leads to stabilisation and a subsequent reduced turbidity removal. The latter was perhaps dominant for FW B-EPS and PE A120V. For the PE A120V, stabilisation is possible due to the high CD (6.2 meq/g at neutral pH). At such high ionic strength where the electrical double layer is completely suppressed

(see Section 3.6), the addition of (excess) divalent cation can lead to some of the polymer chains forming bridges with one another (instead of bridging with the particles) due to the many adsorption sites. For the FW B-EPS, it is possible the low and medium MW fractions first form bridges between the kaolin particles, and instead of the longer chains to aggregate into larger flocs, they can bind with each other with the aid of the added Ca^{2+} [47].

Flocculation under non-saline conditions was also performed using 100 mg Ca^{2+}/L (to mimic Ca^{2+} concentration in natural waters) as a coagulant (Fig. 6B). 50 mg Ca^{2+}/L was initially tested but had a poor flocculation performance (< 50%), possibly concentration was too low to effectively reduce the electrostatic repulsion between the negatively charged kaolin particles. At the tested 100 mg Ca^{2+}/L coagulant dosage, the commercial flocculant showed the highest flocculation efficiency (93.5 ± 0.3 %) for the non-saline kaolin suspension, followed by the FW B-EPS with an efficiency of 89.1 ± 2.0 %. The other EPS fractions achieved more than 74% flocculation performance.

We hypothesized that EPS produced under saline conditions would perform best under saline flocculation conditions and freshwater EPS would perhaps be more efficient during freshwater flocculation. Indeed, of the EPS fractions, the bound-EPS produced under saline condition (Sal B-EPS) showed the best flocculation of kaolin particles in the saline environment and the bound-EPS produced under freshwater condition (FW B-EPS) showed the best flocculation of particles in the non-saline environment.

A higher EPS dosage was required to achieve a flocculation performance comparable to the synthetic PE because of the higher MW and charge density of the synthetic PE. It is well known that the higher the MW, the longer the polymer chain and the more adsorption sites for flocculation. Likewise, a higher charge density implies more repulsion between charged segments and an expansion of the polymer chain, although an optimum CD is necessary for effective flocculation [4]. However, the advantage of a lower CD (as found in EPS compared to PE A120V) is the reduced restabilisation effect at excess polymer dosage (Fig. 6A). This explains why EPS had a wider dosage range for an effective flocculation performance.

Regarding the four EPS fractions and their flocculation performances, the soluble-EPS, due to their more abundant higher MW fractions, were expected to show higher flocculation efficiencies than the corresponding bound-EPS. However, the results showed otherwise. Perhaps the flocculation performances of the soluble-EPS were hampered by the high fraction of building blocks (Fig. 4A). Nonetheless, this study indicates that mixed EPS with little or no building blocks, and having high (> 1000 kDa), medium (1000 - 100 kDa) and low (< 100 kDa) MW [4], as found in the bound-EPS, are potential and promising flocculating agents.

3.6. Proposed flocculation mechanisms

In both the saline and non-saline flocculation conditions, the addition of cations to the suspension reduces the electrostatic repulsion between the kaolinite particles due to the compressed double layer (according to the DLVO theory) [19]. This effect is much stronger in the saline kaolin suspension with higher ionic strength (I = 0.513 M) than with the non-saline suspension coagulated with Ca^{2+}

(*I* = 0.008 M). It has been reported that an ionic strength of at least 0.5 M is needed to achieve complete suppression of the electrostatic repulsions [48,49]. Hence, H-bonds can be easily formed (in the saline kaolin suspension) between the amide group (of EPS-protein) or hydroxyl group (of EPS-polysaccharide) and surface hydroxyl groups of kaolinite such as silanol (Si–OH) and aluminol (Al–OH), thus forming EPS polymer bridges between the kaolin particles – Fig. 7A. A similar flocculation mechanism (polymer bridging by H-bonding) has been reported for anionic polyacrylamide for saline mine tailings and kaolinite particles [4,50]. Ji *et al*. [50] further described a more condensed polymer conformation and enhanced adsorption state due to the high salinity medium. Thus, the reduced electrical repulsion among the particles and the enhanced adsorption of the biopolymers on particle surfaces are the likely reasons for the high flocculation efficiencies of the saline kaolin suspension [50].

In the non-saline kaolin suspension coagulated with 100 mg/L Ca^{2+}, the ionic strength (0.008 M) was perhaps too low to bring about a significant suppression of the DLVO-type electrostatic repulsion for subsequent H-bonding. Hence, the divalent cationic bridging (DCB) mechanism [19] (rather than H-bonding) is more likely to control the flocculation process. Despite electrostatic repulsion, Ca^{2+} can bridge between anionic groups on the polymer and negative sites on the kaolin surface [4] (Fig. 7B).

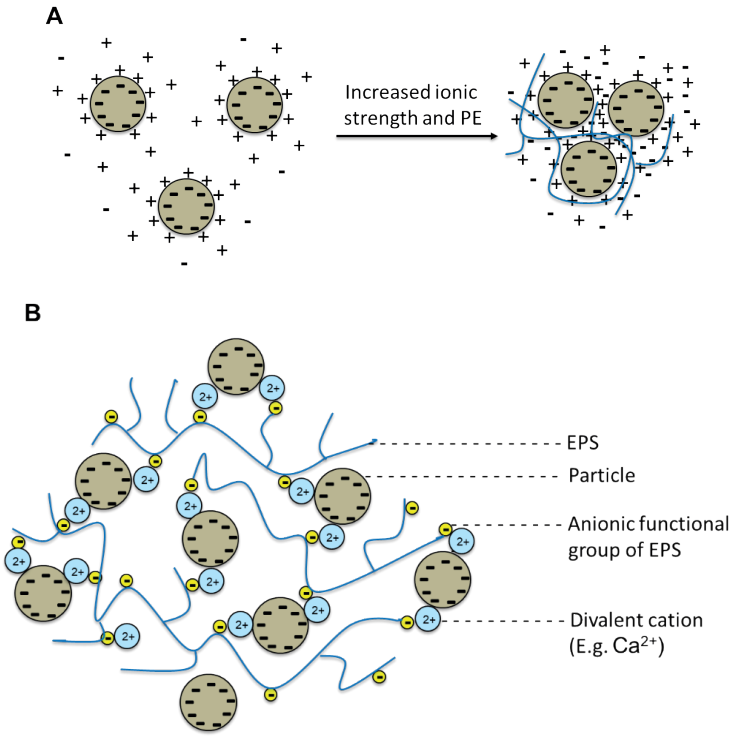

Fig. 7. Schematic illustration of the proposed flocculation mechanisms of EPS in (**A**) saline kaolin suspension (hydrogen bonding after the suppression of the double layer at high ionic strength), (**B**) non-saline kaolin suspension coagulated with 100 mg/L Ca^{2+} (divalent cationic bridging mechanism). Figures not drawn to scale.

4. Conclusions

This work demonstrates the combination of biological wastewater treatment with the production of effective natural flocculants (microbial exopolymers) from both fresh and saline wastewater. Although the extracted soluble and bound EPS fractions had a similar composition (mainly polysaccharides and proteins), their molecular weights (distribution) and charge densities differed. The four EPS fractions had a mixture of high (> 1000 kDa), medium (100 - 1000 kDa) and low (< 100 kDa) molecular weight fractions, but in varying concentrations. Saline-EPS produced higher concentrations of biopolymers than the corresponding freshwater-EPS fraction. The molecular weight distribution of the four EPS fractions was less affected by salinity – both the freshwater and saline soluble EPS had a similar distribution, and the same for the bound fractions. Moreover, the lower charge density of EPS, compared to the anionic polyacrylamide (PE A120V), provided an extensive dosage range for effective flocculation with little or no problem of particle restabilisation at higher dosages. Since EPS recoveries in this study were low (5.8 – 7.6 % influent COD), ongoing research is focused on simple strategies to increase recovery for economic viability. Moreover, the flocculation mechanism of such mixed-EPS needs to be further investigated.

Acknowledgements

This work was performed in the cooperation framework of Wetsus, European Centre of excellence for sustainable water technology (www.wetsus.nl). Wetsus is co-funded by the Dutch Ministry of Economic Affairs and Ministry of Infrastructure and Environment, the European Union Regional Development Fund, the Province of Fryslân and the Northern Netherlands Provinces. This work has also received funding from the European Union's Horizon 2020 research and innovation programme under the Marie Skłodowska-Curie [grant agreement No. 665874]. The authors would like to thank Kemira for providing the anionic polyacrylamide used in this study; Wetterskip Leeuwarden and WLN Netherlands for providing the inocula; and the participants of the research theme 'Natural flocculants' for the fruitful discussions and financial support.

Supplementary information of Chapter 2

S1. Chemical analysis of kaolinite, as provided by Sigma-Aldrich.

Compound	wt%
SiO_2	50.4
Al_2O_3	34.3
K_2O	1.9
Fe_2O_3	0.5
TiO_2	0.4
Na_2O	0.2

Loss on ignition: 11.5%

S2. LC-OCD-OND chromatograms of EPS **(A)**.

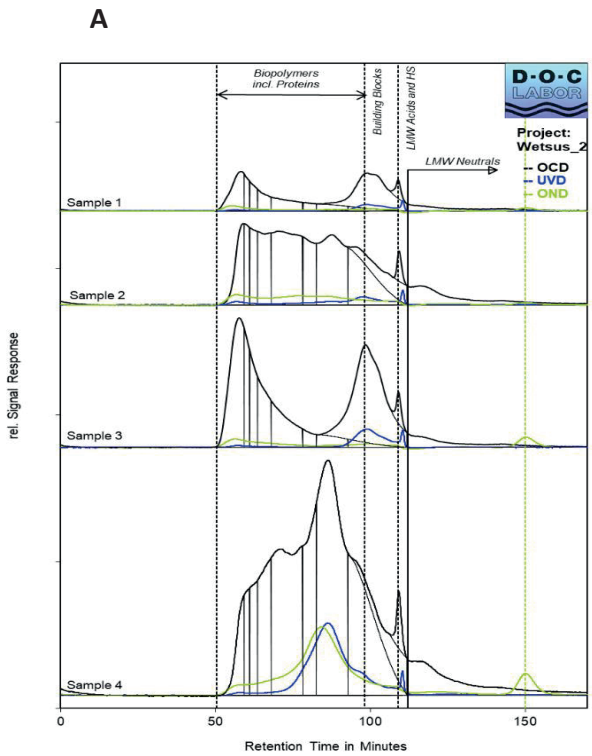

Sample 1: Freshwater soluble-EPS

Sample 2: Freshwater bound-EPS

Sample 3: Saline soluble-EPS

Sample 4: Saline bound-EPS

S2 (B). Dissolved organic carbon and nitrogen concentrations of EPS fractions by LC-OCD-OND.

EPS	EPS fraction	Biopolymer MW fraction	mg DOC/g EPS	mg DON/g EPS
FW S-EPS	Biopolymer	0.45 µm - 2000 kDa	15.1	2.5
		2000 - 1500 kDa	5.1	0.4
		1500 - 1000 kDa	5.5	0.4
		1000 - 500 kDa	6.3	0.5
		500 - 100 kDa	9.2	0.7
		100 - 50 kDa	2.8	0.3
		50 - 10 kDa	5.1	0.5
		< 10 kDa	3.0	0.3
	Building blocks		37.9	-
	LMW neutrals		11.0	-
	LMW acids		3.2	-
FW B-EPS	Biopolymer	0.45 µm - 2000 kDa	8.0	1.8
		2000 - 1500 kDa	4.9	0.5
		1500 - 1000 kDa	6.5	0.6
		1000 - 500 kDa	10.6	0.9
		500 - 100 kDa	24.2	2.5
		100 - 50 kDa	9.4	1.2
		50 - 10 kDa	21.9	2.5
		< 10 kDa	17.2	2.0
	Building blocks		8.4	-
	LMW neutrals		13.8	-
	LMW acids		1.8	-
Sal S-EPS	Biopolymer	0.45 µm - 2000 kDa	53.3	3.9
		2000 - 1500 kDa	16.6	0.9
		1500 - 1000 kDa	17.9	1.0
		1000 - 500 kDa	21.2	1.5
		500 - 100 kDa	25.5	2.2
		100 - 50 kDa	5.5	0.6
		50 - 10 kDa	9.2	1.0
		< 10 kDa	5.4	0.7
	Building blocks		97.2	-
	LMW neutrals		20.3	-
	LMW acids		5.0	-
Sal B-EPS	Biopolymer	0.45 µm - 2000 kDa	4.8	0.9
		2000 - 1500 kDa	3.5	0.3
		1500 - 1000 kDa	5.2	0.5
		1000 - 500 kDa	10.2	1.0
		500 - 100 kDa	26.8	3.9
		100 - 50 kDa	13.3	3.8
		50 - 10 kDa	37.5	9.1
		< 10 kDa	24.7	4.1

S2 (B). (*continued*)

EPS	EPS fraction	Biopolymer MW fraction	mg DOC/g EPS	mg DON/g EPS
Sal B-EPS	Building blocks		6.1	-
	LMW neutrals		13.8	-
	LMW acids		2.0	-

S3. Cation analysis of EPS (mean ± standard deviation, n = 2). PE: Polyelectrolyte.

Cation	FW S-EPS	FW B-EPS	Sal S-EPS	Sal B-EPS	PE A120V
Ammonium (mg/g PE)	1.4 ± 0.0	6.9 ± 0.0	7.1 ± 0.1	19.0 ± 0.7	< 1.0
Sodium (mg/g PE)	3.9 ± 0.2	13.9 ± 0.1	21.1 ± 1.1	21.0 ± 0.3	70.8 ± 0.8
Potassium (mg/g PE)	2.1 ± 0.0	6.2 ± 0.2	6.6 ± 0.2	5.6 ± 0.2	< 1.0
Calcium (mg/g PE)	11.9 ± 0.4	1.9 ± 0.1	17.5 ± 0.4	3.2 ± 0.0	< 1.0
Magnesium (mg/g PE)	2.3 ± 0.0	< 1.0	3.7 ± 0.0	< 1.0	< 1.0

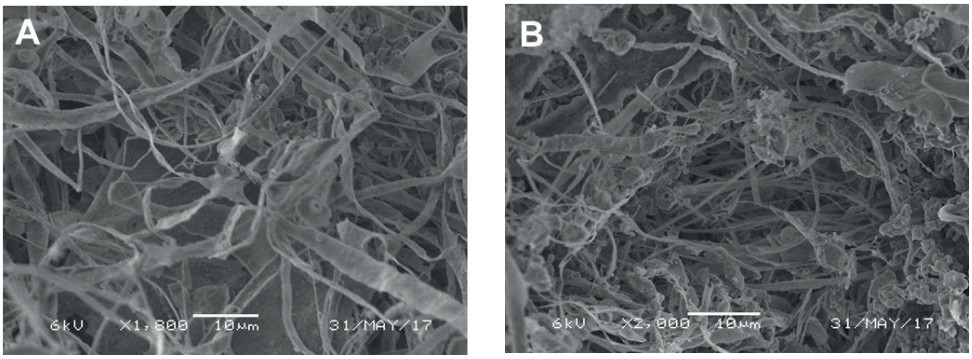

S4. SEM micrograph of bound-EPS produced from (**A**) fresh and (**B**) saline wastewater.

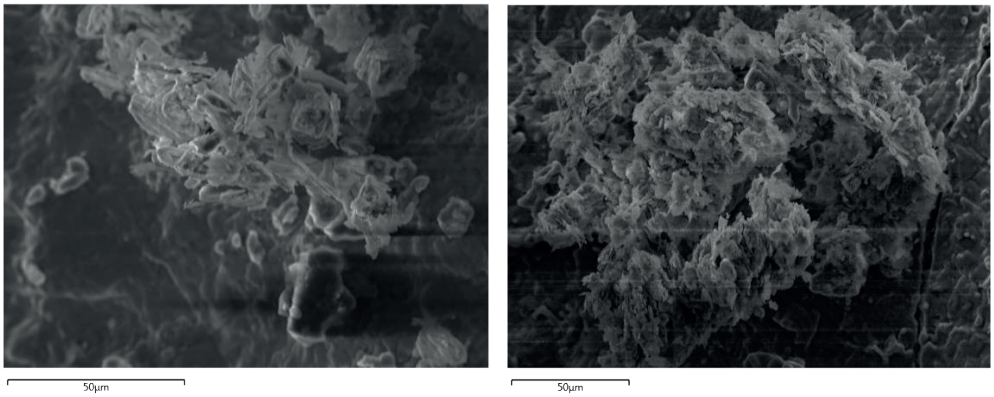

A. Saline kaolin suspension only **B.** Saline kaolin suspension + FW B-EPS

S5. SEM micrograph of non-flocculated (**A**) and flocculated (**B**) particles.

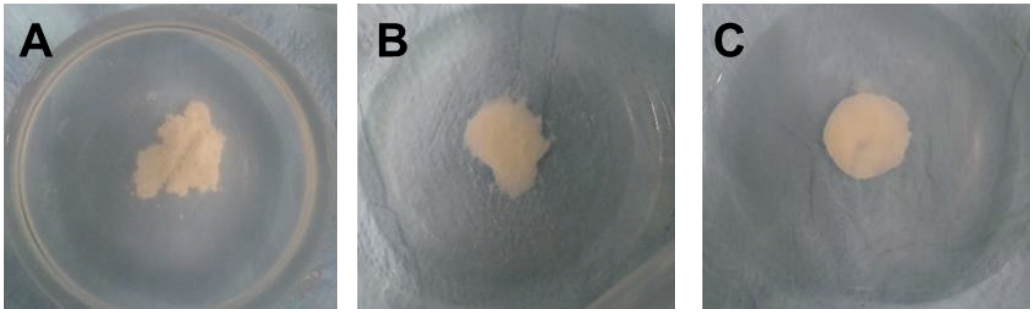

S6. Images of settled flocs formed by (**A**) anionic acrylamide, (**B**) FW B-EPS in non-saline kaolin suspension coagulated with 100 mg /L Ca^{2+}, (**C**) FW B-EPS in saline kaolin suspension without additional Ca^{2+}.

References

[1] O. Lefebvre, R. Moletta, Treatment of organic pollution in industrial saline wastewater: A literature review, Water Res. 40 (2006) 3671–3682. doi:10.1016/j.watres.2006.08.027.

[2] C.S. Lee, J. Robinson, M.F. Chong, A review on application of flocculants in wastewater treatment, Process Saf. Environ. Prot. 92 (2014) 489–508. doi:10.1016/j.psep.2014.04.010.

[3] S.C. Bondy, Low levels of aluminum can lead to behavioral and morphological changes associated with Alzheimer's disease and age-related neurodegeneration, Neurotoxicology. 52 (2016) 222–229. doi:10.1016/j.neuro.2015.12.002.

[4] B. Bolto, J. Gregory, Organic polyelectrolytes in water treatment, Water Res. 41 (2007) 2301–2324. doi:10.1016/j.watres.2007.03.012.

[5] A. Mishra, M. Bajpai, Flocculation behaviour of model textile wastewater treated with a food grade polysaccharide, J. Hazard. Mater. 118 (2005) 213–217. doi:10.1016/j.jhazmat.2004.11.003.

[6] T. Suopajärvi, H. Liimatainen, O. Hormi, J. Niinimäki, Coagulation-flocculation treatment of municipal wastewater based on anionized nanocelluloses, Chem. Eng. J. 231 (2013) 59–67. doi:10.1016/j.cej.2013.07.010.

[7] F. Renault, B. Sancey, J. Charles, N. Morin-Crini, P.M. Badot, P. Winterton, G. Crini, Chitosan flocculation of cardboard-mill secondary biological wastewater, Chem. Eng. J. 155 (2009) 775–783. doi:10.1016/j.cej.2009.09.023.

[8] C. Wu, Y. Wang, B. Gao, Y. Zhao, Q. Yue, Coagulation performance and floc characteristics of aluminum sulfate using sodium alginate as coagulant aid for synthetic dying wastewater treatment, Sep. Purif. Technol. 95 (2012) 180–187. doi:10.1016/j.seppur.2012.05.009.

[9] H. Salehizadeh, N. Yan, Recent advances in extracellular biopolymer flocculants, Biotechnol. Adv. 32 (2014) 1506–1522. doi:10.1016/j.biotechadv.2014.10.004.

[10] T.T. More, J.S.S. Yadav, S. Yan, R.D. Tyagi, R.Y. Surampalli, Extracellular polymeric substances of bacteria and their potential environmental applications, J. Environ. Manage. 144 (2014) 1–25. doi:10.1016/j.jenvman.2014.05.010.

[11] H.-C. Flemming, J. Wingender, The biofilm matrix, Nat. Publ. Gr. 8 (2010) 623–633. doi:10.1038/nrmicro2415.

[12] L. Zhao, Z. She, C. Jin, S. Yang, L. Guo, Y. Zhao, M. Gao, Characteristics of extracellular polymeric substances from sludge and biofilm in a simultaneous nitrification and denitrification system under high salinity stress, Bioprocess Biosyst. Eng. 39 (2016) 1375–1389. doi:10.1007/s00449-016-1613-x.

[13] S. Malamis, A. Andreadakis, Fractionation of proteins and carbohydrates of extracellular polymeric substances in a membrane bioreactor system, Bioresour. Technol. 100 (2009)

3350–3357. doi:10.1016/j.biortech.2009.01.053.

[14] S. Bala Subramanian, S. Yan, R.D. Tyagi, R.Y. Surampalli, Extracellular polymeric substances (EPS) producing bacterial strains of municipal wastewater sludge: Isolation, molecular identification, EPS characterization and performance for sludge settling and dewatering, Water Res. 44 (2010) 2253–2266. doi:10.1016/j.watres.2009.12.046.

[15] S.A. Zaki, M.F. Elkady, S. Farag, D. Abd-El-Haleem, Characterization and flocculation properties of a carbohydrate bioflocculant from a newly isolated *Bacillus velezensis* 40B, J. Environ. Biol. 34 (2013) 51–58.

[16] G. Sathiyanarayanan, G. Seghal Kiran, J. Selvin, Synthesis of silver nanoparticles by polysaccharide bioflocculant produced from marine *Bacillus subtilis* MSBN17, Colloids Surfaces B Biointerfaces. 102 (2013) 13–20. doi:10.1016/j.colsurfb.2012.07.032.

[17] C. Liu, K. Wang, J.H. Jiang, W.J. Liu, J.Y. Wang, A novel bioflocculant produced by a salt-tolerant, alkaliphilic and biofilm-forming strain *Bacillus agaradhaerens* C9 and its application in harvesting Chlorella minutissima UTEX2341, Biochem. Eng. J. 93 (2015) 166–172. doi:10.1016/j.bej.2014.10.006.

[18] W. Li, M. Mutuvulla, X. Chen, M. Jiang, M. Dong, Isolation and identification of high viscosity-producing lactic acid bacteria from a traditional fermented milk in Xinjiang and its role in fermentation process, Eur. Food Res. Technol. 235 (2012) 497–505. doi:10.1007/s00217-012-1779-7.

[19] D.C. Sobeck, M.J. Higgins, Examination of three theories for mechanisms of cation-induced bioflocculation, Water Res. 36 (2002) 527–538. doi:10.1016/S0043-1354(01)00254-8.

[20] M.S. Nasser, A.E. James, The effect of polyacrylamide charge density and molecular weight on the flocculation and sedimentation behaviour of kaolinite suspensions, Sep. Purif. Technol. 52 (2006) 241–252. doi:10.1016/j.seppur.2006.04.005.

[21] L. Faust, H. Temmink, A. Zwijnenburg, A.J.B. Kemperman, H.H.M. Rijnaarts, High loaded MBRs for organic matter recovery from sewage: effect of solids retention time on bioflocculation and on the role of extracellular polymers., Water Res. 56 (2014) 258–66. doi:10.1016/j.watres.2014.03.006.

[22] I. Akanyeti, H. Temmink, M. Remy, A. Zwijnenburg, Feasibility of bioflocculation in a high-loaded membrane bioreactor for improved energy recovery from sewage, Water Sci. Technol. 61 (2010) 1433–1439. doi:10.2166/wst.2010.032.

[23] B. Frølund, R. Palmgren, K. Keiding, P.H. Nielsen, Extraction of extracellular polymers from activated sludge using a cation exchange resin, Water Res. 30 (1996) 1749–1758. doi:10.1016/0043-1354(95)00323-1.

[24] Water Environment, APHA, Standard Methods for the Examination of Water and Wastewater Part 1000 Standard Methods for the Examination of Water and Wastewater, 1999.

[25] M. DuBois, K. a. Gilles, J.K. Hamilton, P. a. Rebers, F. Smith, Colorimetric method for determination of sugars and related substances, Anal. Chem. 28 (1956) 350–356. doi:10.1021/ac60111a017.

[26] W.F. Tan, W. Norde, L.K. Koopal, Humic substance charge determination by titration with a flexible cationic polyelectrolyte, Geochim. Cosmochim. Acta. 75 (2011) 5749–5761. doi:10.1016/j.gca.2011.07.015.

[27] S.J. Yuan, M. Sun, G.P. Sheng, Y. Li, W.W. Li, R.S. Yao, H.Q. Yu, Identification of key constituents and structure of the extracellular polymeric substances excreted by bacillus megaterium TF10 for their flocculation capacity, Environ. Sci. Technol. 45 (2011) 1152–1157. doi:10.1021/es1030905.

[28] S. Sam, F. Kucukasik, O. Yenigun, B. Nicolaus, E.T. Oner, M.A. Yukselen, Flocculating performances of exopolysaccharides produced by a halophilic bacterial strain cultivated on agro-industrial waste, Bioresour. Technol. 102 (2011) 1788–1794. doi:10.1016/j.biortech.2010.09.020.

[29] G. Sheng, H. Yu, X. Li, Extracellular polymeric substances (EPS) of microbial aggregates in biological wastewater treatment systems: A review, Biotechnol. Adv. 28 (2010) 882–894. doi:10.1016/j.biotechadv.2010.08.001.

[30] L. Faust, H. Temmink, A. Zwijnenburg, A.J.B. Kemperman, H.H.M. Rijnaarts, Effect of dissolved oxygen concentration on the bioflocculation process in high loaded MBRs, Water Res. 66 (2014) 199–207. doi:10.1016/j.watres.2014.08.022.

[31] Z. Wang, M. Gao, Z. Wang, Z. She, Q. Chang, C. Sun, J. Zhang, Y. Ren, N. Yang, Effect of salinity on extracellular polymeric substances of activated sludge from an anoxic-aerobic sequencing batch reactor, Chemosphere. 93 (2013) 2789–2795. doi:10.1016/j.chemosphere.2013.09.038.

[32] A. Barth, Infrared spectroscopy of proteins, Biochim. Biophys. Acta - Bioenerg. 1767 (2007) 1073–1101. doi:10.1016/j.bbabio.2007.06.004.

[33] E. Reid, X. Liu, S.J. Judd, Effect of high salinity on activated sludge characteristics and membrane permeability in an immersed membrane bioreactor, J. Memb. Sci. 283 (2006) 164–171. doi:10.1016/j.memsci.2006.06.021.

[34] Z.-J. Zhang, S.-H. Chen, S.-M. Wang, H.-Y. Luo, Characterization of extracellular polymeric substances from biofilm in the process of starting-up a partial nitrification process under salt stress, Appl. Microbiol. Biotechnol. 89 (2011) 1563–1571. doi:10.1007/s00253-010-2947-y.

[35] L. De Temmerman, T. Maere, H. Temmink, A. Zwijnenburg, I. Nopens, Salt stress in a membrane bioreactor: Dynamics of sludge properties, membrane fouling and remediation through powdered activated carbon dosing, Water Res. 63 (2014) 112–124. doi:10.1016/j.watres.2014.06.017.

[36] P.H. Nielsen, A. Jahn, R. Palmgren, Conceptual model for production and composition of exopolymers in biofilms, Water Sci. Technol. 36 (1997) 11–19. doi:10.1016/S0273-1223(97)00318-1.

[37] J. Gregory, S. Barany, Adsorption and flocculation by polymers and polymer mixtures, Adv. Colloid Interface Sci. 169 (2011) 1–12. doi:10.1016/j.cis.2011.06.004.

[38] S.A. Huber, A. Balz, M. Abert, W. Pronk, Characterisation of aquatic humic and non-humic matter with size-exclusion chromatography - organic carbon detection - organic nitrogen detection (LC-OCD-OND), Water Res. 45 (2011) 879–885. doi:10.1016/j.watres.2010.09.023.

[39] M.A.H. Johir, S. Vigneswaran, J. Kandasamy, R. BenAim, A. Grasmick, Effect of salt concentration on membrane bioreactor (MBR) performances: Detailed organic characterization, Desalination. 322 (2013) 13–20. doi:10.1016/j.desal.2013.04.025.

[40] P. Tielen, H. Kuhn, F. Rosenau, K.-E. Jaeger, H.-C. Flemming, J. Wingender, Interaction between extracellular lipase LipA and the polysaccharide alginate of Pseudomonas aeruginosa, BMC Microbiol. 13 (2013) 159. doi:10.1186/1471-2180-13-159.

[41] F. Neemann, S. Rosenberger, B. Jefferson, E.J. McAdam, Non-covalent protein-polysaccharide interactions and their influence on membrane fouling, J. Memb. Sci. 446 (2013) 310–317. doi:10.1016/j.memsci.2013.06.054.

[42] L.H. Mikkelsen, Applications and limitations of the colloid titration method for measuring activated sludge surface charges, Water Res. 37 (2003) 2458–2466. doi:10.1016/S0043-1354(03)00021-6.

[43] S. Cosa, A.M. Ugbenyen, L. V. Mabinya, K. Rumbold, A.I. Okoh, Characterization and flocculation efficiency of a bioflocculant produced by a marine Halobacillus, Environ. Technol. 34 (2013) 2671–2679. doi:10.1080/09593330.2013.786104.

[44] W.W. Li, W.Z. Zhou, Y.Z. Zhang, J. Wang, X.B. Zhu, Flocculation behavior and mechanism of an exopolysaccharide from the deep-sea psychrophilic bacterium *Pseudoalteromonas* sp. SM9913, Bioresour. Technol. 99 (2008) 6893–6899. doi:10.1016/j.biortech.2008.01.050.

[45] L. Wang, F. Ma, Y. Qu, D. Sun, A. Li, J. Guo, B. Yu, Characterization of a compound bioflocculant produced by mixed culture of Rhizobium radiobacter F2 and *Bacillus sphaeicus* F6, World J. Microbiol. Biotechnol. 27 (2011) 2559–2565. doi:10.1007/s11274-011-0726-2.

[46] B.J. Lee, M.A. Schlautman, E. Toorman, M. Fettweis, Competition between kaolinite flocculation and stabilization in divalent cation solutions dosed with anionic polyacrylamides, Water Res. 46 (2012) 5696–5706. doi:10.1016/j.watres.2012.07.056.

[47] A. Costine, J. Cox, S. Travaglini, A. Lubansky, P. Fawell, H. Misslitz, Variations in the molecular weight response of anionic polyacrylamides under different flocculation conditions, Chem. Eng. Sci. 176 (2018) 127–138. doi:10.1016/j.ces.2017.10.031.

[48] H.H.M. Rijnaarts, W. Norde, J. Lyklema, A.J.B. Zehnder, DLVO and steric contributions to bacterial deposition in media of different ionic strengths, Colloids Surfaces B Biointerfaces. 14 (1999) 179–195. doi:10.1016/S0927-7765(99)00035-1.

[49] M.R. Bohmer, O.A. Evers, J.M.H.M. Scheutjens, Weak Polyelectrolytes between Two Surfaces: Adsorption and Stabilization, Macromolecules. 23 (1990) 2288–2301.

[50] Y. Ji, Q. Lu, Q. Liu, H. Zeng, Effect of solution salinity on settling of mineral tailings by polymer flocculants, Colloids Surfaces A Physicochem. Eng. Asp. 430 (2013) 29–38. doi:10.1016/j.colsurfa.2013.04.006.

Chapter 3

Valorization of glycerol/ethanol-rich wastewater to bioflocculants: recovery, properties, and performance

A modified version of this Chapter has been published as:

V. Ajao, S. Millah, M.C. Gagliano, H. Bruning, H. Rijnaarts, H. Temmink, Valorization of glycerol/ethanol-rich wastewater to bioflocculants: recovery, properties, and performance, J. Hazard. Mater. 375 (2019) 273–280. doi:10.1016/j.jhazmat.2019.05.009.

Abstract

Microbial extracellular polymeric substances (EPS) were produced in two membrane bioreactors, each separately treating fresh and saline synthetic wastewater (consisting of glycerol and ethanol), with the purpose of applying them as sustainable bioflocculants. The reactors were operated under nitrogen-rich (COD/N ratios of 5 and 20) and limited (COD/N ratios of 60 and 100) conditions. Under both conditions, high COD removal efficiencies of 87 - 96 % were achieved. However, nitrogen limitation enhanced EPS production, particularly the polysaccharide fraction. The maximum EPS recovery (g EPS-COD/g $COD_{influent}$) from the fresh wastewater was 54% and 36% recovery was obtained from the saline (30 g NaCl/L) wastewater. The biopolymers had molecular weights up to 2.1 MDa and anionic charge densities of 2.3 - 4.7 meq/g at pH 7. Using kaolin clay suspensions, high flocculation efficiencies of 85 - 92 % turbidity removal were achieved at EPS dosages below 0.5 mg/g clay. Interestingly, EPS produced under saline conditions proved to be better flocculants in a saline environment than the corresponding freshwater EPS in the same environment. The results demonstrate the potential of glycerol/ethanol-rich wastewater, namely biodiesel/ethanol industrial wastewater, as suitable substrates to produce EPS as effective bioflocculants.

1. Introduction

One of the challenges faced in the water sector with respect to particle removal is the replacement of synthetic flocculants with effective and eco-friendly flocculants such as natural flocculants, and for this reason, bioflocculants have gained increasing attention [1–3]. They are potential alternatives to fossil-based synthetic flocculants, which are largely non-biodegradable and may cause harmful pollution [3,4]. A class of promising bioflocculants yet to be explored are microbial extracellular polymeric substances (EPS) [5,6]. EPS comprise high molecular weight compounds (namely polysaccharides and proteins) that make them attractive flocculants. Being anionic polyelectrolytes, they can interact with negatively charged particles in the presence of divalent cations, forming divalent cationic bridges between particles and polymers, which lead to bridging flocculation [7].

EPS are often produced by employing pure cultures [1,5,6]. However, this approach requires sterile conditions as well as expensive and unsustainable carbon sources such as glucose [1]. As a more sustainable alternative, we demonstrate a mixed-culture strategy that involves non-sterile cultures and feedstock, such as organic wastewater. Such an approach not only yields cheap and environmentally friendly flocculants but also saves on wastewater treatment costs. Recently, we showed the possibility of producing EPS with excellent flocculation performance from wastewater [8], but the yield of 6 - 8 % (based on wastewater-COD) was relatively low.

Although conflicting results have been obtained, nitrogen limitation is often reported to enhance microbial EPS production [9–13]. This seems a functional strategy to produce bioflocculants from wastewater as many wastewaters such as biodiesel and paper industrial wastewaters are rich in organic carbon but low in nitrogen.

This study investigates the effect of nitrogen limitation as an approach to enhance EPS yield during the treatment of biodiesel/(bio)ethanol wastewater mixture, and to explore the effect of nitrogen limitation on EPS properties and flocculation performances. In addition, EPS obtained from saline wastewater were compared to EPS from fresh wastewater as it was hypothesized that the former might also give a better flocculation performance under saline conditions.

2. Materials and methods

2.1. Wastewater treatment reactors

Two membrane bioreactors (MBRs, 3.3 L effective volume) were operated in parallel, each separately treating fresh and saline synthetic wastewater. The MBRs were equipped with a PVDF submerged flat sheet membrane with a nominal pore size of 0.2 µm [8]. The freshwater (FW) MBR was inoculated with non-saline aerobic sludge (182 ± 62 mg Na^+/L) from a municipal wastewater treatment plant (WWTP) located in Leeuwarden, Netherlands. The saline (Sal) MBR was inoculated with aerobic sludge obtained from a saline industrial WWTP (located in Delfzijl, Netherlands) that treats wastewater from local chemical industries (sludge salinity 11 ± 3 g Na^+/L). Both MBRs were operated at a room temperature of 20 ± 1 °C, a pH of 7.5 ± 0.3, a dissolved oxygen concentration of 2.5 ± 1.5 mg O_2/L, and a solids retention time (SRT) of 3 days. The hydraulic retention time (HRT) varied between 7.3 h and 13.9 h, depending on the membrane fouling (Table 1).

2.2. Wastewater composition

Wastewater influent COD was 1000 ± 25 mg/L, mainly provided from glycerol (410 ± 10 mg/L) and ethanol (240 ± 5 mg/L) in a 1:1 COD ratio, simulating biodiesel and bioethanol wastewater. These substrates make up more than 60% of the wastewater COD of Delfzijl WWTP. The main nitrogen source was NH_4Cl, and its concentration varied based on the utilized COD/N ratio. The nutrient medium composition per litre of tap water comprised 200 mg $MgCl_2{\cdot}6H_2O$, 150 mg $CaCl_2{\cdot}2H_2O$, 15 mg K_2HPO_4, 25 mg KH_2PO_4, and 2 mL trace elements solution (detailed composition in Ajao *et al*. [8]). Yeast extract was also added to the nutrient medium, and the COD of the medium was considered in the total influent COD. The COD/N ratio was calculated based on the ratio of total influent COD to total nitrogen (N), measured in g/L. The COD/N ratios employed were 5, 20, 60 and 100. The amount of NH_4-N and yeast extract required for each COD/N ratio is shown in Table 1.

Table 1. Hydraulic retention time (HRT) of each reactor under freshwater (FW-MBR) and saline (Sal-MBR) conditions, and amount of NH_4-N and yeast extract in the feed.

Reactor	HRT(h) (FW-MBR/Sal-MBR)	COD/N (g/g)	NH_4–N (mg/L)	Yeast extract (mg/L)	Total nitrogen (mg/L)
COD/N 5	7.3/8.6	5	189.5	100.0	200.0
COD/N 20	7.9/9.2	20	39.5	100.0	50.0
COD/N 60	9.9/13.9	60	6.1	100.0	16.7
COD/N 100	9.9/13.9	100	4.7	50.0	10.0

2.3. Wastewater treatment performance analysis

COD, total nitrogen, and NH_4–N concentrations were determined using the Hach Lange test kits (LCK, Hach Lange, UK). The nitrite and nitrate concentrations of reactor effluents were analyzed using ion chromatography (Metrohm IC Compact 761): the stationary phase was packed polyvinyl alcohol with quaternary ammonium groups and the mobile phase was an aqueous solution of 1mM $NaHCO_3$ and 3.2 mM Na_2CO_3.

2.4. EPS extraction

For each COD/N ratio, the MBRs were operated for a period of at least three times the SRT, after which EPS were extracted from the reactor content. The detailed extraction technique has been described by Ajao *et al*. [8], but was slightly modified. In summary, 400 mL sludge was centrifuged at 17000 *g* and 4 °C for 30 min. The sludge supernatant containing soluble (S)-EPS was dialysed successively against demineralised water at least eight times. From the sludge pellets, bound (B)-EPS were extracted into a phosphate buffer saline solution (PBS, pH 7.4) using a cation exchange resin (Sigma-Aldrich's DOWEX Marathon C, sodium form) at a dosage of 70 g/g VSS for 2 h. After extraction, the supernatant containing the B-EPS was centrifuged at 12000 *g* and 4°C for 15 min and dialysed as explained above. Dialysed soluble and bound EPS fractions were frozen at -80 °C and freeze-dried to obtain dry solids. Dried EPS were weighed and measured for COD content. EPS recovery was based on the influent COD using the equation:

$$EPS\ recovery\ (\%) = \frac{Q_{was} * C_{EPS}}{Q_{inf} * COD_{inf}} * COD(EPS) \qquad (1)$$

where Q_{was} and Q_{inf} are the flow rates (L/d) of the waste sludge and influent feed respectively, C_{EPS} is the extracted EPS concentration (g/L), COD_{inf} is the influent COD (g/L), and *COD(EPS)* is the COD of extracted EPS (g COD/g EPS).

2.5. EPS characterisation

2.5.1. Viscosity

As a quick tool to monitor EPS production in the reactors, viscosities of the sludge supernatants (after centrifugation at 17000 *g* for 30 mins) were measured at 10, 12, 20, and 30 rpm at room temperature (21 ^{o}C) using a HAAKE Viscotester 6L plus (Thermo Electron, Germany).

2.5.2. Functional group determination

Fourier transform infrared spectroscopy (FTIR) was carried out on the freeze-dried EPS samples using an FTIR-8400S spectrometer (Shimadzu, Japan) with a scanning range of 4000 - 650 cm^{-1} for 40 scans at a spectral resolution of 2 cm^{-1}.

2.5.3. Total protein and polysaccharide quantification

The total protein content of the EPS was determined using a bicinchoninic acid (BCA) assay kit (Thermo Scientific, USA). The assay was performed in a microplate, where 25 µL of EPS solution (dissolved in PBS, pH 7.4) or standard bovine serum albumin was mixed with 200 µL of BCA working reagent and incubated at 37 °C for 30 min. Afterward, the absorbance was measured at 570 nm using a spectrophotometer (Victor3 1420 Multilabel Counter, Perkin Elmer, USA).

Total polysaccharides/carbohydrates were quantified using the phenol-sulphuric acid method described by Dubois *et al*. [14] using glucose as the standard sugar. Absorbance was measured at 490 nm in the spectrophotometer mentioned above.

2.5.4. Molecular weight determination

A solution of EPS was first passed through 0.45 µm polytetrafluoroethylene filter before molecular weight determination using liquid chromatography-organic carbon detection (LC-OCD – model 8, DOC-LABOR, Germany) with a built-in Siemens Ultramat 6^{E} Non-Dispersive Infra-Red detector, coupled with an Agilent 1260 organic nitrogen detector (UV 220 nm) and a UV detector (254 nm). The column used was a tandem setup with an Agilent BioSec5 5um 1000A (7.8 mm*300 mm) and a Toyopearl HW-50S 30 um (20 mm*250 mm). The mobile phase was a phosphate buffer (28 mmol, pH 6.6). EPS molecular weights were determined using pullulan standards obtained from PSS, Germany.

2.5.5. Charge density

Charge density was determined by colloid titration using a Mütek Particle Charge Detector (PCD03, Germany) described by Tan *et al*. [15] and a titration procedure explained by Ajao *et al*. [8]. The charge density was calculated from the titrant (poly-diallyldimethylammonium chloride, pDADMAC) consumption according to:

$$q = \frac{c*V}{m} \qquad (2)$$

where *q* is the specific charge quantity (eq/g), *c* is the titrant concentration (eq/L), *V* is the consumed titrant volume (L), and *m* is the mass of the EPS sample (g). Charge density was determined at the initial pH of sample solution (5.0 ± 0.2) and at pH 7.0 ± 0.1 (since most waters are flocculated at close to neutral pH) using 1 mM NaOH for pH adjustment.

2.6. Flocculation tests

Flocculation tests were carried out on a jar test flocculation unit, as described by Ajao *et al*. [8]. Naturally-occurring kaolin clay (Sigma-Aldrich's natural kaolinite, $Al_2O_3{\cdot}2SiO_2{\cdot}2H_2O$), possessing a net negative charge, was used as a model for water particles [5,16]. We investigated the potentials of different EPS fractions produced under different COD/N ratios as natural flocculants. For this purpose, two model suspensions were prepared: (i) saline kaolin suspension: 5 g kaolin/L and 30 g NaCl/L (to mimic saline water), and (ii) non-saline kaolin suspension comprising only 5 g kaolin/L. Both were prepared in Milli-Q water. EPS solutions were made by dissolving freeze-dried EPS in Milli-Q water. For the flocculation of the non-saline kaolin suspension, 100 mg Ca^{2+}/L ($CaCl_2{\cdot}2H_2O$) was added as a coagulant. Supernatant turbidity after flocculation was measured with a turbidimeter (2100N IS, Hach) in Nephelometric Turbidity Units (NTU). Flocculation efficiency was calculated as follows:

$$Flocculation\ efficiency\ (\%) = \frac{NTU_{control} - NTU_{test}}{NTU_{control}} \qquad (3)$$

where $NTU_{control}$ is the turbidity value of the control experiment (without EPS addition), and NTU_{test} is the turbidity value of test experiment (with EPS as flocculant).

3. Results and discussion

3.1. Wastewater treatment performance

During the operational period of at least three times the SRT, similar COD removal efficiencies (93 - 97 %) were observed for all the COD/N ratios (except Sal-MBR at COD/N 100) irrespective of the wastewater salinity (Table 2). COD concentrations in the effluent varied between 36 and 58 mg/L. Only at a COD/N ratio of 100 did the Sal-MBR give an average removal efficiency of 87% and an effluent concentration of 130 mg/L.

The high COD removal efficiencies at COD/N of 60 and 100 were rather surprising because nitrogen was clearly limiting under these conditions (effluent NH_4-N concentrations below 0.3 mg/L). To exclude a temporary effect, FW-MBR operation at COD/N 100 was continued for another 105 days, but a high COD removal efficiency of at least 96% could still be maintained. Under the nitrogen-limited condition, excellent COD removals were achieved because influent soluble COD was converted to EPS-COD, which was retained by the membrane. Moreover, the COD mass balances (Fig. S1, see supplementary information) reveal that by limiting nitrogen, mineralisation and biomass production from influent COD were substituted by EPS production. At COD/N 100, 54% of the wastewater COD was converted to EPS and 17% for biomass growth. Mineralisation of wastewater-COD, calculated as a closure of the COD mass balance, was only 16%, implying that the oxygen demand of the process was very low.

Table 2. COD removal efficiency, effluent COD and NH_4-N concentrations in both freshwater (FW) and saline (Sal) membrane bioreactors (MBRs) operated at different COD/N ratios. Data expressed as the mean ± standard deviation of at least four effluent samples analysed during the operational period.

Reactor	COD/N (g/g)	Effluent COD (mg/L)	COD removal (%)	Effluent NH4-N (mg/L)
FW-MBR	5	58 ± 9	94.0 ± 1.0	127 ± 11
	20	50 ± 6	94.8 ± 0.6	9 ± 6
	60	36 ± 8	96.2 ± 0.8	0.05 ± 0.05
	100	36 ± 10	96.0 ± 1.0	0.008 ± 0.006
Sal-MBR	5	57 ± 12	94.0 ± 1.2	170 ± 10
	20	50 ± 5	94.9 ± 0.6	8 ± 4
	60	48 ± 6	94.9 ± 0.6	0.3 ± 0.3
	100	130 ± 50	86.7 ± 5.2	0.2 ± 0.1

3.2. EPS production

The COD/N ratio had a noticeable effect on the sludge viscosity in both the FW- and Sal-MBRs. The sludge viscosity increased at COD/N 60 and 100, especially the FW-MBR sludge, which was slimy and sticky (Figs. 1A and 1B). The associated decrease of S-EPS viscosity with shear rate (Fig. 1C) reveals its non-Newtonian pseudoplastic fluid behavior, a property usually found in exopolysaccharides [17]. This pseudoplastic behaviour was more evident with FW-EPS than with Sal-EPS. Furthermore, the sludge viscosity is proportional to the S-EPS concentration and can, therefore, be used as a quick tool to monitor S-EPS production in bioreactors (Fig. 1D).

The EPS concentrations, particularly those of the S-EPS, generally increased with increasing COD/N ratio (Fig. 2). At COD/N 100, the total EPS (soluble and bound) concentration was 2.32 g/L for the FW-MBR and 1.86 g/L for the Sal-MBR, from which the soluble fractions accounted for 77% and 67%, respectively. The highest concentration of B-EPS was observed at COD/N 60, with values of 0.58 g/L (FW) and 0.98 g/L (Sal) (Figs. 2B and 2D).

A notable observation is the distribution of soluble and bound EPS (Figs. 2A and B, 2C and D). The contribution of S-EPS to the total EPS (soluble and bound) was significantly higher in FW-EPS (62 – 77 %) than in Sal-EPS (36 – 45 %, but 67% at COD/N 100). Considering the S-EPS are likely sheared-off products of cell-bound EPS [18], this implies that EPS produced under saline conditions are more strongly attached to the microbial cells/flocs than FW-EPS, possibly due to the function of EPS to protect against salt stress [19].

The amount of influent COD recovered as EPS-COD (equation 1) is also shown in Fig. 2. A relatively low amount of total EPS (soluble and bound) could be recovered (< 8%) under nitrogen-rich conditions (COD/N 5 and 20). However, a huge increase in EPS recovery was observed when the COD/N ratio increased from 20 to 60, with respective recoveries of 5 to 27 % for the FW-EPS, and 7 to 28 % for the Sal-EPS. At COD/N 100, the highest recoveries were obtained with a total of 54% under freshwater condition (S-EPS 47%, B-EPS 7%), and 36% under saline condition (S-EPS 25%, B-EPS 11%). These high recoveries clearly demonstrate the key role of nitrogen limitation in EPS production.

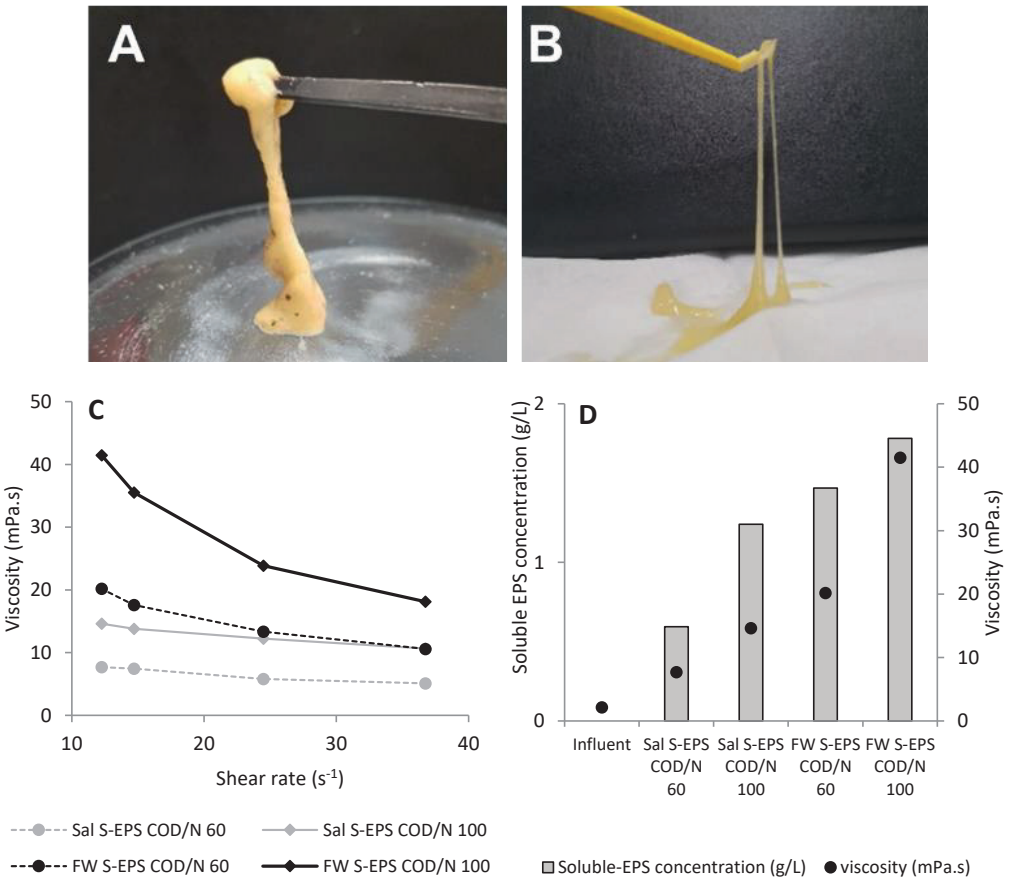

Fig 1. (**A, B**) – Viscous sludge produced from freshwater-MBR at COD/N ratio 60 (**A**) and 100 (**B**). (**C**) – Soluble-EPS viscosity as a function of shear rate at room temperature (21 °C). (**D**) – Soluble-EPS concentration *versus* viscosity at a shear rate of 12.2 s^{-1}. The viscosity of the influent was obtained at a shear rate of 244.8 s^{-1}. Sal S-EPS: saline soluble-EPS, FW S-EPS: freshwater soluble-EPS.

Microbial EPS synthesis can be considered a secondary metabolism that is uncoupled from growth. Russell [20] defined this as 'energy spillage' – non-growth dissipation of excess energy by microorganisms. This excess energy under nitrogen-limited condition is converted to extracellular polymers, especially polysaccharides (which do not contain the growth-limiting nutrient) [21], possibly as a means to store carbon under unbalanced carbon to nitrogen ratios [22]. The COD mass balance in Fig. S1 demonstrates that at high COD/N ratios, EPS production is favoured over biomass growth and vice versa at low COD/N ratios.

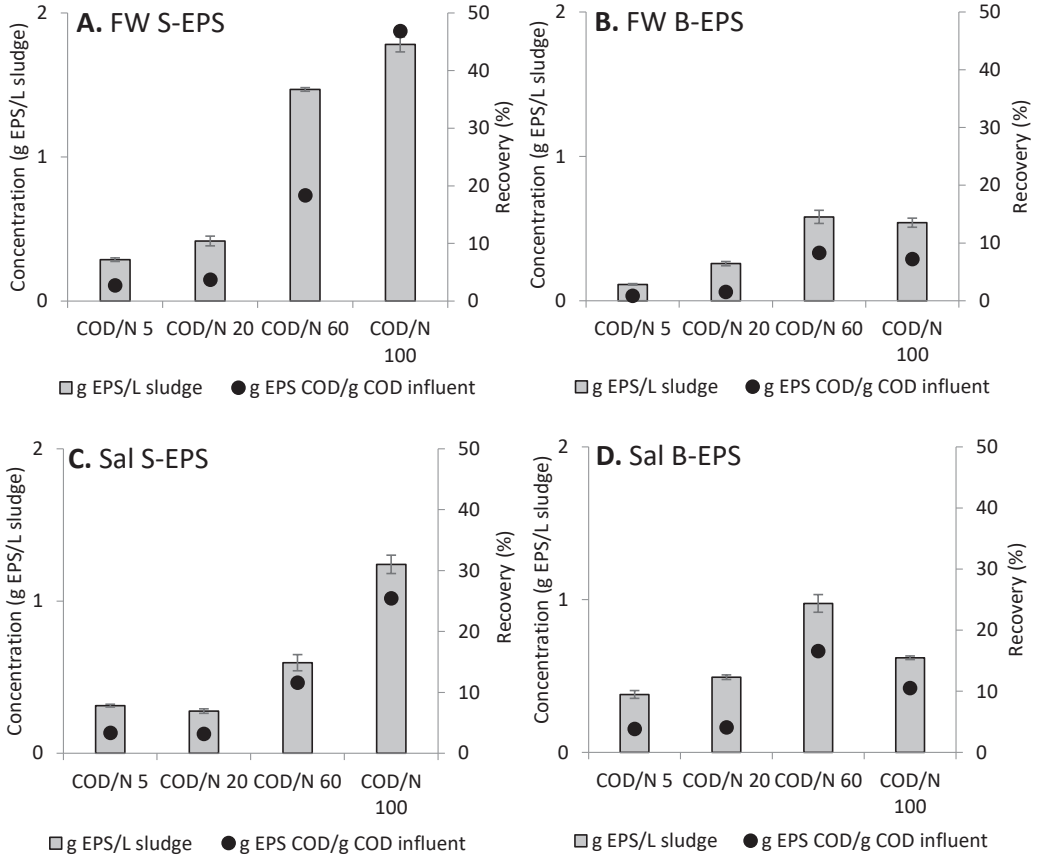

Fig. 2. EPS production at different COD/N ratios. (**A**) FW S-EPS: freshwater soluble-EPS, (**B**) FW B-EPS: freshwater bound-EPS, (**C**) Sal S-EPS: saline soluble-EPS, and (**D**) Sal B-EPS: saline bound-EPS.

Aside from nitrogen limitation as a strategy to increase EPS yield, the carbon/energy source also plays a crucial role in EPS biosynthesis. Studies using pure cultures fed with a mixture of glycerol and ethanol/methanol reported higher EPS production and yields compared to single sources such as glucose, sucrose and soluble starch [5]. Moreover, fortification of bacterial growth medium with glycerol (in the presence of ethanol or methanol) was demonstrated to increase EPS yield [23], and in some cases, more than two-fold [24]. Yields (g EPS/g substrate COD) as high as 51.2 and 57.4 % have been reported by Buthelezi *et al*. [25] and Nouha *et al*. [23] respectively from *Klebsiella terrigena* and *Cloacibacterium normanense* using substrates of glycerol and ethanol mixture in batch cultures. Our study also demonstrates the possibility of very high EPS recoveries from a glycerol/ethanol mixture (54% from fresh wastewater and 36% from saline wastewater), though with mixed cultures (see S2 and Table S1, supplementary information) and in a continuous wastewater treatment process. One possible explanation for the high EPS yield is that glycerol has a shorter pathway towards EPS synthesis compared to most sugar substrates [21]. Another reason may be the combined effects of energy non-equivalent substrates [26,27]. According to this

bioenergetic concept, all growth substrates are either energy excessive or deficient based on the amount of ATP and reducing equivalents formed in the synthesis of phosphoglyceric acid – the key precursor for the synthesis of all cell components. On this basis, glycerol, glucose, and sucrose are energy-deficient substrates, while ethanol and methanol are energy-excessive substrates that can be used as auxiliary substrates [26]. Although the underlying metabolic mechanism is yet to be understood, a combination of these two substrate classes (the former utilized for carbon conversion and the latter as an energy source) at the optimum ratio has been reported to increase carbon conversion efficiencies towards the production of secondary metabolites such as EPS [24,27]. Further studies using different energy non-equivalent substrate mixtures in a continuous system would be justified as this would give insights into the combination of industrial wastewater types needed as best substrates for EPS production.

3.3. EPS properties

3.3.1. Composition

In general, the total polysaccharide (PS) content of the produced EPS increased with increasing COD/N ratios (Fig. 3). In the FW-MBR, the trend of increasing PS content was observed from COD/N 5 to 60 (21.7 - 70.4 wt% for the S-EPS, and 14.0 - 60.7 wt% for the B-EPS). At COD/N 100, the values decreased to 41.8 and 47.8 wt% for the S-EPS and B-EPS, respectively. In the Sal-MBR, the PS content increased steadily from COD/N 5 to 60/100 (17.6 - 61.2 wt% for the Sal S-EPS, and from 13.8 - 49.8 wt% for the Sal B-EPS). In contrast to the PS content, the nitrogen (PN) content decreased or remained rather constant with increasing COD/N ratio, revealing that the carbohydrate fraction was the main EPS component under nitrogen-limited conditions.

It should be noted that, with the colorimetric assays, no distinction could be made between free or bound proteins such as glycoproteins. To further investigate the presence of glycoproteins in the produced EPS, SDS-PAGE (sodium dodecyl sulfate-polyacrylamide gel electrophoresis – see supplementary information) of EPS produced at COD/N 100 was carried out. Fig. S3 reveals that the protein fraction of the produced EPS is bonded with carbohydrates to form neutral and acidic glycoproteins in both the FW- and Sal-EPS fractions.

3.3.2. Molecular weight

Molecular weight (MW) is an important property of EPS if they are to be applied as flocculants. The longer the polymeric chain, the better they can extend into solution (if the chain has a hydrophilic property) to aggregate particles. EPS extracted from COD/N 20 (nitrogen-rich) and 100 (nitrogen-limited) were selected for MW determination. Typical size exclusion chromatograms are shown in Fig. S4, and Table 3 presents the average MW of the EPS biopolymer fractions. The EPS fractions showed two biopolymer chromatographic peaks – one with high (> 1000 kDa) or medium (1000 - ~100 kDa) MW, and the other with low (< 100 kDa) MW, except for the FW-EPS at COD/N 20 where only one peak was detected.

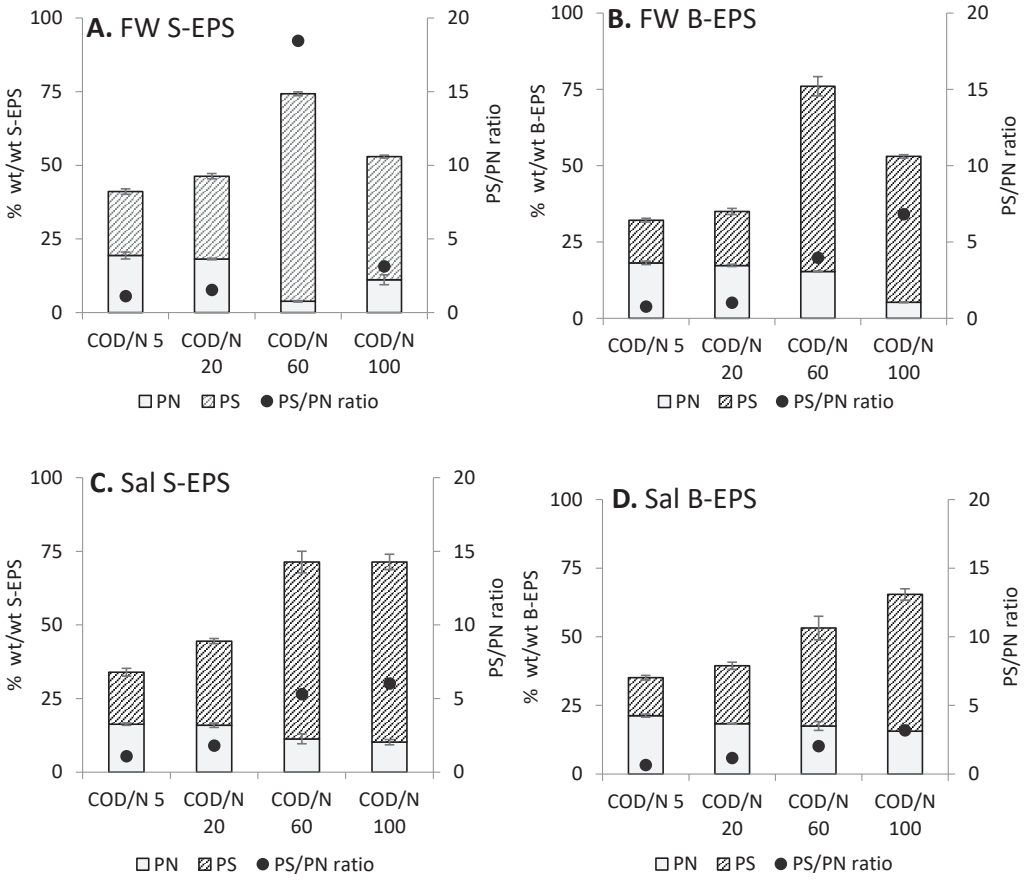

Fig. 3. Total proteins (PN) and polysaccharides (PS) content of EPS fractions from COD/N ratios 5, 20, 60, and 100.

Higher molecular weight EPS were produced under nitrogen-limited conditions compared to EPS from nitrogen-rich sources. This is more evident for the saline EPS, where the polysaccharide fractions at COD/N 100 are much higher than the polysaccharide fractions at COD/N 20 (Figs. 3C and 3D). This demonstrates that nitrogen limitation not only stimulates microorganisms to excrete large quantity of EPS, it also builds longer chain biopolymers compared to the nitrogen-rich counterparts. Another observation is that the soluble and bound fractions under the different conditions had similar molecular weights (except for saline EPS from COD/N 20), suggesting, as was mentioned earlier, that S-EPS were sheared-off products of cell-bound EPS. However, as will be explained below, their charge densities do show differences.

Table 3. Average molecular weights (MW) of the EPS biopolymer fraction.

EPS fraction	MW at COD/N 20	MW at COD/N 100
Freshwater soluble-EPS	1.7 MDa	1.9 MDa, 24.5 kDa
Freshwater bound-EPS	1.6 MDa	2.1 MDa, 24.6 kDa
Saline soluble-EPS	202.3 kDa, 22.5 kDa	1.0 MDa, 22.7 kDa
Saline bound-EPS	98.4 kDa, 39.6 kDa	1.0 MDa, 22.7 kDa

Table 4. Anionic charge density of EPS (meq/g EPS) extracted from COD/N 20 and 100 reactors.

COD/N	pH	Freshwater EPS		Saline water EPS	
		Soluble	Bound	Soluble	Bound
20	5	2.14 ± 0.13	1.94 ± 0.01	3.11 ± 0.02	1.60 ± 0.16
	7	3.50 ± 0.10	3.02 ± 0.01	4.68 ± 0.05	2.69 ± 0.12
100	5	2.25 ± 0.18	2.72 ± 0.13	1.96 ± 0.16	1.40 ± 0.01
	7	3.25 ± 0.07	3.48 ± 0.01	3.06 ± 0.22	2.25 ± 0.00

3.3.3. Charge density

In addition to molecular weight, charge density is another crucial property for flocculation. The charge density of EPS is due to the presence of carboxyl and amino groups as indicated in the FTIR spectra in Fig. S5 (supplementary information). Table 4 shows the anionic charge density of EPS extracted at COD/N 20 and 100 at the initial pH of the sample solution (5) and neutral pH (7).

As expected, the charge density at an elevated pH (pH 7) was higher because of the functional groups in a largely deprotonated form, i.e. $–COO^-$ and $–NH_2$, compared to –COOH and $–NH_3^+$. These values can even go as high as 5 - 6 meq/g at higher pH values, such as 10 [8]. At both studied pH values, charge densities of the S-EPS were higher than those of the corresponding B-EPS (except for the FW-EPS at COD/N 100), likely due to the higher polysaccharide content in the soluble fractions compared to the bound fractions (Fig. 3). In the case of the FW-EPS produced at COD/N 100, where a higher polysaccharide content was in the B-EPS than in the S-EPS (Fig. 3A and 3B), the charge density was also higher in the B-EPS than in the S-EPS. These findings imply that polysaccharides (with functional groups –OH and $–COO^-$) give a higher contribution to the anionic charge density than proteins (with functional groups $–NH_2$ and $–COO^-$), which is consistent with the results of Durmaz and Sanin [9].

3.4. EPS flocculation performance

Flocculation tests were focused on the EPS produced at COD/N 20 and 100 to mimic EPS from excess and limited nitrogen regimes, respectively. First, the flocculation performances of the EPS fractions on non-saline kaolin suspension were tested, with the addition of 100 mg/L Ca^{2+} to facilitate bridging between the anionic particles and EPS (Fig. 4). The maximum flocculation efficiencies that were obtained varied between 81 and 91 %, with no significant difference between the performances of FW-EPS and Sal-EPS at COD/N 100. The maximum efficiency (91%) and optimum dosage (0.2 mg/g) are comparable to that of a commercial synthetic flocculant (anionic polyacrylamide – 93% efficiency at 0.1 mg/g) operated under similar flocculation conditions [8].

The three best dosages (0.1, 0.2 and 0.5 mg/g) were also utilized to flocculate saline kaolin suspension (30 g/L NaCl) without Ca^{2+} addition. A similar flocculation performance pattern was also observed like in Fig. 4 (see supplementary information, Fig. S6), with maximum flocculation efficiencies between 87 and 92 %. However, under the saline conditions, Sal-EPS consistently gave a better performance (by 6 - 13 %) than the corresponding EPS produced under freshwater conditions. Although this cannot be directly related to observed differences in EPS properties such as composition, molecular weight and charge, the implication may be that, for flocculation in saline environments, it is more attractive to use EPS that were produced from saline wastewater.

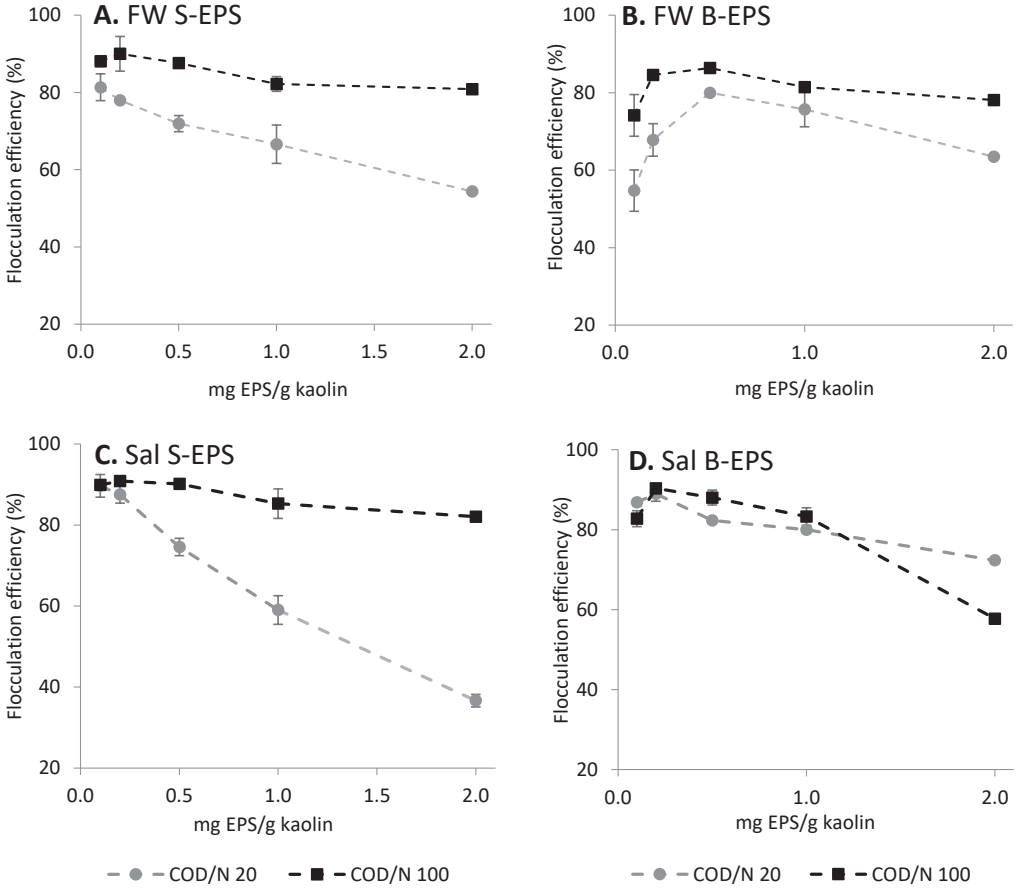

Fig. 4. Non-saline kaolin clay flocculation using EPS from COD/N ratio 20 and 100, with the addition of 100 mg Ca^{2+}/L. (**A**) FW S-EPS: freshwater soluble-EPS, (**B**) FW B-EPS: freshwater bound-EPS, (**C**) Sal S-EPS: saline soluble-EPS, and (**D**) Sal B-EPS: saline bound-EPS.

Overall, three flocculation patterns were seen in the non-saline and saline kaolin experiments. First, the general trend was an increase in flocculation efficiency with increasing EPS concentration in the range of 0.1 – 0.2/0.5 mg/g kaolin, but reduced efficiency at higher concentrations (Fig. 4 and S6). A similar pattern has also been reported with synthetic anionic flocculants and in sludge bioflocculation with EPS [28–30]. This effect is known to be caused by restabilisation of the clay particles at concentrations above the optimum [31]. Secondly, FW and Sal EPS produced from COD/N 100 generally showed better flocculation performances than corresponding EPS from COD/N 20. This is likely due to the higher MW biopolymers in EPS produced under nitrogen-limited conditions (Table 3). It is well established that a higher MW and longer polymer chain facilitates the formation of adsorbed 'loops' and 'tails' that can extend into the solution, thereby enhancing the ability to attach to other clay particles [4]. The third trend is that S-EPS generally had higher maximum flocculation efficiencies than the corresponding B-EPS, which is consistent with the findings of Bala Subramanian *et al*. [32] and Nouha *et al*. [33]. From our study, this is possibly related to the higher charge densities of S-EPS compared to the corresponding B-EPS (except for freshwater EPS of COD/N 100 – Table 4), since both fractions have similar MWs. A higher charge density implies more repulsion between charged segments and a wider expansion of the polymer chain into the solution, increasing the ability to adsorb and bridge between particles [4].

3.5. Practical implications and outlook

The advantage of such mixed EPS (mixed composition and MW) over single-type EPS and single synthetic flocculants could be their resilience and robustness under practical conditions such as different particle type, size, and concentration. However, further research is needed to substantiate this hypothesis.

The use of non-synthetic glycerol/ethanol-rich wastewater is also expected to afford high EPS yield if influent nitrogen is limited. However, the impact of this non-synthetic wastewater on the produced EPS properties and flocculation acitvity, though not expected to differ much from the findings of this study, still needs to be investigated. Also, additional studies should be carried out on (non-synthetic) wastewater mixtures of varying compositions and how these may affect the reproducibility of the produced EPS. Finally, while EPS production from wastewater may have the additional advantage of much lower oxygen demand, the consequent membrane fouling due to a higher sludge viscosity is a challenge that still needs to be addressed.

4. Conclusions

- It is possible to continuously treat glycerol/ethanol-rich wastewater while simultaneously producing, with a mixed microbial population, large amounts of extracellular polymers that can be utilised as bioflocculants.
- Under nitrogen-limited (COD/N 100) and freshwater conditions, up to 54% of the wastewater-COD could be recovered as EPS.
- Under saline conditions, EPS recovery was as high as 36%.

- High flocculation efficiencies were obtained, which can be explained by the relatively high molecular weight (up to 2.1 MDa) and medium charge densities (2-5 meq/g) of the flocculants.
- In the flocculation tests under saline conditions, polymers that were produced under saline conditions gave a consistently higher (6 - 13 %) flocculation performance than polymers produced under freshwater conditions.

Acknowledgements

This work was performed in the cooperation framework of Wetsus, European Centre of excellence for sustainable water technology (www.wetsus.nl). Wetsus is co-funded by the Dutch Ministry of Economic Affairs and Ministry of Infrastructure and Environment, the European Union Regional Development Fund, the Province of Fryslân and the Northern Netherlands Provinces. This work has also received funding from the European Union's Horizon 2020 research and innovation programme under the Marie Skłodowska-Curie [grant agreement No. 665874]. The authors thank the participants of the research theme 'Natural flocculants' for the fruitful discussions and financial support, Mieke Kersaan-Han for developing the molecular weight method, Nora Sutton for the NGS preparation and analysis, Bastian Hornung for assisting with the sequence deposit, Wetterskip Leeuwarden and Northwater Netherlands for providing the inocula, and David Lewis for the English language correction of this manuscript.

Supporting information of Chapter 3

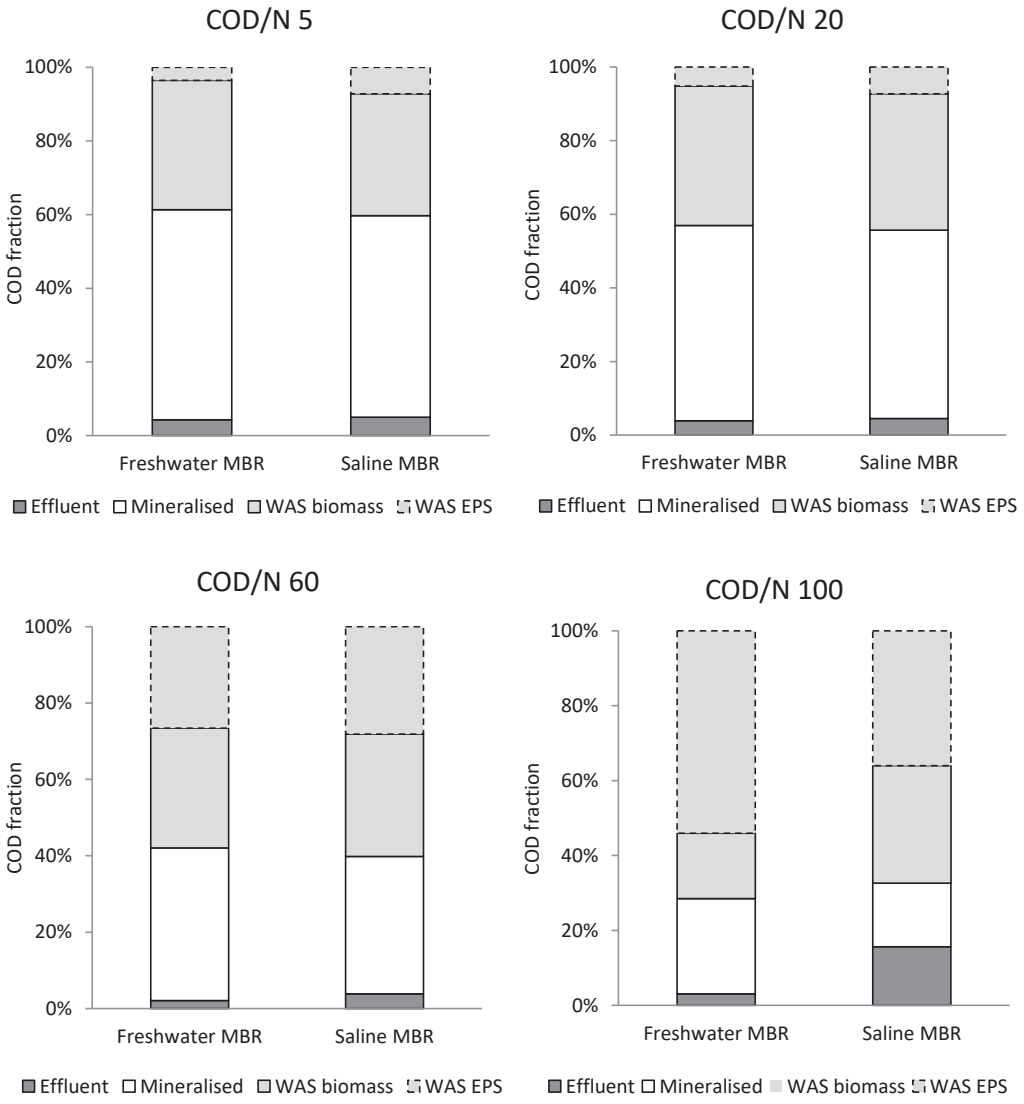

Fig. S1. COD distribution as a fraction of influent COD in the freshwater and saline membrane bioreactors (MBRs). Mineralisation was estimated as the closure of the mass-balance. WAS biomass was also calculated as the difference between the total WAS-COD and EPS-COD. WAS: Waste activated sludge.

S2. Microbial community analysis under nitrogen-limited condition

Fresh mixed liquor samples were collected from the MBRs when operated at COD/N 60 after 20 days of operation. Samples were stored at -20 °C for further DNA extraction. DNA was extracted using the PowerSoil isolation kit (Mo Bio Laboratories, USA), according to the manufacturer instructions. The extracted DNA was concentrated through a speed vacuum step and then quantified via Qbit assay (Themofisher Scientific, Germany). Universal primers based on the V3-V4 hypervariable region of prokaryotic 16S rDNA [34] were applied for the simultaneous detection of Bacteria and Archaea in the reactor samples. The 16S rRNA gene PCR amplification was carried out following the protocol of Takahashi *et al*., (2014). Illumina sequencing and computational analysis of the 16S PCR products are fully described in the supplementary information. The taxonomic assignment for OTUs identified through NGS analysis are reported in Table S1 A and B. The sequences reported in this paper have been deposited in the European Nucleotide Archive (ENA) database (http://www.ebi.ac.uk/ena/) under accession numbers ERR2851470 and ERR2851471.

Illumina Sequencing and Computational analysis of 16S rRNA gene amplicons

The sequencing of the 16S PCR products was conducted using the Illumina MiSeq sequencing system. The sequences generated from the Illumina Miseq analysis of the 16S rRNA gene amplicons were processed (i.e., filtered, clustered, and taxonomically assigned and aligned) using the Quantitative Insights Into Microbial Ecology (QIIME) pipeline version 1.9.1 [35]. The process consisted of quality checking, denoising, and microbial diversity analysis. The primer sequences were removed from the raw 16S sequences readings and then placed in a single fasta file using the add_qiime_labels.py script. OTU picking was performed with the script pick_open_reference_otus.py using the SILVA version 128 16S reference database [36] and the clustering method UCLUST [37]. The RDP classifier (version 2.2) [38] was used to classify the OTUs based on the same SILVA database. The QIIME script core_diversity_analyses.py was used to calculate alpha- and beta-diversity statistics of the samples.

The taxonomic assignment for OTUs identified through NGS analysis are reported in Table S1 A and B. Data has been uploaded to the ENA database under accession numbers ERR2851470 and ERR2851471 for the FW-MBR and the Sal-MBR, respectively.

Microbial diversity

The relative abundance of each microbial component within the microbial community found by NGS analysis was utilised to calculate the biodiversity of the mixed microbial communities using Shannon–Weaver index of diversity (H') and Pielou's evenness index.

Tables S1. In (**A**) and (**B**), taxonomic assignment for OTUs identified through NGS analysis in the aerobic FW- and Sal-MBR operated at COD/N 60. For each OTU, the maximum affiliation level (from phylum to genus) is reported. In **C**, Shannon–Weaver (H') and Pielou's evenness index (E) values calculated for the two different microbial populations.

A

FW-MBR	
Affiliation	**OTU %**
Acidovorax	15.4
Uncultured Sphingobacteriales	13.7
Bdellovibrio	10.1
Flavobacterium	8.7
Sediminibacterium	4.7
Rhodobacter	4.6
Hydrogenophaga	3.9
Uncultured Verrucomicrobiaceae	2.9
Acinetobacter	2
Others	1.9
Citrobacter	1.6
Cloacibacterium	1.5
Verrucomicrobium	1.4
Uncultured Saccharibacteria	2.8
Aeromonas	1.4
Brevundimonas	1.3
Comamonas	1.3
Rhizobium	1.1
Pseudomonas	1.1
Prosthecobacter	0.9
Macellibacteroides	0.9
Uncultured Sphingobacterium sp.	0.9
Acetoanaerobium	0.8
Pedobacter	0.8
Legionella	0.7
Simplicispira	0.6
Chryseobacterium	0.5
Luteolibacter	0.5
Uncultured Chlorobiales	0.5
Runella	0.5

B

Sal-MBR	
Affiliation	**OTU %**
Halomonas	43.2
Uncultured Cryomorphaceae	7.5
Defluviimonas	4.4
Bacteroidetes Incertae Sedis	4.3
Hoeflea	3.2
Vibrio	2.9
Verrucomicrobiales	3.2
Uncultured Hyphomonadaceae	2.7
Marinobacterium	2
Uncultured Cytophagaceae	1.8
Sulfitobacter	1.5
Balneola	1.5
Others	1.5
Idiomarina	1.2
Psychrilyobacter	1.2
Roseovarius	1
SR1 (Absconditabacteria)	1
Uncultured Legionellaceae	0.9
Fusibacter	0.9
Sunxiuqinia	0.9
Cyclobacterium	0.7
Methyloversatilis	0.6
Uncultured Sphingobacteriales	0.5
Rhodobacteraceae	0.5
Bdellovibrio	0.5
Labrenzia	0.5

C

Microbial diversity		
	FW-MBR	*Sal-MBR*
H'	2.32	1.72
E	0.68	0.53

S3. Sodium dodecyl sulfate polyacrylamide gel electrophoresis (SDS-PAGE) analysis

The isolated proteins from EPS were further analyzed using sodium dodecyl sulfate polyacrylamide gel electrophoresis (SDS-PAGE). Coomassie blue, periodic-acid Schiff (PAS), and Alcian blue staining were applied to detect total proteins, neutral, and acidic glycoproteins, respectively. For sample preparation, the proteins were precipitated using trichloroacetic acid (30%, w/v) and washed with cold acetone three times. After centrifugation (12,000 *g* for 30 min), the pellet containing proteins were dissolved in Laemmli sample buffer (Bio-Rad) containing 355 mM of 2-merchaptoethanol to reach a concentration of 1 mg/mL. The samples were then heated at 70 °C for 10 min, and about 15 µL was loaded to a Mini-PROTEAN® TGX™ precast gel (4 – 20 %, 15 wells, Bio-Rad). As a marker, a 10-250 kDa protein ladder of Bio-Rad Precision Plus Protein Dual Colour Standards was applied on the gel. Using a Mini Protean Tetra Cell (Bio-Rad) with 1× Tris-glycine-SDS running buffer (Bio-Rad), electrophoresis was carried out at initially 75 volts for 15 min and subsequently at 150 volts for 45 min. The gel was stained using the following procedures.

Coomassie blue staining

Prior staining, fixation step was carried out to limit the diffusion of proteins from the gel matrix. The gels were immersed in 45% methanol (v/v) and 10% acetic acid (v/v) for 10 min. The step was repeated once to ensure that the SDS was fully removed from the gel. Next, gels were washed twice with 3% acetic acid (v/v) for 10 min each and stained with 0.25% w/v Coomassie blue (Brilliant Blue R-250, Sigma Aldrich) in fixative solution for 1 h. Subsequently, gels were de-stained in 20% ethanol (v/v) and 10% acetic acid (v/v) overnight. All staining steps were done under gentle agitation and at room temperature.

Periodic-acid Schiff (PAS) staining

The PAS staining was done using Pro-Q® Emerald 300 Glycoprotein Gel and Blot Stain Kit from Life Technologies. The staining steps were conducted according to the protocol of the manufacturer [39].

Alcian blue staining

For the Alcian blue staining, the gel was stained with 0.125% Alcian blue (w/v) in 25% ethanol (v/v) and 10% acetic acid (v/v) for a minimum of 2 h. The fixation, washing and de-staining steps were the same as those of Coomassie blue staining.

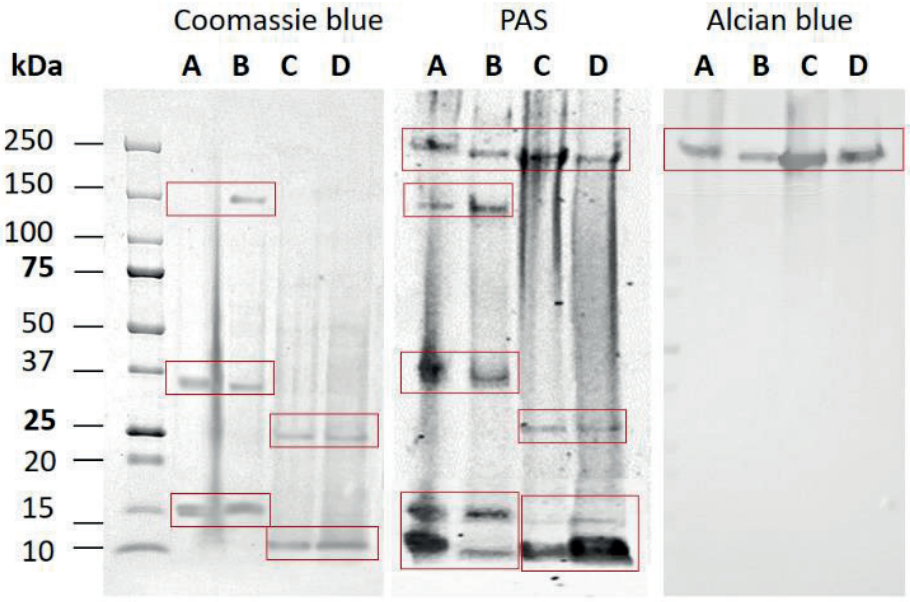

Fig. S3. SDS-PAGE of EPS produced at COD/N 100, stained with Coomassie blue (to visualize total protein), periodic acid-Schiff (PAS – to visualize neutral glycoprotein), and Alcian blue (to visualize acidic glycoprotein). Line **A** and **B**: respective proteins in S-EPS and B-EPS produced from freshwater. Line **C** and **D**: respective proteins in S-EPS and B-EPS produced from saline wastewater.

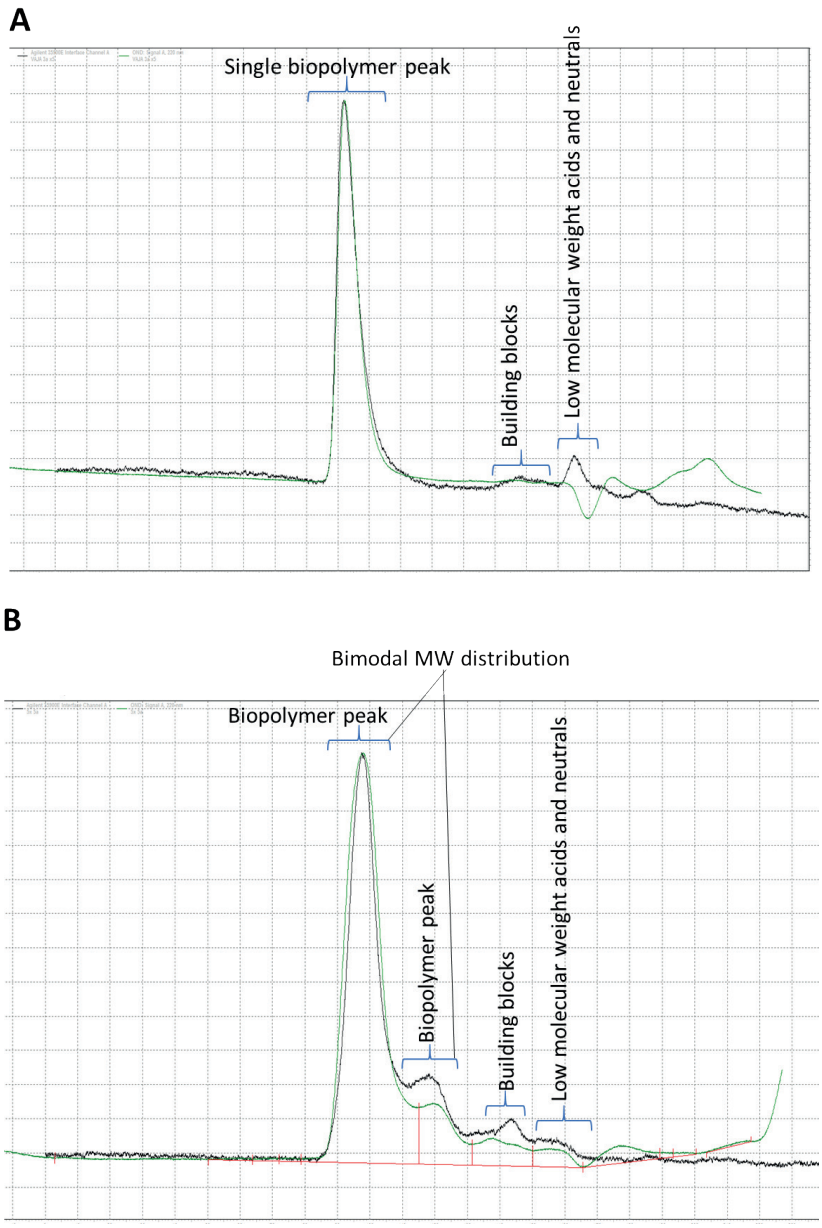

Fig. S4. LC-OCD (based on size exclusion) chromatograms. (**A**) with a single biopolymer peak as found in FW S-EPS and FW B-EPS of COD/N 20, (**B**) with bimodal biopolymer peaks as found in the other EPS fractions in Table 3. Black line is the organic carbon detector signal; green line is the organic nitrogen detector signal.

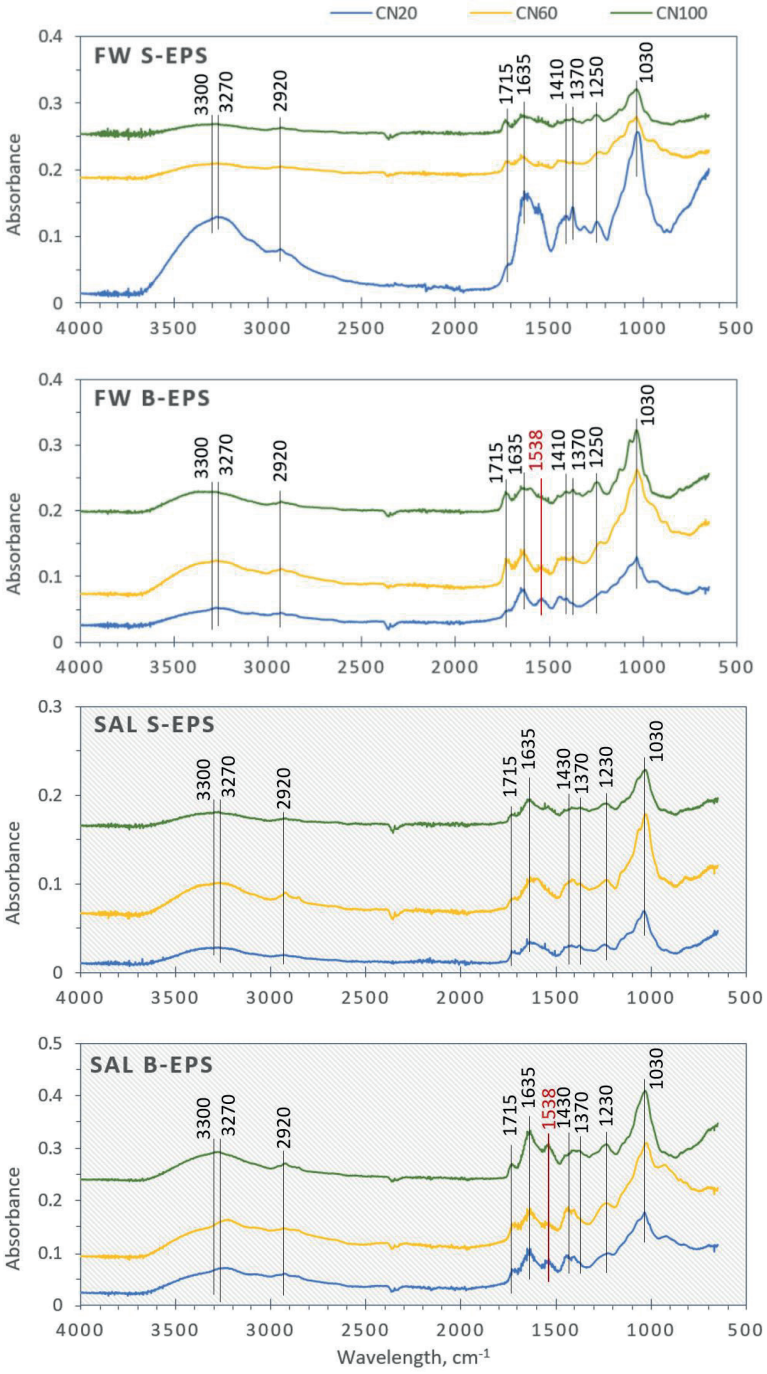

Fig. S5 (**A**). Fourier transform infrared (FTIR) spectra of EPS produced from COD/N ratios 20, 60 and 100. FW S-EPS: freshwater soluble-EPS, FW B-EPS: freshwater bound-EPS, Sal S-EPS: saline soluble-EPS, and Sal B-EPS: saline bound-EPS.

S5 (**B**). FTIR spectra interpretation.

Wavelength (cm^{-1})	Functional group
3300, 3270	O–H and N–H stretching vibrations of polysaccharide and protein, respectively
2920	C–H stretching vibration
1635	C=O stretching vibration of protein amide I band
1538	C–N stretching vibration and out-of-phase N–H bending of protein amide II band
1430, 1410	In-phase N–H bending of protein amide III band
1370	C=O symmetric stretching of $–COO^-$ groups
1250, 1230	C–O stretching of ether or alcohol
1030	C–O–C asymmetric stretching of ester linkage of polysaccharides

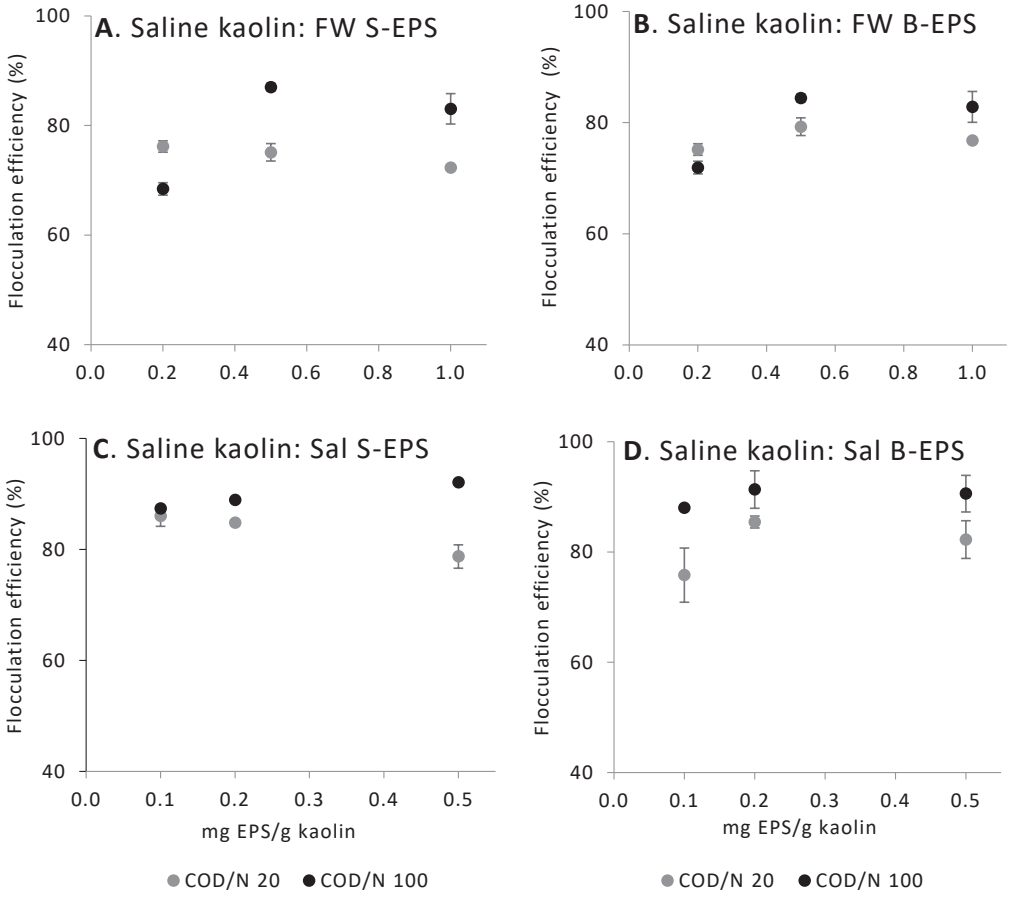

S6. Saline kaolin clay flocculation using EPS from COD/N ratio 20 and 100, with no addition of divalent cations. **A**) FW S-EPS: freshwater soluble-EPS, **B**) FW B-EPS: freshwater bound-EPS, **C**) Sal S-EPS: saline soluble-EPS, and **D**) Sal B-EPS: saline bound-EPS.

References

[1] H. Salehizadeh, N. Yan, Recent advances in extracellular biopolymer flocculants, Biotechnol. Adv. 32 (2014) 1506–1522. doi:10.1016/j.biotechadv.2014.10.004.

[2] F. Renault, B. Sancey, P.M. Badot, G. Crini, Chitosan for coagulation/flocculation processes - An eco-friendly approach, Eur. Polym. J. 45 (2009) 1337–1348. doi:10.1016/j.eurpolymj.2008.12.027.

[3] C.S. Lee, J. Robinson, M.F. Chong, A review on application of flocculants in wastewater treatment, Process Saf. Environ. Prot. 92 (2014) 489–508. doi:10.1016/j.psep.2014.04.010.

[4] B. Bolto, J. Gregory, Organic polyelectrolytes in water treatment, Water Res. 41 (2007) 2301–2324. doi:10.1016/j.watres.2007.03.012.

[5] T.T. More, J.S.S. Yadav, S. Yan, R.D. Tyagi, R.Y. Surampalli, Extracellular polymeric substances of bacteria and their potential environmental applications, J. Environ. Manage. 144 (2014) 1–25. doi:10.1016/j.jenvman.2014.05.010.

[6] M. Shahadat, T.T. Teng, M. Rafatullah, Z.A. Shaikh, T.R. Sreekrishnan, S.W. Ali, Bacterial bioflocculants: A review of recent advances and perspectives, Chem. Eng. J. 328 (2017) 1139–1152. doi:10.1016/j.cej.2017.07.105.

[7] D.C. Sobeck, M.J. Higgins, Examination of three theories for mechanisms of cation-induced bioflocculation, Water Res. 36 (2002) 527–538. doi:10.1016/S0043-1354(01)00254-8.

[8] V. Ajao, H. Bruning, H. Rijnaarts, H. Temmink, Natural flocculants from fresh and saline wastewater: Comparative properties and flocculation performances, Chem. Eng. J. 349 (2018) 622–632. doi:10.1016/j.cej.2018.05.123.

[9] B. Durmaz, F.D. Sanin, Effect of carbon to nitrogen ratio on the physical and chemical properties of activated sludge, Environ. Technol. 24 (2003) 1331–1340. doi:10.1080/09593330309385677.

[10] A.P. Miqueleto, C.C. Dolosic, E. Pozzi, E. Foresti, M. Zaiat, Influence of carbon sources and C/N ratio on EPS production in anaerobic sequencing batch biofilm reactors for wastewater treatment, Bioresour. Technol. 101 (2010) 1324–1330. doi:10.1016/j.biortech.2009.09.026.

[11] S. Feng, N. Zhang, H. Liu, X. Du, Y. Liu, H. Lin, The effect of COD/N ratio on process performance and membrane fouling in a submerged bioreactor, Desalination. 285 (2012) 232–238. doi:10.1016/j.desal.2011.10.008.

[12] F. Ye, Y. Ye, Y. Li, Effect of C/N ratio on extracellular polymeric substances (EPS) and physicochemical properties of activated sludge flocs, J. Hazard. Mater. 188 (2011) 37–43. doi:10.1016/j.jhazmat.2011.01.043.

[13] Z. Wang, M. Gao, S. Wang, Y. Xin, D. Ma, Z. She, Z. Wang, Q. Chang, Y. Ren, Effect of C/N ratio on extracellular polymeric substances of activated sludge from an anoxic–aerobic sequencing batch reactor treating saline wastewater, Environ. Technol. 35 (2014) 2821–2828. doi:10.1080/09593330.2014.924563.

[14] M. DuBois, K. a. Gilles, J.K. Hamilton, P. a. Rebers, F. Smith, Colorimetric method for determination of sugars and related substances, Anal. Chem. 28 (1956) 350–356. doi:10.1021/ac60111a017.

[15] W.F. Tan, W. Norde, L.K. Koopal, Humic substance charge determination by titration with a flexible cationic polyelectrolyte, Geochim. Cosmochim. Acta. 75 (2011) 5749–5761. doi:10.1016/j.gca.2011.07.015.

[16] S.J. Yuan, M. Sun, G.P. Sheng, Y. Li, W.W. Li, R.S. Yao, H.Q. Yu, Identification of key constituents and structure of the extracellular polymeric substances excreted by *Bacillus megaterium* TF10 for their flocculation capacity, Environ. Sci. Technol. 45 (2011) 1152–1157. doi:10.1021/es1030905.

[17] P.L.L. Ribeiro, M.I. Campos, J.I. Druzian, Novel extracellular polymeric substances produced by *Cupriavidus necator* IPT 027 grown on glucose and crude glycerol originated from biodiesel, Polym. Adv. Technol. 28 (2017) 549–556. doi:10.1002/pat.3957.

[18] C.S. Laspidou, B.E. Rittmann, A unified theory for extracellular polymeric substances, soluble microbial products, and active and inert biomass, Water Res. 36 (2002) 2711–2720. doi:10.1016/S0043-1354(01)00414-6.

[19] Z.-J. Zhang, S.-H. Chen, S.-M. Wang, H.-Y. Luo, Characterization of extracellular polymeric substances from biofilm in the process of starting-up a partial nitrification process under salt stress, Appl. Microbiol. Biotechnol. 89 (2011) 1563–1571. doi:10.1007/s00253-010-2947-y.

[20] J.B. Russell, The energy spilling reactions of bacteria and other organisms, J. Mol. Microbiol. Biotechnol. 13 (2007) 1–11. doi:10.1159/000103591.

[21] D.W. Tempest, O.M. Neijssel, Eco-Physiological Aspects of Microbial Growth in Aerobic Nutrient-Limited Environments, (1978) 105–153. doi:10.1007/978-1-4615-8222-9_3.

[22] H.-C. Flemming, J. Wingender, The biofilm matrix, Nat. Publ. Gr. 8 (2010) 623–633. doi:10.1038/nrmicro2415.

[23] K. Nouha, N.V. Hoang, R.D. Tyagi, Fourier Transform Infrared Spectroscopy and Liquid Chromatography – Mass Spectrometry Study of Extracellular Polymer Substances Produced on Secondary Sludge Fortified with Crude Glycerol, J. Mater. Sci. Eng. 5 (2016) 1–10. doi:10.4172/2169-0022.1000240.

[24] J. Lin, C. Harichund, Production and characterization of heavy-metal removing bacterial bioflocculants, African J. Biotechnol. 11 (2012) 9619–9629. doi:10.5897/AJB11.1698.

[25] S.P. Buthelezi, A.O. Olaniran, B. Eillay, Production and characterization of bioflocculants from bacteria isolated from wastewater treatment plant in South Africa, Biotechnol. Bioprocess Eng. 15 (2010) 874–881. doi:10.1007/s12257-009-3002-7.

[26] W. Babel, R.H. Muller, Mixed Substrate Utilization in Micro-organisms: Biochemical Aspects and Energetics, Microbiology. 131 (1985) 39–45. doi:10.1099/00221287-131-1-39.

[27] T.P. Pirog, M.A. Kovalenko, Y. V. Kuz'minskaya, Intensification of exopolysaccharide synthesis by *Acinetobacter* sp. on an ethanol-glucose mixture: Aspects related to biochemistry and bioenergetics, Microbiology. 72 (2003) 305–312. doi:10.1023/A:1024247915758.

[28] M.S. Nasser, A.E. James, The effect of polyacrylamide charge density and molecular weight on the flocculation and sedimentation behaviour of kaolinite suspensions, Sep. Purif. Technol. 52 (2006) 241–252. doi:10.1016/j.seppur.2006.04.005.

[29] B.J. Lee, M.A. Schlautman, E. Toorman, M. Fettweis, Competition between kaolinite flocculation and stabilization in divalent cation solutions dosed with anionic polyacrylamides, Water Res. 46 (2012) 5696–5706. doi:10.1016/j.watres.2012.07.056.

[30] J.I. Houghton, J. Quarmby, T. Stephenson, Municipal wastewater sludge dewaterability and the presence of microbial extracellular polymer, Water Sci. Technol. 44 (2001) 373–379. doi:10.2166/wst.2001.0792.

[31] J. Gregory, S. Barany, Adsorption and flocculation by polymers and polymer mixtures, Adv. Colloid Interface Sci. 169 (2011) 1–12. doi:10.1016/j.cis.2011.06.004.

[32] S. Bala Subramanian, S. Yan, R.D. Tyagi, R.Y. Surampalli, Extracellular polymeric substances (EPS) producing bacterial strains of municipal wastewater sludge: Isolation, molecular identification, EPS characterization and performance for sludge settling and dewatering, Water Res. 44 (2010) 2253–2266. doi:10.1016/j.watres.2009.12.046.

[33] K. Nouha, N. Hoang, Y. Song, R. Tyagi, S. RY, Characterization of Extracellular Polymeric Substances (EPS) Produced by *Cloacibacterium normanense* Isolated from Wastewater Sludge for Sludge Settling and Dewatering, J. Civ. Environ. Eng. 5 (2015) 1–8. doi:10.4172/2165-784X.1000191.

[34] S. Takahashi, J. Tomita, K. Nishioka, T. Hisada, M. Nishijima, Development of a prokaryotic universal primer for simultaneous analysis of Bacteria and Archaea using next-generation sequencing, PLoS One. 9 (2014) 1–9. doi:10.1371/journal.pone.0105592.

[35] J.G. Caporaso, J. Kuczynski, J. Stombaugh, K. Bittinger, F.D. Bushman, E.K. Costello, N. Fierer,

A.G. Peña, J.K. Goodrich, J.I. Gordon, G.A. Huttley, S.T. Kelley, D. Knights, J.E. Koenig, R.E. Ley, C.A. Lozupone, D. Mcdonald, B.D. Muegge, M. Pirrung, J. Reeder, J.R. Sevinsky, P.J. Turnbaugh, W.A. Walters, J. Widmann, T. Yatsunenko, J. Zaneveld, R. Knight, QIIME allows analysis of high- throughput community sequencing data, Nat. Publ. Gr. 7 (2010) 335–336. doi:10.1038/nmeth0510-335.

[36] C. Quast, E. Pruesse, P. Yilmaz, J. Gerken, T. Schweer, P. Yarza, J. Peplies, F.O. Glöckner, The SILVA ribosomal RNA gene database project: Improved data processing and web-based tools, Nucleic Acids Res. 41 (2013). doi:10.1093/nar/gks1219.

[37] R.C. Edgar, Search and clustering orders of magnitude faster than BLAST, Bioinformatics. 26 (2010) 2460–2461. doi:10.1093/bioinformatics/btq461.

[38] Q. Wang, G.M. Garrity, J.M. Tiedje, J.R. Cole, Naïve Bayesian classifier for rapid assignment of rRNA sequences into the new bacterial taxonomy, Appl. Environ. Microbiol. 73 (2007) 5261–5267. doi:10.1128/AEM.00062-07.

[39] Molecular Probes, Pro-Q ® Emerald 300 Glycoprotein Gel and Blot Stain Kit Emerald 300 Glycoprotein Gel and Blot Stain Kit (P21857), Invit. Eur. Hqrs. (2007) 1–4.

Chapter 4

Microbial extracellular polymer production from various substrates mimicking industrial wastewaters: polymer properties and microbial community

Authors:

V. Ajao [a,b], M.C. Gagliano [a], M. Rogowska [c], P. van Veelen [a], M.A. Kabel [d], P. de Gijsel [d], H. Bruning [b], H.H.M. Rijnaarts [b], H. Temmink [a,b]

[a.] Wetsus – European Centre of Excellence for Sustainable Water Technology, Oostergoweg 9, 8911MA Leeuwarden, the Netherlands.

[b.] Sub-department of Environmental Technology, Wageningen University and Research, Bornse Weilanden 9, 6708 WG Wageningen, the Netherlands.

[c.] Wageningen University and Research, Laboratory of Food Microbiology, Bornse Weilanden 9, 6708 WG Wageningen, the Netherlands.

[d.] Wageningen University and Research, Laboratory of Food Chemistry, Bornse Weilanden 9, 6708 WG Wageningen, the Netherlands.

Abstract

Microorganisms that degrade organics in (waste)water also excrete biopolymers referred to as extracellular polymeric substances (EPS). New uses are increasingly found for such EPS in various industries. In this study, we showed how single substrates (glycerol, glucose, acetate, ethanol) and mixtures of two substrates non-equivalent in terms of bioenergetics, influenced mixed-cultured EPS recovery and characteristics. EPS were produced and harvested from membrane bioreactors treating nitrogen-limited (COD/N ratio 100) synthetic wastewater containing the aforementioned substrates. The reactors showed high COD removal and the ratios between the biomass-COD, EPS-COD, and oxidised COD fractions depended on the utilised substrate and the microbial community developed per substrate. Overall, the glycerol-based substrates resulted in the highest EPS recoveries (28 - 45 % of influent-COD recovered as EPS-COD), followed by the glucose-based substrates (25 - 30 %), while the reactors fed with sole ethanol (11%) and acetate/ethanol showed the lowest EPS yields (3 - 11 %). With substrates of acetate and acetate/ethanol mixture, the formation of polyhydroxyalkanoates were observed, which likely decreased EPS production. Although the addition of ethanol as an auxiliary substrate to acetate increased EPS recovery from 3% (sole acetate) to 11% (acetate/ethanol ratio 1:1), reduced EPS recoveries were obtained when ethanol was added to glycerol and glucose substrates. Surprisingly, a higher EPS recovery (69%) was obtained when a mixture of acetate and ethanol was fed to the microbial community already producing high EPS yield from glycerol-based substrates. Microbial community analysis via Next Generation Sequencing (NGS) of 16S rRNA gene revealed the growth of different and diverse communities of EPS-producing bacteria (mostly at the genus level) per reactor, as well as possible EPS-degraders. Furthermore, this study shows the possibility to employ different substrates to modulate basic EPS properties (namely monosaccharide composition, molecular weight and charge density), which is interesting for certain EPS applications such as for particle flocculation, heavy metal adsorption and as additives in the food industry.

1. Introduction

Microorganisms responsible for the biological degradation of organics in wastewater excrete biopolymers, generally referred to as extracellular polymeric substances (EPS). EPS have received increasing attention for water and wastewater treatment applications such as particle flocculation [1,2], heavy metal adsorption [3,4], toxic organic chemical removal [1] and dye decolourisation [1]. This is due to their interesting properties, namely biodegradability, non-toxicity, amphiphilicity, high molecular weight, and cation binding capacity (because of their net anionic charge). However, these properties (specifically amphiphilicity, molecular weight and surface charge) and EPS yield depend on several factors such as the carbon source and carbon/nitrogen ratio of the feed [1,5], the reactor's redox condition (aerobic or anaerobic) [6], solids retention time (SRT) [7], and the microbial community which is determined by the aforementioned factors [8]. In relation to the reactor condition, aerobic systems have been reported to favour EPS production compared to anaerobic systems [1,9,10], probably due to a higher energy gain in the presence of oxygen; hence, more energy is available for microbial EPS synthesis.

Recently, we reported the effect of carbon/nitrogen ratio on the EPS produced from glycerol/ethanol-rich wastewater [5]. Nitrogen limitation (at a chemical oxygen demand (COD)/nitrogen ratio of 100) coupled with a relatively short SRT (3 days) were crucial for high EPS recovery (up to 54% influent-COD recovered as EPS-COD), and at the same time, excellent COD removal was achieved. At a relatively short SRT, wastewater-COD mineralisation is minimised and under nitrogen-limited conditions, excess energy is converted to extracellular polymers, especially polysaccharides (which do not contain the growth-limiting nutrient – in this case, nitrogen) [11], possibly as a means to store carbon under unbalanced carbon/nitrogen ratios [12].

Aside from nitrogen limitation, the types of carbon substrate (and wastewater generally consist of mixtures of substrates) also have a major influence on microbial EPS synthesis [11,13]. Babel and Muller [13] proposed the theory of energy non-equivalent substrates and classified all cellular growth substrates as either energy excessive or deficient based on the amount of ATP and reducing equivalents formed in the synthesis of phosphoglyceric acid – the key precursor for the synthesis of all cellular components. The combination of both substrate types was reported to enhance both microbial biomass and EPS production [14]. Since this theory seems to hold for bacterial strains that produce EPS [14], this principle was used in the present study to select substrate mixtures for EPS production from mixed cultures.

Based on the approach of producing EPS from wastewater, a proposed advantage is the use of mixed cultures, which do not require sterile conditions, unlike pure cultures. From a wastewater resource recovery point of view, it is important to study the wastewater types that can be valorised to EPS, how different wastewater types can be combined to intensify microbial EPS production, and the properties of EPS that may be specific to certain wastewater types (substrate mixtures). These could provide insights on the suitable wastewater types that give a high EPS yield and how to tailor EPS production for a specific application or a range of applications (based on the produced EPS characteristics) using a given substrate. For instance, wastewater rich in a substrate that leads to

the production of high molecular weight (> 1 MDa) EPS may be more interesting for the flocculant industry [15] and one that produces uronic acid-rich EPS may be more attractive as additives (emulsifiers or thickeners) for the food industry [16] or for adsorbing heavy metals [4]. In this study, glycerol, glucose, acetate and ethanol were selected as carbon sources for the microorganisms in four membrane bioreactors (MBRs), to mimic respective wastewaters from the biodiesel industry [17], soda/sugar beet industry, pulp and paper industry [18], and liquor industry. The reactors were operated starting from the same inoculum, and the EPS production and composition were monitored after each substrate-fed operation. The associated microbial communities that developed in time were analysed by means of Next Generation Sequencing (NGS) of 16S rRNA gene.

This study was aimed to: 1) provide insights on the suitable wastewater types to obtain high EPS recovery, 2) verify if the addition of an auxiliary energy-excessive substrate (ethanol) to energy-deficient substrates (glycerol, glucose and acetate) [13] would increase EPS recovery in a mixed culture reactor, 3) examine the characteristics (composition, molecular weight, charge density) of the various types of EPS formed from different wastewater substrates, and 4) investigate the microbial communities that developed from each substrate (mixture) at the genus level.

2. Materials and methods

2.1. Reactor operation, wastewater composition and chemical analysis

Four submerged MBRs (3.3 L effective volume per reactor) were operated in parallel, each treating synthetic wastewaters composed of different carbon sources (Table 1). MBRs were employed to retain and concentrate the produced EPS. Each reactor comprised a PVDF flat sheet membrane (membrane cartridge type 203, Kubota, Japan) with a nominal pore size of 0.2 μm [2]. The reactors were operated at a room temperature of 20 ± 1 °C, a pH of 7.5 ± 0.3, a dissolved oxygen concentration of 3 ± 1 mg O_2/L, and an SRT of 2 days. Level controllers were used to control the influent flow and the working volume of each reactor due to the periodic fouling of the membrane, which influenced the hydraulic retention time, HRT (HRT varied between 5.7 and 7.9 h – Table 1). The reactors (R1, R2, R3 and R4 – Table 1) were inoculated with aerobic sludge from a municipal wastewater treatment plant (WWTP) located in Leeuwarden, Netherlands. There was no re-inoculation when feeds were changed in each reactor.

The reactors were operated under a nitrogen-limited condition (COD/N ratio 100 ± 10, calculated based on g COD/g total nitrogen) since this condition has been reported to enhance EPS yield [5,11]. The influent COD was 600 ± 25 mg/L, mainly provided from the carbon sources listed in Table 1. The main nitrogen source was NH_4Cl (18.1 ± 1.0 mg/L) and yeast extract (12 mg/L) contributed 10.5% of the total nitrogen content. The nutrient medium composition per litre of tap water comprised 203 mg $MgCl_2 \cdot 6H_2O$, 147 mg $CaCl_2 \cdot 2H_2O$, 15 mg K_2HPO_4, 25 mg KH_2PO_4 (COD/P ratio 70 ± 2), and 2 mL trace elements solution (the composition of trace elements has been reported by Ajao *et al*. [2]). The COD of the nutrient medium was considered in the influent COD. COD, total nitrogen and NH_4-N concentrations of the wastewater and reactor effluents were determined using Hach Lange test kits (LCK, Hach Lange, UK).

The COD mass balance was calculated based on the fraction of the influent COD that ended up in the reactor effluent and waste sludge, while the oxidised COD was estimated as the closure of the

mass balance. The COD of the waste sludge was further fractionated into EPS-COD and biomass-COD (Biomass-COD = COD of waste sludge - EPS-COD).

2.2. EPS extraction

The reactors were operated for a period of at least three times the SRT [7], after which EPS were extracted from 1000 mL of sludge. The soluble EPS (S-EPS) were harvested by centrifugation and the bound EPS (B-EPS) were extracted with a cation exchange resin – the detailed extraction protocol has been described elsewhere [5]. Extracted EPS were dialysed and freeze-dried to obtain dry solids. Dried EPS were weighed and measured for COD content using the Hach Lange test kits. EPS recovery was based on the influent COD using the equation:

$$EPS\ recovery\ (\%) = \frac{Q_{was} * C_{EPS}}{Q_{inf} * COD_{inf}} * COD(EPS) \qquad (1)$$

where Q_{was} and Q_{inf} are the flow rates (L/d) of the waste sludge and influent feed respectively, C_{EPS} is the harvested EPS concentration (g/L sludge), COD_{inf} is the influent COD (g/L), and *COD(EPS)* is the COD of extracted EPS (g COD/g EPS).

Table 1. Feed type, concentration and hydraulic retention time (HRT) of each reactor.

Reactor	Carbon source(s)	Concentration of carbon source (mg/L)	HRT (h)
Reactor 1 (R1)	Glycerol/ethanol (4:1)[a]	394.7 / 57.6	7.9
	Glycerol/ethanol (1:1)[a]	246.7 / 144.0	5.7
	Glycerol	493.4	6.5
	Acetate/ethanol (4:1)[a]	1020.6 [b]/ 57.6	5.8
	Acetate	1276.6 [b]	6.1
Reactor 2 (R2)	Acetate	1276.6 [b]	6.5
	Acetate/ethanol (4:1)[a]	1020.6 [b]/ 57.6	5.7
	Acetate/ethanol (1:1)[a]	384.6 [b]/ 144.0	5.8
Reactor 3 (R3)	Glucose	563.0	6.5
	Glucose/ethanol (1:1)[a]	281.5 / 144.0	7.1
Reactor 4 (R4)	Ethanol	287.9	5.8

[a] Ratio based on g COD carbon source 1: g COD carbon source 2.

[b] Mass of acetate reported as Na acetate.

2.3. EPS characterisation

2.3.1. Protein quantification

The total protein content of the dried EPS was determined in triplicates using a bicinchoninic acid (BCA) assay kit (Thermo Scientific, USA). The assay was performed in a microplate, where 25 µL of EPS solution (dissolved in a phosphate buffer saline, pH 7.4 [2]) or bovine serum albumin, BSA (used as a standard protein) was mixed with 200 µL of BCA working reagent and incubated at 37 °C for 30 min. Afterward, the absorbance was measured at 570 nm using a spectrophotometer (Victor3 1420 Multilabel Counter, Perkin Elmer, USA). Protein concentration values are given as BSA equivalent units.

2.3.2. EPS sugar composition and quantification

Previous studies under the same nitrogen-limited condition reveal polysaccharides as the main biopolymer [4,5]. Hence, it was important to further analyse the polysaccharide composition of both the soluble and bound EPS fractions.

Neutral sugar composition was determined in duplicates according to Englyst and Cummings [19]. Briefly, after a pre-hydrolysis with 72% (w/w) H_2SO_4 for 1 h at 30 ^oC, the dried samples were hydrolysed with 1 M H_2SO_4 at 100 ^oC for 3 h. The monosaccharides were derivatised to their alditol acetates and analysed by gas chromatography (Focus-GC, Thermo Scientific, Waltham, MA, USA). Inositol was used as the internal standard [20] and the monosaccharide standards used for comparison were composed of L-rhamnose monohydrate, L-fucose, D-arabinose, D-xylose, D-mannose, D-galactose and D-glucose.

After the hydrolysis step, the uronic acid content was determined in duplicates according to the automated colorimetric m-hydroxydiphenyl assay [21] using an auto-analyser (Skalar Analytical B.V., Breda, Netherlands). Galacturonic acid was used for calibration [20].

2.3.3. Molecular weight determination

EPS solution was first passed through a 0.45 µm hydrophilic polytetrafluoroethylene filter (purchased from Merck, Netherlands) before molecular weight determination using liquid chromatography-organic carbon detection (LC-OCD – model 8, DOC-LABOR, Germany), which has been described elsewhere [5].

2.4. Microbial community analysis

Sludge samples were taken from each reactor at the end of each feeding phase and stored at -20 °C until DNA extraction. Before the procedure, ~ 25 mL sludge was thickened by centrifuging for 5 min at 3750 rpm, and 500 mg of the pellet was transferred into a clean tube. The thickened biomass was washed several times with PBS and the resulting suspension was sonicated (40 kHz, 50 W, 30 s). Subsequently, genomic DNA was extracted using a FastDNA® SPIN kit for soil (MPBio, USA) according to the manufacturer's instructions. DNA concentration and purity were measured with the NanoDrop® spectrophotometer (Thermo Fisher Scientific, Germany).

DNA extracts were sent to MrDNA (Shallowater, USA) for PCR amplification, library preparation and sequencing. Universal primers 515F [22] and 926R [23] were applied to simultaneously amplify the V4-V5 hypervariable region of the prokaryotic 16S rRNA gene of bacteria and archaea. The HotStarTaq PCR Master Mix Kit (Qiagen, USA) was used for PCR, with a programme consisting of 3 min at 94 °C, followed by 30 cycles of 30 s at 94 °C, 40 s at 54 °C and 1 min at 72 °C, and a final elongation of 5 min at 72 °C. Amplicons were checked on 2% agarose gel, pooled in equimolar proportions and purified using AMPure XP beads (Agencourt, USA) before library preparation. The 16S rRNA gene sequences generated were 300 bp paired-end, using Illumina MiSeq sequencing with V3 chemistry (Illumina Inc., USA). Further details on QIIME2 [24] sequence data processing and sequencing statistics are reported in the supplementary information and Table S7. For the data presented in this study, we considered the most dominant ASVs (mean relative abundance > 0.1%), which comprised 72.8% of 417988 sequences generated from the reactor samples with a mean (± SE) coverage of 34832 ± 6993 sequences per sample.

The relative abundance of each microbial group above 1% detected after NGS analysis was utilised to calculate the biodiversity of the mixed microbial communities by means of Shannon–Weaver index of diversity (H') [25] and Pielou's evenness index [26].

3. Results

3.1. Reactors' performances and EPS production

During the reactors' operational period, effluent samples were analysed for COD and NH_4–N. High COD removal efficiencies (84 - 95 %, Fig. 1) were achieved by all the reactors even though nitrogen was clearly limiting (effluent NH_4–N concentration was in the range of 0.003 - 0.1 mg/L).

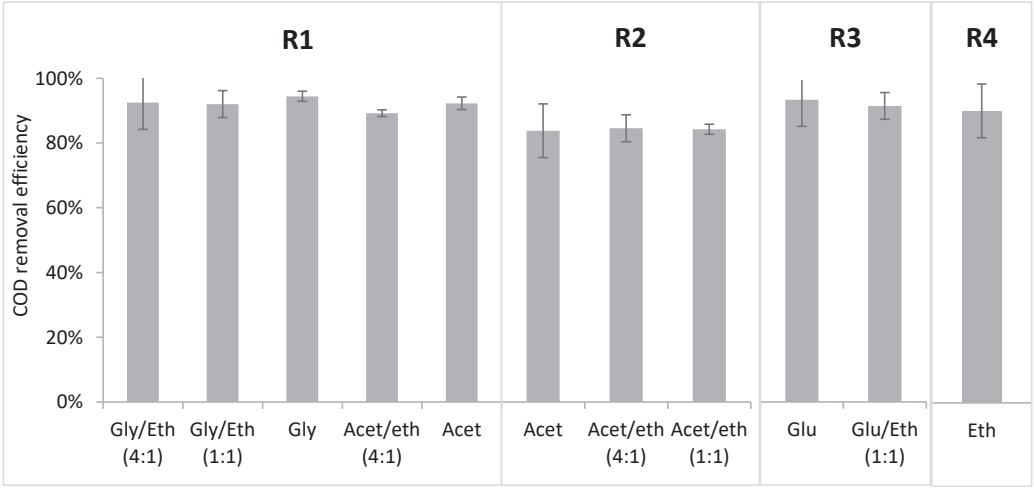

Fig. 1. COD removal efficiencies of the four reactors fed with different substrates. Data expressed as mean ± standard deviation of at least triplicate measurements at different days of operation. Gly: Glycerol; Eth: Ethanol; Acet: Acetate; Glu: Glucose. Displayed ratios are based on g COD carbon source 1**:** g COD carbon source 2.

This high COD removal confirms our previous finding [5], that reactors operating under nitrogen-limited conditions can achieve high COD removal efficiencies, partly because the influent soluble COD can be converted to EPS-COD, which is retained in the reactor by the membrane [5].

As shown in the COD mass balance in Fig. 2, a fraction of the influent COD was used for biomass production and a fraction was lost to oxidation. The ratios between the EPS-COD, biomass-COD, and oxidised COD fractions depend on the utilised substrates and microbial community. With respect to feeding the reactors with single substrates, the produced sludge-COD (comprising biomass- and EPS-COD) from glycerol, glucose and acetate_R1 (R1 – acetate was fed to an EPS-rich sludge, later discussed) were predominantly composed of EPS-COD (83, 81 and 65 %, respectively). For acetate_R2 (R2 – acetate was fed to an inoculum from a WWTP) and ethanol substrates, it was the other way round: 93 and 78 %, respectively, of the sludge-COD was from the biomass.

With the addition of ethanol as a co-substrate to glycerol and acetate_R2, no positive effect on the total biomass and EPS production was observed; however, there was a slight shift from biomass to EPS production with the increasing addition of ethanol to acetate_R2 (Fig. 2 – R2). On the other hand, the addition of ethanol to glucose increased sludge production from 37% to 71% (which was connected to the increased biomass production, not EPS), thereby decreasing the oxidised COD fraction. Similarly, ethanol addition to acetate_R1 increased sludge production from 21% to 77% (in this case, it was associated with increased EPS production, not biomass), thus reducing the fraction of oxidised COD. Overall, these findings show that, depending on the substrate, sludge-COD may predominantly consist of biomass instead of EPS, even under limited nitrogen and excess carbon. However, it is recognized that the biomass-COD here may include internal storage products such as polyhydroxyalkanoates (PHA), as will be discussed later.

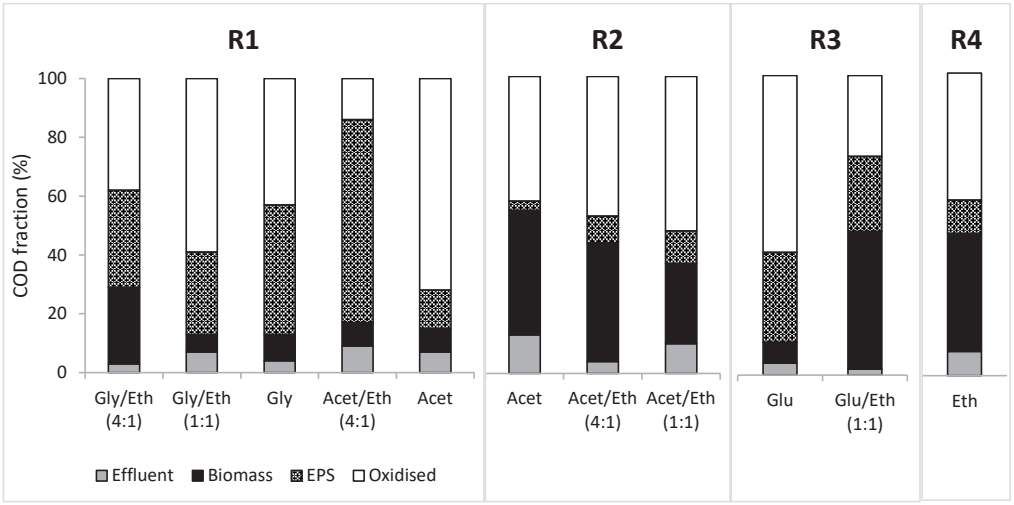

Fig. 2. COD distribution as a fraction of influent COD in the four reactors fed with different substrates. The legends in R1 are also applicable to R2, R3 and R4. Gly: Glycerol; Eth: Ethanol; Acet: Acetate; Glu: Glucose. Displayed ratios are based on g COD carbon source 1**:** g COD carbon source 2. Absolute values are reported in Table S1.

After a stable operation of the reactors (at least three times the SRT and when effluent COD values became consistent), soluble and bound EPS were extracted from the reactor mixed liquor. The concentrations and recovery of EPS in the reactors varied between 0.2 - 3.1 g/L sludge and 3 - 69 %, respectively (Fig. 3 and Fig. S1). Hence, EPS recovery was notably influenced by the type of carbon source(s), despite been operated under a similar nitrogen-limited regime, that has been reported to enhance EPS production [5]. Overall, the highest EPS recoveries were obtained with the glycerol-based substrates in R1 (28 - 45%), followed by the glucose-based substrates (R3, EPS recovery 25 - 30%), while the reactors fed with sole ethanol (11%) and acetate/ethanol showed the lowest EPS recoveries (3 - 11 %).

With glycerol and glucose as substrates, the (increasing) addition of ethanol unexpectedly led to lower EPS recoveries, in contrast to the auxiliary substrate concept proposed by Babel and Muller [13]. Although the recovery of B-EPS increased while that of S-EPS decreased with increasing ethanol addition (Fig. 3, R1 and R3), the total EPS recovery decreased, taking into account that the S-EPS fraction had a higher contribution (56 – 80%) to the total EPS produced. On the other hand, the addition of ethanol positively influenced the recovery of EPS from acetate (Fig. 3 – R2). The total EPS recovery increased from 3% with sole acetate to 8.6% and 10.6% in the acetate/ethanol ratios 4:1 and 1:1, respectively (Fig. 3, R2). In this case, both the S-EPS and B-EPS fractions had increased recoveries with ethanol addition. However, when acetate and acetate/ethanol (4:1) were fed to the microbial community of R1, which was already adapted to produce high concentrations of EPS from glycerol (Table 1), the EPS recovery with sole acetate was 13% (1% S-EPS, 12% B-EPS) and with acetate/ethanol (4:1), the reactor afforded a surprisingly high recovery of 69%, mainly composed of S-EPS (67%) (Fig. 3 – R1).

3.2. EPS characteristics

3.2.1. Chemical composition

Irrespective of the type of carbon source fed to the reactors, the produced EPS generally contained a higher polysaccharide (comprising neutral and acidic sugars) content than proteins (Fig. S2 and S3). In all the reactors, the harvested EPS-protein content was < 7.5 wt%, with the exception of the slightly higher values obtained for the S-EPS extracted from R1 when fed with Gly/Eth(1:1) (11.1 wt%) and the EPS extracted from R4 (S-EPS: 11.5 wt%, B-EPS: 17.5 wt%). The polysaccharide content reached up to 46.3 wt%, with the S-EPS containing a higher sugar content (28.1 – 46.3 wt%) than the corresponding B-EPS. It is worth mentioning that aside from the biopolymeric fractions (polysaccharides and proteins), EPS are expected to also contain other substances, such as acidic and neutral low molecular weight compounds that are encompassed in the total weight of the recovered EPS [2,27].

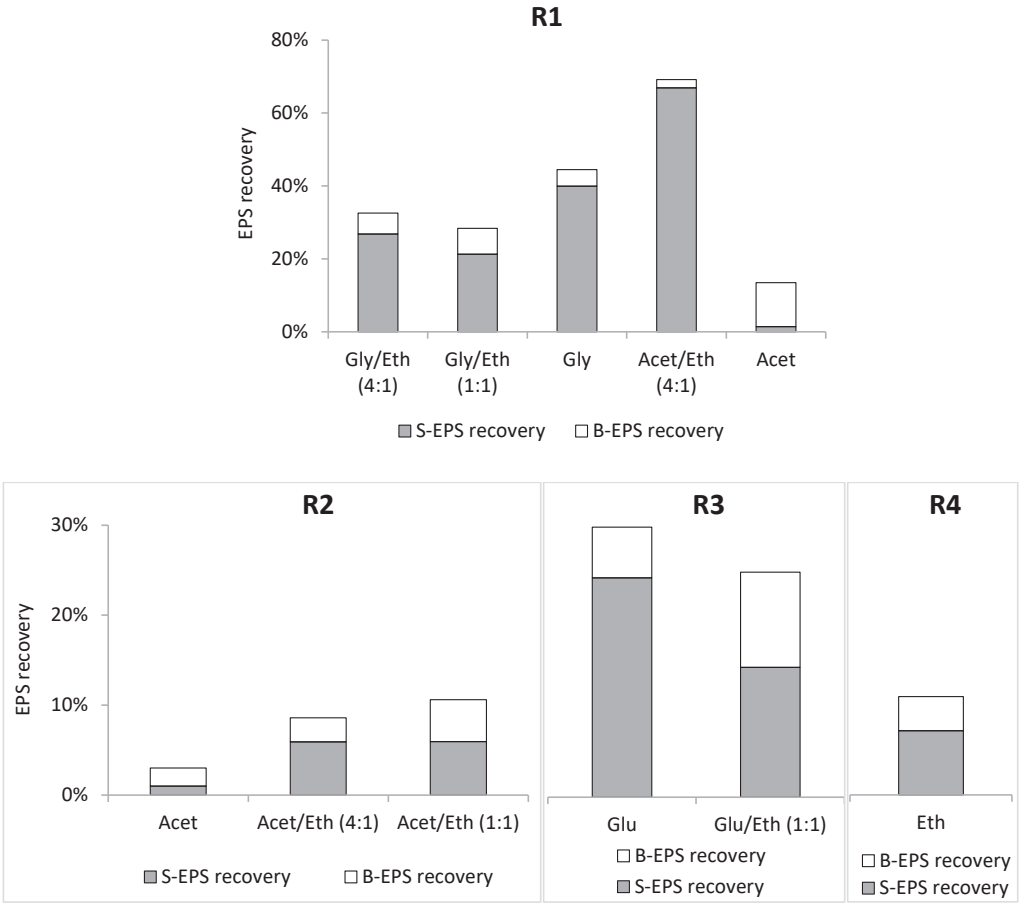

Fig. 3. EPS recoveries (influent COD recovered as EPS-COD) from the four reactors (R1, R2, R3 and R4) fed with different substrates. Gly: Glycerol; Eth: Ethanol; Acet: Acetate; Glu: Glucose. S-EPS: soluble-EPS; B-EPS: bound EPS. Displayed ratios are based on g COD carbon source 1**:** g COD carbon source 2. Error bars are shown for the EPS concentrations in Fig. S1 (supplementary information).

The molar polysaccharide composition of the various EPS' fractions is presented in Fig. 4. Soluble and bound EPS produced from the same carbon source contained the same monosaccharides in a similar proportion, while the EPS produced from different substrates varied in composition and proportion. The EPS produced with glycerol as the sole carbon source contained uronic acids as the main monosaccharides (51 - 58 mol%), but with ethanol as a co-substrate in the ratio 4:1 (glycerol/ethanol ratio), glucose and galactose became the dominant monosaccharides, while uronic acid content decreased to ~ 18 mol%. When the glycerol/ethanol ratio decreased from 4 to 1, the galactose content reduced significantly and again, uronic acids became the dominant residues in the EPS fraction (43 - 47 mol%). With acetate and acetate/ethanol substrates (R1), the synthesised EPS were mainly composed of mannosyl and galactosyl residues, whereas the EPS produced in R4 (ethanol-fed reactor) had a fairly uniform distribution of the main monosaccharides: mannose,

galactose, fucose, rhamnose, glucose and uronic acids. There was also a uniform distribution of the main monosaccharides (fucose, mannose, galactose, glucose, uronic acids) in the EPS produced with Glu/Eth (1:1) as the substrate in R3. With glucose as the only carbon source, the produced EPS were majorly composed of mannosyl residues, and only the EPS produced from this substrate were composed of significant amounts of pentoses (arabinosyl and xylosyl residues) – Fig. 4. Overall, the addition of ethanol as a co-substrate with glycerol, acetate and glucose led to an increase in the amount of rhamnose in both the soluble and bound EPS.

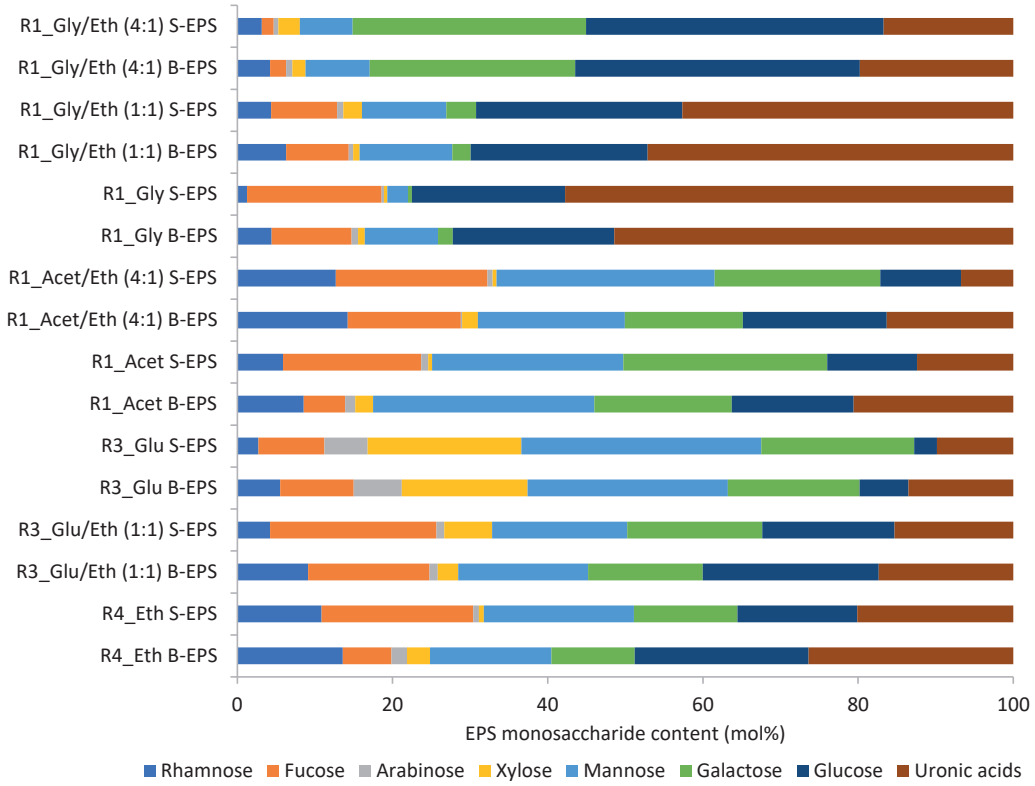

Fig. 4. Relative amounts (mol%) of EPS' monosaccharide composition produced from different substrates. Gly: Glycerol; Eth: Ethanol; Acet: Acetate; Glu: Glucose. S-EPS: soluble-EPS; B-EPS: bound EPS. Displayed ratios are based on g COD carbon source 1**:** g COD carbon source 2. Error bars are standard deviations of duplicate analysis.

3.2.2. Molecular weight (MW) and charge density

The average MWs of the EPS fractions produced from the different substrates are presented in Table 2. The MW values increased in the order: Glucose-based EPS (3.2 ± 0.2 MDa) > acetate-based EPS ≈ ethanol-fed EPS (2.6 ± 0.2 MDa) > glycerol-based EPS (1.6 ± 0.2 MDa). This order cannot be explained based on the polysaccharide or protein content (wt% – Fig. S2 and S3) because, for

instance, the B-EPS produced from sole glucose had the highest MW value but not the highest polysaccharide or protein content (18 wt% total polysaccharides and 5.3 wt% total proteins). Although it is not entirely clear from this study why one substrate affords a higher or lower MW EPS than the other, one inference from this result is that substrates that lead to very high EPS recoveries do not necessarily produce EPS with the highest MWs. Moreover, the addition of ethanol as a co-substrate to glycerol, glucose and acetate did not significantly alter the MW when compared with the EPS produced from the single substrates. Lastly, the MW results in Table 2 reveal that both the bound and corresponding soluble EPS fraction have similar MWs.

Aside from MW, charge density is another property of EPS that determines its suitability as a flocculant and as a heavy metal adsorbent [2,4]. The charge density results presented in Table S2 reveal that the anionic charge density of EPS increased with the content of uronic acids (Fig. 4). The S-EPS produced from sole glycerol had the highest uronic acid content and a high charge density value of 6.7 meq/g (at EPS solution pH of 7), whereas the S-EPS from Acet/Eth (4:1) with the lowest uronic acid content had a low charge density value of 2 meq/g at the same pH.

Table 2. Average molecular weights (MWs) of the EPS biopolymer fraction produced from different substrates.

Substrate (Reactor)	EPS fraction	Average MW (MDa)
Glycerol (R1)	S-EPS	1.72 ± 0.04
	B-EPS	1.50 ± 0.16
Glycerol/ethanol (1:1) (R1)	S-EPS	1.78 ± 0.14
	B-EPS	1.69 ± 0.14
Acetate (R1)	S-EPS	2.49 ± 0.07
	B-EPS	2.50 ± 0.02
Acetate/ethanol (4:1) (R1)	S-EPS	2.71 ± 0.03
	B-EPS	2.41 ± 0.09
Glucose (R3)	S-EPS	3.02 ± 0.08
	B-EPS	3.30 ± 0.09
Glucose/ethanol (1:1) (R3)	S-EPS	3.22 ± 0.10
	B-EPS	3.23 ± 0.37
Ethanol (R4)	S-EPS	2.61 ± 0.14
	B-EPS	2.55 ± 0.12

3.3. Microbial community composition

A microbial community analysis by NGS was carried out on the inoculum sample and samples taken from all the reactors at the end of each feeding phase (Table 1). Each reactor was started from the same inoculum, where the most important bacterial groups were affiliated to the genera *Trichococcus* and *Acinetobacter* (27.5 and 24.5%, respectively) (Table S3). From this profile, very different bacterial populations developed in time in all the reactors, changing significantly when fed with the different substrates. The changes in community structure with each substrate are summarised in Fig. 5 and detailed in Tables S3, S4, S5 and S6 (supplementary information).

In Reactor 1, in the first phase fed with glycerol/ethanol (4:1), *Rickettsiales* SM2D12 (24.2%) and *Xanthobacter* (9.4%) were the dominant groups, followed by family *Burkholderiaceae* (8.7%) and genus *Acinetobacter* (7.6%). With the decrease of glycerol substrate and increase in ethanol (glycerol/ethanol (1:1)), *Luteolibacter,* which was 3% relatively abundant in the 4:1 ratio became highly dominant (40.7%). *Rickettsiales* SM2D12 decreased to 0.4% while *Xanthobacter* and *Acinetobacter* were not detected. Feeding only on glycerol, *Luteolibacter* decreased to a relative abundance of 14%, and the genus *Mucilaginibacter* (27.5%) was rather dominant. *Acinetobacter* (19.8%), *Burkholderiaceae* (15.8%) and *Caulobacter* (12.6%) were the three dominant groups with Acetate/Ethanol (4:1), while *Luteolibacter* (0.4%) and *Mucilaginibacter* (0.2%) became rare. After feeding with only acetate, *Acinetobacter* decreased to 8.3%, with *Erysipelothrix* and *Verrucomicrobium* as the dominant genera (relative abundance of 29.8% and 22.8%, respectively).

In Reactor 2, where the inoculum was first exposed to sole acetate as substrate, *Erysipelothrix* was the main genus (33%), which was also observed in R1 when fed with acetate. When ethanol was added as a co-substrate (acetate/ethanol (4:1)), the number of core OTUs decreased in comparison to the population grown with sole acetate (Table S7), and an increased number of dominant populations developed (Fig. 5). *Erysipelothrix* decreased from 33% to 1.4% and the dominant groups under this condition were the family *Burkholderiaceae* (17.9%) and genera *Romboutsia* (17%) and *Acinetobacter* (13.5%).

In Reactor 3, we observed the most evident influence of substrate change on the number of core OTUs with respect to ethanol as a co-substrate or not (Table S7). When glucose was the sole substrate, *Acinetobacter* (28.5%) was the dominant genus, as also observed in R1 with Acet/Eth (4:1) as substrate (Fig. 5). After ethanol addition (glucose/ethanol (1:1)), core OTUs number (≥ 1%) increased from 10 to 21 (Table S7), with a variety of dominant groups represented by the genera *Flectobacillus* (13.1%), *Sphaerotilus* (11.8%) and *Hydrogenophaga* (11.4%), while *Acinetobacter* decreased to 1.4%.

Reactor 4 was fed with only ethanol (as a reference) for the whole operation time, after which the community was dominated by the family *Burkholderiaceae* (23.7%), which were detected multiple times in other reactors, particularly in reactors where ethanol was added to acetate (R1 and R2). Similarly, *Caulobacter, Romboutsia, Aeromonas*, *Hydrocarboniphaga*, *Sphingobium* and *Xanthobacter*, which were observed in some of the reactors co-fed with ethanol were also detected in R4 fed with sole ethanol (Fig. 5).

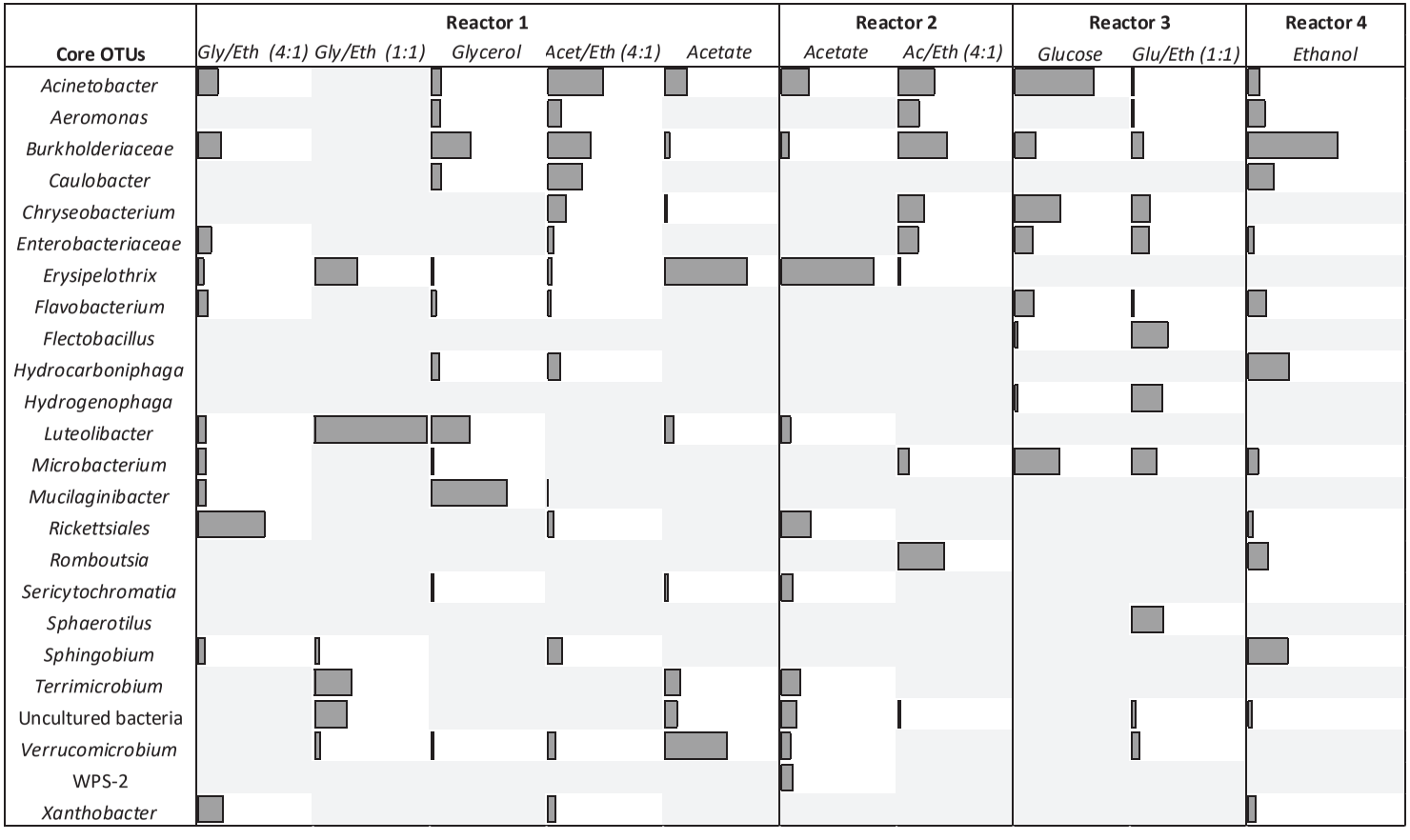

Fig. 5. The main microbial groups detected in all the four aerobic reactors and their relative abundances (as dark grey bars) presented in comparison to the substrates fed. Light grey spots indicate when the relative abundance of the microbial group was below 1% in the specific sample.

4. Discussion

4.1. Effect of substrates on EPS production

With the use of single substrates, EPS recovery was in the order Glycerol > Glucose >> Acetate (R1) > Ethanol > Acetate (R2). Apparently, the waste sludge produced from ethanol and acetate substrates were predominantly composed of biomass (including internal storage products, as discussed below) and not EPS (Fig. 2). Since there was no significant difference in the energy content of the substrates (-14.8 kJ/g COD glycerol, -14.5 kJ/g COD glucose, -14.2 kJ/g COD ethanol, -13.6 kJ/g COD acetate), the differences in EPS recovery may be better explained by the substrate incorporation into the cell/subsequent energy spilling [28] and the difference in metabolic pathways within the cells. Small uncharged molecules such as glycerol can cross the cell membrane via facilitated passive diffusion through its concentration gradient. On the other hand, the movement of most sugars and charged molecules such as acetate involves an active transport system whereby ATP hydrolysis is needed to gain energy to drive the substrate uptake against its concentration gradient [10,17]. In the latter case, it is likely that less energy is spilled (or remains) by microorganisms to synthesise secondary metabolites such as EPS (by the way, rapidly growing cells can spill as much as 25% of their ATP for the synthesis of secondary metabolites) [28]. In the case of ethanol as a substrate, its redox degree (-2) strongly deviates from the redox degree of carbon in EPS, which is zero. Hence, EPS production from ethanol requires net energy and this may justify the low EPS recovery from ethanol.

Another explanation for the significant difference in EPS yield per substrate is based on the different metabolic pathways involved in the biosynthesis of secondary metabolites. For instance, the biosynthesis of alginates involves the oxidation of a carbon source (usually carbohydrates) to acetyl-CoA, which enters the tricarboxylic acid (TCA) cycle where oxaloacetate is formed and subsequently converted to fructose-6-phosphate via gluconeogenesis [29]. Fructose-6-phosphate undergoes a series of transformations to form guanosine diphosphate-mannuronic acid – the nucleotide precursor for alginate synthesis [29]. Similar pathways have also been reported for the synthesis of other extracellular polymers such as xanthan gum and pullulan [30,31]. While glucose substrate must be converted to pyruvate via several steps and then oxidized to acetyl-CoA before entering the TCA cycle, glycerol conversion is possibly shorter and less energy-intensive. Glycerol can directly undergo gluconeogenesis (without entering the TCA cycle) to form dihydroxyacetone phosphate [17] and finally fructose-6-phosphate [11] or its analogue, which may be converted to the nucleotide precursor needed for EPS production. In the case of acetate as a substrate, it can be metabolised via the TCA cycle for cell growth and possibly EPS synthesis, or it can be channelled towards intracellular PHA production via the direct 'PhaABC' process [32,33]. The latter pathway is more probable under stress conditions such as nutrient limitation/starvation or aerobic dynamic feeding, where PHA production is energetically cheaper [34,35].

Although the addition of ethanol to acetate in R2 increased EPS recovery from 3% (sole acetate) to 10.6% (acetate/ethanol (1:1)), this is still a low value compared to the recovery values obtained from the glycerol (R1) and glucose-fed (R3) reactors. Through microscopic imaging (which by the

way is strictly qualitative), we observed PHA accumulation within the biomasses of the acetate-fed (Fig. S4 A and B) and acetate/ethanol (4:1)-fed of R2 (Fig. S4 C and D), and in R3 when fed with glucose (Fig. S4 E and F). But PHAs were not detected in the biomass from the glycerol-fed reactor. Furthermore, higher biomass-COD/EPS-COD ratios in R2 (fed with acetate and acetate/ethanol) were observed compared to the glycerol-based reactors (R1) (Fig. 2). These findings suggest that the production of EPS from acetate and acetate/ethanol under the studied conditions may have been less due to some level of carbon flux to intracellular PHA production. This is not particularly surprising since acetate is reported as a principal substrate for PHA production [36] and many species of heterotrophic bacteria can synthesise PHA under aerobic conditions [34,37]. Moreover, the start-up inoculum was obtained from a WWTP that employs a biological nutrient removal process. Hence, it naturally contains PHA-accumulating organisms, at least to some extent, which were further enriched when acetate was fed into R1 [38].

However, when the biomass producing high EPS yield in R1 (grown on glycerol) was fed with acetate and acetate/ethanol, EPS yield was higher than in R2, where the start-up inoculum was directly fed with acetate. Compared to R2, the influent COD channelled towards biomass production in R1 was considerably lower (8%, Fig. 2). Most of the influent COD in R1 was converted to EPS-COD (69%) when fed with Acet/Eth (4:1), and to oxidised-COD (about 72%) when fed with sole acetate. Although it is not entirely clear why the type of start-up biomass can significantly influence substrate effect on EPS production, a similar strategy has also been reported for PHA intensification, which involved the selection of a glycerol-fed enrichment culture and a subsequent PHA accumulation phase with acetate as the substrate [39]. Hence, the use of such enriched microbial cultures (EPS-rich sludge) may be a good strategy to intensify EPS production from substrate mixtures such as acetate/ethanol. However, this still needs to be verified with longer experiments and with various substrates, as this may pave the way for substrate versatility for EPS production.

Overall, although the addition of ethanol as an auxiliary substrate to acetate increased EPS recoveries, reduced recoveries were obtained when ethanol was added to glycerol and glucose substrates. Hence, the auxiliary substrate concept proposed by Babel and Muller [13] to intensify EPS production in pure cultures [14] may not be absolutely applicable for mixed cultures, particularly under nitrogen-limited conditions. Further experimental evidence (such as isotope labelling and tracing) will be needed to substantiate the (metabolic) roles of energy-excessive and deficient substrates for either EPS synthesis, PHA production or energy generation.

4.2. Microbial population and EPS recovery from different substrates

The microbial community analysis of 16S rRNA amplicon sequencing resolved the community composition mostly at the genus level, although in some cases, the major protagonists could only be classified at the family, order or phylum level (or even as uncultured bacteria). This is the case with the orders *Rickettsiales* and *Enterobacteriaceae*, and the family *Burkholderiaceae*. For this reason, a detailed understanding of the microbial dynamics in relation to the different substrates and EPS production is not possible. Nonetheless, interesting discussion points develop when comparing the relative abundances of the core OTUs, as summarised in Fig. 5. This discussion will

focus on the most relevant results in relation to the EPS recoveries, i.e. those obtained from R1 and R2 with glycerol- and acetate-based substrates.

The change in substrate fed into each reactor strongly influenced the composition of the microbial community, probably also stimulated by the strong selection pressure exerted by the relatively short SRT of 2 days, which causes the wash-out of slow-growing microorganisms. Considering the narrow substrate range, especially for the single substrates, the microbial diversity was high. However, no specific group was always dominant in the same reactor. In most cases, two or more possible EPS-producing genera developed within the same reactor when fed with different substrates.

Reactor 1, successively fed with the glycerol-based substrates Gly/Eth (4:1), Gly/Eth (1:1) and Gly gave relatively high EPS recoveries (28 – 45 %) (Fig. 3). This can be connected to the presence of EPS-producing genera *Xanthobacter* [40] and *Acinetobacter* [41,42] when fed with Gly/Eth (4:1), *Erysipelothrix* [43] and *Terrimicrobium* [44] when fed with Gly/Eth (1:1), and the genus *Mucilaginibacter* [45] when fed with Gly. Interestingly, although not surprising, known EPS degraders were found, in particular, *Luteolibacter* [46,47] when the feed consisted of Gly/Eth (1:1). Their presence implies that, when upscaling EPS production from mixed cultures, it should be taken into account that possible EPS-degraders may grow under high EPS production rates. How the presence of such EPS degraders affects the yield of EPS and how to control a reactor to avoid or minimise their presence is unknown, but it would be worthwhile to further investigate.

When acetate was used as a single substrate in both R1 and R2, the EPS producers *Acinetobacter* and *Erysipelothrix* were present, the latter even at significantly higher relative abundancy than with the glycerol-based substrates. In spite of this, the EPS recoveries were much lower (3 - 13 %). Under nitrogen-limited conditions and with acetate as a substrate, it is possible these genera, particularly *Acinetobacter* prefer to accumulate PHA (also see Section 4.1) over EPS excretion, or specific strains were enriched that have this preference [48,49]. Although *Erysipelothrix* has been reported to grow on acetate [50], there has been no report on its ability to accumulate PHA. Furthermore, the genus *Verrucomicrobium*, a known polysaccharide degrader [51,52] was present in R1 at significantly higher relative abundancy than in R2 when fed with sole acetate. This can be explained from the high EPS production that was observed during the previous feeding phase with Acet/Eth (4:1), which will be discussed below, but it also implies that the wash-out of this microorganism was much slower than expected based on an SRT of 2 days.

The most striking result was that the EPS recovery in R1 with Acet/Eth (4:1) was much higher (69%) than in R2 fed with the same substrate (11%). The only operational difference being the substrate that was previously fed to these reactors, i.e., glycerol in R1 and acetate in R2, which led to different microbial communities. The main difference in terms of microbial population is the presence of *Caulobacter*, *Sphingobium* and *Xanthobacter* in R1, members of which are known EPS producers [40,53,54]. However, no explanation is available why these genera were able to develop towards a high relative abundance in R1 but not in R2. Still, considering the very high EPS yield in R1, this outcome certainly deserves more research (also see Section 4.1). Nevertheless, the result suggests that feeding an inoculum with a substrate like glycerol could be the required step to develop a

microbial community able to maintain high EPS yield when switching to acetate-based substrates, especially in the presence of ethanol as a co-substrate.

4.3. Effect of substrates on EPS characteristics

Regardless of the fed carbon source, the produced EPS were complex in composition, comprising proteins, different carbohydrates (neutral and acidic), and other substances (neutral and acidic low molecular weight compounds [2,27]). Even when fed with single substrates, the synthesized EPS were heterogeneous in composition, most likely due to the complex microbial community that comprised various EPS-producers.

Under nitrogen-limited conditions, polysaccharides were found as the main biopolymer component, which agrees with our previous studies [4,5] and the reports of other researchers [55,56]. Consistent with other studies, exopolysaccharides produced from mixed-cultures are compositionally mixed (comprising different monosaccharides) [57], whether produced from single or dual substrates, as shown in this study. This study further demonstrates that the sugar composition and content of mixed-cultured EPS vary with the utilised substrate (Fig. 4 and Fig. S2). While ethanol, glycerol- and acetate- based substrates produced EPS with aldohexoses and uronic acids as the main sugar components, significant amounts of pentose sugars (arabinose and xylose) were found only in the glucose-based reactors, especially when glucose was used as the sole substrate. This differs from what has been obtained by a single bacterial strain that produces one type of EPS. For instance, Pirog *et al*. [41] showed that the EPS (ethapolan) synthesised by *Acinetobacter* sp. 12S were identical in monosaccharide composition and content regardless of the utilised carbon source (glucose, ethanol or their mixture).

The content of oxidised substituents (such as uronic acids) in the produced EPS gives an indication of the energy requirement per substrate during EPS biosynthesis. The higher the content of the oxidised groups, the lower the energy invested (instead energy is generated) by the microorganisms (compared to the synthesis of neutral exopolysaccharides) [14,58], perhaps further justifying why glycerol yields more EPS than the other substrates. Therefore, substrates such as glycerol that lead to the production of uronic acids as their main polysaccharide component are likely to be sufficient for both microbial cell growth and high EPS yield. This is because, the energy required for acidic exopolysaccharide synthesis can potentially come from both catabolism and the oxidation process when certain polysaccharide substituents (such as acidic groups) are formed [58].

This study further revealed the parallel between the soluble and bound EPS fractions of the same origin. Soluble and bound EPS produced from the same substrate had similar MW and were composed of the same sugar type in a somewhat similar proportion. These results suggest that both the soluble (sludge supernatant after centrifugation) and bound (attached to the microbial cells or flocs) EPS fractions are not different fractions but are fundamentally similar, at least biochemically, although their concentrations in a reactor may differ. This concurs with the proposition by Laspidou and Rittman [59] and Hsieh *et al* [60], that soluble EPS to a large extent are products (sheared-off or dissolved products) of the bound EPS.

4.4. Practical implications and outlook

The results of this study demonstrate that glycerol-rich (such as wastewater from the biodiesel industry) and glucose-rich wastewater (e.g., soda/sugar beet industrial wastewater) prove to be suitable wastewater types for substantial EPS recovery. Although substrates containing acetate (as found in pulp and paper industrial wastewater) showed low EPS recoveries, the use of an inoculum already adapted to produce high EPS yield may pave the way for substrate versatility for enhanced EPS production. However, this needs to be further investigated with much longer reactor operation times and additional analyses to assess the evolution and function of the microbial community members.

EPS produced from sole glycerol were mainly composed of uronic acids, consequently leading to a highly charged anionic biopolymer. The advantage of such EPS is their potential application as heavy metal adsorbents, where polymers with a high charge density are preferred for the ion-exchange mechanism [4]. Moreover, uronic acid-rich EPS are interesting for the food industry as thickeners or gelling agents, coupled with the non-Newtonian fluid behaviour of EPS produced from glycerol-based wastewater, as found in exopolysaccharides such as gellan gum [5,61]. Although for food application, clean (void of pollutants, heavy metals and pathogens) substrates and processes would be needed to produce mixed EPS that are rich in uronic acids.

The high MWs of the produced EPS (irrespective of the utilised carbon source) make them potential bioflocculants for particle removal. Since flocculation capabilities of anionic polymers generally increase with MW [62], it is expected that EPS produced from glucose-based substrates would show higher flocculation performance compared to EPS obtained from glycerol and acetate. However, this may not necessarily be the case since the MW differences are not significant (order of magnitude ~ 2) from a flocculation viewpoint.

5. Conclusions

This study confirms that the type of wastewater for the set conditions of nitrogen limitation not only affects the recoveries of microbial EPS but also the development of the microbial community that is responsible for EPS production, and the characteristics of the produced EPS. Although the addition of ethanol as an auxiliary substrate to acetate increased EPS recovery from 3% (sole acetate) to 11% (acetate/ethanol ratio 1:1), reduced EPS recoveries were obtained when ethanol was added to glycerol and glucose substrates. However, the preliminary acclimation of the biomass with a substrate like glycerol may help the microbial community to establish anabolic pathways toward EPS production that remain active even with other substrates like acetate/ethanol mixture. Overall, by employing different substrates, it is possible to modulate the basic EPS properties, namely monosaccharide composition, molecular weight and charge density, which are important for different EPS applications.

Acknowledgements

This work was performed in the cooperation framework of Wetsus, European Centre of Excellence for Sustainable Water Technology (www.wetsus.nl). Wetsus is co-funded by the Dutch Ministry of Economic Affairs and Ministry of Infrastructure and Environment, the European Union Regional Development Fund, the Province of Fryslân and the Northern Netherlands Provinces. This work has also received funding from the European Union's Horizon 2020 research and innovation programme under the Marie Skłodowska-Curie [grant agreement No. 665874]. The authors thank Ema Ižaković for the charge density analysis, Caroline Plugge and Alan Werker for their scientific inputs, and the participants of the research theme 'Natural flocculants' for the fruitful discussions and financial support.

Supplementary information of Chapter 4

Table S1. COD distribution as a fraction of influent COD in the four reactors fed with different substrates. Gly: Glycerol; Eth: Ethanol; Acet: Acetate; Glu: Glucose. Displayed ratios are based on g COD carbon source 1**:** g COD carbon source 2.

Reactor	Substrates	Effluent-COD	Biomass-COD	EPS-COD	Oxidised COD
R1	Gly/Eth (4:1)	3	26	33	38
	Gly/Eth (1:1)	7	6	28	59
	Gly	4	9	44	43
	Acet/Eth (4:1)	9	8	69	14
	Acet	7	8	13	72
R2	Acet	13	42	3	42
	Acet/Eth (4:1)	4	40	9	47
	Acet/Eth (1:1)	10	27	11	52
R3	Glu	4	7	30	59
	Glu/Eth (1:1)	2	46	25	27
R4	Eth	8	39	11	42

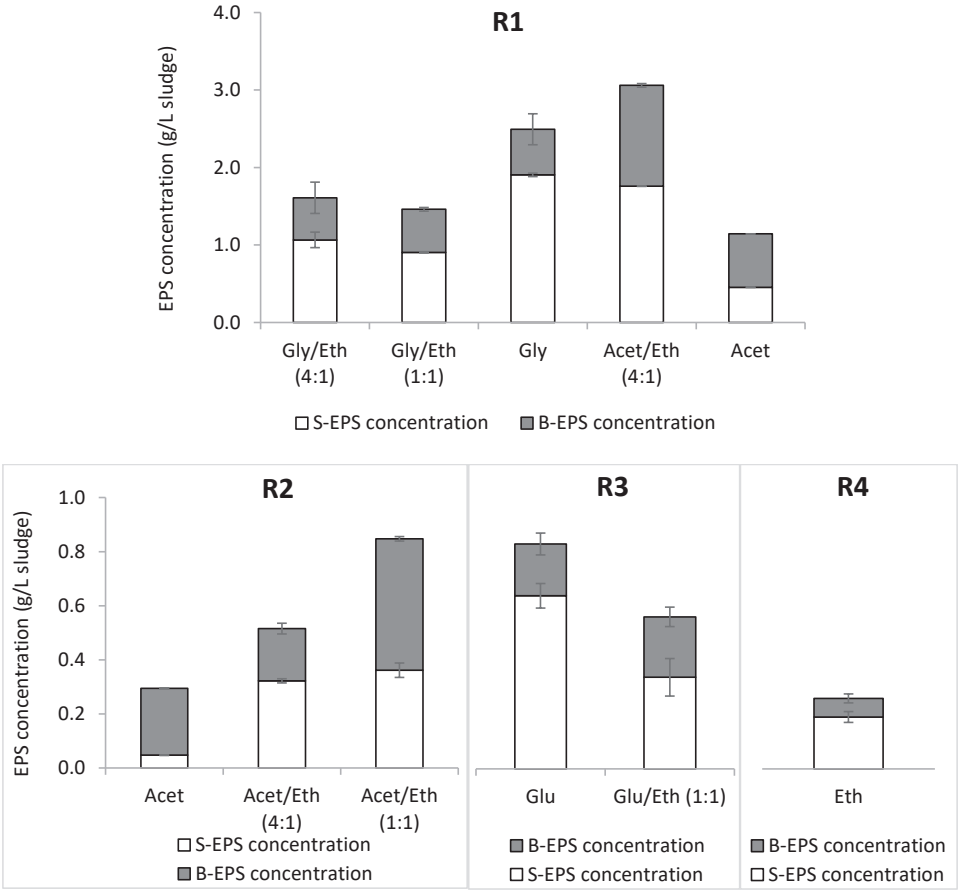

Fig. S1. EPS concentration from the four reactors (R1, R2, R3 and R4) treating different substrates. Gly: Glycerol; Eth: Ethanol; Acet: Acetate; Glu: Glucose. S-EPS: soluble-EPS; B-EPS: bound EPS. Displayed ratios are based on g COD carbon source 1**:** g COD carbon source 2. Error bars are standard deviations of duplicate extraction.

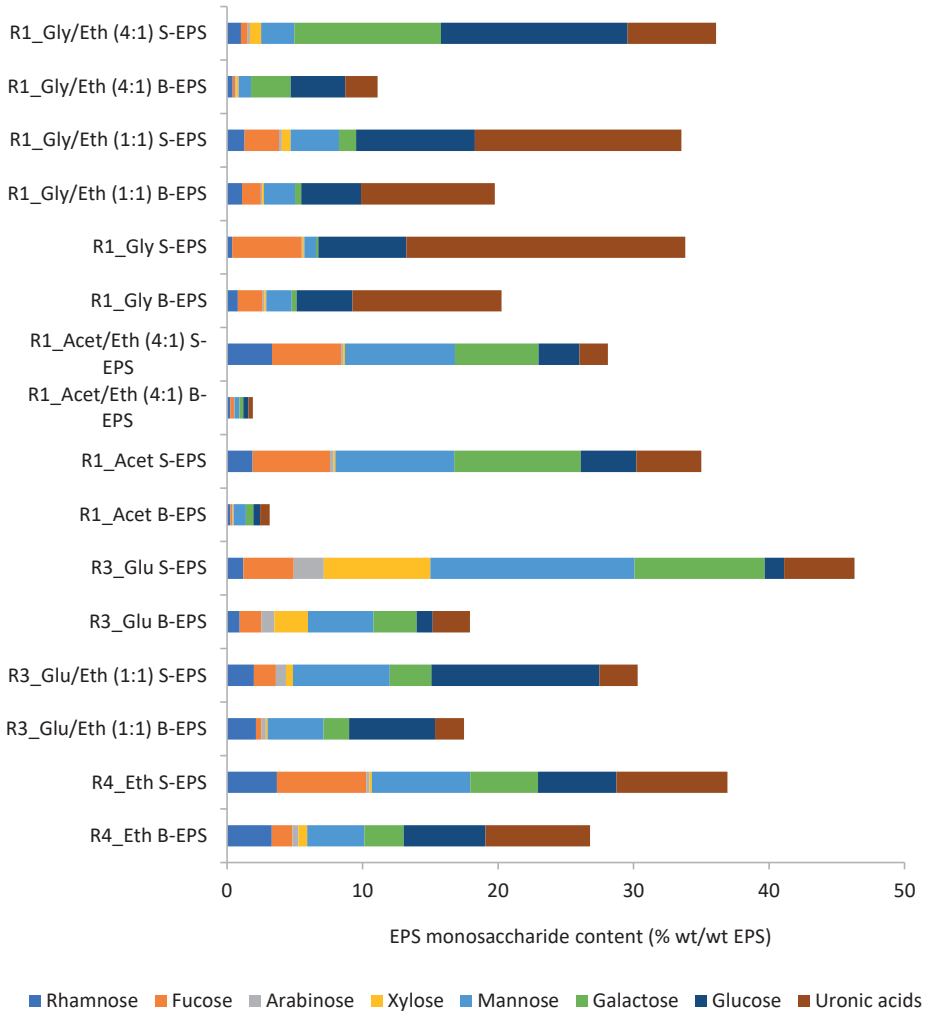

Fig. S2. Sugar composition (% wt/wt EPS) of EPS fractions from different substrates. Gly: Glycerol; Eth: Ethanol; Acet: Acetate; Glu: Glucose. S-EPS: soluble-EPS; B-EPS: bound EPS. Displayed ratios are based on g COD carbon source 1**:** g COD carbon source 2.

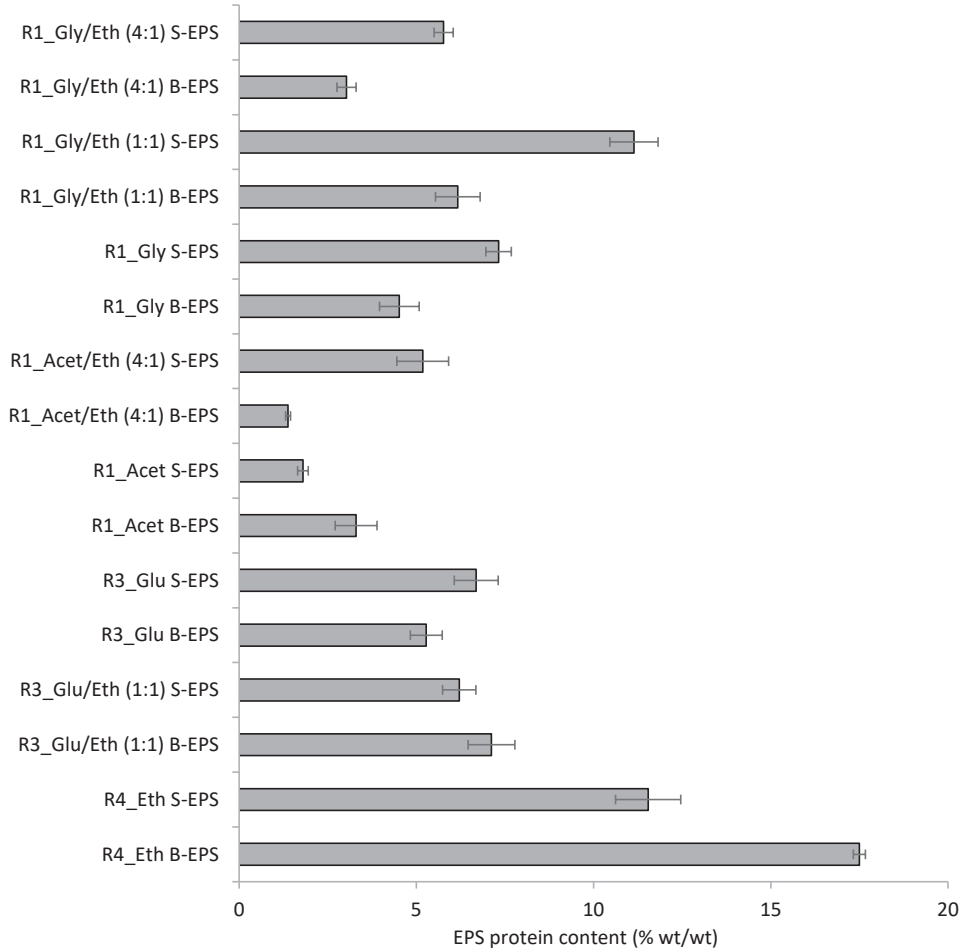

Fig. S3. Total protein content (expressed as wt% BSA equivalent units) of EPS fractions from different substrates. Gly: Glycerol; Eth: Ethanol; Acet: Acetate; Glu: Glucose. S-EPS: soluble-EPS; B-EPS: bound EPS. Displayed ratios are based on g COD carbon source 1**:** g COD carbon source 2. Error bars are standard deviations of triplicate measurements.

Charge density determination

EPS' charge density was determined by colloid titration using a Mütek Particle Charge Detector (PCD03, Germany) described by Tan *et al*. [63] and a titration procedure explained by Ajao *et al*. [2]. The charge densities were determined at a sample solution pH of 7.0 ± 0.1 and calculated from the titrant (polydiallyldimethylammonium chloride, pDADMAC) consumption according to the equation:

$$q = \frac{c*V}{m} \qquad (2)$$

where *q* is the specific charge quantity (eq/g), *c* is the titrant concentration (eq/L), *V* is the consumed titrant volume (L), and *m* is the mass of the sample (g).

Table S2. Charge density values of selected soluble EPS from reactors 1 - 3. Mean ± standard deviation of duplicate measurements.

EPS and reactor/substrate	Charge density (meq/g) at pH 7
Soluble EPS (R1 - Glycerol)	6.67 ± 0.23
Soluble EPS (R2 - Acetate/ethanol, 4:1)	2.01 ± 0.10
Soluble EPS (R3 - Glucose)	2.32 ± 0.03

Table S3. Bacterial 16S rRNA gene analysis by means of Next Generation Sequencing (NGS) of samples taken from Reactor 1. The relative abundance of core operational taxonomic units (OTUs) (> 1% relative abundance, 100% occupancy) and their taxonomic classification at the identified level (mostly genus level). All OTUs < 1% are summed together and presented as unclassified. The inoculum and samples taken from reactor R1 are compared. Light grey spots indicate when the microbial group was not present in the specific sample.

	Relative abundance (%)					
	Inoculum	*Gly/Eth (4:1)*	*Gly/Eth (1:1)*	*Glycerol*	*Acet/Eth (4:1)*	*Acetate*
Classification	**day 0**	**day 11**	**day 18**	**day 42**	**day 57**	**day 64**
Rickettsiales SM2D12	0.1	24.2	0.4	0.1	2.2	0.8
Xanthobacter		9.4		0.6	2.9	0.7
Burkholderiaceae	1.2	8.7	0.9	14.4	15.8	1.9
Acinetobacter	24.5	7.6		3.9	19.8	8.3
Enterobacteriaceae	4.3	5.2		0.2	2.5	0.7
Pseudomonas		4.0		4.7	0.4	2.1
Flavobacterium		3.8	0.4	1.9	1	
Microbacterium	0.4	3.2		1	0.2	
Mucilaginibacter	0.2	3		27.5	0.2	
Luteolibacter		3	40.7	14.1	0.4	3.6
Sphingobium		2.7	2	0.3	5.4	
Erysipelothrix	0.3	2.4	15.6	1	1.5	29.8
Microscillaceae		2.3		0.9	0.2	
Brevundimonas	0.2	1.7		1.1	1.7	
Rhizobiaceae		1.6		0.1	0.6	
Terrimicrobium		0.9	13.8	0.1	0.8	5.9
Rickettsiales		0.9	4.5	0.2	1.0	7.2
Aeromonas	7.4	0.5		3.5	4.9	0.9
Verrucomicrobium		0.5	2.3	1	3.3	22.8
Uncultured *Bacteria*		0.5	11.7	0.1	0.3	4.6
Trichococcus	27.5	0.5			0.3	
Dokdonella		0.4		0.4	2.3	
Bosea		0.4		1.5	0.8	
Exiguobacterium	0.3	0.2		0.1	1.7	0.3
Chryseobacterium		0.2		0.8	6.5	1.2
Afipia		0.2		2.6	2.5	
Hydrocarboniphaga	0.2	0.1	0.7	3.1	4.8	
Micavibrionales		0.1		3.8		
Saprospiraceae	11.4					
Caldilineaceae	6.4					
Anaerolineaceae	6.3		0.1			
Romboutsia	4.8			0.2		
Kouleothrix	1.4					
Anaerolineae	1.3					
Caulobacter	0.3			3.9	12.6	0.9
Sericytochromatia				1.4	0.1	1.5
Sediminibacterium				2.5		
Unclassified	1.7	11.9	7	3.4	3.1	6.6

Table S4. Bacterial 16S rRNA gene analysis by means of Next Generation Sequencing (NGS) of samples taken from Reactor 2. The relative abundance of core operational taxonomic units (OTUs) (> 1% relative abundance, 100% occupancy) and their taxonomic classification at the identified level (mostly genus level). All OTUs < 1% are summed together and presented as unclassified. The inoculum and samples taken from reactor R1 are compared. Light grey spots indicate when the microbial group was not present in the specific sample.

	Relative abundance (%)		
	Inoculum	*Acetate*	*Acet/Eth (4:1)*
Classification	**day 0**	**day 26**	**day 33**
Erysipelothrix	0.3	33.1	1.4
Rickettsiales		10.9	0.6
Acinetobacter	24.5	10.2	13.5
Terrimicrobium		7.1	
Uncultured *Bacteria*		6.0	1.0
WPS-2	0.3	4.5	
Sericytochromatia		4.2	0.1
Luteolibacter		3.6	0.1
Verrucomicrobium		3.4	0.1
Burkholderiaceae		3.2	17.9
Methanosaeta	0.2	2.2	0.3
Mollicutes	0.7	2.2	0.3
Proteobacteria		2	0.2
Atribacteria	0.2	1.6	0.4
Curvibacter		1.1	0.1
Thermovirga	0.2	1.1	0.2
Pseudoxanthomonas		0.7	1.1
Anaerolineaceae	6.3	0.2	
Chryseobacterium			9.9
Pseudomonas			1.9
Afipia			3.3
Devosia			2.4
Microbacterium	0.4		4.5
Anaerolineae	1.3		
Kouleothrix	1.4		
Enterobacteriaceae	4.3		7.6
Romboutsia	4.8		17
Caldilineaceae	6.4		
Aeromonas	7.4		8
Saprospiraceae	11.4		
Trichococcus	27.5		0.2
Unclassified	2.6	2.7	8.2

Table S5. Bacterial 16S rRNA gene analysis by means of Next Generation Sequencing (NGS) of samples taken from Reactor 3. The relative abundance of core operational taxonomic units (OTUs) (> 1% relative abundance, 100% occupancy) and their taxonomic classification at the identified level (mostly genus level). All OTUs < 1% are summed together and presented as unclassified. The inoculum and samples taken from reactor R1 are compared. Light grey spots indicate when the microbial group was not present in the specific sample.

	Relative abundance (%)	
	Inoculum	*Ethanol*
Classification	**Day 0**	**Day 18**
Burkholderiaceae	1.2	23.7
Hydrocarboniphaga	0.2	10.7
Sphingobium		10.7
Caulobacter	0.3	6.8
Romboutsia	4.8	5.5
Flavobacterium		5.0
Aeromonas	7.4	4.6
Afipia		3.6
Acinetobacter	24.5	3.0
Microbacterium	0.4	2.9
Sphingomonadaceae		2.3
Xanthobacter		2.2
Flectobacillus		2.1
Brevundimonas	0.2	1.6
Enterobacteriaceae	4.3	1.6
Rickettsiales		1.5
Sediminibacterium		1.4
Methanosaeta	0.2	1.4
Uncultured *Bacteria*		1.1
Exiguobacterium	0.3	0.9
Opitutaceae		0.5
WPS-2		0.4
Sericytochromatia		0.3
Prosthecobacter		0.2
Terrimicrobium		0.1
Gemmataceae	0.2	
Anaerolineae SBR1031	1.3	
Kouleothrix	1.4	
Anaerolineaceae	6.3	
Caldilineaceae	6.4	
Saprospiraceae	11.4	
Trichococcus	27.5	
Unclassified	2	5.9

Table S6. Bacterial 16S rRNA gene analysis by means of Next Generation Sequencing (NGS) of samples taken from Reactor 4. The relative abundance of core operational taxonomic units (OTUs) (> 1% relative abundance, 100% occupancy) and their taxonomic classification at the identified level (mostly genus level). All OTUs < 1% are summed together and presented as unclassified. The inoculum and samples taken from reactor R1 are compared. Light grey spots indicate when the microbial group was not present in the specific sample.

	Relative abundance (%)		
	Inoculum	*Glucose*	*Glu/Eth (1:1)*
Classification	**day 0**	**day 20**	**day 39**
Acinetobacter	24.5	28.5	1.4
Chryseobacterium		17.0	6.9
Microbacterium	0.4	16.5	9.4
Burkholderiaceae	1.2	7.9	4.5
Flavobacterium		7.2	1
Enterobacteriaceae	4.3	6.5	6.6
Pseudomonas		5.9	1.4
Hydrogenophaga		1.3	11.4
Flectobacillus		1.2	13.1
Pseudoxanthomonas		1.1	2.5
Verrucomicrobium		0.9	2.9
Dyadobacter		0.8	3.2
Microbacteriaceae		0.8	1.6
Brevundimonas	0.2	0.8	2.7
Haliangium		0.6	2.9
Pleomorphomonadaceae		0.6	2.3
Microscillaceae		0.5	3.5
Aeromonas	7.4	0.2	1.1
Uncultured *Bacteria*		0.1	2.1
Trichococcus	27.5	0.1	0.1
Sphaerotilus			11.8
Dokdonella			1.3
Anaerolineae SBR1031	1.3		0.2
Kouleothrix	1.4		0.1
Romboutsia	4.8		0.1
Anaerolineaceae	6.3		
Caldilineaceae	6.4		
Saprospiraceae	11.4		
Unclassified	3.1	1.7	5.8

Table S7. Diversity index (H') and evenness index (E) values calculated for each reactor, in the different feeding conditions, compared with the inoculum. The most significant operational taxonomic units (OTUs) per each sample out of the total number of sequences were considered, setting a cut-off value of 1%.

Reactor R1

	Substrate		*Gly/Eth (4:1)*	*Gly/Eth (1:1)*	*Glycerol*	*Acet/Eth (4:1)*	*Acetate*
	Sample	*Inoculum*	*day 11*	*day 18*	*day 42*	*day 57*	*day 64*
Core OTUs		11	16	7	16	17	11
H'		1.94	2.21	1.48	2.13	2.32	1.80
E		1.24	1.25	1.31	1.30	1.22	1.33

Reactor R2

	Substrate		*Acetate*	*Acet/Eth (4:1)*
	Sample	*Inoculum*	*day 26*	*day 33*
Core OTUs		11	16	12
H'		1.94	2.32	2.23
E		1.24	1.19	1.11

Reactor R3

	Substrate		*Glucose*	*Glu/Eth (1:1)*
	Sample	*Inoculum*	*day 20*	*day 39*
Core OTUs		11	10	21
H'		1.94	1.85	2.62
E		1.24	1.24	1.16

Reactor R4

	Substrate		*Ethanol*
	Sample	*Inoculum*	*day 18*
Core OTUs		11	19
H'		1.94	2.39
E		1.24	1.23

S4. Polyhydroxyalkanoate (PHA) visualisation in bacterial cells

Sludge samples from R1_Glycerol, R2_Acetate, R2_Acetate/ethanol (4:1), and R3_Glucose were selected to visualise PHA accumulation in the bacterial cells using Nile blue A dye (Sigma Aldrich, Netherlands). Sludge samples from the glycerol- and glucose-fed reactors were first diluted 100 times in PBS (due to the high EPS concentration in the sludge) while those from the acetate- and acetate/ethanol (4:1)-fed reactors were diluted once because their sludges were watery and had low EPS concentration.

10 µL of each diluted sludge sample (in duplicates) was placed in the well of a multi-well microscope slide and dried at 55 °C for 5 mins. Afterwards, the glass slide was immersed in a petri dish with 1% aqueous solution of Nile blue A dye and incubated at 55 °C for 10 mins. After the incubation, the slide was washed with Milli-Q water and incubated with 8% aqueous solution of acetic acid for 1 min to remove excess stain. The glass slide was once again washed with Milli-Q water and air-dried. For the microscopy analysis, the glass slide was mounted with VECTASHIELD® Antifade Mounting Medium (Vector Laboratories, USA) and then observed with a Leica DM5000B fluorescence microscope with blue excitation wavelengths (filter BP 450-490).

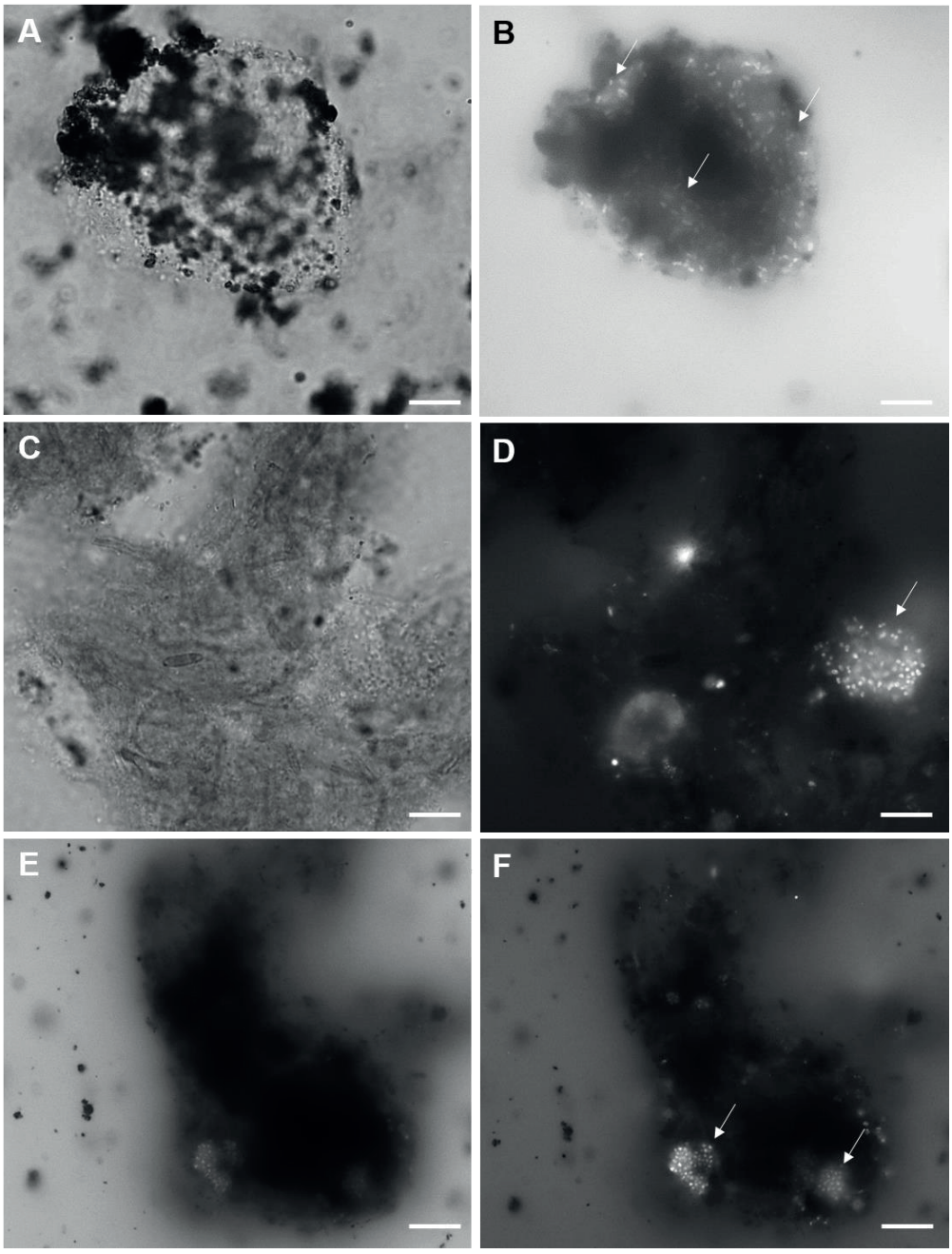

Fig. S4. Bright field (on the left) and epifluorescence (on the right) micrographs after Nile blue staining of samples taken from R2 fed with acetate (**A** and **B**), R2 fed with acetate/ethanol (4:1) (**C** and **D**), and R3 fed with glucose (**E** and **F**). No PHA accumulating cells were detected in R1 fed with glycerol. White arrows indicate the positive spots within the sludge aggregates. Scale bar is 10 µm.

S7. Next generation sequencing - QIIME 16S rRNA gene analysis

Paired-end 300 bp sequence data were imported as sequence .qza data artefact in QIIME2 v. 2018.11 [24]. Raw sequence processing comprised demultiplexing with quality filtering (i.e., 0 errors in barcodes and trimming primer sequences). Subsequent denoising of forward and reverse reads was performed by removing the first 10 bases and at truncating reads at position 235 (where median Phred > 30), error-correction, joining paired reads, amplicon sequence variant (ASV) calling, dereplication and chimeric sequence removal using the DADA2 plugin [64]. Only merged sequences were used in subsequent analyses, and the non-overlapping pairs were discarded. Representative sequences for each ASV were used to assign taxonomy using a naive Bayes classifier trained on primer set-specific 411 bp fragments of curated 16S rRNA gene sequences from the SILVA database v.132 [65–67]. The ASV feature table and taxonomic classification were exported and subsequently imported with *phyloseq* [68] in R statistical software [69]. ASVs with no Kingdom assignment were discarded and the ASV table was filtered to retain ASVs with a mean relative abundance of 0.1%. Sample coverage and alpha diversity were then estimated based on non-rarefied data (Table S3).

Table S7. Detected OTUs and alpha diversity obtained after amplicon sequencing.

		Reactor 1					**Reactor 2**		**Reactor 3**		**Reactor 4**
	Inoculum	day 11	day 18	day 42	day 57	day 64	day 26	day 33	day 20	day 39	day 18
Sequences	8928	31408	6201	56430	41980	3381	3121	26908	49779	26010	45839
OTUs	42	114	49	103	101	42	43	87	83	80	99
Core OTUs (Occupancy = 100%, abundance > 1&)	11	16	7	16	17	11	16	12	10	21	19

References

[1] T.T. More, J.S.S. Yadav, S. Yan, R.D. Tyagi, R.Y. Surampalli, Extracellular polymeric substances of bacteria and their potential environmental applications, J. Environ. Manage. 144 (2014) 1–25. doi:10.1016/j.jenvman.2014.05.010.

[2] V. Ajao, H. Bruning, H. Rijnaarts, H. Temmink, Natural flocculants from fresh and saline wastewater: Comparative properties and flocculation performances, Chem. Eng. J. 349 (2018) 622–632. doi:10.1016/j.cej.2018.05.123.

[3] K. Raj, U.R. Sardar, E. Bhargavi, I. Devi, B. Bhunia, O.N. Tiwari, Advances in exopolysaccharides based bioremediation of heavy metals in soil and water: A critical review, Carbohydr. Polym. 199 (2018) 353–364. doi:10.1016/j.carbpol.2018.07.037.

[4] V. Ajao, K. Nam, P. Chatzopoulos, E. Spruijt, H. Bruning, H. Rijnaarts, H. Temmink, Regeneration and reuse of microbial extracellular polymers immobilised on a bed column for heavy metal recovery, Water Res. 171 (2020) 115472. doi:10.1016/j.watres.2020.115472.

[5] V. Ajao, S. Millah, M.C. Gagliano, H. Bruning, H. Rijnaarts, H. Temmink, Valorization of glycerol/ethanol-rich wastewater to bioflocculants: recovery, properties, and performance, J. Hazard. Mater. 375 (2019) 273–280. doi:10.1016/j.jhazmat.2019.05.009.

[6] G.P. Sheng, H.Q. Yu, Characterization of extracellular polymeric substances of aerobic and anaerobic sludge using three-dimensional excitation and emission matrix fluorescence spectroscopy, Water Res. 40 (2006) 1233–1239. doi:10.1016/j.watres.2006.01.023.

[7] L. Faust, H. Temmink, A. Zwijnenburg, A.J.B. Kemperman, H.H.M. Rijnaarts, High loaded MBRs for organic matter recovery from sewage: effect of solids retention time on bioflocculation and on the role of extracellular polymers., Water Res. 56 (2014) 258–66. doi:10.1016/j.watres.2014.03.006.

[8] S.P. Buthelezi, A.O. Olaniran, B. Eillay, Production and characterization of bioflocculants from bacteria isolated from wastewater treatment plant in South Africa, Biotechnol. Bioprocess Eng. 15 (2010) 874–881. doi:10.1007/s12257-009-3002-7.

[9] P.H. Nielsen, B. Frølund, K. Keiding, Changes in the composition of extracellular polymeric substances in activated sludge during anaerobic storage, Appl. Microbiol. Biotechnol. 44 (1996) 823–830. doi:10.1007/BF00178625.

[10] F. Freitas, V.D. Alves, M.A.M. Reis, Advances in bacterial exopolysaccharides: From production to biotechnological applications, Trends Biotechnol. 29 (2011) 388–398. doi:10.1016/j.tibtech.2011.03.008.

[11] D.W. Tempest, O.M. Neijssel, Eco-Physiological Aspects of Microbial Growth in Aerobic Nutrient-Limited Environments, (1978) 105–153. doi:10.1007/978-1-4615-8222-9_3.

[12] H.-C. Flemming, J. Wingender, The biofilm matrix, Nat. Publ. Gr. 8 (2010) 623–633. doi:10.1038/nrmicro2415.

[13] W. Babel, R.H. Muller, Mixed Substrate Utilization in Micro-organisms: Biochemical Aspects and Energetics, Microbiology. 131 (1985) 39–45. doi:10.1099/00221287-131-1-39.

[14] T.P. Pirog, M.A. Kovalenko, Y. V. Kuz'minskaya, Intensification of exopolysaccharide synthesis by *Acinetobacter* sp. on an ethanol-glucose mixture: Aspects related to biochemistry and bioenergetics, Microbiology. 72 (2003) 305–312. doi:10.1023/A:1024247915758.

[15] J. Gregory, S. Barany, Adsorption and flocculation by polymers and polymer mixtures, Adv. Colloid Interface Sci. 169 (2011) 1–12. doi:10.1016/j.cis.2011.06.004.

[16] P.L.L. Ribeiro, M.I. Campos, J.I. Druzian, Novel extracellular polymeric substances produced by *Cupriavidus necator* IPT 027 grown on glucose and crude glycerol originated from biodiesel, Polym. Adv. Technol. 28 (2017) 549–556. doi:10.1002/pat.3957.

[17] G.P. da Silva, M. Mack, J. Contiero, Glycerol: A promising and abundant carbon source for industrial microbiology, Biotechnol. Adv. 27 (2009) 30–39. doi:10.1016/j.biotechadv.2008.07.006.

[18] J. Bhathena, B.T. Driscoll, T.C. Charles, F.S. Archibald, Effects of nitrogen and phosphorus limitation on the activated sludge biomass in a kraft mill biotreatment system., Water Environ. Res. 78 (2006) 2303–2310. doi:10.2175/106143006x95401.

[19] H.N. Englyst, J.H. Cummings, Simplified method for the measurement of total non-starch polysaccharides by gas - liquid chromatography of constituent sugars as alditol acetates, Analyst. 109 (1984) 937–942. doi:10.1039/an9840900937.

[20] A.M. Pustjens, H.A. Schols, M.A. Kabel, H. Gruppen, Characterisation of cell wall polysaccharides from rapeseed (*Brassica napus*) meal, Carbohydr. Polym. 98 (2013) 1650–1656. doi:10.1016/j.carbpol.2013.07.059.

[21] J. Thibault, Automatisation du dosage des substances pectiques par la methode au meta-hydroxydiphenyl, Leb. Wiss. Und Technol. 21 (1979) 247–251.

[22] A.E. Parada, D.M. Needham, J.A. Fuhrman, Every base matters: Assessing small subunit rRNA primers for marine microbiomes with mock communities, time series and global field samples, Environ. Microbiol. 18 (2016) 1403–1414. doi:10.1111/1462-2920.13023.

[23] C. Quince, A. Lanzen, R.J. Davenport, P.J. Turnbaugh, Removing Noise From Pyrosequenced Amplicons, BMC Bioinformatics. 12 (2011). doi:10.1186/1471-2105-12-38.

[24] E. Bolyen, J.R. Rideout, M.R. Dillon, N.A. Bokulich, C.C. Abnet, G.A. Al-Ghalith, H. Alexander, E.J. Alm, M. Arumugam, F. Asnicar, Y. Bai, J.E. Bisanz, K. Bittinger, A. Brejnrod, C.J. Brislawn, C.T. Brown, B.J. Callahan, A.M. Caraballo-Rodríguez, J. Chase, E.K. Cope, R. Da Silva, C. Diener, P.C. Dorrestein, G.M. Douglas, D.M. Durall, C. Duvallet, C.F. Edwardson, M. Ernst, M. Estaki, J. Fouquier, J.M. Gauglitz, S.M. Gibbons, D.L. Gibson, A. Gonzalez, K. Gorlick, J. Guo, B. Hillmann, S. Holmes, H. Holste, C. Huttenhower, G.A. Huttley, S. Janssen, A.K. Jarmusch, L. Jiang, B.D. Kaehler, K. Bin Kang, C.R. Keefe, P. Keim, S.T. Kelley, D. Knights, I. Koester, T.

Kosciolek, J. Kreps, M.G.I. Langille, J. Lee, R. Ley, Y.X. Liu, E. Loftfield, C. Lozupone, M. Maher, C. Marotz, B.D. Martin, D. McDonald, L.J. McIver, A. V. Melnik, J.L. Metcalf, S.C. Morgan, J.T. Morton, A.T. Naimey, J.A. Navas-Molina, L.F. Nothias, S.B. Orchanian, T. Pearson, S.L. Peoples, D. Petras, M.L. Preuss, E. Pruesse, L.B. Rasmussen, A. Rivers, M.S. Robeson, P. Rosenthal, N. Segata, M. Shaffer, A. Shiffer, R. Sinha, S.J. Song, J.R. Spear, A.D. Swafford, L.R. Thompson, P.J. Torres, P. Trinh, A. Tripathi, P.J. Turnbaugh, S. Ul-Hasan, J.J.J. van der Hooft, F. Vargas, Y. Vázquez-Baeza, E. Vogtmann, M. von Hippel, W. Walters, Y. Wan, M. Wang, J. Warren, K.C. Weber, C.H.D. Williamson, A.D. Willis, Z.Z. Xu, J.R. Zaneveld, Y. Zhang, Q. Zhu, R. Knight, J.G. Caporaso, Reproducible, interactive, scalable and extensible microbiome data science using QIIME 2, Nat. Biotechnol. 37 (2019) 852–857. doi:10.1038/s41587-019-0209-9.

[25] C.E. Shannon, W. Weaver, The mathematical theory of communication, 1964. doi:10.1145/584091.584093.

[26] C. Heip, A New Index Measuring Evenness, J. Mar. Biol. Assoc. United Kingdom. 54 (1974) 555–557. doi:10.1017/S0025315400022736.

[27] S.A. Huber, A. Balz, M. Abert, W. Pronk, Characterisation of aquatic humic and non-humic matter with size-exclusion chromatography - organic carbon detection - organic nitrogen detection (LC-OCD-OND), Water Res. 45 (2011) 879–885. doi:10.1016/j.watres.2010.09.023.

[28] J.B. Russell, The energy spilling reactions of bacteria and other organisms, J. Mol. Microbiol. Biotechnol. 13 (2007) 1–11. doi:10.1159/000103591.

[29] S.N. Pawar, K.J. Edgar, Alginate derivatization: A review of chemistry, properties and applications, Biomaterials. 33 (2012) 3279–3305. doi:10.1016/j.biomaterials.2012.01.007.

[30] K. Nouha, R.S. Kumar, S. Balasubramanian, R.D. Tyagi, Critical review of EPS production, synthesis and composition for sludge flocculation, J. Environ. Sci. (China). 66 (2018) 225–245. doi:10.1016/j.jes.2017.05.020.

[31] S. Rosalam, R. England, Review of xanthan gum production from unmodified starches by *Xanthomonas comprestris* sp., Enzyme Microb. Technol. 39 (2006) 197–207. doi:10.1016/j.enzmictec.2005.10.019.

[32] A. Kawakoshi, H. Nakazawa, J. Fukada, M. Sasagawa, Y. Katano, S. Nakamura, A. Hosoyama, H. Sasaki, N. Ichikawa, S. Hanada, Y. Kamagata, K. Nakamura, S. Yamazaki, N. Fujita, Deciphering the genome of polyphosphate accumulating Actinobacterium *Microlunatus phosphovorus*, DNA Res. 19 (2012) 383–394. doi:10.1093/dnares/dss020.

[33] J.M.L. Dias, P.C. Lemos, L.S. Serafim, C. Oliveira, M. Eiroa, M.G.E. Albuquerque, A.M. Ramos, R. Oliveira, M.A.M. Reis, Recent advances in polyhydroxyalkanoate production by mixed aerobic cultures: From the substrate to the final product, Macromol. Biosci. 6 (2006) 885–906. doi:10.1002/mabi.200600112.

[34] B. Basak, O. Ince, N. Artan, N. Yagci, B.K. Ince, Effect of nitrogen limitation on enrichment of

activated sludge for PHA production, Bioprocess Biosyst. Eng. 34 (2011) 1007–1016. doi:10.1007/s00449-011-0551-x.

[35] K. Johnson, R. Kleerebezem, M.C.M. van Loosdrecht, Influence of ammonium on the accumulation of polyhydroxybutyrate (PHB) in aerobic open mixed cultures, J. Biotechnol. 147 (2010) 73–79. doi:10.1016/j.jbiotec.2010.02.003.

[36] A.S.M. Chua, H. Takabatake, H. Satoh, T. Mino, Production of polyhydroxyalkanoates (PHA) by activated sludge treating municipal wastewater: Effect of pH, sludge retention time (SRT), and acetate concentration in influent, Water Res. 37 (2003) 3602–3611. doi:10.1016/S0043-1354(03)00252-5.

[37] F. Morgan-Sagastume, Characterisation of open, mixed microbial cultures for polyhydroxyalkanoate (PHA) production, Rev. Environ. Sci. Biotechnol. 15 (2016) 593–625. doi:10.1007/s11157-016-9411-0.

[38] L. Marang, M.C.M. van Loosdrecht, R. Kleerebezem, Enrichment of PHA-producing bacteria under continuous substrate supply, N. Biotechnol. 41 (2018) 55–61. doi:10.1016/j.nbt.2017.12.001.

[39] H. Moralejo-Gárate, R. Kleerebezem, A. Mosquera-Corral, J.L. Campos, T. Palmeiro-Sánchez, M.C. van Loosdrecht, Substrate versatility of polyhydroxyalkanoate producing glycerol grown bacterial enrichment culture, Water Res. 66 (2014) 190–198. doi:10.1016/j.watres.2014.07.044.

[40] J. Wiegel, The Genus *Xanthobacter*, The Prokaryotes. (2006) 290–314. doi:10.1007/0-387-30745-1_16.

[41] T.P. Pirog, M.A. Kovalenko, Y. V. Kuzminskaya, S.K. Votselko, Physicochemical properties of the microbial exopolysaccharide ethapolan synthesized on a mixture of growth substrates, Microbiology. 73 (2004) 14–18. doi:10.1023/B:MICI.0000016361.71744.6f.

[42] K.J. Towner, The Genus *Acinetobacter*, in: 1992: pp. 3137–3143.

[43] E.K. Pomaranski, E. Soto, The Formation, Persistence, and Resistance to Disinfectant of the *Erysipelothrix piscisicarius* Biofilm, J. Aquat. Anim. Health. (2020) 1–6. doi:10.1002/aah.10097.

[44] Y. Yin, J. Sun, F. Liu, L. Wang, Effect of nitrogen deficiency on the stability of aerobic granular sludge, Bioresour. Technol. 275 (2019) 307–313. doi:10.1016/j.biortech.2018.12.069.

[45] J.H. Ahn, B.C. Kim, J.H. Joa, S.J. Kim, J. Song, S.W. Kwon, H.Y. Weon, *Mucilaginibacter ginsengisoli* sp. Nov., Isolated from a ginseng-cultivated soil, Int. J. Syst. Evol. Microbiol. 65 (2015) 3933–3937. doi:10.1099/ijsem.0.000519.

[46] J. Park, G.S. Baek, S.G. Woo, J. Lee, J. Yang, J. Lee, *Luteolibacter yonseiensis* sp. nov., isolated from activated sludge using algal metabolites, Int. J. Syst. Evol. Microbiol. 63 (2013) 1891–

1895. doi:10.1099/ijs.0.046664-0.

[47] T. Ohshiro, N. Harada, Y. Kobayashi, Y. Miki, H. Kawamoto, Microbial fucoidan degradation by *Luteolibacter algae* H18 with deacetylation, Biosci. Biotechnol. Biochem. 76 (2012) 620–623. doi:10.1271/bbb.110911.

[48] V. Tandoi, M. Majone, J. May, R. Ramadori, The behaviour of polyphosphate accumulating *Acinetobacter* isolates in an anaerobic-aerobic chemostat, Water Res. 32 (1998) 2903–2912. doi:10.1016/S0043-1354(98)00079-7.

[49] G.N. Rees, G. Vasiliadis, J.W. May, R.C. Bayly, Production of poly-beta-hydroxybutyrate in *Acinetobacter* spp. isolated from activated sludge, Appl. Microbiol. Biotechnol. 38 (1993) 734–737. doi:10.1007/BF00167136.

[50] A. Mielcarek, J. Rodziewicz, W. Janczukowicz, D. Dabrowska, S. Ciesielski, A. Thornton, J. Struk-Sokołowska, Citric acid application for denitrification process support in biofilm reactor, Chemosphere. 171 (2017) 512–519. doi:10.1016/j.chemosphere.2016.12.099.

[51] M. Muchová, J. Růžička, M. Julinová, M. Doležalová, J. Houser, M. Koutný, L. Buňková, Xanthan and gellan degradation by bacteria of activated sludge, Water Sci. Technol. 60 (2009) 965–973. doi:10.2166/wst.2009.443.

[52] Z. Cardman, C. Arnosti, A. Durbin, K. Ziervogel, C. Cox, A.D. Steen, A. Teske, *Verrucomicrobia* are candidates for polysaccharide-degrading bacterioplankton in an Arctic fjord of Svalbard, Appl. Environ. Microbiol. 80 (2014) 3749–3756. doi:10.1128/AEM.00899-14.

[53] Y. Zhang, F. Wang, X. Yang, C. Gu, F.O. Kengara, Q. Hong, Z. Lv, X. Jiang, Extracellular polymeric substances enhanced mass transfer of polycyclic aromatic hydrocarbons in the two-liquid-phase system for biodegradation, Appl. Microbiol. Biotechnol. 90 (2011) 1063–1071. doi:10.1007/s00253-011-3134-5.

[54] Z. Ur Rehman, L. Fortunato, T. Cheng, T. Leiknes, Metagenomic analysis of sludge and early-stage biofilm communities of a submerged membrane bioreactor, Sci. Total Environ. 701 (2020). doi:10.1016/j.scitotenv.2019.134682.

[55] L. Hao, S.N. Liss, B.Q. Liao, Influence of COD:N ratio on sludge properties and their role in membrane fouling of a submerged membrane bioreactor, Water Res. 89 (2015) 132–141. doi:10.1016/j.watres.2015.11.052.

[56] F. Ye, Y. Ye, Y. Li, Effect of C/N ratio on extracellular polymeric substances (EPS) and physicochemical properties of activated sludge flocs, J. Hazard. Mater. 188 (2011) 37–43. doi:10.1016/j.jhazmat.2011.01.043.

[57] D. Al-Halbouni, W. Dott, J. Hollender, Occurrence and composition of extracellular lipids and polysaccharides in a full-scale membrane bioreactor, Water Res. 43 (2009) 97–106. doi:10.1016/j.watres.2008.10.008.

[58] T.R. Jarman, G.W. Pace, Energy requirements for microbial exopolysaccharide synthesis, Arch. Microbiol. 137 (1984) 231–235. doi:10.1007/BF00414549.

[59] C.S. Laspidou, B.E. Rittmann, A unified theory for extracellular polymeric substances, soluble microbial products, and active and inert biomass, Water Res. 36 (2002) 2711–2720. doi:10.1016/S0043-1354(01)00414-6.

[60] K.M. Hsieh, G.A. Murgel, L.W. Lion, M.L. Shuler, Interactions of microbial biofilms with toxic trace metals: 1. Observation and modeling of cell growth, attachment, and production of extracellular polymer, Biotechnol. Bioeng. 44 (1994) 219–231. doi:10.1002/bit.260440211.

[61] S. Sharma, S. Bhattacharya, Flow behaviour of gellan sol with selected cations, J. Food Sci. Technol. 52 (2014) 1233–1237. doi:10.1007/s13197-014-1453-0.

[62] B. Bolto, J. Gregory, Organic polyelectrolytes in water treatment, Water Res. 41 (2007) 2301–2324. doi:10.1016/j.watres.2007.03.012.

[63] W.F. Tan, W. Norde, L.K. Koopal, Humic substance charge determination by titration with a flexible cationic polyelectrolyte, Geochim. Cosmochim. Acta. 75 (2011) 5749–5761. doi:10.1016/j.gca.2011.07.015.

[64] B.J. Callahan, P.J. McMurdie, M.J. Rosen, A.W. Han, A.J.A. Johnson, S.P. Holmes, DADA2: High-resolution sample inference from Illumina amplicon data, Nat. Methods. 13 (2016) 581–583. doi:10.1038/nmeth.3869.

[65] F. Pedregosa, R. Weiss, M. Brucher, Scikit-learn : Machine Learning in Python, J. Mach. Learn. 12 (2011) 2825–2830.

[66] N.A. Bokulich, B.D. Kaehler, J.R. Rideout, M. Dillon, E. Bolyen, R. Knight, G.A. Huttley, J. Gregory Caporaso, Optimizing taxonomic classification of marker-gene amplicon sequences with QIIME 2's q2-feature-classifier plugin, Microbiome. 6 (2018) 1–17. doi:10.1186/s40168-018-0470-z.

[67] C. Quast, E. Pruesse, P. Yilmaz, J. Gerken, T. Schweer, P. Yarza, J. Peplies, F.O. Glöckner, The SILVA ribosomal RNA gene database project: Improved data processing and web-based tools, Nucleic Acids Res. 41 (2013). doi:10.1093/nar/gks1219.

[68] P.J. McMurdie, S. Holmes, Phyloseq: An R Package for Reproducible Interactive Analysis and Graphics of Microbiome Census Data, PLoS One. 8 (2013). doi:10.1371/journal.pone.0061217.

[69] R Core Team, R: A language and environment for statistical computing, Foundation for Statiscal Computing (2018).

Chapter 5

Bioflocculants from wastewater: insights into adsorption affinity, flocculation mechanisms and mixed particle flocculation based on biopolymer size-fractionation

A modified version of this Chapter has been published as:

V. Ajao, R. Fokkink, F. Leermakers, H. Bruning, H. Rijnaarts, H. Temmink, Bioflocculants from wastewater: insights into adsorption affinity, flocculation mechanisms and mixed particle flocculation based on biopolymer size-fractionation, J. Colloid Interface Sci. 581 (2020) 533–544. doi:10.1016/j.jcis.2020.07.146.

Abstract

Microbial extracellular polymeric substances (EPS) have received considerable attention as effective and biodegradable flocculants for (waste)water treatment. In this study, wastewater-produced EPS, which are generally heterodispersed, were size-fractionated and each fraction was investigated for its role in the overall flocculation mechanism of EPS in clay systems. The harvested EPS were fractionated into three molecular weights (MWs): high (HMW: 1.99 MDa), medium (MMW: 0.78 MDa) and low (LMW: 0.13 MDa). The produced EPS and its fractions were mainly composed of polysaccharides and proteins and their ratios increased with increasing MW. The harvested unfractionated EPS and the HMW-EPS fraction showed similar and excellent flocculation of kaolinite (93% turbidity removal at a dosage of 0.1 mg/g kaolinite) and montmorillonite (98 - 99 % at 0.5 mg/g) in single clay systems, revealing that the presence of LMW-EPS in the harvested EPS did not hinder its flocculation performance. However, the sole use of the LMW-EPS poorly flocculated any of the clay particles. In the dual clay system, the harvested mixed EPS proved to be more efficient than the HMW-EPS fraction. Optical reflectometry, used to monitor the adsorption of each fraction on a silica surface, revealed site-blocking effects in mixed EPS: the LMW and MMW EPS first adsorbed to the surface due to higher diffusivities and faster mass transfer to the interface, while the HMW-EPS were slowly transported but were attached to the surface irreversibly and stronger than the LMW/MMW-EPS. We propose from this, a mixed EPS adsorption mechanism: extended anionic polymer tails in solution, thereby enhancing particle flocculation.

1. Introduction

The coagulation/flocculation process has been employed for centuries as a simple and effective way to destabilise, agglomerate and remove particles from water and wastewater. Currently, this process is widely achieved with the use of inorganic coagulants and fossil-based organic flocculants. Flocculants are particularly important because they are efficient at low dosages and able to form strong flocs [1]. However, most synthetic flocculants biodegrade poorly and some of the degradation products/monomer residues are toxic, with acrylamide from polyacrylamide as a well-known example [1].

As an alternative, bioflocculants have gained increasing attention for water treatment due to their biodegradability, non-toxic property, and effective flocculation performances sometimes comparable with synthetic flocculants [2–6]. Quite recently, microbial extracellular polymeric substances (EPS) are being explored as promising bioflocculants due to their relatively high molecular weight [6–8]. EPS are products of microbial biochemical secretions and may either be produced by pure or mixed cultures. The usual approach is the enrichment of pure cultures with single organic substrates (such as glucose) to obtain a single type of EPS, usually polysaccharides [7,9–11]. Although this strategy produces biodegradable EPS, the disadvantage is that it necessitates sterile conditions and expensive carbon sources. On the contrary, a mixed-culture approach requires no sterility and can be fed with low-cost feedstocks such as organic wastewater. One outcome of the mixed-culture approach is the production of a heterogeneous and heterodispersed EPS matrix, comprising different compounds with different molecular weights (MWs) and charge densities (CDs) [6,12]. These two characteristics (MW and CD), especially the former, govern the flocculation process and performance of anionic flocculants such as EPS [13]. Previous studies reported wastewater-produced EPS to comprise a mixture of varying MWs [6,12,14,15], which according to Bolto and Gregory [16], can be generally classified as high (> 1000 kDa), medium (100 – 1000 kDa) and low (< 100 kDa) MW fractions.

High MW polymers have been reported to favour polymer bridging between particles since such molecules expand further in suspension (>> 50 nm [17]), escape the electrostatic field of the attached particle (generally < 50 nm at ionic strengths in wastewater [17]), adsorb on other particles and result in big and fast-settling flocs [13]. However, very high MW (typically > 15 MDa) can have an adverse effect on adsorption and flocculation. Such polymers tend to have fewer chains per gram (specifically for linear polymers), a higher chain entanglement and result in a highly viscous polymer solution that is poorly distributed in suspension [18]. In the last few decades, the use of polymer mixtures, especially dual-polymer systems (low and high MW or medium and high MW polymers) has gained considerable interest due to some significant advantages over the use of single-type polymers [13]. The studied dual-polymer systems typically involved a cationic low MW polymer and a subsequent anionic high MW polymer [13,19–21]. The advantage of this approach is the synergistic effect of two flocculation mechanisms – charge neutralisation by the cationic polymer and bridge formation by the anionic polymer [13,19]. While the polycation adsorbs to the particles via electrostatic interaction, it also provides adsorption sites for the polyanion to form bridges with itself and other particles [13]. For instance, Yu and Somasundaran [19] showed that by pre-

adsorbing polydiallyldimethylammonium chloride (pDADMAC, 240 kDa) on alumina particles, the subsequent adsorption of polyacrylic acid (PAA, 100 kDa) was enhanced and the settling rate tripled compared to the addition of pDADMAC alone. In the same vein, Fan *et al*. [22] reported that the use of a dual polymer system (cationic Percol, 1.8 MDa and anionic PAA, 10 kDa) increased the turbidity removal efficiency of alumina particles by 11 - 15 % compared to the sole use of PAA, and by 30 - 33 % compared to the use of Percol.

Wastewater-produced EPS comprise a mixture of different MW fractions (mixed EPS consisting of high, medium and low MW fractions) and have also been reported to show excellent flocculation of particles with performances comparable to some synthetic flocculants such as anionic polyacrylamide [6]. Due to the net negative charge of EPS [6], polymer bridging (particularly divalent cationic bridging) has been proposed and reported as the flocculation mechanism – a phenomenon also found in synthetic anionic flocculants [16,23]. However, there has been no report on the role of each MW fraction on the overall flocculation mechanism. More so, the use of (synthetic) polymer mixtures composed of anionic polymers is yet to be studied. The advantage of such mixtures (and in this case, mixed EPS) may be the synergistic effect of these MW fractions on single or mixed suspensions or the ability of different fractions to selectively adsorb to different particles in a mixture. We conjectured that in the presence of di/multi-valent cations, the low MW (LMW) EPS fraction would (preferentially) adsorb to the smaller particles in a mixture while the high MW fractions will bridge to the tails of the adsorbed LMW EPS and adsorb to the bigger particles.

To study polymer adsorption in a controlled system, optical reflectometry has been reported as an effective technique [24–26]. With this technique, we can monitor the *in situ* adsorption of polymers on a flat reflective surface in a stagnation point flow cell. Due to its high sensitivity and controlled hydrodynamic condition, it is possible to determine (low) amounts of adsorbed polymers and to characterise the kinetics of adsorption. As reported by Wågberg and Nygren [26], the combination of optical reflectometry with flocculation measurements can be very powerful in gaining insights into the working mechanism of flocculants.

This study, for the first time, investigates the effect of the different MW fractions of EPS on single and dual clay (kaolinite and montmorillonite as models) particle flocculation and mechanism of flocculation. We imagined that mixed EPS would better flocculate a mixture of particles than a single MW EPS. Optical reflectometry was used to observe the *in situ* adsorption of the different MW fractions on a flat silica surface, from which we could determine the adsorption affinity and kinetics of each fraction and mixtures of fractions. From these experiments, we elucidated the mechanism on how the various MW fractions of EPS adsorb to single and dual clay mixtures.

2. Materials and method

2.1. Production, harvesting and fractionation of EPS

A submerged membrane bioreactor (MBR) with a working volume of 3.3 L was operated to produce EPS. The MBR operation, wastewater composition (fresh wastewater consisting of glycerol and ethanol at a COD/N ratio of 100) and EPS yield have been thoroughly described elsewhere [27].

During the steady-state reactor operation, soluble (S)-EPS were harvested from the reactor content, having been reported to be the major EPS fraction (62 - 77 wt%) when operating a reactor under nitrogen-limited conditions [27]. S-EPS were harvested via centrifugation: 1000 mL sludge was centrifuged at 17000 *g* and 4 °C for 1 h, after which the supernatant containing the S-EPS (henceforth called 'mixed EPS' in this Chapter) was dialysed (tubular dialysis membrane, 12 - 14 kDa molecular weight cut-off, MWCO – Spectra/Por 2) against demineralised water to remove salts and ultra-low MW compounds.

Dialysed mixed EPS were size-fractionated into three MW fractions (Fig. 1) using membrane filters (with different MWCO) fitted in Amicon® dead-end filtration cells operated at 2.5 bars. The first filtration was performed using a 0.1 µm hydrophilic polyethersulfone membrane disc (Pall Corporation, Supor®). The retentate was collected by carefully scraping and washing (with demineralised water) the biopolymer film on the membrane. The permeate was further filtered using a 100 kDa polysulfone membrane (Microdyn Nadir PM US100) and the retentate and permeate were collected separately. The 0.1 µm membrane retentate, 100 kDa membrane retentate and 100 kDa membrane filtrate were classified as high, medium and low MW (HMW, MMW and LMW) EPS fractions, respectively. Each fraction and the mixed EPS were frozen at -80 °C and freeze-dried.

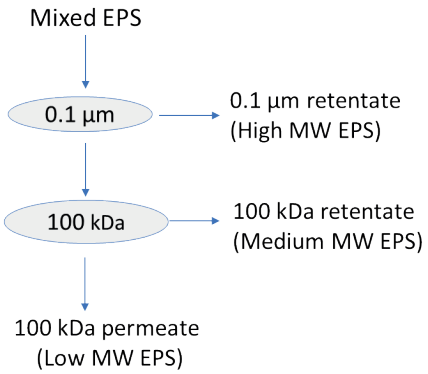

Fig. 1. Mixed EPS fractionation into the three molecular weight fractions – high, medium and low molecular weight fractions.

2.2. EPS characterisation

2.2.1. Molecular weight and charge density measurement

The mixed EPS and its fractions were further analysed for MW using liquid chromatography-organic carbon detection (LC-OCD – model 8, DOC-LABOR, Germany). The detailed method has been described by Ajao *et al*. [27]. Prior to the analysis, each sample was dissolved in Milli-Q water and passed through a 0.45 µm hydrophilic polytetrafluoroethylene filter.

The CDs were determined by colloid titration using a Mütek Particle Charge Detector (PCD03, Germany) described by Tan *et al*. [28] and a titration procedure explained by Ajao *et al*. [6]. The CDs

were determined at a sample solution pH of 7.0 ± 0.1 (because the clay suspensions were prepared at this pH) and calculated from the titrant (pDADMAC) consumption according to the equation:

$$q = \frac{c*V}{m} \qquad (1)$$

where q is the specific charge quantity (eq/g), c is the titrant concentration (eq/L), V is the consumed titrant volume (L), and m is the mass of the sample (g).

2.2.2. Functional group determination

Fourier transform infrared spectroscopy (FTIR) was carried out on the freeze-dried EPS samples using an IRTracer-100 spectrometer (Shimadzu, Japan) with a scanning range of 4000 - 450 cm^{-1} for 40 scans at a spectral resolution of 4 cm^{-1}.

2.2.3. Total protein and polysaccharide quantification

Previous studies under the same conditions reported polysaccharides and proteins as the main components of (soluble) EPS [27,29]. Hence, each component was measured colorimetrically to determine the total protein and polysaccharide content.

The total protein content of the dried EPS samples was determined using a bicinchoninic acid (BCA) assay kit (Thermo Scientific, USA). The assay was performed in a microplate, where 25 µL of EPS solution (dissolved in a phosphate buffer saline, pH 7.4 [27]) or bovine serum albumin, BSA (used as a standard protein) was mixed with 200 µL of BCA working reagent and incubated at 37 °C for 30 min. Afterward, the absorbance was measured at 570 nm using a spectrophotometer (Victor3 1420 Multilabel Counter, Perkin Elmer, USA).
Total polysaccharides were quantified using the phenol-sulphuric acid method described by Dubois *et al*. [30], using glucose as the standard sugar. Absorbance was measured at 490 nm in the spectrophotometer mentioned above.

2.3. Clay characteristics and flocculation tests

Flocculation tests were carried out in a jar test flocculation unit, as described by Ajao *et al*. [8]. Naturally occurring kaolinite (purchased from Sigma-Aldrich, Netherlands) and montmorillonite (purchased from VWR, Netherlands) were used as model particles. These clay particles were selected due to their different characteristics (Table 1), to mimic mixed particles in natural environments. Although kaolinite is the most common clay in many mining and oil sand operations, other clay types such as montmorillonite are also major components [31]. Montmorillonite behaves differently from kaolinite because of its swelling character, which is attributed to the Na^+ and Ca^{2+} exchange on the clay surface. The swollen clay retains much water and contributes to the poor dewaterability of tailings ponds [31]. For this reason, montmorillonite suspensions are also important model systems to investigate.

We investigated the potential of the harvested mixed EPS, its fractions and the combination of fractions to flocculate single and dual clay mixtures. For this purpose, three clay suspensions (a working volume of 100 mL) were prepared: (i) 5 g/L kaolinite suspension, as extensively used in

several studies to determine the flocculation performance of EPS [8] (ii) 1.5 g/L montmorillonite suspension [32] – a lower montmorillonite concentration was used due to its swelling property, and (iii) a mixture of kaolinite and montmorillonite (1.5 g/L each). Each suspension was prepared in Milli-Q water, stirred overnight and neutralised to pH 7 by adding a few drops of NaOH. EPS samples were also dissolved in Milli-Q water at a concentration of 0.1 g/L.

Table 1. Clay characteristics.

Kaolinite ($Al_2O_3 \cdot 2SiO_2 \cdot 2H_2O$)	Montmorillonite $(Na,Ca)_{0.33}(Al,Mg)_2(Si_4O_{10})(OH)_2 \cdot nH_2O$
1:1 clay: 1 silica tetrahedral sheet and 1 alumina octahedral sheet	2:1 clay: 2 silica tetrahedral sheets and 1 alumina octahedral sheet
Layers held by hydrogen bond – restricts expansion	Layers held by van der Waals bond
Low swelling capacity	High swelling capacity
Low cation exchange capacity, (~ 0.09 meq/g)	High cation exchange capacity (~1 meq/g) [33]
Volume-based particle size: 2.93 ± 1.51 µm [a]	Particle size (after swelling): 5.97 ± 2.51 µm [a]
Surface area (BET): 7.52 m^2/g [b]	Surface area (BET): 25.68 m^2/g [b]
Total pore area (NLDFT): 5.75 m^2/g [b]	Total pore area (NLDFT): 19.10 m^2/g [b]

[a] Particle size was measured using a DIPA 2000 (Doner Technologies, Israel).
[b] Surface area and porosity were determined using a Micromeritics Tristar 3000 (USA). The detailed method has been described by Suresh Kumar *et al*. [34]. BET: Brunauer-Emmett-Teller; NLDFT: Non-Local Density Functional Theory.

First, we determined for each EPS fraction and the mixed EPS the optimum concentration required to best flocculate each clay. (As shown later in Section 3.5.1, the flocculation tests were carried out in a 'starved' polymer regime, i.e., an excess particle surface area compared to the polymer dosage.) From this result, the best performing EPS fractions, different combinations of fractions and the mixed EPS were investigated for mixed particle flocculation. In all the tests, 100 mg/L Ca^{2+} (from $CaCl_2 \cdot 2H_2O$) was added as a coagulant to reduce the electrostatic repulsion between the negatively charged clay particles and to facilitate bridging between the anionic particles and EPS [6,27]. (About this Ca^{2+} concentration is frequently observed in natural waters.) Supernatant turbidity after flocculation was measured with a turbidimeter (2100N IS, Hach) in Nephelometric Turbidity Units (NTU). Flocculation efficiency (*FE*) was calculated as follows:

$$FE\ (\%) = \frac{NTU_{control} - NTU_{test}}{NTU_{control}} \qquad (2)$$

where $NTU_{control}$ is the turbidity value of the control experiment (without EPS addition but with Ca^{2+} addition), and NTU_{test} is the turbidity value of test experiment (with Ca^{2+} and EPS added). The supernatant was also analysed with LC-OCD to measure the biopolymer organic carbon [6] that was not adsorbed in the flocs (supernatant-phase EPS concentration or non-adsorbed EPS concentration), and by subtracting this from the total dosed EPS concentration, we obtained the

fraction of EPS adsorbed (adsorbed EPS). Additionally, the zeta (ζ) potential of the supernatants, clay suspensions and EPS were calculated from electrophoretic measurements (Malvern Mastersizer 2000, UK) using the Smoluchowski equation [35]. It is important to note that the ζ potential is not affected by the clay concentration [35]. All experiments and analyses were done in at least duplicates.

2.4. Optical reflectometry test

A stagnation point optical reflectometer (manufactured by the Laboratory of Physical Chemistry and Soft Matter, Wageningen University and Research, Netherlands) was used to determine the adsorbed amount and build-up behaviour of the EPS fractions. A full description of the device and its underlying theory have been thoroughly described elsewhere [24,36], but in the supplementary information, there is a description of the stagnation point region. Reflectometry is an optical technique used to observe the *in situ* adsorption of molecules on an optically flat surface, such as a silicon wafer. The changes in signal measured upon adsorption on the surface (ΔS) is directly proportional to the adsorbed amount, Γ (mg/m^2) according to the equation:

$$\Gamma = Q_f \frac{\Delta S}{S_0} \qquad (3)$$

where S_0 is the starting output signal of the bare silicon wafer, $\Delta S = S - S_0$ is a change in the signal upon adsorption on the surface, and Q_f (mg/m^2) is the sensitivity factor, calculated with the *Prof. Huygens* v1.3 program (Dullware software) using the refractive index increments (d*n*/d*c*) of the adsorbate (in this case, EPS). To determine the d*n*/d*c*, the refractive indexes (*n*) of mixed EPS at different concentrations (*c* = 0.5, 1.0, 2.5, 5, 10, 15, 20 g/L; dissolved in Milli-Q water) were measured at room temperature (21 ± 1 °C) using a J47 refractometer (Rudolph, USA). The d*n*/d*c*, which is the slope of *n versus c* was obtained as 0.135 mL/g (see supplementary information, Fig. S1), a value close to that of poly(ethylene oxide), the most studied polymer in optical reflectometry ($dn/dc_{\text{poly(ethylene oxide)}}$ = 0.134 mL/g).

Since both kaolinite and montmorillonite clays (and most clay particles) are silica-based, the reflectometry tests were performed on a silica surface, which is largely representative of most clay types. Silicon wafers (obtained from Wafernet, USA) were heated at 1000 °C for 1 h to form an oxide layer of silica. The oxidised wafers with a silica layer thickness of 70 ± 10 nm (measured by ellipsometry) were cut into strips of approximately 1 x 4 cm^2, immersed in a freshly prepared piranha solution (1 part of 30% H_2O_2 and 3 parts of 95% H_2SO_4) for 20 minutes and rinsed in Milli-Q water.

Each adsorption measurement typically involved a wafer being placed in the reflectometer cell, rinsed with a solvent (200 mg/L Ca^{2+}, except stated otherwise) to establish the baseline signal (S_0), followed by the introduction of an EPS sample solution and its adsorption was monitored, in most cases, until a plateau was reached. In some cases, this was followed by rinsing with the same solvent until a new plateau was reached, and in other cases, another EPS sample solution was directly introduced. All reported values were calculated based on the amounts that remained adsorbed on the surface after rinsing with the solvent (referred to as the irreversible adsorbed amounts) unless mentioned otherwise. All EPS samples were tested at pH 7.

3. Results

3.1. EPS characteristics

3.1.1. Composition and functional groups

FTIR analysis was carried out to compare the chemical composition of the mixed EPS (the harvested soluble-EPS) and its fractions (Fig. 2). The mixed EPS, HMW EPS and MMW EPS showed similar absorption bands (interpreted in Table 2), revealing the presence of polysaccharides and proteins as the main components. Although this FTIR analysis mainly gives qualitative information, a clear difference is observed between the LMW EPS spectrum and the other spectra. The typically broad and sharp O–H stretching vibrations at around 3282 cm^{-1} was rather obscure for the LMW EPS. Similarly, the band at 1018 cm^{-1} (C–O–C asymmetric stretching) was noticeably smaller in the LMW EPS spectrum compared to the other spectra that have sharp and distinct peaks. These two groups are associated with carbohydrates, suggesting that the LMW EPS have a much lower polysaccharide content than the MMW and HMW fractions (confirmed later by other characterisation techniques). On the other hand, the amide III band at 1396 cm^{-1} was more conspicuous in the LMW EPS spectrum than the other spectra, signifying a higher protein content in the LMW EPS than the other EPS fractions. The fingerprint region between 866 and 650 cm^{-1} (found only in the LMW EPS spectrum) is associated with the ring vibrations from aromatic amino acids and nucleotides [37].

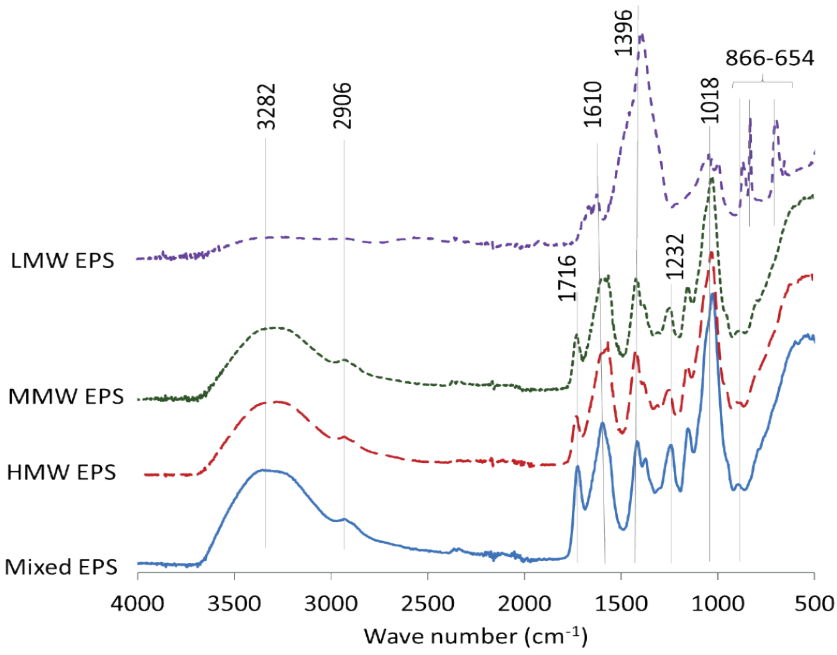

Fig. 2. FTIR spectra of mixed EPS and its fractions – HMW (high molecular weight), MMW (medium molecular weight) and LMW (low molecular weight).

Table 2. Band assignment for the FTIR spectral features of mixed EPS and its fractions [37–39].

Wavenumber (cm^{-1})	Functional group assignment
3282	O–H stretching vibrations
2906	C–H stretching vibration
1716	C=O stretching vibration of protein amide I band
1610	Out-of-phase N–H bending and C–N stretching vibrations of protein amide II band
1396	In-phase N–H bending of protein amide III band
1365	C=O symmetric stretching of $–COO^-$ groups
1232	C–O stretching of alcohol
1018	C–O–C asymmetric stretching of ester linkage of polysaccharides
866-654	Ring vibrations from aromatic amino acids and nucleotides

Further quantification of the total polysaccharide and protein content is given in Table 3. The mixed EPS were composed of about 76 wt% biopolymers and the remaining 24 wt% accounts for non-biopolymeric components such as building blocks, low molecular weight acids and neutrals [6]. Out of the 76% biopolymers, 65 ± 3 wt% were polysaccharides and the remaining 11 ± 2 wt% were composed of proteins. The polysaccharides could be further fractionated into approximately 36 wt% HMW, 28 wt% MMW, and 3 wt% LMW fractions (MW characterisation on Table 3). The reverse trend was observed for the protein fractionation, which is consistent with the FTIR result in Fig. 2: out of the 11 wt% EPS proteins, the fractions comprised 3 wt% HMW, 4 wt% MMW and 5 wt% LMW proteins. Hence, the order of the polysaccharide/protein ratio was HMW > MMW > LMW (Table 3). Apparently, polysaccharides were the main constituents in the high and medium MW EPS fractions while the LMW EPS fraction contained more proteins than polysaccharides.

3.1.2. Molecular weight and charge density

The average MW of the mixed EPS and its fractions are also presented in Table 3. The high MW of the mixed EPS (1.7 MDa) is similar to that previously reported [27], showing the possibility to obtain consistent EPS MW under similar operational conditions. A further size-fractionation of the mixed EPS reveals that the high, medium and low MW fractions have average MW values of 1.99, 0.78 and 0.13 MDa, respectively. The obtained MW value for the smallest EPS fraction (0.13 MDa) was however higher than the membrane's MWCO (0.1 MDa), indicating that some pores were larger than the manufacturer's reported average MWCO.

Table 3. Properties of mixed EPS and its fractions – HMW (high molecular weight), MMW (medium molecular weight) and LMW (low molecular weight). Polysaccharides and proteins values are mean ± standard deviation of triplicate assays. Values of MW and CD are mean ± standard deviation of duplicate measurements.

Parameter	Mixed EPS	HMW EPS	MMW EPS	LMW EPS
Polysaccharide content [a] (g/g EPS)	0.65 ± 0.03	0.36 ± 0.04	0.28 ± 0.03	0.03 ± 0.00
Protein content [b] (g/g EPS)	0.11 ± 0.02	0.03 ± 0.01	0.04± 0.01	0.05 ± 0.01
Polysaccharide/protein ratio	6	12	7	0.6
Average molecular weight (MDa)	1.68 ± 0.15	1.99 ± 0.05	0.78 ± 0.03	0.13 ± 0.01
Charge density at pH 7 (meq/g)	5.10 ± 0.15	6.46 ± 0.12	5.12 ± 0.12	1.30 ± 0.11

[a] based on glucose equivalent units.
[b] based on BSA equivalent units.

Each MW fraction possesses functional groups (particularly carboxyl and amine groups from polysaccharides and proteins) that are responsible for their charge. The charge density (CD) values in Table 3 are directly proportional to the polysaccharide/protein ratios: the HMW EPS with the highest ratio (12) have the highest CD value (6.46 meq/g). Likewise, the LMW EPS have the lowest CD value (1.30 meq/g). These findings imply that the EPS polysaccharides (with functional groups –OH and $–COO^-$) gave a higher contribution to the anionic CD than the proteins (with functional groups $–NH_2$ and $–COO^-$), which is consistent with other studies [27,40].

3.3. Flocculation in single clay systems

Flocculation tests were performed on kaolinite and montmorillonite suspensions separately, with the addition of 100 mg/L Ca^{2+} as a coagulant. A preliminary test without Ca^{2+} addition showed no flocculating effect and even led to negative flocculation efficiency values. The flocculation efficiencies of mixed EPS and its fractions toward these clay particles, in the presence of Ca^{2+}, are given in Fig 3A and B. Clearly, the sole use of the LMW EPS showed poor flocculation of both kaolinite and montmorillonite particles. Above 0.5 mg LMW EPS/g kaolinite (1.0 - 20.0 mg/g kaolinite – results not shown), negative flocculation efficiencies were even obtained. At the optimum dosage of 0.2 mg/g kaolinite and 1.0 mg/g montmorillonite, the maximum flocculation efficiencies with LMW EPS were only 12% and 19%, respectively. In contrast, the MMW, HMW and mixed EPS exhibited good flocculation of kaolinite particles with average efficiencies of 87.4, 93.9, and 92.9 % respectively, each at an (estimated) optimum dosage of 0.1 mg/g kaolinite. Above this dosage, flocculation performances decreased, likely caused by the restabilisation of clay particles at concentrations above the optimum. Although the HMW EPS showed the highest efficiency with kaolinite (93.9%), the performance of mixed EPS was not significantly lower (92.9%).

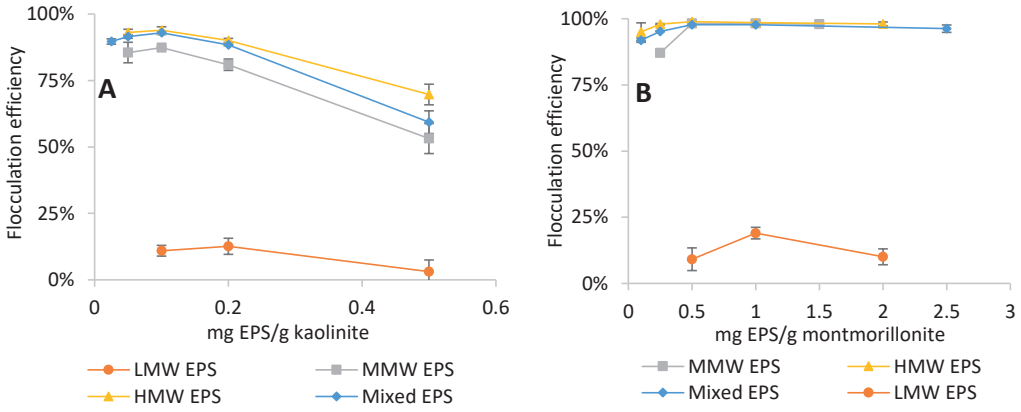

Fig. 3. Flocculation performances of mixed EPS and its fractions (with 100 mg/L Ca^{2+}) on kaolinite (**A**) and montmorillonite (**B**) clays.

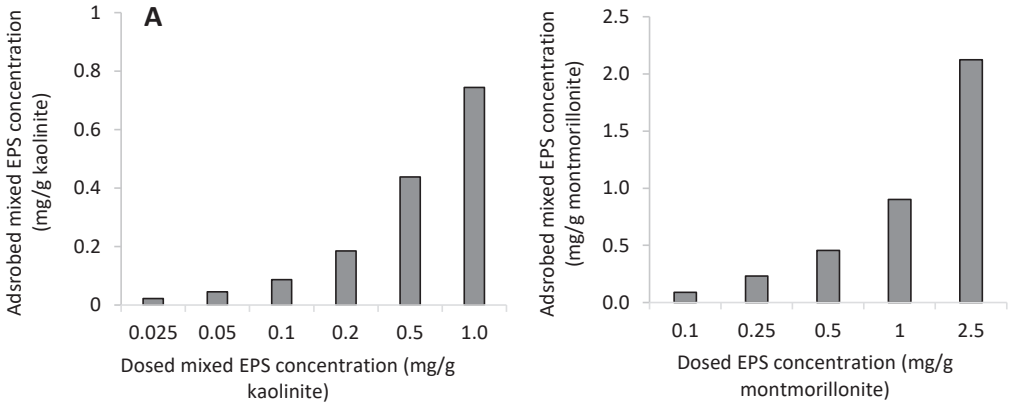

Fig. 4. The dosed mixed EPS concentration compared to the adsorbed mixed EPS concentration. (**A**) Kaolinite flocculation, (**B**) montmorillonite flocculation.

With montmorillonite, higher flocculation efficiencies were obtained compared to kaolinite. The highest average performances of the MMW, HMW, and mixed EPS were 98.3, 98.9, and 97.7 %, respectively, at a dosage of 0.5 mg/g montmorillonite. Above this dosage, up to 2.5 mg/g, the flocculation efficiencies remained relatively constant for each EPS type. Thus, in contrast to kaolinite, the restabilisation effect was not observed with montmorillonite at higher dosages.

The relationship between the dosed and adsorbed mixed EPS concentrations are presented in Fig. 4. At EPS dosages above 0.5 mg/g clay, an increasing surface saturation starts to become apparent since the amount adsorbed becomes significantly smaller than the amount dosed. The adsorbed EPS concentrations required to achieve the best flocculation performance were 0.09 mg/g kaolinite and 0.46 mg/g montmorillonite. These two values are close to the dosed mixed EPS concentrations

of 0.1 mg/g kaolinite and 0.5 mg/g montmorillonite, respectively, demonstrating that, at the optimum dosages, 90% of the dosed mixed EPS was adsorbed on the kaolinite flocs and 92% was adsorbed on the montmorillonite flocs. These adsorbed concentrations (0.09 mg/g kaolinite and 0.46 mg/g) correspond to surface coverage areas of 0.012 mg/m^2 kaolinite and 0.018 mg/m^2 montmorillonite (using the BET values on Table 1). The higher coverage area for montmorillonite may have contributed to the higher flocculation performance compared to kaolinite flocculation performance.

3.4. Dual clay flocculation

The optimum flocculation dosages of each EPS fraction on kaolinite and montmorillonite were used to flocculate a 1:1 mixture of both clays (1.5 g/L each). Additionally, flocculation tests were carried out to determine the optimum concentrations for the mixed particles. The results are presented in the Supplementary information – Table S1. The main findings, illustrated in Fig. 5, show the effect of different EPS mixtures on mixed particle flocculation. With the HMW EPS (0.5 mg/g), a flocculation efficiency of 95.7% was achieved. At an equal dosage of the LMW and HMW EPS fractions (0.5 mg/g each), the efficiency was 96.2%. At equal concentrations (0.25 mg/g each) of the MMW and HMW EPS, the flocculation performance was 98%, and with the harvested mixed EPS, the efficiency was 98.7% at a dosage of 0.25 mg/g. These results show that, with a mixture of MW fractions, the flocculation of mixed clay particles could be increased compared to using a single MW fraction (HMW EPS). Furthermore, the lower dosage required by the mixed EPS compared to the single MW fraction and the dual EPS mixtures is beneficial from a practical point of view.

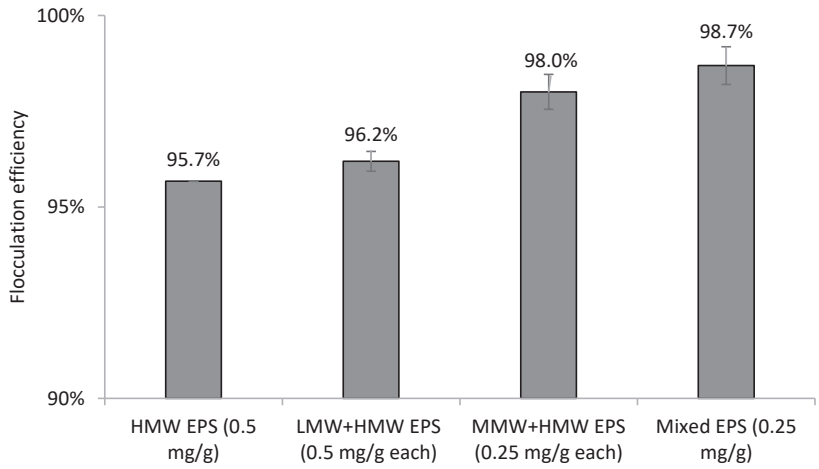

Fig. 5. Flocculation performance of mixed EPS and its fractions (with 100 mg/L Ca^{2+}) on a 1:1 mixture of kaolinite and montmorillonite clays at the optimal EPS concentrations.

3.5. EPS adsorption on a silica surface

While the jar tests of the clay particles provide useful information on the flocculation performances of the EPS (fractions), other important parameters such as the adsorption kinetics and the understanding of how each EPS fraction contributes to particle adsorption cannot be obtained by jar tests, hence optical reflectometry was employed (described in Sections 1 and 2.4).

3.5.1. Effect of calcium concentration

Since both the silica surface and EPS (fractions) were negatively charged, the addition of cations, especially divalent cations, was needed to reduce the electrostatic repulsion. Hence, the adsorption tests were carried out for all the EPS samples dissolved in a $CaCl_2 \cdot 2H_2O$ solution.

First, we established the optimum Ca^{2+} concentration needed for maximum irreversible adsorption (undesorbed EPS after rinsing the silica surface with the solvent) of EPS on the silica surface. Fig. 6 shows the adsorbed amount of mixed EPS at different Ca^{2+} concentrations – 100, 200, and 400 mg/L Ca^{2+} (i.e. 2.5, 5 and 10 mM Ca^{2+}, respectively). In 200 mg/L Ca^{2+}, the highest adsorbed amount (Γ) of EPS (1.1 mg/m^2) was obtained and the adsorption was irreversible. This Ca^{2+} concentration was also obtained by Zhu *et al*. [41] as the optimum concentration for EPS deposition on silica using quartz crystal microbalance with dissipation (QCM-D), in lieu of an optical reflectometer.

Lower adsorbed amounts (Γ = 0.6 mg/m^2 each) were obtained in the 100 and 400 mg/L Ca^{2+} solutions. This suggests that in both solutions, there was insufficient Ca^{2+} available for binding between the EPS and the silica surface. In the 100 mg/L Ca^{2+} solution, the adsorption reached an equilibrium faster than the other two solutions (Fig. 6). However, the maximum adsorbed amount of 1.1 mg/m^2 was not attained, perhaps due to insufficient Ca^{2+} to form complete polymer-surface bridges. On the other hand, above the optimum Ca^{2+} concentration required for adsorption (in the case of 400 mg/L Ca^{2+}), Lee *et al*. [42] described the occurrence of polymer-polymer binding instead of polymer-surface binding, which hampers the irreversible anchoring of polymers to surfaces (illustrated in Fig. 7). This phenomenon was substantiated by the desorption that occurred after the solvent injection in Fig. 6 (the vertical grey line).

It is worth mentioning that the optimum Ca^{2+} concentration and EPS surface coverage areas for the reflectometry and flocculation tests are different because, while the former involves an 'overdose' polymer regime, the latter operates in an 'underdose' or 'starved' polymer system. In reflectometry, the maximum adsorbed amount (a fully covered surface) is measured while in the flocculation process, a low surface coverage (low adsorption density) is needed [13] because a polymer adsorbed on one particle should be able to find a free spot on another particle. Comparing the optimum concentration of mixed EPS adsorbed on the clay particles (0.012 mg/g kaolinite and 0.018 mg/g montmorillonite – section 3.3) with the maximum adsorbed amount (Γ) on the silica surface (0.6 mg/m^2 at 0.5 g/L EPS and 100 mg/L Ca^{2+}), the optimal mixed EPS surface coverage for good flocculation was about 2% for kaolinite and 3% for montmorillonite.

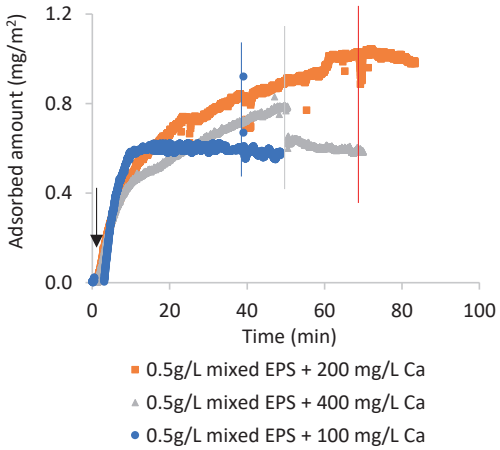

Fig. 6. Adsorbed amounts of mixed EPS dissolved in solutions of different Ca^{2+} concentrations on a silica surface. The black arrow is the point of EPS injection after establishing the baseline with the solvent (Ca^{2+} solution); the coloured vertical lines are the points of solvent injection after EPS adsorption on the surface: blue line for 100 mg/L Ca^{2+}, grey line for 400 mg/L Ca^{2+} and red line for 200 mg/L Ca^{2+}.

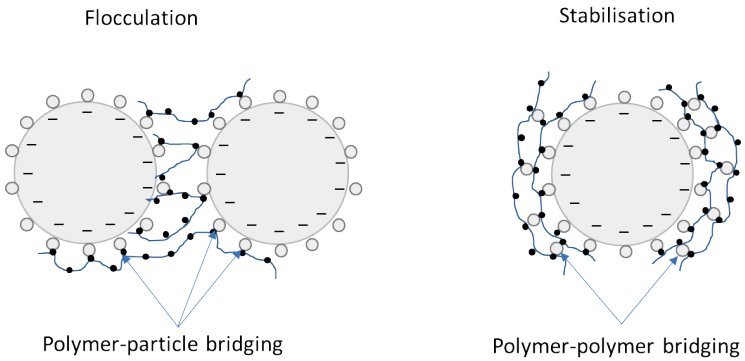

Fig. 7. Lee *et al.*'s [42] illustration of anionic polymer adsorption on kaolinite for two different types of divalent cationic bridging (flocculation and stabilisation).

3.5.2. Adsorption of mixed EPS and its fractions

At the optimum Ca^{2+} concentration (200 mg/L Ca^{2+}), varying concentrations of mixed EPS (0.1 - 2.0 g/L) were adsorbed on the silica surface to establish an adsorption isotherm. Fig. S2 (see supplementary information) shows that the isotherm reached a plateau at EPS concentrations above 0.5 g/L, with no significant difference in the adsorbed amounts at these concentrations (~ 1.1 mg/m^2). Hence, 0.5 g/L was used as the optimum EPS concentration (for the study of the maximum adsorbed amounts by reflectometry) for the mixed EPS, and also the HMW and MMW EPS since these three EPS types had the same optimum flocculation dosage (0.1 mg/g kaolinite and 0.5 mg/g montmorillonite).

Table 4. Adsorbed amounts (Γ) of mixed EPS and its fractions on silica surface in the presence of 200 mg/L Ca^{2+}. Unless otherwise stated (denoted as [a]), all Γ values were taken after solvent injection (irreversible adsorbed amounts). Hence, values with the superscript '[a]' are those before the solvent injection.

EPS (fraction)	EPS concentration (g/L)	Ca^{2+} concentration (mg/L)	Γ (mg/m^2)	Γ (μeq/m^2)
Mixed EPS	0.5	200	1.07	5.43
HMW EPS	0.5	200	0.79	5.07
MMW	0.5	200	1.00 [a]	
MMW	0.5	200	0.42	2.15
LMW	0.5	200	1.50 [a]	
LMW	0.5	200	0.00	
LMW	1.0	200	2.78 [a]	
LMW	1.0	200	0.49	0.64
LMW, then HMW	1.0, 0.5	5	0.49 [a], 1.20	

[a] Adsorbed amount before solvent (200 mg/L Ca^{2+}) injection.

Each EPS fraction had a lower irreversible adsorbed amount than the mixed EPS. The HMW, MMW and LMW EPS had irreversible Γ values of 0.79, 0.42 and 0.49 mg/m^2 at concentrations of 0.5, 0.5 and 1 g/L, respectively, (Table 4). Out of these three fractions, only the HMW EPS did not desorb significantly after rinsing with the solvent (Fig. S3). The MMW-EPS (at a concentration of 0.5 g/L) desorbed from 1.0 to 0.42 mg/m^2 (Fig. 8) while the 0.5 g/L LMW EPS was completely desorbed (from 1.5 mg/m^2 before solvent injection to 0 mg/m^2 after solvent injection). However, the adsorbed amount of LMW EPS was concentration-dependent. At 1 g/L, about 2.8 mg/m^2 of LMW-EPS was adsorbed on the silica surface, out of which 0.49 mg/m^2 was irreversible (Fig. 9). Hence, 82% of the initial adsorbed amount was desorbed as opposed to 58% for the MMW-EPS.

Each EPS fraction also displayed different adsorption rates, in the order LMW EPS > MMW EPS > HMW EPS (Table 5). The LMW EPS (composed of short polymeric chains relative to the other fractions) were rapidly deposited on the silica surface, with an initial adsorption rate, $[d\Gamma/dt]_0$ of 0.41 mg/m^2/s, followed by the MMW EPS with a $[d\Gamma/dt]_0$ of 0.096 mg/m^2/s. The $[d\Gamma/dt]_0$ of the HMW EPS and the mixed EPS were much lower (0.0004 mg/m^2/s for the HMW EPS and 0.0012 mg/m^2/s for the mixed EPS).

To obtain more information on the adsorption mechanism, we compared the initial adsorption rate, $[d\Gamma/dt]_0$ with the rate at which the polymers arrived at the interface (silicon wafer), given by the theoretical flux (J) [36]. When at the initial stage of the adsorption process, all the molecules that arrive the interface do adsorb, then $[d\Gamma/dt]_0 = J$. Table 5 shows that both the initial adsorption rate and the theoretical flux are inversely proportional to the MW (and most likely, the chain length) of

the EPS fractions. About 85% of the LMW EPS molecules and 81% of the MMW EPS molecules that arrived at the interface adsorbed while only 0.4% of the HMW EPS molecules were adsorbed.

It is worth mentioning that each of the EPS fractions (LMW, MMW and HMW) was somewhat polydisperse and the mixed EPS was very polydisperse. As *J* is directly proportional to the diffusion coefficient *D*, this means that small molecules (with a relatively high *D*) arrive at the surface first and thus, the adsorption kinetics is dominated by the smallest molecules within the EPS fraction. However, *D* was determined by dynamic light scattering (see supplementary information) and this technique is governed by the largest (and slowest) molecules because these scatter light the most. Hence, it is possible that we underestimated the flux of the molecules towards the surface and overestimated the percentage of polymers that adsorbed at the interface. However, we may safely conclude from the results in Table 5 (specifically from the percentage of EPS fractions adsorbed at the interface) that the adsorption kinetics of the LMW and MMW EPS fractions were (at least) mass transport-limited, while the adsorption kinetics of the HMW EPS fraction must have been limited by other factors aside mass transport, such as the unfolding of the polymer or conformational transitions [13].

Table 5. The initial adsorption rate, $[d\Gamma/dt]_0$ and the rate at which each EPS fraction arrived at the interface (theoretical flux, *J*).

EPS (fraction)	Initial adsorption rate, $[d\Gamma/dt]_0$ (mg/m²/s)	Theoretical flux, *J* (mg/m²/s)	% of EPS adsorbed at the interface (%)
LMW EPS	0.41	0.48	85
MMW EPS	0.096	0.12	81
HMW EPS	0.0004	0.10	0.4

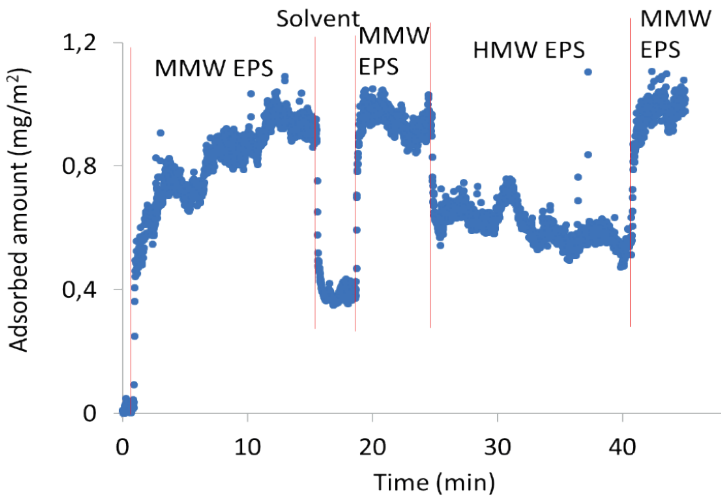

Fig. 8. Adsorption of HMW EPS fraction (0.5 g/L) on pre-adsorbed MMW EPS fraction (0.5 g/L).

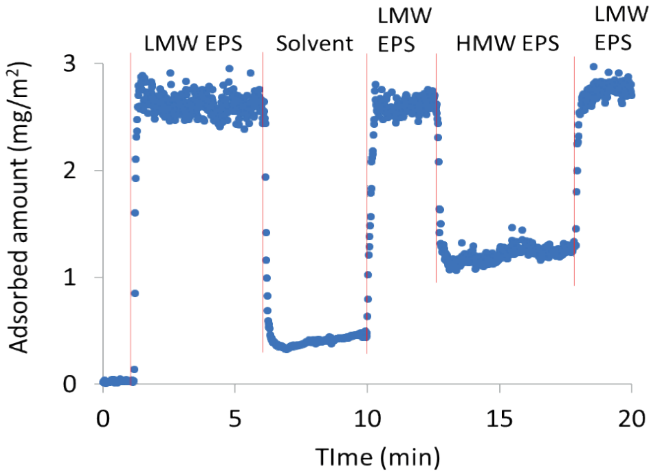

Fig. 9. Adsorption of HMW EPS fraction (0.5 g/L) on pre-adsorbed LMW EPS fraction (1.0 g/L).

4. Discussion

4.1. Mixed EPS characteristics

Since bacterial EPS, particularly wastewater-produced EPS, are a heterogeneous mixture of biomacromolecules, understanding the properties of each MW fraction is crucial in gaining insights into their flocculation behaviour. We can determine if it is expedient to extract the individual fractions (particularly the HMW fraction) for single or mixed clay flocculation or to use the produced mixed EPS without further fractionation.

Having shown in previous studies that nitrogen limitation coupled with a relatively short solids retention time (1 - 3 days) is essential for increased EPS recovery from wastewater [27,43], the outcome of such a strategy, as also shown in this study, is the production of polysaccharide-rich mixed EPS with low protein content (at least when glycerol/ethanol-rich wastewater is used as the substrate). In addition, the results of this study reveal that about 93 wt% of the biopolymers are in the high and medium MW range, from which 84% are polysaccharides. These two fractions (the HMW and MMW EPS), majorly comprising polysaccharides, are largely responsible for the overall high MW (1.68 MDa) and charge density (5.10 meq/g) of the mixed EPS (Table 3) and determine its flocculation capacity. The MW of the produced mixed EPS tested in this study is within the range (500 - 2000 kDa) reported for other exopolysaccharides such as alginate and xanthan gum [44]. Extracellular proteins, on the other hand, are typically in the LMW range (10 - 250 kDa) [27,45] and have also been reported to play a critical role in flocculation [46]. Hence, the effect of protein-rich LMW EPS fraction on particle adsorption could not be overlooked and was studied alongside the polysaccharide-rich MMW and HMW EPS fractions.

4.2. Adsorption and flocculation of single clay particles

Preliminary flocculation tests done in the absence of Ca^{2+} showed, as expected, that EPS, having a net negative charge, could not flocculate negatively charged particles (such as kaolinite and montmorillonite) suspended in a medium of low ionic strength or one void of multivalent cations [6,32,41]. This is due to the electrostatic repulsion between the polymer adsorption sites and the clay particles according to the classical DLVO theory [6,41]. This phenomenon was confirmed with the zeta (ζ) potential measurements in Table S2 (supplementary information), which demonstrate that (i), the sole addition of EPS to the clay suspension did not increase the ζ potential value, as would be the case for cationic polymers [47]. This implies that the interaction between clay particles and EPS is governed by the presence of di/multivalent cations, whereby Ca^{2+}, for instance, can bridge between the anionic groups (COO^- – Table 2) of EPS and the negative sites of the clay particles [16]. (ii) Above the optimum EPS dosage, the ζ potential values decreased due to the increasing concentration of non-adsorbed EPS in the supernatant (Fig. 4).

Above the optimum EPS dosage needed to flocculate the kaolinite particles, flocculation efficiencies decreased (Fig. 3A). This phenomenon has also been reported for the flocculation of kaolinite with excess anionic polyacrylamide [42]. During polyelectrolyte attachment to adsorption sites, bridges are developed between polymers and particles via divalent cationic bridging or hydrogen bonding [6,48]). Once the adsorption sites are occupied, higher polymer dosages result in higher concentrations of non-adsorbed polymer molecules in solution [42], as seen in Fig. 4. The effect of this is a reduction in particle flocculation because polymer-polymer bridges (which lead to stabilisation) become more dominant than polymer-particle bridges (which lead to flocculation), as illustrated in Fig. 7 [42]. Polymers with a relatively high CD (as found in the MMW, HMW and mixed EPS – Table 3) are more susceptible to this effect due to the presence of unoccupied sites that can engage in intramolecular bonding [6,27,42].

As regards montmorillonite flocculation with MMW, HMW and mixed EPS, colloid restabilisation did not occur at the tested dosages of 0.5 - 2.5 mg/g (Fig. 3B). A similar outcome has also been reported for montmorillonite and bentonite (the major fraction of bentonite is montmorillonite [49]) flocculation with anionic polyacrylamide [49], cationic polyacrylamide [32], non-ionic guar gum, non-ionic hydroxypropyl guar gum and cationic hydroxypropyl guar gum [50]. This implies that the absence of restabilisation in montmorillonite at increased polymer dosages is likely not governed by the polymer type, polymer charge or charge density but more related to the clay property. A possible explanation is the high cation exchange capacity of montmorillonite (Table 1), whereby Ca^{2+} (used as the coagulant in this study) can replace Na^+ in the clay, thereby increasing montmorillonite's adsorption sites for polymer-particle bridging, instead of polymer-polymer bridging that leads to stabilisation.

The LMW EPS (in the presence of 100 mg/L Ca^{2+}) might have been confined within the electrostatic repulsion layer because of their short polymeric chains [51], thus unable to effectively bridge between particles, leading to poor flocculation performances. The reflectometry tests further revealed that at low concentrations (< 1 g/L), LMW EPS rapidly but reversibly adsorbed to the silica

surface. In general, it is easier for small molecules to desorb from a surface due to their low binding affinity (as a result of their low adsorption energy per chain [36]), whereas, large polymers (with a high adsorption energy per chain) are bound to a surface by several 'trains' [16]. For desorption to occur, all trains of a chain must get loose at the same time, and the chance of this happening is smaller with increasing polymer length. At high concentrations of the LMW-EPS fraction (≥ 1 g/L), the bigger polymers in this fraction are large enough to be irreversibly adsorbed (Table 4).

In the same vein, the MMW, HMW and mixed EPS induced particle flocculation. Apparently, the MW of these EPS types played significant roles in the flocculation process, especially when bridging is the underlying mechanism. This agrees with literature that flocculation is driven by 'high' MW components (>> 100 kDa) that can expand into the bulk and bridge with particles [16,39]. As observed in the adsorption tests, the mixed EPS and the HMW fraction were not desorbed after the solvent rinse. This irreversible adsorption is due to the strong attachment of the long polymeric and highly charged chains to the surface [36]. Although slow in the initial adsorption kinetics, the HMW polymers have a higher binding to the surface than the fast-adsorbing LMW and MMW fractions, and this may suggest that with time, the HMW EPS may replace the weakly bound smaller polymers. However, Fig 8 and 9 show that this is not the case.

Overall, the flocculation of single clay particles shows no significant differences among the performances of the MMW, HMW and mixed EPS types, although, for kaolinite, the HMW and mixed EPS would be preferred. More importantly, this study reveals that the presence of short polymeric chains (LMW EPS) in the harvested mixed EPS does not hinder its flocculation performance. Hence, mixed EPS can flocculate single clay particles as effectively as single-type HMW EPS.

4.3. Adsorption and flocculation in a dual particle system

One of the hypotheses prior to this study was that wastewater-derived mixed EPS (consisting of LMW, MMW and HMW fractions) could better flocculate a mixture of particles compared to the use of HMW EPS, perhaps due to the different MW fractions that may work synergistically for mixed particle flocculation.

The results in Fig. 5 show that mixtures of EPS can better flocculate mixed particles than the single HMW fraction. Furthermore, there is a 50% lower dosage requirement when using mixed EPS instead of the HMW EPS. The reflectometry results in Fig. 8 and 9 nicely explain the underlying adsorption mechanism of dual EPS fractions. Both figures reveal that the subsequent adsorption of the HMW EPS fraction did not displace the already adsorbed LMW and MMW EPS, which differs from what is found when homopolymers adsorb to silica surfaces [25]. For instance, the co-adsorption of the LMW and HMW EPS fractions in Fig. 9 resulted in a total adsorbed amount of 1.2 mg/m^2, a slightly higher value than the mixed EPS adsorbed amount (1.1 mg/m^2). The higher value may be due to the higher concentration of each tested EPS fraction compared to what was found in the harvested mixed EPS.

Additionally, the LC-OCD results in Table S3 (see supplementary information) also confirm the co-adsorption (rather than competitive adsorption) of both the LMW and HMW EPS fractions, and the MMW and HMW EPS fractions. At the optimum dosages, the EPS fractions were adsorbed in the flocs and their concentrations in the supernatant phase were found to be below the equipment's detection limit, even after concentrating the supernatant five times. However, above the optimum mixed EPS concentration (dosed concentration of 0.5 mg/g), not all the EPS fractions were adsorbed in the flocs. About 24.4 µg/L (= 0.05 mg/g clay), attributed to the HMW EPS fraction, was measured in the supernatant phase.

Based on these results, we mechanistically deduce that when (mixtures of) particles are to be flocculated with mixed EPS comprising low, medium and high MW fractions, the LMW and MMW EPS, which are least affected by mass transport limitation, first adsorb to the (smallest) particles, while the HMW-EPS slowly attach to the bigger particles and the anchor sites of the LMW chains, both processes taking place in the presence of di/multi-valent cations (Fig. 10). This mechanism is analogous to the 'site blocking' effect, which to the best of our knowledge, has only been reported for dual cationic polymer systems (typically composed of a LMW polymer that acts as a cationic site-blocking agent, and a cationic polymer) [13,52,53]. The vital component of this effect is the ability of the site-blocking agent (in our case, the LMW or MMW EPS fraction) to adsorb to the particle's surface site to which the flocculation polymer (the HMW EPS fraction) can adsorb (illustrated in Fig. 9) [52]. This effect is even more likely when both the site-blocking agent and the flocculation polymer have the same charge type, such that the former can adsorb to the same vacant sites that would have been available for the latter. The advantage of this effect is that the limited adsorption opportunity of the (HMW) flocculation polymer (as a result of site blocking) leads to more extended tails and enhanced bridging possibilities, thus improved flocculation.

A practical implication of these findings is that it would not be necessary to further separate the HMW biopolymer fraction from the harvested EPS before they can be applied as effective flocculants. The harvested mixed EPS can effectively flocculate particles in single and dual clay systems, with performances comparable to the HMW EPS fraction during single clay flocculation, and a better performance than the HMW EPS during dual clay flocculation.

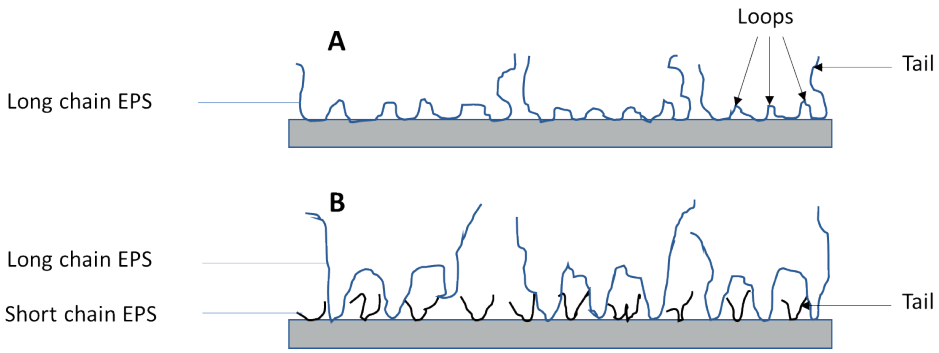

Fig. 10. (**A**) The expected configuration of an adsorbed HMW EPS fraction. (**B**) The co-adsorption of short (LMW EPS) and long (MMW or HMW) chain EPS fractions.

5. Conclusions

Wastewater-derived mixed EPS were successfully fractionated into three MW fractions (high, medium and low MW fractions) and each fraction was further characterised and examined to elucidate the flocculation mechanism of such complex biomacromolecules. This study shows that the MMW, HMW and harvested mixed EPS could effectively flocculate single clay systems, namely kaolinite or montmorillonite, in the presence of divalent cations. However, in a dual clay system, the mixed EPS proved to be more efficient (higher flocculation performance at a lower dosage) than the HMW EPS fraction, implying that the effect of mixed EPS on dual clay systems is higher than for single clay systems. Optical reflectometry coupled with LC-OCD analysis reveal site-blocking effect in EPS mixtures. In this mechanism, the LMW and MMW EPS fractions, which were least affected by mass transport limitation, first adsorbed to the silica surface, while the HMW-EPS slowly attached to the unoccupied sites on the surface. We propose from this, a mixed EPS adsorption mechanism leading to extended anionic polymer tails in solution, thereby enhancing particle flocculation.

Acknowledgements

This work was performed in the cooperation framework of Wetsus, European Centre of Excellence for Sustainable Water Technology (www.wetsus.nl). Wetsus is co-funded by the Dutch Ministry of Economic Affairs and Ministry of Infrastructure and Environment, the European Union Regional Development Fund, the Province of Fryslân and the Northern Netherlands Provinces. This work has also received funding from the European Union's Horizon 2020 research and innovation programme under the Marie Skłodowska-Curie [grant agreement No. 665874]. The authors thank the participants of the research theme 'Natural flocculants' for the fruitful discussions and financial support, and Claire Chassagne from Delft University of Technology for the zeta potential measurements.

Supplementary information of Chapter 5

Table S1. Flocculation performance of EPS fractions (top table: at the optimum EPS dosages for single clay particles; bottom table: at different EPS dosages) on a 1:1 mixture of kaolinite and montmorillonite clays. 100 mg/L Ca^{2+} was added as a coagulant. LMW: Low molecular weight; MMW: medium molecular weight EPS; HMW: High molecular weight EPS.

EPS fraction(s)	Flocculation efficiency (%)
0.1 mg/g HMW EPS (optimum concentration for kaolinite)	92.7 ± 0.2
0.5 mg/g HMW EPS (optimum concentration for montmorillonite)	95.7 ± 0.0
1.0 mg/g LMW EPS, then 0.5 mg/g HMW EPS [a]	95.6 ± 0.4
0.2 mg/g LMW EPS, then 0.1 mg/g HMW EPS [a]	92.5 ± 0.6
1.0 mg/g LMW EPS, then 0.1 mg/g HMW EPS [a]	90.8 ± 0.3
0.2 mg/g LMW EPS, then 0.5 mg/g HMW EPS [a]	94.8 ± 0.0
0.5 mg/g LMW EPS and 0.5 mg/g HMW EPS [b]	96.2 ± 0.3
0.25 mg/g MMW EPS and 0.25 mg/g HMW EPS [b]	98.0 ± 0.1
0.5 mg/g MMW EPS and 0.5 mg/g HMW EPS [b]	96.7 ± 1.3
0.05 mg/g mixed EPS	96.5 ± 0.2
0.1 mg/g mixed EPS	97.4 ± 0.2
0.25 mg/g mixed EPS	98.7 ± 0.5
0.5 mg/g mixed EPS	98.0 ± 0.3
1.0 mg/g mixed EPS	97.2 ± 0.6

[a] The EPS fractions were dosed sequentially: the LMW EPS was first dosed for 4 mins, then the HMW EPS was dosed for 6 mins.

[b] The EPS fractions were mixed and dosed as a single solution.

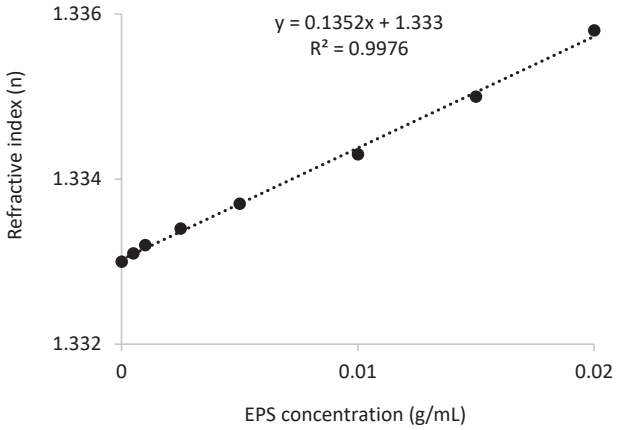

Fig. S1. Determination of the refractive index increments of mixed EPS dissolved in Milli-Q water (dn/dc_{EPS} = slope = 0.135 mL/g).

Table S2. Zeta (ζ) potential values of mixed EPS, its fractions and the supernatant phase after flocculation.

Sample	ζ potential value (mV)
0.1 g L^{-1} mixed EPS only	-43.4 ± 1.9
0.1 g L^{-1} HMW EPS only	-33.4 ± 1.3
0.1 g L^{-1} MMW EPS only	-27.1 ± 2.3
0.1 g L^{-1} LMW EPS only	-8.61 ± 1.3
Montmorillonite only	-18.0 ± 0.5
Kaolinite only	-25.0 ± 1.4
[a] Kaolinite/0.1 mg g^{-1} mixed EPS *	-24.2 ± 1.1
[a] Kaolinite/Ca^{2+} **	-17.9 ± 0.8
[a] Kaolinite/Ca^{2+}/0.1 mg g^{-1} mixed EPS *	-19.7 ± 1.7
[a] Kaolinite/Ca^{2+}/0.5 mg g^{-1} mixed EPS	-21.4 ± 1.9

* Optimum dosage of mixed EPS for the flocculation of kaolinite.

** 100 mg/L Ca^{2+} was used as the coagulant.

[a] Flocculation supernatant phase was measured.

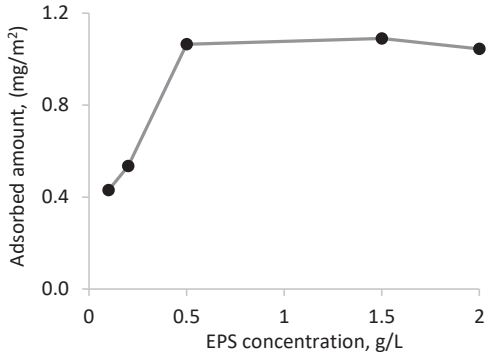

Fig. S2. Adsorption isotherm of mixed EPS (dissolved in 200 mg/L Ca^{2+} solution) on a silica surface.

Table S3. LC-OCD analysis of the supernatant phase after the flocculation of kaolinite and montmorillonite mixtures. N/A: Not applicable, since the biopolymer organic carbon concentration was below the detection limit even after a 5-time concentration of the supernatant.

Dosed EPS (concentration)	Biopolymer OC [a] (µg/L)	MW [b] (MDa)
HMW (0.5 mg/g)	< 2.5 [c]	N/A
LMW + HMW (0.5 mg/g each)	< 2.5 [c]	N/A
MMW + HMW (0.5 mg/g each)	< 2.5 [c]	N/A
Mixed EPS (0.25 mg/g)	< 2.5 [c]	N/A
Mixed EPS (0.5 mg/g)	24.4	1.2

[a] Biopolymer organic carbon of EPS in the supernatant phase after flocculation.
[b] MW of EPS in the supernatant phase after flocculation.
[c] Below the detection limit of the LC-OCD equipment.

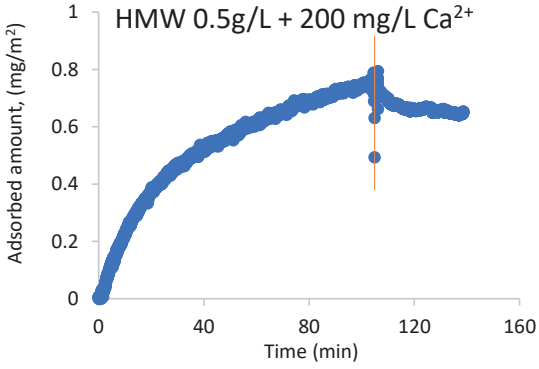

Fig. S3. Adsorption of HMW EPS (dissolved in 200 mg/L Ca^{2+} solution) on silica surface. The red line is the point of solvent injection (200 mg/L Ca^{2+}) after EPS adsorption on the surface.

The stagnation point flow of the optical reflectometer

The experimental set-up of the reflectometer (Fig. S4) is such that there are well defined hydrodynamic circumstances at the point where the incoming laser beam (1) hits the collector surface (2). This enables us to calculate the flux of molecules towards the surface. The solution (5) is impinged perpendicular to the collector surface. The point where the axis of the impinging jet (3) intersects with the surface (2) is called the stagnation point (4). On this point, the solution does not flow, which can be seen from Fig. S4. At and around the stagnation point, the molecules are deposited rather homogeneously. The reflectometer was aligned such that the laser spot was exactly in this stagnation point.

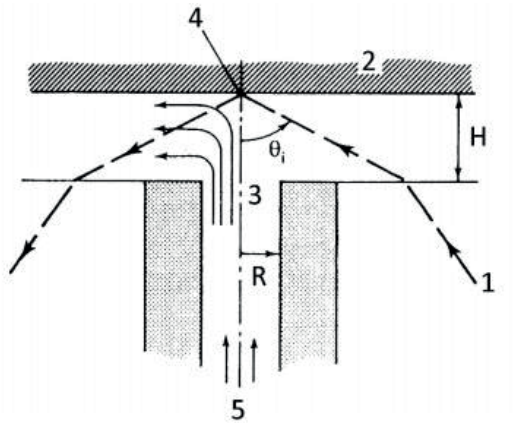

Fig. S4. Description of the stagnation point region (figure taken by permission from the Manufacturer's manual).

Diffusion coefficient (*D*) measurement

To determine the diffusion coefficient (*D*) of each EPS fraction, dynamic light scattering experiment was done with an ALV light-scattering setup, consisting of an ALV5000/60X0 external Correlator, an ALV-125 Goniometer, an ALV/HIGH QE APD single photon detector with an ALV static and dynamic enhancer fiber optics. The laser used was a Cobolt Flamenco DPSS Laser operating at 660 nm and at a power of 300 mW. For the MMW and HMW EPS samples, a 3.1% Transmission attenuator was used. The LMW EPS was measured without attenuator (so 100% transmission). Measurements were performed at an angle of 90 degrees and a second-order cumulant was used to calculate the D. Each sample underwent 30 measurement runs and each run lasted 10 seconds. All samples were paper-filtered prior to the DLS measurement.

The obtained average *D* values are:

High molecular weight (HMW) EPS: $1.6 * 10^{-13}$ m^2/s

Medium molecular weight (MMW) EPS: $2.1 * 10^{-13}$ m^2/s

Low molecular weight (LMW) EPS: $6.0 * 10^{-13}$ m^2/s

References

[1] C.S. Lee, J. Robinson, M.F. Chong, A review on application of flocculants in wastewater treatment, Process Saf. Environ. Prot. 92 (2014) 489–508. doi:10.1016/j.psep.2014.04.010.

[2] A. Mishra, M. Bajpai, Flocculation behaviour of model textile wastewater treated with a food grade polysaccharide, J. Hazard. Mater. 118 (2005) 213–217. doi:10.1016/j.jhazmat.2004.11.003.

[3] T. Suopajärvi, H. Liimatainen, O. Hormi, J. Niinimäki, Coagulation-flocculation treatment of municipal wastewater based on anionized nanocelluloses, Chem. Eng. J. 231 (2013) 59–67. doi:10.1016/j.cej.2013.07.010.

[4] F. Renault, B. Sancey, J. Charles, N. Morin-Crini, P.M. Badot, P. Winterton, G. Crini, Chitosan flocculation of cardboard-mill secondary biological wastewater, Chem. Eng. J. 155 (2009) 775–783. doi:10.1016/j.cej.2009.09.023.

[5] C. Wu, Y. Wang, B. Gao, Y. Zhao, Q. Yue, Coagulation performance and floc characteristics of aluminum sulfate using sodium alginate as coagulant aid for synthetic dying wastewater treatment, Sep. Purif. Technol. 95 (2012) 180–187. doi:10.1016/j.seppur.2012.05.009.

[6] V. Ajao, H. Bruning, H. Rijnaarts, H. Temmink, Natural flocculants from fresh and saline wastewater: Comparative properties and flocculation performances, Chem. Eng. J. 349 (2018) 622–632. doi:10.1016/j.cej.2018.05.123.

[7] H. Salehizadeh, N. Yan, Recent advances in extracellular biopolymer flocculants, Biotechnol. Adv. 32 (2014) 1506–1522. doi:10.1016/j.biotechadv.2014.10.004.

[8] T.T. More, J.S.S. Yadav, S. Yan, R.D. Tyagi, R.Y. Surampalli, Extracellular polymeric substances of bacteria and their potential environmental applications, J. Environ. Manage. 144 (2014) 1–25. doi:10.1016/j.jenvman.2014.05.010.

[9] S.A. Zaki, M.F. Elkady, S. Farag, D. Abd-El-Haleem, Characterization and flocculation properties of a carbohydrate bioflocculant from a newly isolated *Bacillus velezensis* 40B, J. Environ. Biol. 34 (2013) 51–58.

[10] G. Sathiyanarayanan, G. Seghal Kiran, J. Selvin, Synthesis of silver nanoparticles by polysaccharide bioflocculant produced from marine *Bacillus subtilis* MSBN17, Colloids Surfaces B Biointerfaces. 102 (2013) 13–20. doi:10.1016/j.colsurfb.2012.07.032.

[11] C. Liu, K. Wang, J.H. Jiang, W.J. Liu, J.Y. Wang, A novel bioflocculant produced by a salt-tolerant, alkaliphilic and biofilm-forming strain *Bacillus agaradhaerens* C9 and its application in harvesting Chlorella minutissima UTEX2341, Biochem. Eng. J. 93 (2015) 166–172. doi:10.1016/j.bej.2014.10.006.

[12] B. Bin Wang, X.T. Liu, J.M. Chen, D.C. Peng, F. He, Composition and functional group characterization of extracellular polymeric substances (EPS) in activated sludge: the impacts

of polymerization degree of proteinaceous substrates, Water Res. 129 (2018) 133–142. doi:10.1016/j.watres.2017.11.008.

[13] J. Gregory, S. Barany, Adsorption and flocculation by polymers and polymer mixtures, Adv. Colloid Interface Sci. 169 (2011) 1–12. doi:10.1016/j.cis.2011.06.004.

[14] T.J. Stewart, J. Traber, A. Kroll, R. Behra, L. Sigg, Characterization of extracellular polymeric substances (EPS) from periphyton using liquid chromatography-organic carbon detection-organic nitrogen detection (LC-OCD-OND), Environ. Sci. Pollut. Res. 20 (2013) 3214–3223. doi:10.1007/s11356-012-1228-y.

[15] M. Ras, D. Lefebvre, N. Derlon, E. Paul, E. Girbal-Neuhauser, Extracellular polymeric substances diversity of biofilms grown under contrasted environmental conditions, Water Res. 45 (2011) 1529–1538. doi:10.1016/j.watres.2010.11.021.

[16] B. Bolto, J. Gregory, Organic polyelectrolytes in water treatment, Water Res. 41 (2007) 2301–2324. doi:10.1016/j.watres.2007.03.012.

[17] H.H.M. Rijnaarts, W. Norde, J. Lyklema, A.J.B. Zehnder, DLVO and steric contributions to bacterial deposition in media of different ionic strengths, Colloids Surfaces B Biointerfaces. 14 (1999) 179–195. doi:10.1016/S0927-7765(99)00035-1.

[18] A. Costine, J. Cox, S. Travaglini, A. Lubansky, P. Fawell, H. Misslitz, Variations in the molecular weight response of anionic polyacrylamides under different flocculation conditions, Chem. Eng. Sci. 176 (2018) 127–138. doi:10.1016/j.ces.2017.10.031.

[19] X. Yu, P. Somasundaran, Role of Polymer Conformation in Interparticle-Bridging Dominated Flocculation, J. Colloid Interface Sci. 177 (1996) 283–287.

[20] Y. Sang, H. Xiao, Clay flocculation improved by cationic poly(vinyl alcohol)/anionic polymer dual-component system, J. Colloid Interface Sci. 326 (2008) 420–425. doi:10.1016/j.jcis.2008.06.058.

[21] S. Bárány, R. Meszaros, L. Marcinova, J. Skvarla, Effect of polyelectrolyte mixtures on the electrokinetic potential and kinetics of flocculation of clay mineral particles, Colloids Surfaces A Physicochem. Eng. Asp. 383 (2011) 48–55. doi:10.1016/j.colsurfa.2011.01.051.

[22] A. Fan, N.J. Turro, P. Somasundaran, A study of dual polymer flocculation, Colloids Surfaces A Physicochem. Eng. Asp. 162 (2000) 141–148. doi:10.1016/S0927-7757(99)00252-6.

[23] D.C. Sobeck, M.J. Higgins, Examination of three theories for mechanisms of cation-induced bioflocculation, Water Res. 36 (2002) 527–538. doi:10.1016/S0043-1354(01)00254-8.

[24] J.C. Dijt, M.A.C. Stuart, G.J. Fleer, Reflectometry as a tool for adsorption studies, Adv. Colloid Interface Sci. 50 (1994) 79–101. doi:10.1016/0001-8686(94)80026-X.

[25] J.C. Dijt, M.A.C. Stuart, G.J. Fleer, Competitive Adsorption Kinetics of Polymers Differing in Length Only, Macromolecules. 27 (1994) 3219–3228. doi:10.1021/ma00090a015.

[26] L. Wågberg, I. Nygren, The use of stagnation point adsorption reflectometry to study molecular interactions relevant to papermaking chemistry, Colloids Surfaces A Physicochem. Eng. Asp. 159 (1999) 3–15. doi:10.1016/S0927-7757(99)00158-2.

[27] V. Ajao, S. Millah, M.C. Gagliano, H. Bruning, H. Rijnaarts, H. Temmink, Valorization of glycerol/ethanol-rich wastewater to bioflocculants: recovery, properties, and performance, J. Hazard. Mater. 375 (2019) 273–280. doi:10.1016/j.jhazmat.2019.05.009.

[28] W.F. Tan, W. Norde, L.K. Koopal, Humic substance charge determination by titration with a flexible cationic polyelectrolyte, Geochim. Cosmochim. Acta. 75 (2011) 5749–5761. doi:10.1016/j.gca.2011.07.015.

[29] V. Ajao, K. Nam, P. Chatzopoulos, E. Spruijt, H. Bruning, H. Rijnaarts, H. Temmink, Regeneration and reuse of microbial extracellular polymers immobilised on a bed column for heavy metal recovery, Water Res. 171 (2020) 115472. doi:10.1016/j.watres.2020.115472.

[30] M. DuBois, K. a. Gilles, J.K. Hamilton, P. a. Rebers, F. Smith, Colorimetric method for determination of sugars and related substances, Anal. Chem. 28 (1956) 350–356. doi:10.1021/ac60111a017.

[31] T. Robert, S.M. Mercer, T.J. Clark, B.E. Mariampillai, P. Champagne, M.F. Cunningham, P.G. Jessop, Nitrogen-containing polymers as potent ionogens for aqueous solutions of switchable ionic strength: application to separation of organic liquids and clay particles from water, Green Chem. 14 (2012) 3053. doi:10.1039/c2gc36074h.

[32] S.M.R. Shaikh, M.S. Nasser, I.A. Hussein, A. Benamor, Investigation of the effect of polyelectrolyte structure and type on the electrokinetics and flocculation behavior of bentonite dispersions, Chem. Eng. J. 311 (2017) 265–276. doi:10.1016/j.cej.2016.11.098.

[33] G. Lagaly, S. Ziesmer, Colloid chemistry of clay minerals: The coagulation of montmorillonite dispersions, Adv. Colloid Interface Sci. 100–102 (2003) 105–128. doi:10.1016/S0001-8686(02)00064-7.

[34] P. Suresh Kumar, T. Prot, L. Korving, K.J. Keesman, I. Dugulan, M.C.M. van Loosdrecht, G.J. Witkamp, Effect of pore size distribution on iron oxide coated granular activated carbons for phosphate adsorption – Importance of mesopores, Chem. Eng. J. 326 (2017) 231–239. doi:10.1016/j.cej.2017.05.147.

[35] F. Mietta, C. Chassagne, A.J. Manning, J.C. Winterwerp, Influence of shear rate, organic matter content, pH and salinity on mud flocculation, Ocean Dyn. 59 (2009) 751–763. doi:10.1007/s10236-009-0231-4.

[36] J.C. Dijt, M.A.C. Stuart, J.E. Hofman, G.J. Fleer, Kinetics of polymer adsorption in stagnation point flow, Colloids and Surfaces. 51 (1990) 141–158. doi:10.1016/0166-6622(90)80138-T.

[37] A.R. Badireddy, S. Chellam, P.L. Gassman, M.H. Engelhard, A.S. Lea, K.M. Rosso, Role of extracellular polymeric substances in bioflocculation of activated sludge microorganisms

under glucose-controlled conditions, Water Res. 44 (2010) 4505–4516. doi:10.1016/j.watres.2010.06.024.

[38] A. Barth, Infrared spectroscopy of proteins, Biochim. Biophys. Acta - Bioenerg. 1767 (2007) 1073–1101. doi:10.1016/j.bbabio.2007.06.004.

[39] S.J. Yuan, M. Sun, G.P. Sheng, Y. Li, W.W. Li, R.S. Yao, H.Q. Yu, Identification of key constituents and structure of the extracellular polymeric substances excreted by bacillus megaterium TF10 for their flocculation capacity, Environ. Sci. Technol. 45 (2011) 1152–1157. doi:10.1021/es1030905.

[40] B. Durmaz, F.D. Sanin, Effect of carbon to nitrogen ratio on the physical and chemical properties of activated sludge, Environ. Technol. 24 (2003) 1331–1340. doi:10.1080/09593330309385677.

[41] P. Zhu, G. Long, J. Ni, M. Tong, Deposition kinetics of extracellular polymeric substances (EPS) on silica in monovalent and divalent salts, Environ. Sci. Technol. 43 (2009) 5699–5704. doi:10.1021/es9003312.

[42] B.J. Lee, M.A. Schlautman, E. Toorman, M. Fettweis, Competition between kaolinite flocculation and stabilization in divalent cation solutions dosed with anionic polyacrylamides, Water Res. 46 (2012) 5696–5706. doi:10.1016/j.watres.2012.07.056.

[43] L. Faust, H. Temmink, A. Zwijnenburg, A.J.B. Kemperman, H.H.M. Rijnaarts, High loaded MBRs for organic matter recovery from sewage: effect of solids retention time on bioflocculation and on the role of extracellular polymers., Water Res. 56 (2014) 258–66. doi:10.1016/j.watres.2014.03.006.

[44] P. Lembre, C. Lorentz, P. Di, Exopolysaccharides of the Biofilm Matrix: A Complex Biophysical World, in: The Complex World of Polysaccharides, 2012. doi:10.5772/51213.

[45] B. Bin Wang, Q. Chang, D.C. Peng, Y.P. Hou, H.J. Li, L.Y. Pei, A new classification paradigm of extracellular polymeric substances (EPS) in activated sludge: Separation and characterization of exopolymers between floc level and microcolony level, Water Res. 64 (2014) 53–60. doi:10.1016/j.watres.2014.07.003.

[46] M.J. Higgins, J.T. Novak, Characterization of exocellular protein and its role in bioflocculation, J. Environ. Eng. 123 (1997) 479–485. doi:doi:10.1061/(ASCE)0733-9372(1997)123:5(479).

[47] E.A. López-Maldonado, M.T. Oropeza-Guzmán, A. Ochoa-Terán, Improving the efficiency of a coagulation-flocculation wastewater treatment of the semiconductor industry through zeta potential measurements, J. Chem. 2014 (2014) 6–9. doi:10.1155/2014/969720.

[48] M.S. Nasser, A.E. James, The effect of polyacrylamide charge density and molecular weight on the flocculation and sedimentation behaviour of kaolinite suspensions, Sep. Purif. Technol. 52 (2006) 241–252. doi:10.1016/j.seppur.2006.04.005.

[49] D. Liu, M. Edraki, L. Berry, Investigating the settling behaviour of saline tailing suspensions using kaolinite, bentonite, and illite clay minerals, Powder Technol. 326 (2018) 228–236. doi:10.1016/j.powtec.2017.11.070.

[50] B. Zhang, H. Su, X. Gu, X. Huang, H. Wang, Effect of structure and charge of polysaccharide flocculants on their flocculation performance for bentonite suspensions, Colloids Surfaces A Physicochem. Eng. Asp. 436 (2013) 443–449. doi:10.1016/j.colsurfa.2013.07.017.

[51] B.J. Lee, M.A. Schlautman, Effects of polymer molecular weight on adsorption and flocculation in aqueous kaolinite suspensions dosed with nonionic polyacrylamides, Water (Switzerland). 7 (2015) 5896–5909. doi:10.3390/w7115896.

[52] B. Brotherson, Y. Deng, Site blocking effect on the conformation of adsorbed cationic polyacrylamide on a solid surface, J. Colloid Interface Sci. 326 (2008) 324–328. doi:10.1016/j.jcis.2008.06.035.

[53] S. Behl, B. Moudgil, Control of active sites in selective flocculation III. Mechanism of site blocking, J. Collloid Interface Sci. 161 (1993) 430–436.

Chapter 6

Regeneration and reuse of microbial extracellular polymers immobilised on a bed column for heavy metal recovery

A modified version of this Chapter has been published as:

V. Ajao, K. Nam, P. Chatzopoulos, E. Spruijt, H. Bruning, H. Rijnaarts, H. Temmink, Regeneration and reuse of microbial extracellular polymers immobilised on a bed column for heavy metal recovery, Water Res. 171 (2020) 115472. doi:10.1016/j.watres.2020.115472.

Abstract

Microbial extracellular polymeric substances (EPS) have gained increasing attention for various water treatment applications. In this study, EPS produced from nitrogen-limited glycerol/ethanol-rich wastewater were used to recover Cu^{2+} and Pb^{2+} from aqueous solutions. Continuous flow-through tests were conducted on a column packed with silica gel coated with polyethyleneimine, to which EPS were irreversibly attached as shown by optical reflectometry. These immobilised EPS excellently adsorbed Cu^{2+} and Pb^{2+}, with 99.9% of influent metal adsorbed before the breakthrough points. Metal desorption was achieved with 0.1 M HCl, with an average recovery of 86% for Cu^{2+} and 90% recovery for Pb^{2+}. For the first time, we successfully showed the possibility to regenerate and reuse the immobilised EPS for five adsorption-desorption cycles (using Cu^{2+} as an example) with no reduction in the adsorbed amount at the breakthrough point (q_{bp}). Based on the mass balance of the associated metal ions participating in the adsorption process, ion exchange was identified as the major mechanism responsible for Cu^{2+} and Pb^{2+} adsorption by EPS. The results demonstrate the potential of wastewater-produced EPS as an attractive and perhaps, cost-effective biosorbent for heavy metal removal (to trace effluent concentrations) and recovery (86 - 99 %).

1. Introduction

Heavy metal pollution is one of the most critical environmental concerns today due to the hazard caused on human health and the environment. Heavy metals are directly toxic to exposed organisms and indirectly by accumulation in soil and suspended matter in water bodies [1,2]. They are found in high concentrations in wastes discharged into the environment by various industries such as metallurgy, mining and smelting, electroplating, electrolysis, iron and steel, photography, and electric appliance manufacturing [3]. At the same time, the provision of these metals (which are essential and critical elements for our lifestyles) to many industries and economies is at risk due to depleting natural reserves and their concentration in a few nations, thus subjected to geopolitical risks [4]. The recovery of metals from waste streams is, therefore, of increasing economic interest. Hence, treating heavy metal waste streams has two important objectives: removal to environmental standards and recovery to economic standards.

Conventional methods for removing metal ions from aqueous solutions, such as chemical precipitation and filtration, are ineffective in removing low metal concentrations (< 1 - 50 mg/L) and produce large quantities of sludge, which are expensive to dispose of [3,5]. On the other hand, technologies that do not generate such secondary waste streams and are efficient for metal removal and recovery, are very costly. Examples of these are ion exchange, reverse osmosis, adsorption on activated carbon, and evaporation [5].

Biosorption has been proposed and has received increasing attention as a promising technology for heavy metal removal and recovery [6]. Biosorbents (defined as biomass and products of microbial biomass such as extracellular polymers [7]) offer some advantages: they can be cheap and effective when using the adequate type of biomass and processing method, and in some cases can be regenerated for multiple uses just like ion-exchange resins, and are therefore eco-friendly [3,5]. One of the most promising biosorbents from an economically viable point of view are microbial extracellular polymeric substances (EPS). These are products of microbial biochemical secretions, typically comprising polysaccharides and proteins. These biopolymers have functional groups such as carboxyl, hydroxyl, and amine groups that bind with heavy metals either via ion exchange (where the COOH groups are involved) or complexation mechanism (where COOH, OH and NH_2 groups may be involved) [7–9]. EPS are either produced from pure cultures which necessitate sterile conditions and are therefore expensive, or from mixed cultures that require non-sterile cultures and feedstocks (e.g., organic wastewater), making the latter a more sustainable alternative.

Although there are various reports on the use of EPS for heavy metal adsorption [10], most are still far from an economically feasible application in practice due to various limitations: the use of pure-cultured EPS requiring sterile conditions [11], a focus on adsorption only and not on recovery, the use of unrealistically high EPS concentrations in batch studies without practical significance in an industrial or environmental context [7], and the lack of information on the possibility to regenerate and reuse the sorbent.

In this study, we investigated, (i) the immobilisation of wastewater-derived EPS (EPS harvested from waste/surplus sludge) on a column for continuous flow-through tests, (ii) the adsorption and subsequent desorption of heavy metals (using Cu^{2+} and Pb^{2+} as examples) present in another (waste)water, (iii) the possibility to regenerate and reuse the immobilised EPS for several cycles, and (iv) the predominant mechanism involved in the EPS-metal interaction. To our knowledge, this is the first study to prove the regeneration and reuse of EPS for several adsorption and recovery cycles in a continuous process.

2. Materials and methods

2.1. EPS-producing bioreactor

A submerged membrane bioreactor (MBR) with a working volume of 67 L was operated to combine wastewater treatment with EPS production. The MBR was equipped with two PVDF flat sheet membranes (membrane cartridge type 510, Kubota, Japan) with an effective area of 0.8 m^2 each and nominal pore size of 0.2 µm. Perforated tubes made of polyvinyl chloride were placed underneath the membrane to provide aeration.

The reactor was inoculated with aerobic sludge from a municipal wastewater treatment plant located in Leeuwarden, the Netherlands. It was operated at a room temperature of 20 ± 1 °C, a pH of 7.5 ± 0.2, a dissolved oxygen concentration of 2.5 ± 1.0 mg O_2/L, a solids retention time of 3 days to minimise COD mineralisation, and a hydraulic retention time of 10 h.

The reactor was operated under a nitrogen-limited condition (a COD/N ratio of 85, calculated based on g COD/g N). Nitrogen limitation has been previously reported to enhance EPS recovery from glycerol/ethanol-rich wastewater – up to 54% of wastewater-COD recovered as EPS-COD [12]. Influent COD was 2000 ± 100 mg/L, mainly provided from glycerol (820 ± 20 mg/L) and ethanol (480 ± 10 mg/L) in a 1:1 COD ratio, simulating biodiesel and bioethanol wastewater. The main nitrogen source was NH_4Cl (75 ± 5 mg/L) and yeast extract (30 mg/L) contributed 10.5% of the total nitrogen content. The nutrient medium composition per litre of tap water comprised 100 mg $MgCl_2{\cdot}6H_2O$, 150 mg $CaCl_2{\cdot}2H_2O$, 40 mg K_2HPO_4, 60 mg KH_2PO_4, and 2 mL trace elements solution (the composition of trace elements has been reported by Ajao *et al*. [13]).

2.2. EPS harvesting

After operating the reactor at a steady state for at least 30 days, the soluble (S)-EPS were harvested from the waste sludge, having been reported to be the major EPS fraction (62 - 77 wt%) in a nitrogen-limited system [12]. S-EPS were recovered via centrifugation: 400 mL sludge was centrifuged at 17000 *g* and 4 °C for 1 h, after which the supernatant containing the S-EPS (henceforth called 'EPS' in this Chapter) was dialysed successively against demineralised water. Dialysed EPS were freeze-dried to obtain dry solids that were used for the metal adsorption tests.

2.3. EPS characterisation

2.3.1. Functional group determination

Fourier transform infrared spectroscopy (FTIR) was carried out on the freeze-dried EPS samples using an IRTracer-100 spectrometer (Shimadzu, Japan) with a scanning range of 4000 - 450 cm^{-1} for 40 scans at a spectral resolution of 4 cm^{-1}.

2.3.2. Total protein, polysaccharide, and uronic acids quantification

The total protein content of the dried EPS was determined using a bicinchoninic acid (BCA) assay kit (Thermo Scientific, USA). The assay was performed in a microplate, where 25 µL of EPS solution (dissolved in a phosphate buffer saline, pH 7.4 [13]) or bovine serum albumin, BSA (used as a standard protein) was mixed with 200 µL of BCA working reagent and incubated at 37 °C for 30 min. Afterward, the absorbance was measured at 570 nm using a spectrophotometer (Victor3 1420 Multilabel Counter, Perkin Elmer, USA).

Total polysaccharides were quantified using the phenol-sulphuric acid method described by Dubois *et al*. [14], using glucose as the standard sugar. Absorbance was measured at 490 nm in the spectrophotometer mentioned above. The sugar composition was further analysed according to Englyst and Cummings [15] – see supplementary information.

2.3.3. Molecular weight determination

A solution of EPS was first passed through 0.45 µm hydrophilic polytetrafluoroethylene filter (purchased from Merck, the Netherlands) before molecular weight determination using liquid chromatography-organic carbon detection (LC-OCD – model 8, DOC-LABOR, Germany). Detailed method described by Ajao *et al*. [12]. LC-OCD was also used to analyse the different EPS fractions: biopolymers (such as polysaccharides, proteins, glycoproteins), building blocks/humic acids, low molecular weight (LMW) acids and LMW neutrals [13,16].

2.3.4. Charge density measurements

The charge densities of EPS and polyethyleneimine (PEI) were determined by colloid titration using a Mütek Particle Charge Detector (PCD03, Germany) described by Tan *et al*. [17] and a titration procedure explained by Ajao *et al*. [13]. The charge densities were calculated from the consumption of the titrant (polydiallyldimethylammonium chloride for EPS titration and polyethylenesulfonate for PEI titration) according to the equation:

$$q = \frac{c*V}{m} \qquad (1)$$

where q is the specific charge quantity (eq/g), c is the titrant concentration (eq/L), V is the consumed titrant volume (L), and m is the mass of the polymer sample (g). The charge density of EPS was determined at pH 10 (pH of the EPS solution flowed into the column to attach to PEI: freeze-dried EPS was dissolved in Milli-Q and alkalinised to pH 10 with drops of 1 M NaOH) and pH 7. At pH 10,

the functional groups are largely deprotonated and the EPS have a high anionic charge density, from which a fraction is sacrificed to bind with the PEI.

2.4. Chemical analysis

Metals were measured by inductively coupled plasma-optical emission spectrometry, ICP-OES (Perkin Elmer Optima 5300 DV). Total organic carbon (TOC) of EPS, PEI, and column effluents was measured using a TOC analyser (Shimadzu TOC-L). All samples were passed through 0.45 µm hydrophilic polytetrafluoroethylene filter (Merck) before ICP-OES and TOC analysis.

2.5. Optical reflectometry test

For a continuous metal adsorption process, EPS was supported in a column packed with silica gel. Since silica gel is negatively charged, a cationic polymer such as PEI (branched, MW = 10 kDa, purchased from VWR, Netherlands) was first attached to the silica gel, followed by EPS attachment. To assess the attachment of anionic EPS on the cationic PEI, an adsorption test was carried out using fixed-angle stagnation point optical reflectometry described by Dijt *et al.* [18]. Reflectometry is an optical technique used to observe *in situ* adsorption of molecules on an optically flat surface, such as a silicon wafer. The changes in signal measured upon adsorption on the surface (ΔS) is directly proportional to the adsorbed amount, Γ (mg/m^2) according to the equation:

$$\Gamma = Q_f \frac{\Delta S}{S_0} \qquad (2)$$

where Q_f is the sensitivity factor (mg/m^2), S_0 is the starting output signal of the bare silicon wafer, and $\Delta S = S - S_0$ is a change in the signal upon adsorption on the surface. Instead of using mass uptake (Γ), we used the relative signal increase ($\Delta S/S_0$) to interpret the surface adsorption process since both parameters are directly proportional to each other.

Silicon wafers were first baked at 1000 ^oC for 1 h to form an oxide layer on the silicon. The oxidised wafers with a silica layer thickness of 81.5 nm were cut into strips of approximately 1 x 4 cm^2, immersed in a freshly prepared piranha solution (1 part of 30% H_2O_2 and 3 parts of 95% H_2SO_4) for 20 minutes and rinsed in Milli-Q water.

Although 10 g/L PEI and 10 g/L EPS were used for the column preparation, much lower concentrations were needed for the reflectometry tests in order to monitor the adsorption of the polymers on the flat surface. Thus, 0.5 g/L of each polymer was used. The adsorption sequence on the oxidised wafer was as follows: solvent (demineralised water) was passed to establish the baseline, then 0.5 g/L PEI was injected until adsorption reached saturation, the solvent was passed again to know if the adsorption was (ir)reversible, 0.5 g/L EPS was then injected until adsorption reached saturation, after which the solvent was passed.

2.6. Biosorption tests

2.6.1. Batch tests

Batch tests were conducted using dialysis bags according to the method described by Wang *et al*. [19]. 50 mg/L each of Cu^{2+}, Pb^{2+} and Zn^{2+} solutions were prepared by dissolving $CuSO_4 \cdot 5H_2O$, $Pb(NO_3)_2$ and

$Zn(NO_3)_2 \cdot 6H_2O$, respectively in Milli-Q water. A dialysis bag (12 - 14 kDa molecular weight cut-off) filled with 5 mL undialysed and undried EPS was suspended in 100 mL heavy metal solution and stirred continuously at 400 rpm at room temperature (21 ± 1 °C). An aliquot of the heavy metal solution was taken for ICP-OES measurement.

2.6.2. Small-scale syringe test

To assess the feasibility of a continuous column experiment and to test the possibility of coating an EPS layer on a solid surface, a small-scale syringe test was carried out. First, a glass microfibre filter (25 mm diameter, Camlab Ltd, UK) was treated in a low-pressure oxygen plasma system (Diener Electronic Femto, Germany) for 20 seconds to activate the anionic silica groups. Subsequently, a series of solvents/solution was passed through the glass microfibre filter in the following order: 10 mL of Milli-Q water to clean the filter, 1mL of 10 g/L cationic PEI to bind to the anionic groups on the filter, 10 mL of Milli-Q water to remove any residual PEI, 1 mL of 10 g/L EPS (anionic polymer) to attach to the cationic PEI, and 10 mL of Milli-Q water to remove any excess unattached EPS (Fig. 1). The flow rate of the syringe pump was set at 2 mL/min throughout the tests. This feasibility experiment was tested for Cu^{2+} adsorption on the attached EPS.

2.6.3. Fixed-bed column set-up, adsorption and desorption studies

Upflow lab-scale columns (height = 11 cm, internal diameter = 1.5 cm, bed volume [BV] = 19 mL) were made from transparent polyvinylchloride (Fig. 2). Silica gel (pore size 60 Å, 35 - 60 mesh, purchased from Sigma Aldrich) was used in lieu of the previously used glass filter to act as a support for EPS attachment. The silica groups were activated by (re)circulating 50 mL of 10 mM KOH (instead of using a plasma system) for 3 h [20]. Afterwards, 50 mL of 10 g/L PEI was (re)circulated for 1 h and finally, 50 mL of 10 g/L EPS was (re)circulated for 1 h. Between each step and after the final step, 60 mL Milli-Q water was flushed through the column for 1 h. The flow rate of the peristaltic pump was set at 1 mL/min (3.16 BV/h) throughout the column preparation process.

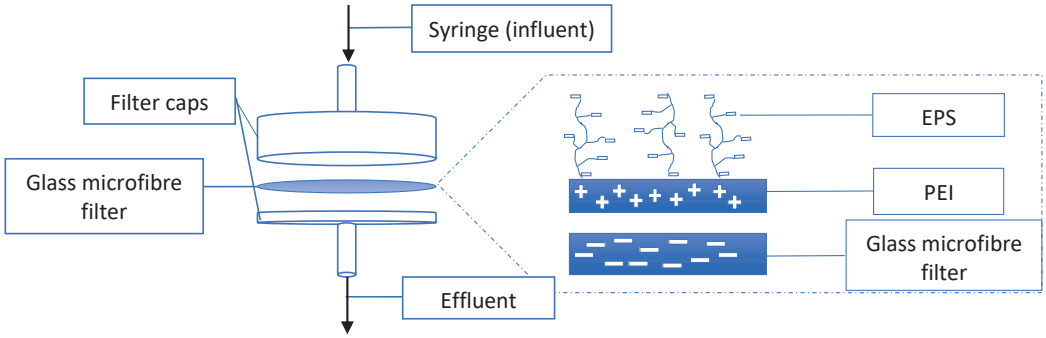

Fig. 1. Schematic depiction of the filter structure for Cu^{2+} adsorption. PEI: Polyethyleneimine.

To determine the mass of EPS immobilised in the column, the TOC values of influent and effluent EPS solution were measured (full calculations in the supplementary information – Table S1). Out of 5.3 g/L TOC_{EPS} entering the column, 1.6 g/L TOC_{EPS} was retained after flushing with water. Thus, about 31% of the influent EPS concentration (3.1 g/L out of 10 g/L) was immobilised in the column. However, not all the sites of the immobilised EPS are available for metal adsorption. A fraction of the charges was attached to the PEI, leaving the remaining free sites available for metal adsorption. Typically, about 45.4 mg of PEI was immobilised in the column, which corresponds to a charge of 0.66 meq. From the charge density values of PEI and EPS (see section 3.12), we established a stoichiometry ratio of 1.6 meq of EPS to 1 meq of PEI for their interaction, assuming all the measured sites are available for binding. Thus, 1.06 meq of EPS was attached to PEI, corresponding to 115.4 mg of EPS, leaving 39.1 mg EPS (charge equivalent of 0.35 meq) available for metal adsorption.

Metal adsorption and desorption studies were carried out on 50 mg/L Cu^{2+} and 50 mg/L Pb^{2+} from metal salt solutions of $CuSO_4 \cdot 5H_2O$ (solution pH 5.7) and $Pb(NO_3)_2$ (solution pH 5.6), respectively. The flow rate of the metal solution was set at 1 mL/min (3.16 BV/h), except stated otherwise. The desorption test was done with the aim of concentrating the adsorbed metal to 10 times the original concentration. To achieve this, the volume of the desorbent (0.1 M HCl) used was 10 times less than that of the metal solution that had flowed through the column during the preceding adsorption phase. The desorption was carried out at a flow rate of 0.25 mL/min (0.79 BV/h). The adsorbed amount (q, mg/g available EPS), and the desorption recovery (%) of metal ions were calculated from equations (3) and (4):

$$Adsorbed\ amount, q = \frac{mass\ of\ metal\ ion\ adsorbed}{mass\ of\ EPS\ available\ for\ adsorption} \quad (3)$$

$$Desorption\ recovery\ (\%) = \frac{mass\ of\ metal\ ion\ desorbed}{mass\ of\ metal\ ion\ adsorbed} \quad (4)$$

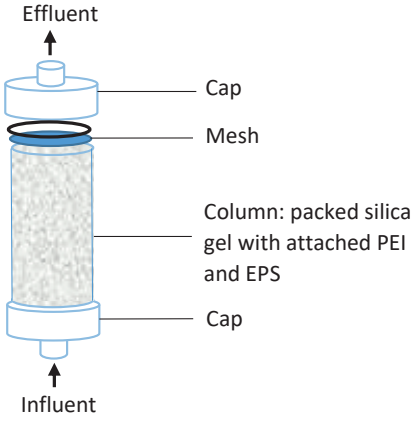

Fig. 2. Upflow fixed-bed column for heavy metal adsorption and desorption. PEI: Polyethyleneimine.

At the end of the desorption test, an HCl volume equivalent to the total volume of HCl used for the desorption process was also flowed through the column at a rate of 2 mL/min to flush out any residual metal ion present in the column. To reuse the EPS for another cycle, the column was first washed with Milli-Q water (as stated above) and recirculated with 10 mM KOH for 2 h (flow rate = 1 mL/min) to deprotonate the EPS for another adsorption process (hence, the immobilised EPS was in the K^+ form), after which Milli-Q water was flushed again for an hour.

3. Results and Discussion

3.1. EPS characteristics

3.1.1. Functionality and composition

EPS, being a mixture of compounds, provide different functional groups that are relevant for heavy metal adsorption. The FTIR spectrum in Fig. 3 shows distinct and sharp absorption bands at 3280 cm^{-1} (–OH and/or $–NH_2$ groups), 2905 cm^{-1} (C–H groups), 1717 cm^{-1} (C=O of amide I), 1593 cm^{-1} (out-of-phase N–H bending and C–N of amide II), 1406 cm^{-1} (in-phase N–H bending of amide III) [21], 1368 cm^{-1} (C=O of $–COO^-$ groups), 1234 cm^{-1} (C–O of ether or alcohol) and 1022 cm^{-1} (C–O–C) [22]. These bands suggest the presence of polysaccharides and proteins with carboxyl, hydroxyl and amino groups as the main functional groups. This result is also consistent with our previous studies and reports of other studies [12,13,22].

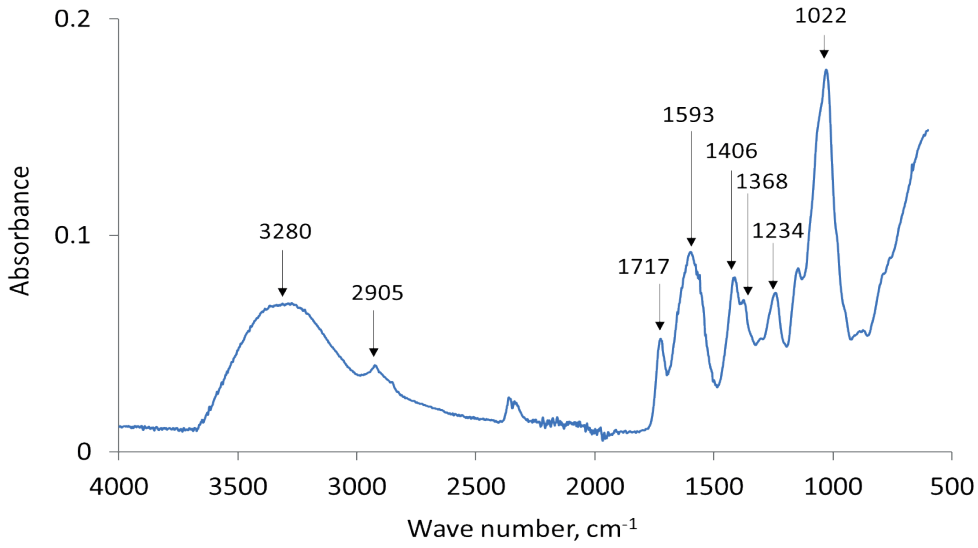

Fig. 3. FTIR spectrum of the harvested EPS.

Table 1. Properties of the produced EPS.

Parameter	Value
Polysaccharide content [a] (g/g EPS)	0.44 ± 0.05
of which uronic acids (g/g EPS)	0.27 ± 0.01
Protein content [b] (g/g EPS)	0.12 ± 0.02
Molecular weight fractions (kDa)	1326.4, 187.1, 92.2, 40.3
Charge density at pH 10 (meq/g EPS)	9.0 ± 0.2
Charge density at pH 7 (meq/g EPS)	5.1 ± 0.2

[a] based on glucose equivalent units.
[b] based on BSA equivalent units.

The quantification of the total polysaccharide and protein content shows that the EPS were composed of 12 wt% proteins and 44 wt% polysaccharides (this value is close to that obtained from the EPS-sugar compositional analysis – see supplementary information), out of which uronic acids account for 26.5 wt% (Table 1). LC-OCD analysis revealed that the EPS also contain building blocks/humic acids (molecular weight 500 - 2500 Da), LMW acids and neutrals (< 500 Da), and a hydrophobic organic fraction [16], which together account for the remaining 44 wt% (see supplementary information – Table S2). In general, the biopolymer fraction of this particular EPS produced from biodiesel/(bio)ethanol wastewater under nitrogen-limited condition (high COD/N ratio) has polysaccharides as its main EPS component [12].

3.1.2. Molecular weight and charge density

Molecular weight (MW) is an important property for (irreversible) attachment of EPS with PEI. The longer the polymeric chains, the stronger the attachment with PEI [18]. The result of the LC-OCD analysis reveals four biopolymer chromatographic peaks of the EPS (Fig S1 – supplementary information, and Table 1). The peaks can be categorised into high (> 1000 kDa), medium (100 - 1000 kDa) and low (< 100 kDa) MW fractions, indicating the heterogeneous macromolecular characteristics of microbial EPS, a phenomenon also found in other studies [13,23,24].

In addition to MW, charge density is another crucial property of EPS for their successful attachment with cationic PEI and as active sites for binding with heavy metals. The charge density of EPS is due to the presence of carboxyl and amino groups and is pH-dependent. At pH 10 (the pH of the EPS solution flowed into the column to attach to PEI), the anionic charge density was 9 meq/g EPS (Table 1). This high value is owing to the functional groups in a largely deprotonated form ($–COO^-$ and $–NH_2$) at such an elevated pH. The highly charged form of the EPS is desirable to maximise the fraction of the sites that binds with the PEI (cationic charge density of PEI = 14.6 ± 0.1 meq/g PEI), leaving the remaining fraction available for metal adsorption (see Table S1).

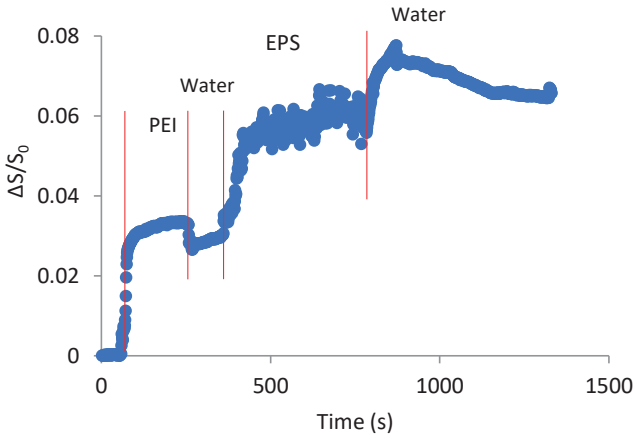

Fig. 4. Optical reflectometry signal for irreversible EPS adsorption on polyethyleneimine (PEI).

3.2. Adsorption of EPS on polyethyleneimine

The result presented in Fig. 4 shows the sequential adsorption of PEI and EPS on an activated silicon wafer. First, cationic PEI showed a fast, largely irreversible adsorption on the silica surface, after which anionic EPS was adsorbed on the PEI layer. After a subsequent solvent injection (demineralised water), no desorption took place, implying that the EPS was irreversibly attached to the PEI. (The sudden increase after solvent injection was due to the change in ionic strength between the EPS solution and water and stabilised at values not lower than that reached with EPS previously.) This is likely due to the strong attachment of the long EPS chains to PEI, which has a large number of adsorption sites [18]. Moreover, the layer-by-layer adsorption suggests that the interaction between PEI and EPS was governed by electrostatic attraction.

3.3. Cu^{2+} adsorption on a modified glass filter

Having established the strong attachment of EPS on PEI, a small-scale syringe test was carried out to assess the feasibility of metal adsorption on an EPS-coated glass filter. The result in Fig. 5 proves this possibility – 89% of Cu^{2+} in the first 10 bed volumes (0.5 mL flowed through the filter) was adsorbed by the EPS. It is important to state that this was not an optimised experiment and the adsorption was limited due to the very small bed volume (~0.05 mL) and a relatively high flow rate (2 mL/min), hence the retention time of Cu^{2+} was very short.

3.4. Fixed-bed adsorption and desorption of Cu^{2+}

The results of the column experiment show that the recovered EPS have a high affinity for Cu^{2+} (Fig. 6A). In all the five cycles, 99.9 % of the influent Cu^{2+} was adsorbed in the column in the first six bed volumes, corresponding to effluent Cu^{2+} concentrations < 50 µg/L (our quantifiable limit). These concentrations are much lower than the US Environmental Protection Agency (USEPA) maximum permissible concentration of 1.3 mg/L Cu^{2+} in drinking water [25].

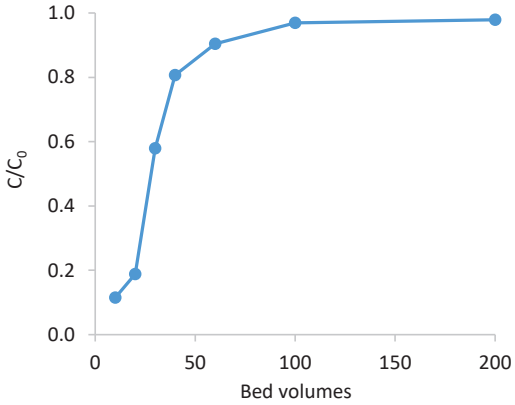

Fig. 5. Cu^{2+} adsorption (on an EPS-coated glass microfibre filter) as a function of effluent concentrations and bed volumes. C_0 = 61.6 mg Cu^{2+} /L.

Fig. 6 shows that the adsorption cycles were not continued long enough to obtain full breakthrough curves, i.e. to reach a $C/C_0 = 1$. During the first cycle, which was operated at twice the flow rate (2 mL/min, 6.32 BV/h) of the other cycles, 151.6 mg Cu^{2+}/g EPS was adsorbed at the breakthrough point, q_{bp} (defined as $C/C_0 = 0.001$) at 6.3 BV and after 31.6 BV, 562.4 mg Cu^{2+}/g EPS had been adsorbed. It is important to mention that this value was not the EPS' maximum adsorption capacity (q_{max}) for Cu^{2+} but the q_{max} could be as high as 787 mg/g EPS as determined in the batch experiments (see supplementary information – Fig. S2). (The q values reported for the column tests are based on the mass of EPS available for binding and do not take into account the amount of EPS sacrificed to attach to PEI.) Nevertheless, these q_{max} values are not as important as the q_{bp} from the practical viewpoint and can even be misleading when solely reported, since they do not take into account the limits of metals permitted in drinking water or industrial effluent discharge [26].

Attractive from an application perspective is the possibility to regenerate and reuse the EPS for subsequent adsorption-desorption cycles without a reduction in the adsorbed amount at the breakthrough point (q_{bp}). Table 2 shows that the q_{bp} for Cu^{2+} was fairly constant (151.6 - 160.1 mg/g) in all the five tested cycles and the cycles had their breakthrough points at approximately the same bed volume (Fig. 6A). Comparing the q values at a common bed volume of 15.8 (the total bed volume of the 2nd to 5th adsorption cycles), the q value of the first adsorption cycle was 357.6 mg/g and that of the second cycle was 316.1 mg/g, implying that only about 11.6% of the EPS' adsorption capacity was lost either during the first cycle metal desorption or EPS regeneration process. In spite of this loss in capacity, the q values of the reused EPS in this study (somewhat constant between 294 - 316 mg/g) are much higher than the q_{max} values of most reported commercial ion-exchange resins (9 - 71 mg/g resin) [27–29] and other adsorbents: zeolites (2 - 5 mg/g), activated carbon (12 – 32 mg/g), chitosan composites (25 - 200 mg/g), activated sludge (19 mg/g), seaweed (8 - 108 mg/g), microbial biomass such as bacteria, fungi and algae (2 - 133 mg/g), and lignocellulosic materials such as rice shell, hazelnut shell, orange peel, modified orange peel (8 - 289 mg/g) [29–34]. For the EPS-producing biomasses such as activated sludge, seaweed and microbial biomass, their much lower q_{max} values

(mg/g biomass) compared to our study may be due to a low amount of available EPS charge or functional group when EPS is attached to biomass. It may be that a fraction of the EPS functional groups needed for adsorption has been sacrificed for biomass attachment [35]. Moreover, biomass composition does not vary significantly, at least between different species of the same genus or order, and will usually result in similar metal adsorption capacities [7]. For instance, different bacteria species studied for Cr^{4+} adsorption showed comparable metal sorption affinities [36]. On the contrary, microbial EPS can differ considerably, based on factors such as the utilised substrates and operational conditions, consequently leading to new EPS properties [1,37].

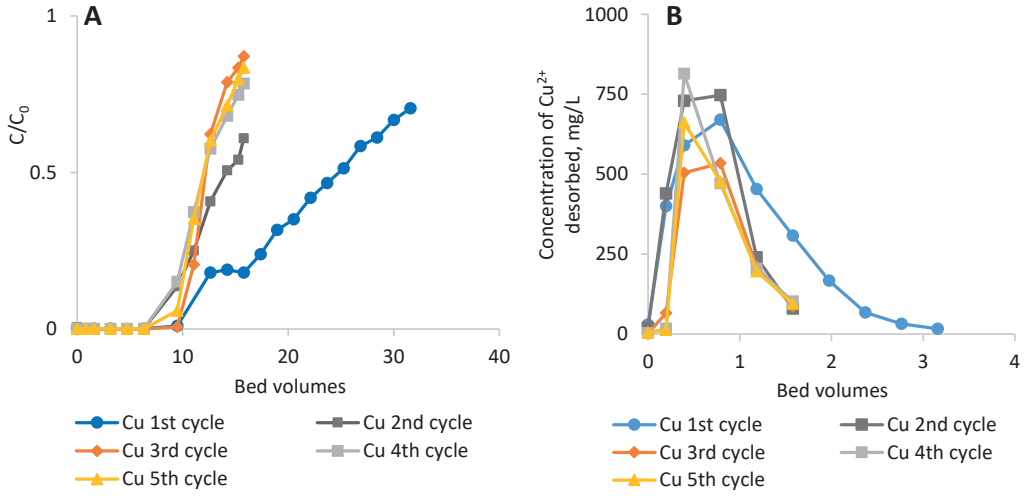

Fig. 6. Adsorption-desorption cycles for Cu^{2+} recovery from EPS. **(A)** Cu^{2+} adsorption as a function of effluent concentrations and bed volumes; C_0 = 50 mg/L. **(B)** Desorption of adsorbed Cu^{2+} from EPS in a 10-time concentrated Cu^{2+} solution.

Table 2. Adsorption capacities of EPS for Cu^{2+} and subsequent recovery in a 10-time and 5-time concentration.

(De)sorption cycle	q [a] (mg/g)	q_{bp} [b] (mg/g)	Recovery [c] (%)	Recovery [d] (%)
1st	562.4	151.6	80	
2nd	316.1	151.6	109	120
3rd	301.3	151.7	76	88
4th	294.0	151.7	88	102
5th	313.3	160.1	75	87

[a] Adsorbed amount at 31.6 bed volume (for the 1st cycle) and 15.8 bed volume (for the 2nd – 5th cycles).
[b] Adsorbed amount at the breakthrough point (C/C_0 = 0.001).
[c] 10 times concentrated (3.2 bed volume for the 1st cycle, 1.6 bed volume for 2nd – 5th cycles).
[d] 5 times concentrated (3.2 bed volume for the for 2nd – 5th cycles).
Values higher than 100% means that Cu^{2+} retained in the column after the previous desorption cycle also got eluted in the next desorption cycle.

As a control, Cu^{2+} adsorption was performed on only the silica particles (without PEI or EPS attachment) to check if they likely participated in the EPS adsorption process. Results (see supplementary information – Fig. S3) showed that the lowest C/C_0 value attained was 0.2, which is much higher than what was obtained with EPS ($C/C_0 = 0.001$). Therefore, the values obtained in this study were solely from the attached EPS and not from the silica gel.

3.5. Pb^{2+} adsorption and desorption

The ability of EPS to adsorb other heavy metals such as $Pb^{2+}$and Zn^{2+}, and monovalent cations such as NH_4^+ was shown by preliminary batch experiments (see supplementary information – Fig. S2). Pb^{2+} was also tested in a newly prepared column for an adsorption-desorption cycle. Like the Cu^{2+} adsorption, EPS also showed an excellent affinity for Pb^{2+} (Fig. 7A). Close to 100% adsorption before the breakthrough point was reached with $C/C_0 = 0.001$, corresponding to effluent concentration of Pb^{2+} < 20 µg/L, which may be lower than the USEPA maximum permissible concentration of 15 µg/L [38]. The q_{bp} for Pb^{2+} was 1204 mg/g EPS, which is in the same order of magnitude as the q_{max} of the acidic polysaccharide produced by *Bacillus firmus* (1103 mg/g) [37], higher than the q_{max} reported for EPS from aerobic granular sludge (900 mg/g at 50 mg/L Pb^{2+}) [1], and much higher than the q_{max} of most reported ion-exchange resins (62 - 110 mg/g) [28,39,40].

The EPS' q_{bp} for Pb^{2+} (5.8 mmol/g EPS) was higher than that of Cu^{2+} (2.4 mmol/g EPS) and was also at a much higher bed volume (49 BV for Pb^{2+} compared to 6 BV for Cu^{2+}). This is likely due to the difference in EPS adsorption affinities between the two metal ion species. The binding affinity of metal ions is strongly dependent on the ion's charge density, which in turn is inversely related to the hydrated ionic radius [9,41]. Since Pb^{2+} has a smaller hydrated ionic radius than Cu^{2+}, it, therefore, has a higher charge density and a stronger affinity to adsorb to EPS.

The desorption test with 0.1 M HCl shows a recovery of 90% in a 10-time concentrated Pb^{2+} solution (Fig. 7B), demonstrating the possibility to also successfully recover Pb^{2+} from aqueous solution with EPS.

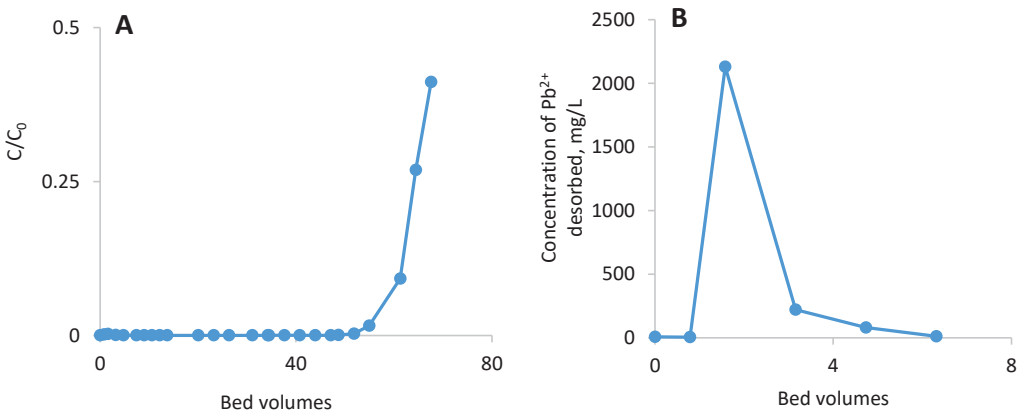

Fig. 7. **(A)** Pb^{2+} adsorption as a function of effluent concentrations and bed volumes; C_0 = 50 mg/L. **(B)** Desorption of adsorbed Pb^{2+} from EPS.

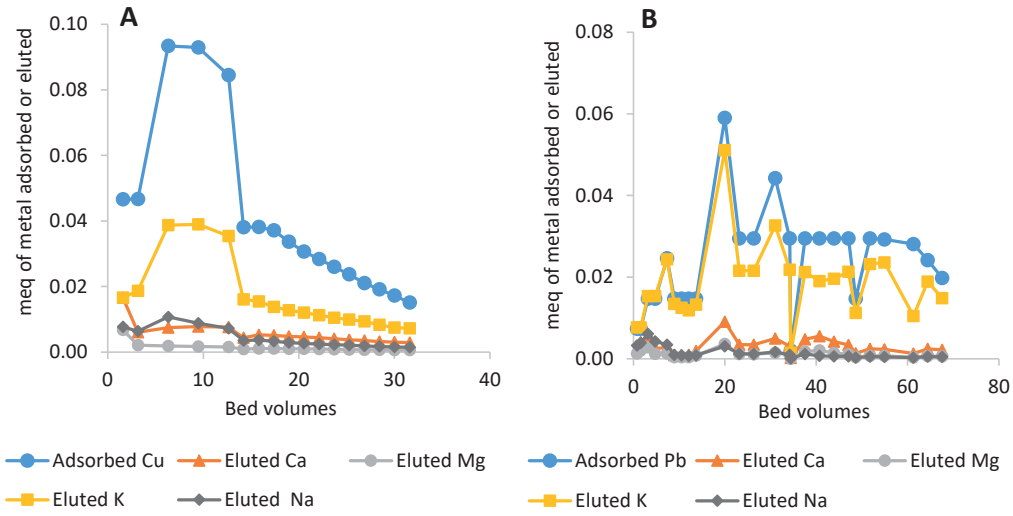

Fig. 8. Molar equivalents of the eluted EPS counter ions (K^+, Ca^{2+}, Na^+, Mg^{2+}) compared to the adsorbed Cu^{2+} (**A**) and Pb^{2+} (**B**) over the bed volumes.

Table 3. Total molar equivalents of adsorbed metal ions (Cu^{2+} and Pb^{2+}) and the eluted EPS counter ions.

Metal ions	Cu^{2+} adsorption (meq)	Pb^{2+} adsorption (meq)
Adsorbed metal ion	0.69	0.61
Eluted K^+	0.28	0.47
Eluted Ca^{2+}	0.10	0.08
Eluted Na^+	0.07	0.04
Eluted Mg^{2+}	0.02	0.03
Total eluted metal ions	0.47	0.61

3.6. Adsorption mechanism

Apparently, mixed EPS (mixed composition – consisting polysaccharides and proteins, and mixed MW – high, medium and low MW fractions) produced aerobically under the nitrogen-limited condition have an excellent affinity for heavy metals, namely Cu^{2+}, Pb^{2+}, and also for Au^{3+} (see supplementary information – Fig. S4). This can be explained based on their composition, charge density and molecular weights. The main functional groups of the EPS polysaccharides and proteins ($–COO^-$, $–NH_2$, OH) can serve as effective binding sites [9]. With more than half of the polysaccharides being uronic acids, the carboxyl group is likely the main functional group contributing to the binding ability and has been reported to have the strongest binding affinity out of the three functional groups present [9]. The hydroxyl group of neutral polysaccharides and the amine group of proteins have

also been found to bind with metals, although they typically exhibit a weaker binding ability than carboxyl groups due to their relatively higher pK_a values [8,9]. The presence of carboxyl and amine groups also makes the charge density of EPS pH-dependent. At a high pH (> 10), the carboxyl and amine groups are deprotonated, leading to a high charge density [13] and more metal adsorption via the ion exchange mechanism [9]. Furthermore, the distribution of the many charges on the long polymeric chains and associated electrostatic repulsion is likely to keep the polymer in an uncoiled conformation and provide accessible binding sites for adsorption. It is also worth mentioning that these two EPS properties (high molecular weight and high charge density) also make EPS effective flocculants for particle adsorption and agglomeration [12].

From the column experiment, we could also determine if the metal adsorption by EPS was exclusively based on ion exchange or not, by determining the molar equivalents of the EPS counter ions (K^+, Ca^{2+}, Na^+, Mg^{2+}) in the effluent. Although summarised in Table 3, Fig. 8A and B give a more vivid picture of the exchange of the counter-ions with Cu^{2+} and Pb^{2+}, respectively. In both Figures, K^+ was the main EPS counter-ion (due to the washing step with 10 mM KOH) and was predominantly eluted. K^+, along with the other counter-ions, followed the same trend as the adsorbed metal, demonstrating that, as Cu^{2+} or Pb^{2+} was being adsorbed, the counter-ions were simultaneously being eluted from the EPS. Overall, Pb^{2+} adsorption by EPS appears to be exclusively via ion exchange (99.7% molar equivalents exchange) with K^+ exchange contributing the most (76%) (Fig 8B). Ion exchange for Cu^{2+} adsorption (in the first cycle, Fig 8A) accounted for 68%, with K^+ exchange also contributing the most (40.8%) and the remaining 32% may be attributed to other mechanisms such as complexation or precipitation [7,9]. Although complexation was more likely to occur due to the presence of COO^-, OH, and NH_2 groups on the EPS that can serve as metal-binding ligands [9], precipitation is also possible (considering the pH in the column during adsorption was 6 - 8). For instance, $Cu(OH)_2$ precipitate was reported as the major form of Cu^{2+} at pH above 6.6 [9]. Notwithstanding, ion exchange mechanism proves to play the leading role in Pb^{2+} and Cu^{2+} adsorption on EPS. This is also in accordance with the findings of Wei *et al.* [42] where 85.7% molar equivalents of K^+ and Mg^{2+} in EPS (produced by *Klebsiella sp.* J1) was exchanged with Pb^{2+}.

3.7. Practical implications and outlook

Although EPS was produced from a specific wastewater, we expect that some other biodegradable industrial wastewater types would also be suitable substrates, provided nitrogen is limiting. Generally, EPS produced under nitrogen-limited conditions, which mainly consist of polysaccharides, may have a higher MW and anionic CD than those produced from excess nitrogen [12]. These two properties govern the immobilization and metal adsorption efficiency of the EPS.

One advantage of this technology is the ability to adsorb heavy metals (in low concentrations) to reach trace concentrations in the effluent. This is important to meet the limits for drinking water or effluent discharge quality for surface water. In addition, the alkali solution used for EPS regeneration could be reused for several regeneration processes instead of disposing of after a one-time use.

Although we have proved the reusability of an immobilised EPS for five adsorption-desorption cycles, more extended experiments will be needed to thoroughly test their durability for multiple

cycles as found in ion-exchange resins. However, compared to commercial resins, EPS are considered low-cost biosorbents [11], which could be beneficial from a business case perspective. The studied system could be further optimised by using a cationic polymer with a lower charge demand since a significant fraction (about 75%) of the flowed EPS had to be sacrificed to bind with the PEI.

Selective separation is an important factor that still needs further study. It may be necessary to study how different EPS fractions (soluble and bound EPS) or EPS produced under different conditions (fresh *versus* saline wastewater grown on different substrates, with and without nitrogen limitation) may have different selectivity for specific metals. Furthermore, the desorption process needs to be optimised to obtain higher concentration factors compared to a factor of 10 used in this study.

4. Conclusions

EPS produced from nitrogen-limited wastewater were immobilised in a column and used to adsorb Cu^{2+} and Pb^{2+} in a continuous process. For the first time, the possibility to regenerate and reuse the immobilised EPS for repetitive adsorption-desorption cycles was successfully shown for Cu^{2+}, with no reduction in the adsorption capacity as indicated by stable breakthrough points (q_{bp}). In all the cycles, 99.9% of influent Cu^{2+} was adsorbed before the breakthrough points (effluent concentrations < 50 µg/L), and an average of 86% could be recovered in a 10-time concentrated Cu^{2+} solution and 99% recovery in a 5-time concentrated Cu^{2+} solution. Quite similar results were also obtained for the adsorption-desorption cycle of Pb^{2+} (close to 100% adsorption and 90% desorption in a 10-time concentrated Pb^{2+} solution).

Interestingly, the mechanism of adsorption was discovered to be via ion-exchange, especially for Pb^{2+} adsorption, with 99.7% molar equivalents exchanged between the adsorbed Pb^{2+} and the eluted EPS counter ions. For the EPS-Cu^{2+} interaction, ion-exchange accounted for 68% of the binding, suggesting other mechanisms also in operation.

Acknowledgements

This work was performed in the cooperation framework of Wetsus, European Centre of Excellence for Sustainable Water Technology (www.wetsus.nl). Wetsus is co-funded by the Dutch Ministry of Economic Affairs and Ministry of Infrastructure and Environment, the European Union Regional Development Fund, the Province of Fryslân and the Northern Netherlands Provinces. This work has also received funding from the European Union's Horizon 2020 research and innovation programme under the Marie Skłodowska-Curie [grant agreement No. 665874]. The authors thank the participants of the research theme 'Natural flocculants' for the fruitful discussions and financial support; Eliane Rodenburg and Gerjanne Bergsma from the Wetsus Honours Programme for some of the experimental work; Dainis Sudmalis, Peter de Gijsel and Mirjam Kabel from Wageningen University and Research for the sugar composition analysis; and Wetterskip Leeuwarden for providing the inoculum.

Supporting information of Chapter 6

Table S1. Calculations of the amount (mass and charge equivalent) of PEI and EPS immobilised in the column.

TOC value of influent PEI	5.7 ± 0.1 g/L
TOC value of (re)circulated PEI	4.5 ± 0.2 g/L
TOC value of PEI retained in column	1.2 g/L (calculated by difference)
TOC value of PEI adsorbed in the column (after flushing with water)	0.51 g/L
Fraction of PEI concentration immobilised in the column	0.09
Mass of PEI immobilised in the column	45.4 mg
Charge equivalent of PEI immobilised in the column	0.66 meq
TOC value of influent EPS	5.3 ± 0.3 g/L
TOC value of (re)circulated EPS	2.2 ± 0.0 g/L
TOC value of EPS retained in column	3.1 g/L (calculated by difference)
TOC value of EPS adsorbed in the column (after flushing with water)	1.6 g/L
Fraction of EPS concentration immobilised in the column	0.31
Charge equivalent of EPS attached to PEI	1.06 meq (using a stoichiometry ratio of 1.6 meq of EPS to 1 meq of PEI)
Thus, mass of EPS attached to PEI	115.4 mg
Mass of EPS with sites available for binding with heavy metals	39.1 mg
Charge equivalent of EPS available for binding with heavy metals	0.35 meq

Table S2. EPS organic fractions measured by size exclusion chromatography using liquid chromatography-organic carbon detection (LC-OCD). LMW: low molecular weight.

EPS organic fraction	Concentration mg/g EPS	Percentage of fraction in DOC
Biopolymer organic carbon	239.0	54%
Biopolymer organic nitrogen	9.6	
Building blocks organic carbon	109.5	25%
Building blocks organic nitrogen	9.0	
LMW neutrals organic carbon	21.4	5%
LMW acids organic carbon	11.3	3%
Hydrophobic organic carbon [a]	58.7	13%
Chromatographic dissolved [b] organic carbon	380.0	87%
Dissolved organic carbon	438.7	100%

[a] Hydrophobic organic fraction (HOC) is the fraction of the dissolved organic carbon (DOC) that is retained in the column due to hydrophobic interactions.

[b] Chromatographic DOC is the fraction of DOC that passes through the column and is separated into the biopolymer organic carbon, building blocks organic carbon, and organic carbon of the LMW neutrals and acids [16].

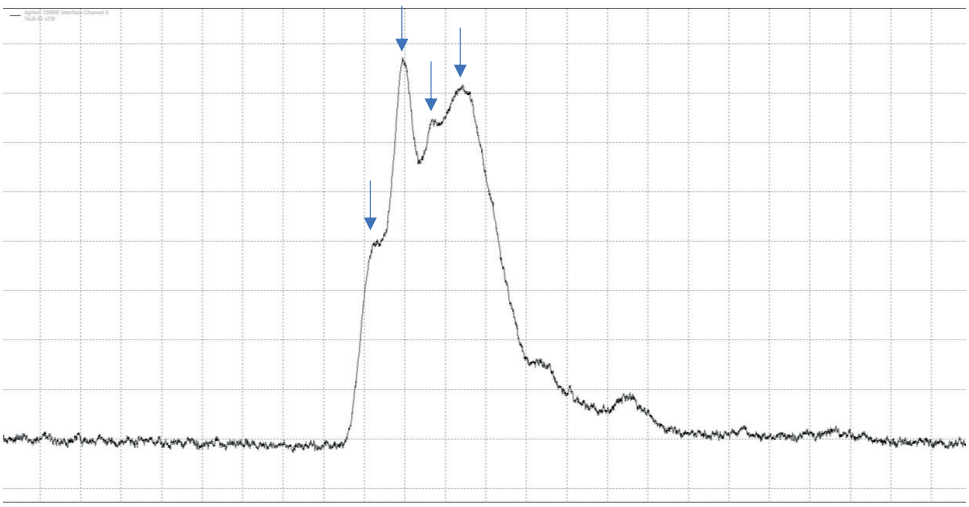

Fig. S1. LC-OCD chromatogram of the produced EPS showing the four biopolymer chromatographic peaks of EPS (shown with arrows).

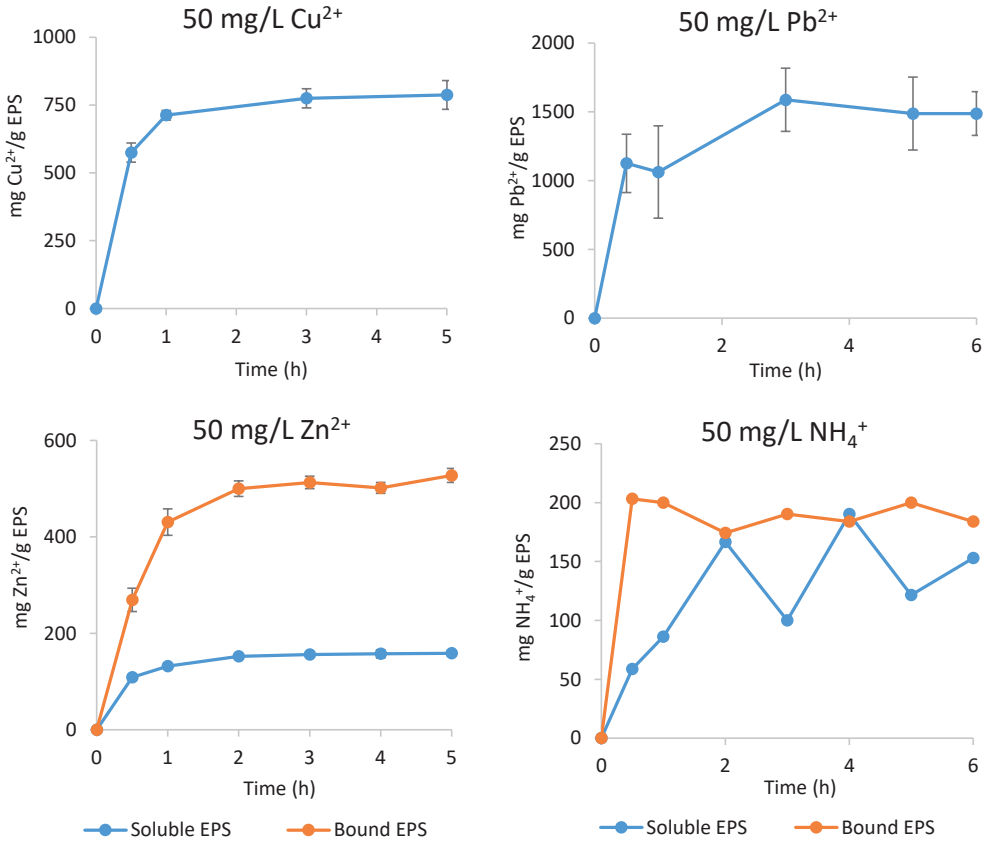

Fig. S2. Batch studies on the removal of Cu^{2+}, Pb^{2+}, Zn^{2+} and NH_4^+ from aqueous solution using EPS. Cu^{2+} and Pb^{2+} were tested for S-EPS, while Zn^{2+} and NH_4^+ were tested for both soluble and bound EPS fractions. Bound EPS were extracted according to the method described by Ajao *et al*. [12].

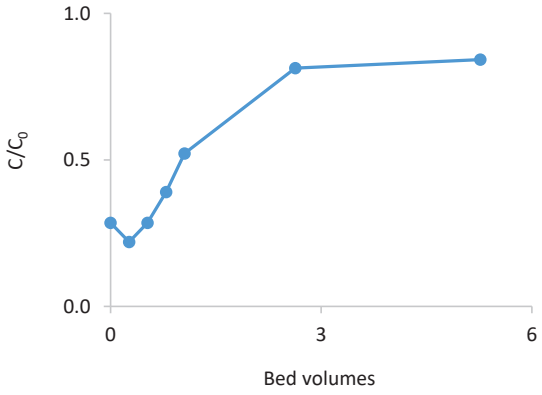

Fig. S3. Adsorption of Cu^{2+} by silica gel packed in a column (control experiment).

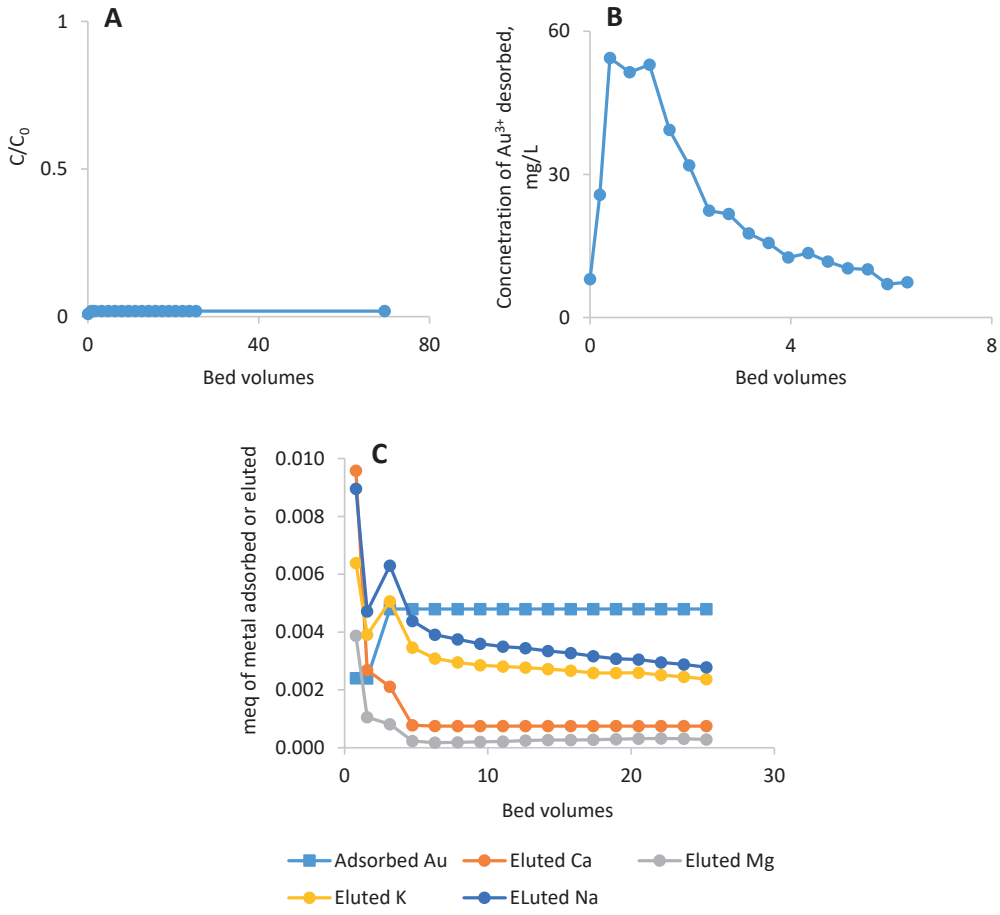

Fig. S4. **A** - Adsorption of Au^{3+} (from $AuCl_3 \cdot 2H_2O$) in a column packed with EPS, C_0 = 10.7 mg/L. **B** - Desorption of adsorbed Au^{3+} from EPS. **C** - Molar equivalents of the eluted EPS counter ions (K^+, Ca^{2+}, Na^+, Mg^{2+}) compared to the adsorbed Au^{3+}.

S5. Analysis of EPS sugar composition

Neutral sugar composition was determined in duplicates according to Englyst and Cummings (1984). After a pre-hydrolysis with 72% (w/w) H_2SO_4 for 1 h at 30 °C, the samples were hydrolysed with 1 M H_2SO_4 at 100 °C for 3 h. The monosaccharides were derivatised to their alditol acetates and analysed by gas chromatography (Focus-GC, Thermo Scientific, Waltham, MA, USA). Inositol was used as the internal standard.

Uronic acid content was determined according to the automated colorimetric m-hydroxydiphenyl assay [43] using an auto-analyser (Skalar Analytical B.V., Breda, the Netherlands). Galacturonic acid was used for calibration [44].

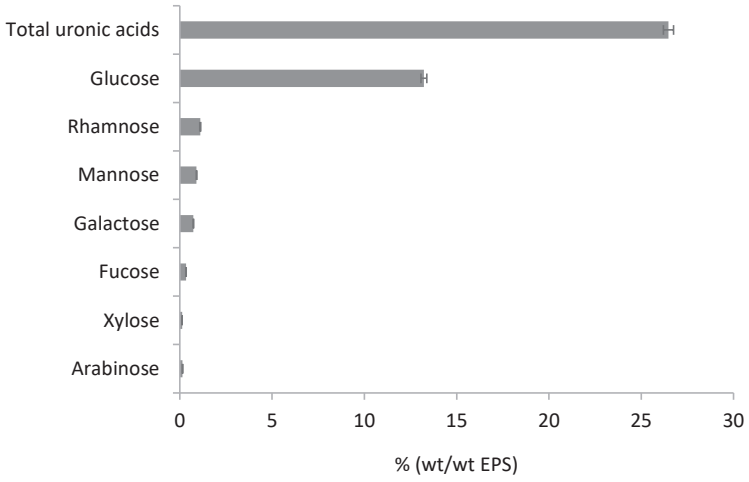

Fig. S5. Harvested EPS sugar composition.

References

[1] W. Liu, J. Zhang, Y. Jin, X. Zhao, Z. Cai, Adsorption of Pb(II), Cd(II) and Zn(II) by extracellular polymeric substances extracted from aerobic granular sludge: Efficiency of protein, J. Environ. Chem. Eng. 3 (2015) 1223–1232. doi:10.1016/j.jece.2015.04.009.

[2] J.J. Gray, The interaction of proteins with solid surfaces, Curr. Opin. Struct. Biol. 14 (2004) 110–115. doi:10.1016/j.sbi.2003.12.001.

[3] J. Wang, C. Chen, Biosorbents for heavy metals removal and their future, Biotechnol. Adv. 27 (2009) 195–226. doi:10.1016/j.biotechadv.2008.11.002.

[4] J.R. Dodson, H.L. Parker, A. Muñoz García, A. Hicken, K. Asemave, T.J. Farmer, H. He, J.H. Clark, A.J. Hunt, Bio-derived materials as a green route for precious & critical metal recovery and re-use, Green Chem. 17 (2015) 1951–1965. doi:10.1039/C4GC02483D.

[5] B. Volesky, Detoxification of metal-bearing effluents: Biosorption for the next century, Hydrometallurgy. 59 (2001) 203–216. doi:10.1016/S0304-386X(00)00160-2.

[6] B. Volesky, Biosorption and me. Review, Water Res. 41 (2007) 4017–4029. doi:10.1016/j.watres.2007.05.062.

[7] G.M. Gadd, Biosorption: Critical review of scientific rationale, environmental importance and significance for pollution treatment, J. Chem. Technol. Biotechnol. 84 (2009) 13–28. doi:10.1002/jctb.1999.

[8] H. Liu, H.H.P. Fang, Characterization of electrostatic binding sites of extracellular polymers by linear programming analysis of titration data, Biotechnol. Bioeng. 80 (2002) 806–811. doi:10.1002/bit.10432.

[9] W.W. Li, H.Q. Yu, Insight into the roles of microbial extracellular polymer substances in metal biosorption, Bioresour. Technol. 160 (2014) 15–23. doi:10.1016/j.biortech.2013.11.074.

[10] T.T. More, J.S.S. Yadav, S. Yan, R.D. Tyagi, R.Y. Surampalli, Extracellular polymeric substances of bacteria and their potential environmental applications, J. Environ. Manage. 144 (2014) 1–25. doi:10.1016/j.jenvman.2014.05.010.

[11] K. Raj, U.R. Sardar, E. Bhargavi, I. Devi, B. Bhunia, O.N. Tiwari, Advances in exopolysaccharides based bioremediation of heavy metals in soil and water: A critical review, Carbohydr. Polym. 199 (2018) 353–364. doi:10.1016/j.carbpol.2018.07.037.

[12] V. Ajao, S. Millah, M.C. Gagliano, H. Bruning, H. Rijnaarts, H. Temmink, Valorization of glycerol/ethanol-rich wastewater to bioflocculants: recovery, properties, and performance, J. Hazard. Mater. 375 (2019) 273–280. doi:10.1016/j.jhazmat.2019.05.009.

[13] V. Ajao, H. Bruning, H. Rijnaarts, H. Temmink, Natural flocculants from fresh and saline wastewater: Comparative properties and flocculation performances, Chem. Eng. J. 349 (2018) 622–632. doi:10.1016/j.cej.2018.05.123.

[14] M. DuBois, K. a. Gilles, J.K. Hamilton, P. a. Rebers, F. Smith, Colorimetric method for determination of sugars and related substances, Anal. Chem. 28 (1956) 350–356. doi:10.1021/ac60111a017.

[15] H.N. Englyst, J.H. Cummings, Simplified method for the measurement of total non-starch polysaccharides by gas - liquid chromatography of constituent sugars as alditol acetates, Analyst. 109 (1984) 937–942. doi:10.1039/an9840900937.

[16] S.A. Huber, A. Balz, M. Abert, W. Pronk, Characterisation of aquatic humic and non-humic matter with size-exclusion chromatography - organic carbon detection - organic nitrogen detection (LC-OCD-OND), Water Res. 45 (2011) 879–885. doi:10.1016/j.watres.2010.09.023.

[17] W.F. Tan, W. Norde, L.K. Koopal, Humic substance charge determination by titration with a flexible cationic polyelectrolyte, Geochim. Cosmochim. Acta. 75 (2011) 5749–5761. doi:10.1016/j.gca.2011.07.015.

[18] J.C. Dijt, M.A.C. Stuart, J.E. Hofman, G.J. Fleer, Kinetics of polymer adsorption in stagnation point flow, Colloids and Surfaces. 51 (1990) 141–158. doi:10.1016/0166-6622(90)80138-T.

[19] J. Wang, Q. Li, M.M. Li, T.H. Chen, Y.F. Zhou, Z.B. Yue, Competitive adsorption of heavy metal by extracellular polymeric substances (EPS) extracted from sulfate reducing bacteria, Bioresour. Technol. 163 (2014) 374–376. doi:10.1016/j.biortech.2014.04.073.

[20] P. Chandra, D.S. Doke, S.B. Umbarkar, K. Vanka, A. V Biradar, Silica microspheres containing high density surface hydroxyl groups as efficient epoxidation catalysts, RSC Adv. 5 (2015) 21125–21131. doi:10.1039/c5ra00374a.

[21] A. Barth, Infrared spectroscopy of proteins, Biochim. Biophys. Acta - Bioenerg. 1767 (2007) 1073–1101. doi:10.1016/j.bbabio.2007.06.004.

[22] S.J. Yuan, M. Sun, G.P. Sheng, Y. Li, W.W. Li, R.S. Yao, H.Q. Yu, Identification of key constituents and structure of the extracellular polymeric substances excreted by *Bacillus megaterium* TF10 for their flocculation capacity, Environ. Sci. Technol. 45 (2011) 1152–1157. doi:10.1021/es1030905.

[23] B. Bin Wang, X.T. Liu, J.M. Chen, D.C. Peng, F. He, Composition and functional group characterization of extracellular polymeric substances (EPS) in activated sludge: the impacts of polymerization degree of proteinaceous substrates, Water Res. 129 (2018) 133–142. doi:10.1016/j.watres.2017.11.008.

[24] T.J. Stewart, J. Traber, A. Kroll, R. Behra, L. Sigg, Characterization of extracellular polymeric substances (EPS) from periphyton using liquid chromatography-organic carbon detection-organic nitrogen detection (LC-OCD-OND), Environ. Sci. Pollut. Res. 20 (2013) 3214–3223. doi:10.1007/s11356-012-1228-y.

[25] EPA, 4. What are EPA's drinking water regulations for mercury? – Ground Water & Drinking Water, United States Environ. Prot. Agency. (2019).

https://safewater.zendesk.com/hc/en-us/articles/211402978-4-What-are-EPA-s-drinking-water-regulations-for-copper- (accessed July 11, 2019).

[26] A. Saeed, M. Iqbal, M.W. Akhtar, Removal and recovery of lead(II) from single and multimetal (Cd, Cu, Ni, Zn) solutions by crop milling waste (black gram husk), J. Hazard. Mater. 117 (2005) 65–73. doi:10.1016/j.jhazmat.2004.09.008.

[27] A.A. Swelam, A.M.A. Salem, A.A. Ayman, Copper (II) Removal using Three Cation Exchange Resins : Ion Exchange Equilibrium and Kinetics, Middle East J. Appl. Sci. 5 (2015) 1017–1027. http://www.curresweb.com/mejas/mejas/2015/1017-1027.pdf (accessed June 17, 2019).

[28] E. Pehlivan, T. Altun, Ion-exchange of Pb^{2+}, Cu^{2+}, Zn^{2+}, Cd^{2+}, and Ni^{2+} ions from aqueous solution by Lewatit CNP 80, J. Hazard. Mater. 140 (2007) 299–307. doi:10.1016/j.jhazmat.2006.09.011.

[29] E.L. Cochrane, S. Lu, S.W. Gibb, I. Villaescusa, A comparison of low-cost biosorbents and commercial sorbents for the removal of copper from aqueous media, J. Hazard. Mater. 137 (2006) 198–206. doi:10.1016/j.jhazmat.2006.01.054.

[30] V. Krstić, T. Urošević, B. Pešovski, A review on adsorbents for treatment of water and wastewaters containing copper ions, Chem. Eng. Sci. 192 (2018) 273–287. doi:10.1016/j.ces.2018.07.022.

[31] W.S. Wan Ngah, L.C. Teong, M.A.K.M. Hanafiah, Adsorption of dyes and heavy metal ions by chitosan composites: A review, Carbohydr. Polym. 83 (2011) 1446–1456. doi:10.1016/j.carbpol.2010.11.004.

[32] A. Kapoor, Fungal biosorption – an alternative treatment option for heavy metal bearing wastewaters: a review, Bioresour. Technol. 53 (2002) 195–206. doi:10.1016/0960-8524(95)00072-1.

[33] A. Hammaini, F. González, A. Ballester, M.L. Blázquez, J.A. Muñoz, Biosorption of heavy metals by activated sludge and their desorption characteristics, J. Environ. Manage. 84 (2007) 419–426. doi:10.1016/j.jenvman.2006.06.015.

[34] S. Aslan, S. Yildiz, M. Ozturk, Biosorption of Cu^{2+} and Ni^{2+} Ions From Aqueous Solutions Using Waste Dried Activated Sludge Biomass, Polish J. Chem. Technol. 20 (2018) 20–28. doi:10.2478/pjct-2018-0034.

[35] H.-C. Flemming, J. Wingender, The biofilm matrix, Nat. Publ. Gr. 8 (2010) 623–633. doi:10.1038/nrmicro2415.

[36] C. Quintelas, B. Fernandes, J. Castro, H. Figueiredo, T. Tavares, Biosorption of Cr(VI) by three different bacterial species supported on granular activated carbon-A comparative study, J. Hazard. Mater. 153 (2008) 799–809. doi:10.1016/j.jhazmat.2007.09.027.

[37] H. Salehizadeh, S.A. Shojaosadati, Removal of metal ions from aqueous solution by

polysaccharide produced from *Bacillus firmus*, Water Res. 37 (2003) 4231–4235. doi:10.1016/S0043-1354(03)00418-4.

[38] CDC - Lead - Tips - Sources of Lead - Water, https://www.cdc.gov/nceh/lead/tips/water.htm (accessed July 12, 2019).

[39] A. Demirbas, E. Pehlivan, F. Gode, T. Altun, G. Arslan, Adsorption of Cu(II), Zn(II), Ni(II), Pb(II), and Cd(II) from aqueous solution on Amberlite IR-120 synthetic resin, J. Colloid Interface Sci. 282 (2005) 20–25. doi:10.1016/j.jcis.2004.08.147.

[40] A. Bożęcka, M. Orlof-Naturalna, S. Sanak-Rydlewska, Removal of lead, cadmium and copper ions from aqueous solutions by using ion exchange resin C 160, Gospod. Surowcami Miner. 32 (2016) 129–140. doi:10.1515/gospo-2016-0033.

[41] S.B. Chen, Y.B. Ma, L. Chen, K. Xian, Adsorption of aqueous Cd^{2+}, Pb^{2+}, Cu^{2+} ions by nano-hydroxyapatite: Single-and multi-metal competitive adsorption study, Geochem. J. 44 (2010) 233–239. doi:10.2343/geochemj.1.0065.

[42] W. Wei, Q. Wang, A. Li, J. Yang, F. Ma, S. Pi, D. Wu, Biosorption of Pb (II) from aqueous solution by extracellular polymeric substances extracted from *Klebsiella* sp. J1: Adsorption behavior and mechanism assessment, Sci. Rep. 6 (2016) 1–10. doi:10.1038/srep31575.

[43] J. Thibault, Automatisation du dosage des substances pectiques par la methode au meta-hydroxydiphenyl, Leb. Wiss. Und Technol. 21 (1979) 247–251.

[44] A.M. Pustjens, H.A. Schols, M.A. Kabel, H. Gruppen, Characterisation of cell wall polysaccharides from rapeseed (*Brassica napus*) meal, Carbohydr. Polym. 98 (2013) 1650–1656. doi:10.1016/j.carbpol.2013.07.059.

Chapter 7

General Discussion and Outlook

1. Microbial EPS: from nuisance to application

The occurrence or production of EPS in systems such as water distribution and membrane-based water treatment systems are undesirable and poses a serious issue, namely biofouling. Biofouling in the aforementioned systems decreases water flow rates and may lead to increased chemical and energy consumption. However, a closer study of EPS properties reveals much more: they are composed of high molecular weight (MW) substances such as polysaccharides and proteins, possess a net anionic charge, are generally non-toxic, biodegradable and amphiphilic [1]. These properties make them attractive biopolymers that can be used as biodegradable flocculants and cost-effective heavy metal adsorbents.

The focus of this research was to investigate how to select and valorise industrial wastewater to EPS while simultaneously treating the wastewater, the applications of the produced EPS as biodegradable flocculants and heavy metal adsorbents, and to understand the flocculation and metal-adsorbing mechanisms of these biopolymers. A systematic approach was followed to study three aspects of the technology value chain (EPS production, characteristics and application) and how they are linked to one another. This resulted in scientific findings regarding suitable wastewaters to produce EPS in practice and how carbon substrates and reactor conditions influence the composition, characteristics and application of EPS (summarised in Fig. 5).

2. EPS production and operational considerations

2.1. Wastewater suitability

EPS, being secondary products of microbial metabolism, require energy for their biosynthesis. This energy typically comes from the break down (catabolism) of assimilated substrates. First, suitable wastewater for EPS production should contain a significant fraction of small, soluble and biodegradable substrates. Thus, wastewater containing biomacromolecules would need to be first hydrolysed before they can be taken up by microorganisms. In practice, most wastewaters contain both soluble and insoluble (particulate and colloidal) COD and their ratios may influence the suitability of a substrate to produce EPS. While biodegradable soluble COD may be metabolised to produce secondary metabolites such as EPS, insoluble but biodegradable organics can be hydrolysed but perhaps not completely within the short solids retention time (SRT) that is required to obtain high EPS yields (later discussed).

Second, the type of soluble organic compound (carbon source) present in the wastewater also determines how it is assimilated into the microbial cell and how it is metabolised to EPS within the cell. Small uncharged molecules such as glycerol can cross the cell membrane via facilitated passive diffusion through its concentration gradient. On the other hand, the movement of most sugars and charged molecules such as acetate involves an active transport system whereby ATP hydrolysis is needed to gain energy to drive the substrate uptake against its concentration gradient [2,3]. In the latter case, it is likely that less energy is spilled (or remains) by microorganisms to synthesize secondary metabolites such as EPS [4]. Moreover, substrates (such as glycerol) that lead to the production of EPS rich in oxidised substituents (e.g., uronic acids) have been reported to have high

EPS (particularly exopolysaccharides) yield due to the low energy demand needed to synthesize acidic exopolysaccharides [5,6] (Chapter 4).

In Chapter 4, the concept of non-equivalent substrates in terms of bioenergetics [6,7] was investigated, whereby ethanol (an energy-rich substrate) was added as a co-substrate to energy-deficient substrates such as glycerol, glucose and acetate, to increase the yield of EPS compared to the use of a single substrate. Although the addition of ethanol to glycerol and glucose led to lower EPS yields, ethanol addition to acetate increased EPS yield when compared to EPS produced from sole acetate. Hence, the non-equivalent substrates concept proposed by Babel and Muller [7] to intensify EPS production in single cultures [6] may not be absolutely applicable for mixed cultures.

The more surprising result, which still needs to be further investigated, was the high EPS recovery (69% wastewater-COD recovered as EPS-COD) obtained when acetate/ethanol substrate was fed to an EPS-rich sludge. Although the results are promising as it may pave the way for intensifying EPS production, further experimental evidence (such as isotope labelling and tracing) is still needed to substantiate the metabolic roles of energy-excessive and deficient substrates in mixed cultures producing EPS. A practical application of this finding is that, to obtain high EPS yield from paper factory wastewater (which is acetate-rich), it may be vital to first enrich the reactor with EPS-producing microorganisms by first operating with glycerol (or biodiesel wastewater) and then switch to the paper wastewater, with the continued addition of a little ethanol to the reactor.

In Chapter 4, we also discussed the microbial population in the reactors producing EPS from different substrates. Even for a narrow substrate range, many bacterial groups (typically the fast growers, due to the 2-day SRT) were surprisingly present under the different feeding conditions. However, none of them was always dominant in the same reactor when switched from a single substrate (e.g., glycerol) to dual substrates (e.g., glycerol + ethanol). In most cases, two or more possible EPS-producing genera (such as *Mucilaginibacter*, *Xanthobacter*, *Acinetobacter*, *Caulobacter* and *Sphingobium*) developed within the same reactor when fed with different substrates. But with surplus EPS in some reactors, some EPS-degraders (*Luteolibacter* and *Verrucomicrobium*) were also present. Worthy of note is the likely competition between extracellular and intracellular polymer (EPS and polyhydroxyalkanoate, respectively) production when one of the reactors (inoculated with aerobic sludge from WWTP) was fed with acetate. In the reactor, *Erysipelothrix* and *Acinetobacter* were the dominant genera and some of their members may be responsible for the PHA production.

Third, the wastewater COD/nitrogen ratio: EPS biosynthesis has been reported to be generally induced by various stress factors such as salinity [8], nutrient limitation [9], or even the presence of toxic substances such as heavy metals [1]. Of particular interest is the effect of nutrient (nitrogen or phosphorus) limitation [9]. Although not studied in this thesis, phosphorus limitation (100:5:0) was reported by Bura *et al*. [10] to enhance EPS production. However, the effect of phosphorus limitation seems to have a lower impact on EPS yield [10] compared to the effect of nitrogen limitation investigated in Chapter 3. Hence, waste streams with a high COD/N ratio (such as biodiesel, soda/sugar beet, pulp and paper, and liquor industrial wastewaters) would be preferred to obtain high EPS yields. This makes high strength industrial wastewaters with high COD and limited

nitrogen content the most suitable wastewater type for EPS production, while municipal wastewater (which usually has low COD levels and contains excess nitrogen) is less appropriate. Moreover, unlike municipal wastewater, it is also possible to select industrial waste streams that are of known chemical composition and free of particles, pathogens and heavy metals. Since EPS can adsorb to heavy metals, the use of a heavy metal-polluted wastewater will lead to the production of a heavy metal-contaminated EPS, which may result in the undesired leaching of metals into the environment. Ditto when the utilised wastewater contains pathogens.

2.2. Reactor design and operation

2.2.1. Maximising EPS volumetric productivity

To upscale EPS recovery from wastewater, the concentration of EPS produced and retained in the reactor should be high enough for cost-effective harvesting, purification (if desirable) and drying. The highest EPS concentration obtained in this thesis was 3.1 g EPS/L sludge (Chapter 4) and is the highest reported for sludge systems, although not surprising because this study was dedicated to obtaining high EPS yields. However, the concentrations obtained in this thesis are lower than what can be attained with pure cultures – which can be as high as 28 g/L [11]. With respect to the MBR used in this study (effective volume 3.3 L), one way to increase the EPS concentration is to simply use a smaller reactor. On a large scale, the solids concentration factor will play a crucial role. With complete membrane retention and in the absence of mineralisation, the solids concentration factor is determined as the ratio between the solids and hydraulic retention times (SRT/HRT ratio) [12]. Although the effect of SRT will be discussed in the next section, it is desirable to keep the HRT as short as possible, provided good wastewater treatment is not jeopardised.

Keeping in mind the high viscosity of EPS in reactors dedicated for this purpose (Fig. 1 and Chapter 3), when upscaling, EPS production should be aimed at the highest possible concentration that can still ensure adequate mixing and sufficient oxygen transfer. Effective mixing is vital to reduce the formation of undesired biofilms on surfaces instead of floating flocs, minimise membrane fouling if an MBR is employed, and more importantly, ensure good oxygen diffusion within the EPS-rich sludge. The physical limit of oxygen transfer rate in aerated reactors is reported to be approximately 5 g/L/h, but it should be noted that this involves expensive industrial fermentation reactors with a very high volumetric power input [13,14]. Although it is possible to apply intensive oxygen input in EPS-producing reactors, it is likely more profitable to optimise mixing and make a compromise between maximising volumetric productivity and optimising aeration and mixing, which are both energy-consuming.

2.2.2. Membrane *versus* membraneless bioreactor for EPS production

Although the use of membrane bioreactors (MBRs) for combined wastewater treatment and EPS production (as employed in this thesis) looks counter-intuitive due to the expected fouling of the membrane (Fig. 2 A and B), they were employed in this research for two reasons. First, biomass and EPS can be effectively retained and concentrated in the reactor, especially under high EPS production rate when the sludge becomes viscous (Fig. 1). In this case, systems such as the

sequencing batch reactor will be ineffective because the produced viscous sludge has a low settleability. Second, MBRs provide an adequate solution to the sedimentation problems often encountered under saline conditions [15].

Fig. 1. Viscous sludge produced from the MBR treating fresh wastewater at a COD/N ratio of 100 (Chapter 3).

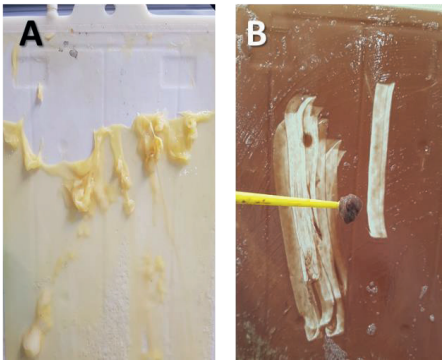

Fig. 2. Fouling of membranes submerged in the membrane bioreactors (MBRs): (**A**) – membrane of the MBR treating fresh wastewater at a COD/N ratio, of 100, (**B**) - membrane of the MBR treating saline wastewater at a COD/N ratio of 100 (Chapter 3).

In practice, the use of MBRs would be cumbersome and costly due to the constant fouling of the membranes. An alternative would be to use the foulant (EPS) itself as a membrane by developing a self-forming dynamic layer of EPS on a porous support (pore size can be as small as 10 - 100 µm or as large as 2 mm [16]). The use of such a separation system has received increasing interest in recent years and is reported to show excellent organic pollutant removal with stable and high quality effluents [16–19]. Although this reactor system has not been employed for dedicated EPS production coupled with wastewater treatment, it could be a cheaper alternative to the conventional MBR systems, while still retaining the aforementioned advantages of using an MBR. However, it is worth mentioning that the performance of a dynamic membrane for wastewater treatment depends on factors such as the cake density, cake structure and cake components [20], which in turn depend on the bulk composition. Hence, these factors still need to be further researched in light of combining biological wastewater treatment with high EPS recovery.

While a retention system is necessary for wastewater with low COD to concentrate and accumulate the produced EPS, it may not be needed when the wastewater COD is high and the HRT of the system is short (as previously discussed). In this case, the produced EPS will have a high concentration that can be harvested from the reactor effluent.

2.2.3. Effect of solids retention time (SRT) on EPS production

With respect to reactor operation, SRT is a crucial parameter for achieving a high EPS yield. In most conventional WWTPs, relatively long SRTs (typically 8 - 30 d) are employed to primarily keep the

very slow-growing nitrifying bacteria in the system, as well as to reduce sludge production and ensure high quality effluents. However, this is done at the expense of high oxygen (and energy) consumption, which leads to mineralisation of about 50 - 60 % of the wastewater organics.

In another study (not reported in this thesis) where we investigated the effect of different SRTs on EPS recovery (Fig. 3), EPS recovery first increased with increasing SRT (typically 1 - 3 d), after which it drastically declined as the SRT was further increased (8 - 15 d). Faust *et al*. [21] also observed a similar phenomenon with municipal wastewater. With increasing sludge retention (SRT > 5 d, according to Faust *et al*. [21]), a large fraction of the wastewater-COD is oxidised instead of being converted to secondary metabolites such as EPS. Furthermore, a short SRT helps to avoid hydrolysis of the produced biopolymer and, perhaps, to wash out the EPS degraders from the system as much as possible. Thus, reactor operation should be such that the SRT is as low as possible to ensure maximum EPS recovery and optimal wastewater treatment. With this approach, as high as 54% of the wastewater-COD can be converted to EPS-COD, reducing the fraction of oxidised COD to 20 - 25%, and the remaining 20 - 25% for biomass growth (Chapter 3, supplementary information).

The minimum SRT that is required is determined by the maximum specific growth rate of the key EPS-producers, which are typically the fast-growing bacteria, such as is reported in Chapter 4. More than 80% of the main EPS-producers highlighted in Chapter 4 belong to the phylum *Proteobacteria*, which have also been reported to grow in high-loaded MBRs operated at extremely short SRTs (≤ 1 d) [22]. Such rapidly growing cells are reported to spill more energy (as much as 25% of their ATP) to produce secondary metabolites, compared to the slow-growing bacteria [4].

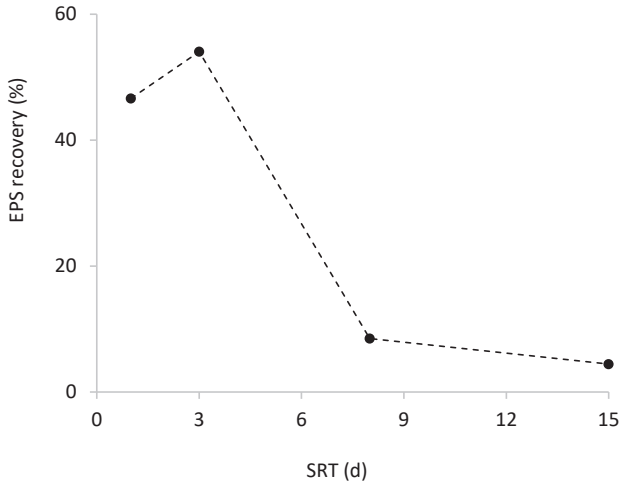

Fig. 3. The influence of solids retention time (SRT) on EPS recovery. Substrates: glycerol/ethanol mixture (ratio 1:1 based on g COD glycerol: g COD ethanol); COD/N ratio 87 ± 6; Influent COD: 1 g/L. Dashed lines are to guide the eye.

3. EPS characteristics

Over the past decades, numerous techniques (both physical and chemical methods) have been explored for characterising EPS in biofilms, effluents and sludges from biological processes, and soils (Table A1 - Appendix). Despite these available techniques, little is known regarding the metabolic pathways involved in EPS biosynthesis, their molecular composition and structure, structure-function relationships that could lead to the identification of new applications and markets, to mention a few [23]. These hurdles exist primarily due to the complexity and diversity of EPS in multi-species biofilms and wastewater sludges. In light of these barriers, this thesis provides more insight into the molecular composition of EPS produced from nitrogen-limited wastewater from different substrates (Chapter 4), and the interconnectedness between EPS composition, chemical characteristics and applications (Chapters 3, 4, 5 and 6).

3.1. EPS composition

The chemical nature of wastewater-produced EPS is diverse and heterogeneous, generally comprised of polysaccharides, proteins, humic substances, lipids and nucleic acids [1]. Polysaccharides and proteins are the major components (50 - 90 %) and their ratios depend on several factors such as the SRT and the wastewater carbon/nitrogen ratio [1]. At long SRTs (typically ≥ 5 d), most studies reported higher EPS-protein content than polysaccharides [21,24–26], perhaps due to the preferential hydrolysis of polysaccharides at an increasing sludge or biofilm age [21]. A similar phenomenon was also observed in this thesis. In Chapter 2, where the SRT was 15 d, the polysaccharide/protein ratio was 0.7, compared to the result in Chapter 3 where a ratio of 1.3 was obtained for an SRT of 3 d (other reactor conditions were similar: glycerol/ethanol-rich wastewater; COD/N 16 and 20, respectively).

Additionally, the COD/N ratio of wastewater also influences the ratio of EPS-polysaccharides to proteins. As reported in Chapter 3 and by other researchers [27–29], reactors operating under nitrogen-limited conditions (i.e., wastewater with a high COD/N ratio) produce EPS with a higher polysaccharide content than proteins, provided other conditions are kept constant. Excess energy under limited nitrogen is converted to extracellular polymers, especially polysaccharides (which do not contain the growth-limiting nutrient) [9], possibly as a means to store carbon under unbalanced C/N ratios [30]. Moreover, microbial polysaccharides are less energy expensive (~ 12.6 mmol ATP/g) to synthesize compared to proteins (~ 36.4 mmol ATP/g) [4].

It is however surprising that EPS-proteins (these may be or include peptides or exoenzymes) are produced even under nitrogen-limited conditions (such as COD/N of 100 in Chapters 3 and 4), which is contrary to the 'stoichiometric' expectation of COD/N ratios in biological wastewater treatment processes (typically COD/N ratio 20 ± 10). One would have imagined the exclusive production of exopolysaccharides, while microorganisms utilise the insufficient influent nitrogen for survival (cell growth and maintenance). However, Redmile-Gordon *et al*. [31] demonstrated that microorganisms are able to invest extracellularly after 'speculating' nitrogen shortage. In this way, they accumulate peptides or proteins as a means to harvest nitrogen from the environment for cell growth, with the aid of hydrolytic enzymes retained in the EPS-rich matrix. A similar phenomenon was also reported

by Wang and Yu [32]. A further investigation into the energy requirement for producing extracellular proteins in *Escherichia coli* (as a model) reveals the conservative nature of microorganisms in producing economic amino acids extracellularly [33]. In other words, the average energy cost for producing extracellular proteins was found to be significantly lower than the costs of intracellular proteins (cytoplasmic, periplasmic, and membrane proteins). These findings may justify the considerable amount of EPS-proteins (up to 15 wt%) recovered in our nitrogen-limited systems, but overall, EPS-polysaccharide content was much higher than proteins.

While carbon is a vital requirement for substantial EPS production, excess or shortage of (inorganic) nitrogen affects the microbial secretion of both EPS-polysaccharides and proteins (Chapter 3). The interesting implication of this is that EPS composition can be fine-tuned by using influent nitrogen (and perhaps SRT) as a 'switch' to either produce protein-rich EPS or polysaccharide-rich EPS, depending on the intended application, but keeping in mind that excess nitrogen results in a reduced EPS yield (Chapter 3).

Based on the results in Chapter 3 that reveal the positive effects of nitrogen limitation on EPS production, composition and characteristics (for our intended applications), the experiments in Chapters 4 to 6 were carried out under the same condition (limited nitrogen). Hence, the produced EPS were mainly composed of polysaccharides as the biopolymer, with low amounts of proteins. For this reason, the sugar composition of the EPS produced from different carbon substrates was characterised using Gas Chromatography. As reported in Chapter 4, EPS sugar composition and content varied with the utilised substrate. While the glycerol-containing substrates led to the production of uronic acid-rich EPS, the acetate-containing substrates were mainly composed of mannose and galactose, while ethanol substrate resulted in a fairly uniform distribution of mannose, galactose, fucose, rhamnose, glucose and uronic acids in the produced EPS. EPS synthesized from the glucose-containing substrate were mainly composed of mannose, galactose and xylose, and only the EPS from this substrate also contained significant amounts of pentoses (arabinose and xylose). It has been reported that polysaccharides with oxidised substituents such as uronic acids require a lower energy investment (and even result in energy generation) compared to neutral exopolysaccharides. This may partly justify the higher EPS yields obtained from glycerol substrates compared to the other substrates mentioned above.

3.2. Average molecular weights of EPS

The general biosynthetic pathway of extracellular polymers, namely exopolysaccharides, can be divided into four stages: (i) the synthesis of a precursor substrate, (ii) cytoplasmic membrane transfer and polymerization, (iii) periplasmic transfer and modification, and (iv) export through the outer membrane [34,35]. The second stage determines the MW and chain length of the produced EPS, while the EPS' charge densities are determined during the second and third stages (during the polymerisation and post-polymerisation modification stages, respectively). In mixed cultures, the degree of polymerisation and post-polymerisation modification vary with the EPS-producing bacteria, leading to heterodispersed molecular weights.

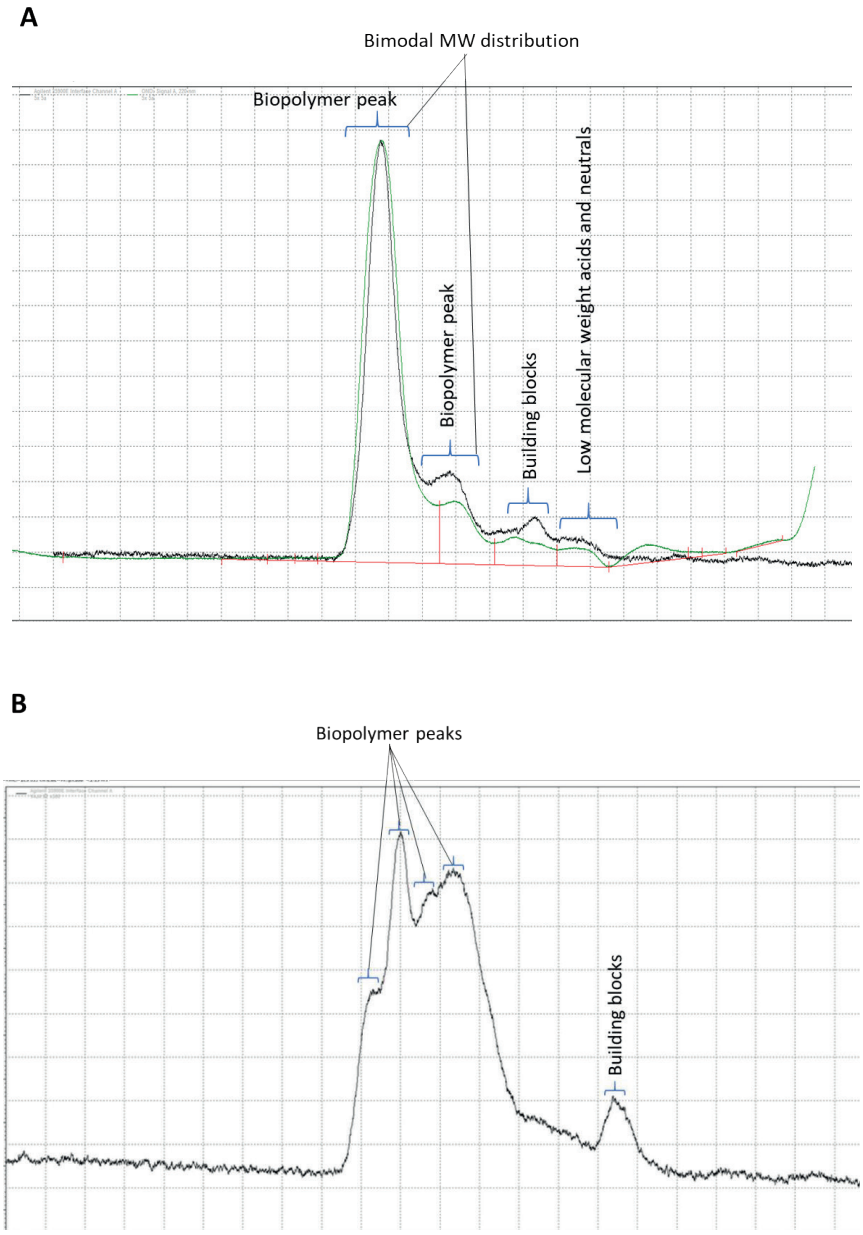

Fig. 4. Molecular weight distribution profile of soluble-EPS extracted from Chapter 6 (**A**) and Chapter 3 (**B**); analysed with liquid-chromatography-organic carbon detection (LC-OCD).

Hence, aside from the compositional heterogeneity of wastewater-derived EPS, they are also heterodispersed in size (Fig. 4 A and B), with MW typically ranging between 1 kDa to as high as 4000 kDa [1,36,37], depending on the sludge origin, which in turn is contingent on several factors that

affect EPS biosynthesis (highlighted in Chapter 1, Section 2.1). Ras *et al*. [37] believed that the different size clusters are related to the different metabolic activities and functions of EPS in microbial aggregates. For instance, the lowest MW EPS (3 - 10 kDa) have been reported to be involved in the initial steps of cell/biofilm adhesion to surfaces [30,37], perhaps due to their higher diffusivities and faster mass transfer to surfaces (Chapter 5). The largest polymeric fraction (≥ 1000 kDa [37]), which are slowly transported but irreversibly adsorb to surfaces, are likely involved in the long-term attachment of biofilms (Chapter 5, [30]). Furthermore, EPS ≥ 180 kDa have been associated with the mechanical stability of biofilms, which is achieved via the formation of a hydrated polymeric network, often in combination with di/multivalent cations [30,37].

Although commercially developed exopolysacharides such as alginate, xanthan gum and gellan gum are in the high MW range, typically between 500 - 2000 kDa [30,38], most studies have however reported lower MWs (<1 - <600 kDa) for EPS-polysaccharides produced from wastewater [36,37,39–41]. There can be several reasons for the lower MW reported, but the most plausible explanations are (i) the high SRT (10 - 60 d) operation of these studies, and (ii) the low COD/N ratio of the (waste)water. At long SRTs, EPS components, particularly polysaccharides, are degraded to low MW products that can be further utilised as carbon and energy sources [30]. But as shown in Chapters 3 – 6, high MW polysaccharide-rich EPS (1000 - 4000 kDa) can be preferentially produced at shorter SRTs irrespective of the consumed carbon source. Chapter 3 further revealed that by employing a nitrogen-limited (waste)water, the produced EPS had a (slightly) higher MW than the corresponding EPS produced under an excess nitrogen condition.

3.3. Charge densities of EPS

Most EPS possess at neutral pH a net negative charge due to the predominant presence of anionic functional groups like carboxyl and phosphoryl groups, outweighing positive charges such as amino groups present in lower numbers. Hence, the charge density (CD) of EPS is pH-dependent: CD increases with pH due to increased deprotonation degree of the functional groups ($–COO^-$ and $–NH_2$), and vice versa at lower pH (having the protonated forms of –COOH and $–NH_3^+$) – Chapter 2.

Although several studies have investigated the electrokinetic potential (zeta potential, mV) of EPS under different conditions [42–45], only a few studies [46–48] have examined the actual charge density (equivalents of charge per weight of EPS). Boyette *et al*. [48] and Morgan *et al*. [47] reported EPS anionic CD values of 0.2 - 0.9 meq/g at neutral pH, while Mikkelsen reported 1 - 3 meq/g (SRT 30 - 35 d). Similarly, the produced EPS in Chapter 2 of this thesis (at an SRT of 15 d) had anionic charge density values between 1.5 - 2.9 meq/g at pH 7. The corresponding EPS in Chapter 3, which were produced at a shorter SRT of 3 days, had a higher charge density (2.7 - 4.7 meq/g at pH 7). This implies that the charge densities of EPS depend on the sludge age. As reported in Chapters 3, 4 and 5, the anionic charge density of EPS increased with a higher polysaccharide (especially uronic acids – Chapter 4) content in EPS, and the other way around. Hence, at a long SRT that leads to reduced polysaccharide content, the produced EPS have been observed to have a low anionic charge density (typically < 3 meq/g). This gives the possibility to control (to some extent) the charge of EPS to be produced.

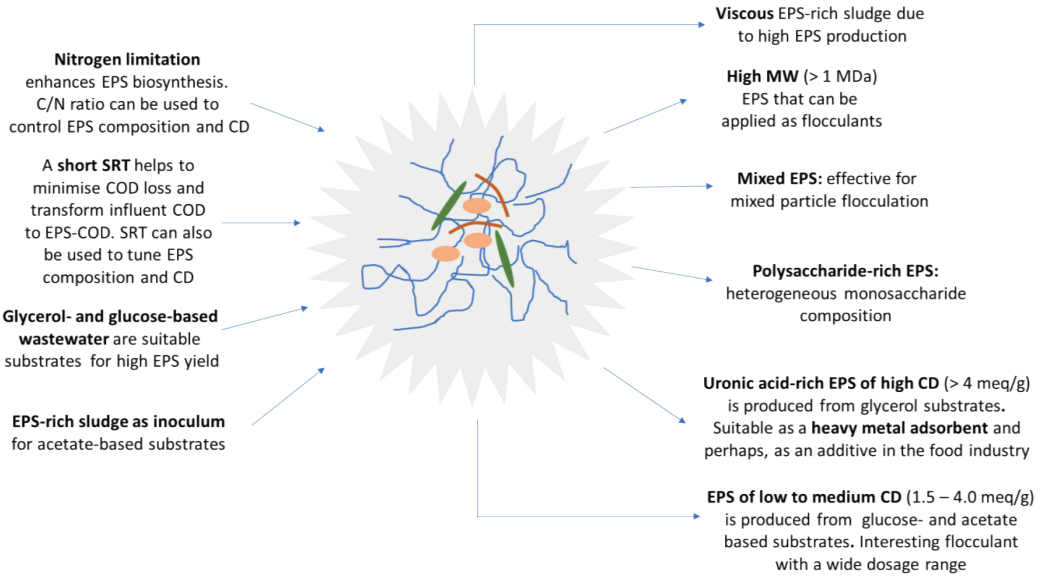

Fig. 5. Summary of the key factors influencing EPS production (left) and the resultant EPS characteristics linked to some applications (right).

4. Application of EPS as flocculants

The relatively high MW of EPS and their solubility in water make them suitable polymers for flocculation. Due to their net negative charge, their application is, however, limited to (some) environments where anionic flocculants can be employed (listed in Table 1). By the way, about 70% of the flocculant market is dominated by anionic flocculants (personal communication with Ronald van Rossum, Kemira, Netherlands); hence, EPS could be an attractive alternative for some environments where synthetic flocculants are used.

Like synthetic anionic flocculants, the flocculation mechanisms of EPS involve divalent cationic bridging and/or hydrogen bonding, depending on the particle type, ionic strength, and the type of cation present in the flocculation environment. In suspensions of high ionic strength (typically ≥ 0.5 M), the electrostatic repulsion between particles are completely suppressed [49,50], leading to hydrogen bond formation between the hydroxy group of EPS-polysaccharide (or the amide group of EPS-protein) and the surface hydroxy groups of particles, namely clay particles such as kaolinite. But at lower ionic strength (<< 0.5 M), hydrogen bonding can barely occur due to the expanded electrostatic repulsion between particles (Chapters 2 and 5). Hence, di/multivalent cationic bridging, rather than hydrogen bonding, governs the flocculation process in such systems. Despite electrostatic repulsion, Ca^{2+}, for instance, can bridge between anionic groups on EPS and the negative sites of the particles [51,52]. This is not to say that both mechanisms (hydrogen bonding and divalent cationic bridging) cannot take place concurrently in some environments, for example, in systems with a moderately high ionic strength (0.3 - 0.5 M) having sufficient di/multivalent cation concentration.

Table 1. Applications of synthetic anionic flocculants.

Industry	Flocculant application
Dredging and land reclamation	To enhance settling of clays, sediments and soil slurry; as a pretreatment to improve the dewatering of soil slurry for land reclamation [53].
Clay mineral processing	To enhance settling and separation of clay particles from suspension [54].
Oil: drilling and fracking	Drilling: to aggregate and separate clay minerals present in waste drilling fluids before disposal of this fluid to the environment [55]. Fracking: Viscous polyelectrolytes are added to fluid to push oil and gas to the well [56,57].
Extrusion and tunnelling	To aggregate and separate clay particles (e.g. bentonite) from their slurry.
Water and wastewater treatment	To remove suspended and colloidal particles, thereby decreasing water turbidity. Wastewaters from different industries such as food, pharmaceuticals, paint, dyes, cement, and paper making, contain (clay) particles that need to be removed before further (biological) treatment [54].
Cosmetics	As thickening agents in cosmetic products; to remove clay minerals from industrial effluents – clays such as kaolinite are used in the cosmetic industry [54].
Mining	To aggregate and separate particles from copper tailings, coal tailings, and the like; to remove particulate phosphates; for brine clarification; barite thickening; to mention a few [58–60].

4.1. Advantages, limitations and potential markets

With a large fraction of synthetic anionic flocculants used in open system applications (such as dredging and land reclamation, oil drilling and fracking, tunnelling and mining – see Table 1), this can hardly be considered a sustainable (waste) water treatment approach due to the poor (bio)degradability of these polymers and their possible toxic effects (discussed in Chapter 1, Section 2.2.1). As also highlighted in Chapter 1 and summarised in Table 2, wastewater-produced EPS can be attractive alternatives in such applications. Particularly interesting are their effectiveness at very low dosages (typically between 0.1 - 0.5 mg/g particles) and their ability to efficiently flocculate mixed particles due to their mixed MW composition (Chapter 5). Furthermore, EPS with a low CD (< 3.5 meq/g) are not prone to colloid restabilisation, unlike most polyacrylamide-based flocculants (Chapters 2 and 3, [51,61]).

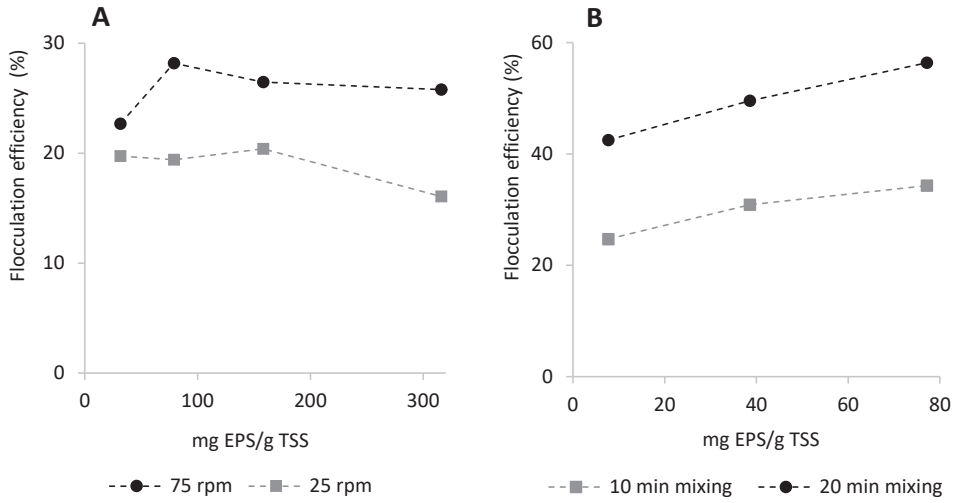

Fig. 6. Effect of mixing speed (**A**) and time (**B**) on the flocculation of Twentekanaal surface water.

However, wastewater-based flocculant is also not without its limitations (listed in Table 2). The main challenge is the polymer property dependence on the utilised substrates and the reactor condition (Chapter 4). In practice, varying substrate composition is likely to affect the main polymer properties, namely MW and CD. Nonetheless, it is expected that under a nitrogen-limited condition and at a relatively short SRT, the produced EPS would have an average MW of at least 1 MDa and a CD of at least 2 meq/g at neutral pH (as the minimum viable product, based on Chapters 3 and 4). Another limitation is their reduced effectiveness in flocculating water particles of low concentration (typically < 100 mg particles/L) in fresh waters having a relatively low ionic strength (< 0.01 M). For instance, flocculation tests on the Twentekanaal (Netherlands) surface water (15 mg/L TSS) resulted in lower flocculation performances (Fig. 6) and required a higher EPS dosage compared to flocculating high particle concentrations (Chapters 2, 3 and 5). In low solids concentrations, the collision rate between particles and EPS is low, subsequently limiting particle destabilisation and flocculation. However, this barrier can be partly overcome by increasing the mixing speed (high enough to induce flocs but not break them) and time, as shown in Fig. 6A and B, respectively.

In this thesis, the application of EPS as flocculants focuses on its ability to agglomerate and separate clay particles from suspension. This is particularly interesting for (open system) applications that involve clay particle removal, such as dredging, extrusion and tunnelling, oil drilling and clay mineral processing. In Chapters 2, 3 and 5, EPS was reported to show high kaolin clay (5 g/L clay) turbidity removal, with efficiencies between 80 - 95 %, under both freshwater and saline flocculation conditions, and in most cases, at an optimum dosage of 0.1 or 0.2 mg EPS/g clay. With montmorillonite clay, the flocculation performances of EPS were even much higher (96 - 98 % turbidity removal).

Table 2. Characteristics, advantages and disadvantages of wastewater-based flocculants compared to common synthetic flocculants (partly adapted from [62]).

Polymer	Studied MW	Studied CD	Advantages	Disadvantages
Wastewater-derived EPS (based on this thesis, unless stated otherwise)	Anionic: 1 – 4 MDa	2.7 – 5.1 meq/g, depends on the substrate and reactor conditions.	- Biodegradable and generally non-toxic [1,63]. - Effective at low dosage (0.1 – 0.5 mg/g particles), lower than some synthetic flocculants. - Easier dosage control (for low CD EPS, <3.5 meq/g) due to wide dosage range without restabilisation. - Effective for mixed particle flocculation. - Its production utilises wastewater as a feedstock, thereby contributing to a circular economy. - Its production contributes to a lower CO_2 footprint. - Likely to have a lower cost than synthetic PAM.	- Polymer properties depend on the utilised substrate and reactor condition. - Social perception bias may undermine its utilisation in drinking water application due to its source (wastewater). - MW not as high as some synthetic polyacrylamide. - May not be suitable for water with low particle concentration (typically < 100 mg/L). - Limited extent of fine-tuning EPS to a specific MW and CD.
Polyacrylamide (PAM) or acrylamide-acrylic acid co-polymers	Anionic: 0.2 – 20 MDa Non-ionic: 5 – 20 MDa Cationic: 1.7 – 7 MDa	- Anionic: 5 – 25 mol% Anionic CD dependent on pH. - Non-ionic: 0	- Commercially available through a broad range of MW and CD. - MW can be as high as 20 MDa. - Least expensive synthetic flocculant (2 - 4 €/kg).	- Polymer/monomer toxicity. - Fossil-based. - Dosage limited to 1 mg/L for drinking water application in North America

Table 2 (*continued*).

Polymer	Studied MW	Studied CD	Advantages	Disadvantages
		- Cationic: 10 – 38 mol%	- Very stable due to its low (bio)degradation. - Long linear structure improves interparticle bridging.	and 0.2 mg/L in European states. - PAMs of very high MW (> 10 MDa) hardly homogenise during solubilisation/implementation. - Sludge containing PAM is not allowed as agricultural fertilizer in some countries.
Polyacrylic acid (PAA)	Anionic: 2 kDa – 4 MDa	Generally highly anionic due to the sole presence of carboxyl groups.	- Anionic PAA is efficient in dual polymer. systems when combined with cationic flocculants - Stable due to its low degradation.	- CD mainly controlled by pH and drops near 0 for pH under 4.5 – 5 (pK_a of carboxyl groups).
	Non-ionic: 5 – 8 MDa	Non-ionic	- Can be co-polymerised with acrylamide to offer a wide range of anionic CD.	- Generally smaller in size than PAM.

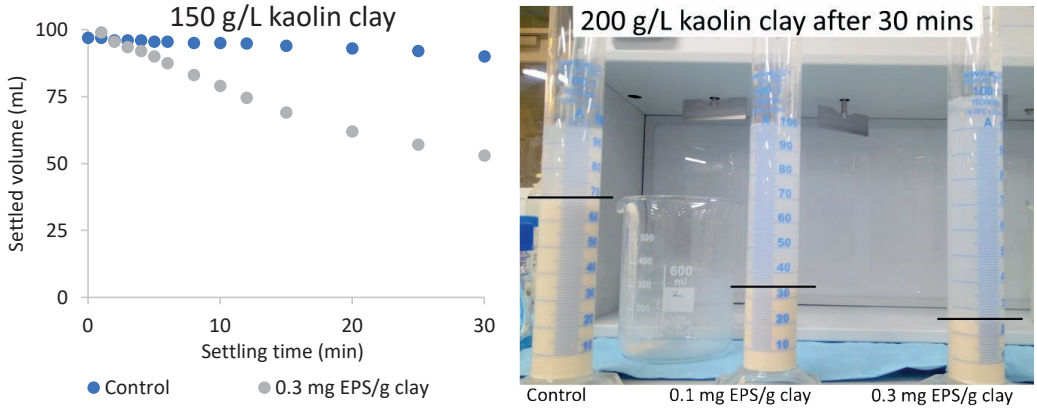

Fig. 7. Enhanced settling of kaolin clay by using EPS as flocculant. *Left*: graph showing the settled clay volume over time. *Right*: image of settled clay 30 mins after flocculation. Control – clay slurry with no addition of EPS. Flocculation with EPS was carried out with no extra addition of Ca^{2+}. Clay was suspended in tap water, which contained 66.6 mg/L Na^{+} and 38.1 mg/L Ca^{2+}. The utilised EPS for both experiments were from Chapter 3 – freshwater synthetic wastewater comprising glycerol/ethanol at a COD/N ratio of 100.

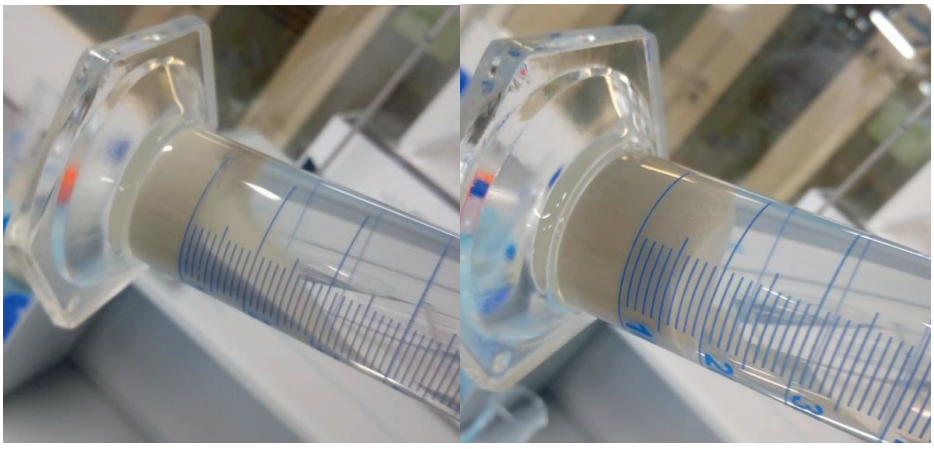

Fig. 8. Tilted kaolin clay flocs after settling. *Left* – unflocculated slurry (control); *right* – flocculated slurry.

To mimic EPS application in industries that flocculate high clay concentrations such as the dredging industry, 150 and 200 g/L of naturally occurring kaolin clay were flocculated with the polysaccharide-rich soluble-EPS produced from the glycerol/ethanol-fed reactor of Chapter 3. As shown in Fig. 7, the addition of EPS to the clay slurry enhanced the settling speed by 43% for the 150 g/L clay concentration (left) and by 61% for the 200 g/L clay concentration (right, 0.3 mg/g clay) after 30 mins of settling. Additionally, the flocculated clay was observed to have a more compact sediment that did not flow after tilting at an approximate angle of 70°, compared to the unflocculated slurry that flowed (Fig. 8).

Based on the above results, environments containing moderate to high clay particles (typically ≥ 2 g/L) that need to be settled or removed would make up potential markets for wastewater-based flocculants. As previously listed, this includes dredging and land reclamation, tunnelling, clay mineral processing, to mention a few industries. These industries do not require very pure polymer product, which is needed in sectors such as drinking water and cosmetics.

4.2. Cationised EPS for a broader application

Although the anionic flocculant market is the major one in the flocculant industry and anionic EPS could be an attractive alternative (discussed above in Section 4), the EPS market can still be broadened by the introduction of cationised EPS. For instance, sludge dewaterability and (micro)algae flocculation can hardly be achieved with anionic flocculants [64,65]. Instead, cationic flocculants work effectively and are employed for such applications [64,66]. These applications rely on an effective flocculation process to lower the cost of downstream processing such as sludge disposal or biomass valorisation to other products, e.g., microalgae for biofuel production [67] and hydrogen-oxidising bacteria as a protein source [68].

The utilisation of anionic EPS to flocculate *Synechocystis* sp. PCC6803 (a freshwater cyanobacterium), *Chlorella sorokiniana* (a freshwater green microalga) and a mixed community of hydrogen-oxidising bacteria proved abortive. Despite the addition of Ca^{2+} (incrementally from 50 - 250 mg/L) prior to EPS addition (EPS concentrations between 1 - 80 mg/L), no visible floc was formed, hence no phase separation and no change in the turbidity values of both the test and control experiments. Granados *et al* [69] and 't Lam *et al*. [66] also reported the unsuitability of anionic and non-ionic flocculants to aggregate freshwater (*Chlorella vulgaris*, *Chlorella fusca*, *Scenedesmus subspicatus* and *Scenedesmus* sp.) and marine algae (*Phaeodactylum tricornutum* and *Neochloris oleoabundans*), respectively. In both instances, cationic polyelectrolytes showed excellent flocculation and recovery of algae, which is explained by charge neutralization between the negatively charged algal cell wall and the positive active sites of the polymer. The outcome of our study and that of others suggest that the presence or addition of di/multivalent cations to algal cultures does not reduce the electrostatic repulsion between cells for subsequent bridging by anionic flocculants.

Due to the above reason, the functionalisation of EPS from a net anionic state to a net cationic state became interesting to investigate. EPS cationisation was carried out via the reaction of EPS with glycidyltrimethylammonium chloride (GTMAC, purchased from Sigma Aldrich) in the presence of NaOH (see appendix for the synthesis description).

A quick flocculation test revealed that one of the produced cationised EPS (9h reaction time) showed good flocculation of *Synechocystis* sp. PCC6803 (81% turbidity removal) at a dosage of 5 mg/L (Fig. 9). A similar test was carried out on a saline (0.5 M Na^{+}) mixed culture comprising hydrogen-oxidizing bacteria. The results, shown in Fig. 10, demonstrate the possibility to employ cationic EPS for the flocculation and concentration of such biomass, albeit at a higher dosage (≥ 75 mg/L to obtain at least a 90% concentration) than what was required for the cyanobacterial flocculation. The higher

dosage requirement may be as a result of the low cationic charge density (0.4 meq/g) of the cationised EPS.

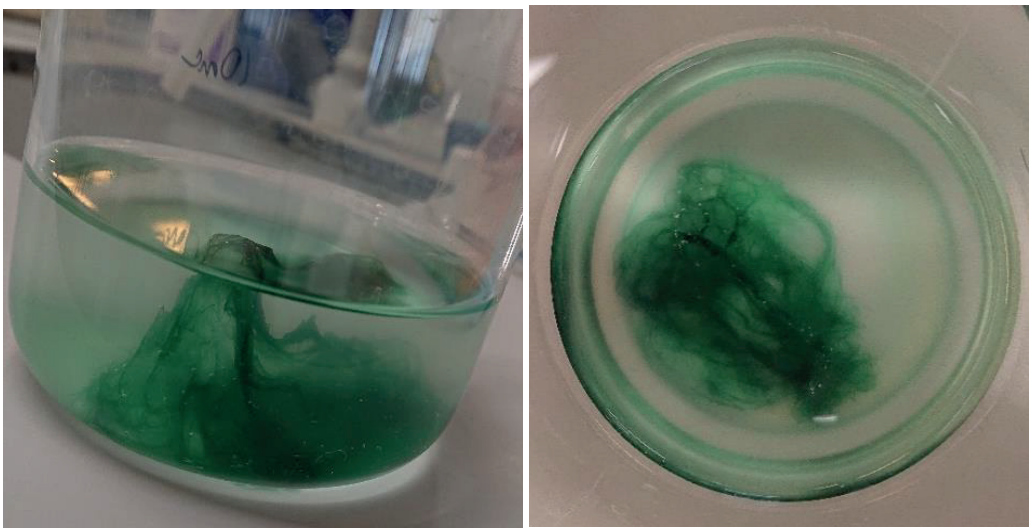

Fig. 9. Flocculation of freshwater *Synechocystis* sp. PCC6803 cyanobacterial culture with cationised EPS.

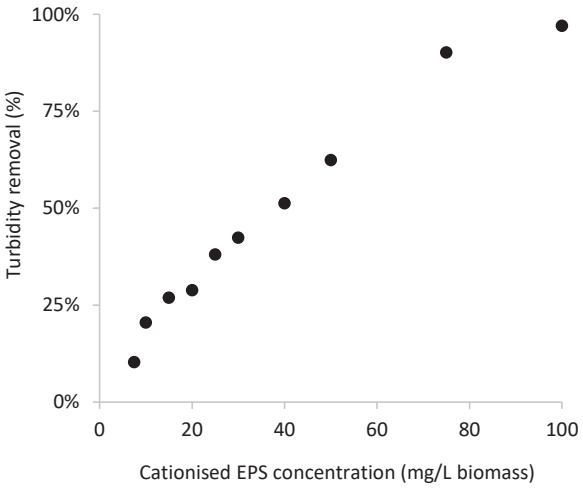

Fig. 10. Flocculation of a mixed culture comprising hydrogen-oxidizing bacteria with the use of cationised EPS.

5. Concluding remarks and outlook

This thesis was primarily aimed at combining biological wastewater treatment with the recovery of extracellular polymers as effective flocculants. The positive results in Chapters 2 and 3 (high flocculation performance and high EPS recovery under nitrogen-limited condition) allowed us to further investigate: other suitable substrates to produce these valuable biopolymers, the fundamental flocculation mechanisms of these complex biomacromolecules, their application as highly effective heavy metal adsorbents, and the use of techniques such as optical reflectometry and gas/liquid chromatography to study their properties. The findings of this thesis can help WWTPs valorise the organics in wastewater to useful extracellular polymers while reducing the volume of sludge to be disposed of and the CO_2 footprint of the plant. This will have a significant impact on our quest for a circular economy and in turning WWTPs to resource recovery facilities. However, a few research and practical questions still need to be answered to better understand EPS biosynthesis and see the commercial fruition of this research. These are highlighted below, together with other research directions that can further broaden the application of microbial EPS in other fields.

i. Further insights on EPS biosynthesis and its competition with PHA production

As described in Chapter 4, microorganisms may store excess carbon as EPS and/or PHA, since some of the conditions for EPS production also apply to PHA synthesis (for instance, nitrogen limitation with excess carbon) [70]. However, it is still not entirely clear when (under what conditions) and why (the overflow metabolism [4] and preferred metabolic route) bacteria decide to store PHA or secrete EPS. As reported in Chapter 4 and by Pal *et al*. [71], high PHA or EPS yield is carbon source-specific, hence further experimental evidence, such as isotope labelling and tracing, will be vital to substantiate the roles of carbon source for either EPS or PHA biosynthesis, particularly under nutrient-limiting conditions. This should be coupled with RNA-based techniques, which could unravel the real utilisation path of carbon sources and the range of enzymatic functions present per substrate.

ii. Pilot studies using real wastewater

For research purposes and to better understand the different parameters that may affect EPS productivity, synthetic wastewater was used in this thesis. However, it will be important to use the knowledge gained from this project to scale-up the EPS production from different real wastewaters and study the properties of the produced EPS and their flocculation performances. The following bottlenecks noticed on lab-scale tests can be better solved by a pilot study:

- Low daily production in a lab-scale experiment which prevents large scale testing on real (waste)water streams.
- Uncertainty about a consistent flocculant quality and quantity if produced under real-life, fluctuating wastewater concentrations and varying temperatures.
- Unknown productivities from wastewaters other than glycerol/ethanol, acetate or glucose-containing wastewater, which if possible, may increase the production volume.

- Establishing on the pilot scale the ability to use EPS produced from real saline wastewater (e.g., wastewater from the cheese industry) to flocculate real saline (waste)water streams.
- Insufficient data to be able to set-up a detailed business case, even though preliminary data show a positive outcome.

iii. EPS produced from saline wastewater to flocculate particles under saline environment

One of the observations in Chapters 2 and 3 was that in flocculating particles in saline environments, EPS produced from saline wastewater (referred to as 'saline EPS') consistently showed higher flocculation performance (4 - 13 % turbidity removal) than the corresponding EPS produced under freshwater condition (referred to as 'freshwater EPS'). Although the reason for this could not be further investigated during the period of this project (and could not be explained based on their MW and CD values), a further structural elucidation of the saline and freshwater EPS may give valuable insights on the flocculation mechanism under saline or high ionic strength conditions. One possibility is that the structure of the saline EPS has a lower branching degree than the freshwater EPS. Under saline or high ionic strength flocculation condition, the repulsion between the charged segments of anionic polyelectrolytes is 'screened' by the cations in suspension, leading to a shrinking of the polymeric chain [51]. Although this affects both linear and branched polymers, the shrinking effect increases with the branching degree of the polymer.

Therefore, to fully substantiate the observed phenomenon of saline EPS to flocculate particles in saline environments, further research is needed, perhaps on the structural level, to further understand the difference between saline and freshwater EPS, and its effect on particle flocculation at different salinities/ionic strengths. We hypothesize that saline microorganisms produce EPS suitable for saline (waste)water flocculation.

iv. EPS extraction and harvesting

Another critical issue in the EPS technological process, which was not within the scope of the thesis but important to consider when upscaling, is the EPS harvesting and extraction process. For research purpose, centrifugation coupled with the use of a cation exchange resin were employed to obtain the soluble and bound EPS fractions, respectively. Since both fractions have been shown to have similar chemical characteristics (namely molecular weight, charge density and monosaccharide composition), harvesting the soluble EPS will be the preferred option if a choice is to be made (Chapter 3 and 4). The soluble EPS is the major fraction (typically 60 - 95 wt%) when EPS is produced under a nitrogen-limited condition (Chapter 3 and 4). However, the use of a centrifuge to harvest EPS on an industrial scale is energy-intensive. Hence, there is a need for a cost-effective technological process. Furthermore, it may be interesting to selectively extract an EPS component for a specific application. For instance, (acidic) polysaccharides can be extracted as heavy metal adsorbents, or EPS-proteins for food/feed application. A promising class of extractants for such a purpose are ionic liquids [72]. Ionic liquids are regarded as 'green' alternatives to organic solvents due to their low volatility and non-flammability [73]. More importantly, they have inherent diversities that allow them to be tailored towards optimising EPS extraction, selectivity and subsequent EPS desorption [74]. Although ionic liquids in themselves are not cheap, the ability to

regenerate and reuse them for several extraction cycles may make them cost-effective in the long run.

Aside from the use of ionic liquids to selectively recover specific EPS components, it will be worthwhile to further investigate how the different EPS-MW fractions can be recovered for various applications. For instance, anionic polyelectrolytes in the $10^3 – 10^4$ Da range are used as antiscalants and dispersants [75,76], those in the $10^4 – 10^5$ Da range are employed as coagulant aid for cationic polymers in dual polymer systems [77,78], those between $10^5 – 10^6$ Da are used as paper strength and drilling mud additives [79], and the highest MW (> 10^6 Da) polyelectrolytes are used as flocculants and viscosifiers [51,56]. Hence, the different EPS fractions could be recovered and explored for some of these interesting applications.

v. Cationised EPS for a wider application

Although this thesis demonstrates, for the first time, the possibility to cationise microbial EPS and employ for biomass flocculation, it will be worthwhile to follow-up on this approach to further investigate:

- the use of cheaper cationising agents, such as the deep eutectic solvent formed when choline chloride reacts with urea [80,81].
- how anionic EPS can be functionalised to give a desired cationic charge density for a specific application.
- the biodegradability and toxicity of cationised EPS in comparison to the corresponding anionic EPS and other synthetic cationic polymers.
- other applications where cationic flocculants give improved performance than anionic flocculants, such as sludge dewatering and flocculation of particles in low concentrations. The biggest market for cationic EPS could be in the dewatering of municipal waste sludge, where about 3700 ton (≈ € 11 million) of synthetic cationic flocculants are used annually to dewater waste sludge in the Netherlands [82].

vi. EPS application as heavy metal adsorbents

Chapter 6 showed the possibility to regenerate and reuse EPS immobilised on a column for repetitive adsorption-desorption cycles. Compared to commercial ion-exchange resins [83–85], EPS showed much higher adsorption capacities for heavy metals such as Cu (~ 780 mg/g EPS), Pb (~ 1200 mg/g EPS) and Zn (520 mg/g EPS), and even for NH_4^+ (~ 200 mg/g EPS), which is interesting for ammonium removal in WWTPs. Being only a proof-of-principle in Chapter 6, further research is needed to fully test its durability as a low-cost adsorption technology, with respect to:

- the number of adsorption-desorption cycles of EPS before it is rendered unusable.
- selectivity for specific metals: selective separation of metals is an important factor that still needs further study. It may be necessary to study how different EPS fractions (soluble and bound EPS) or EPS produced under different conditions (fresh *versus* saline wastewater grown on different substrates, with and without nitrogen limitation) may have different selectivity for specific metals.

- ammonium ion adsorption and recovery: this is particularly important in WWTPs where NH_4^+ recovery is attractive both for environmental and economic reasons.
- optimising the desorption process to obtain highly concentrated metal effluent that can be further valorised via processes such as electrowinning to obtain the recovered metal.

In conclusion, EPS are ubiquitous compounds relevant in other applications such as the food industry, biomedical field, and soil science. Therefore, a better understanding of EPS will increase the breadth and depth of strategies available to intensify their production and control their characteristics for various applications.

Appendix

Table A1. Chemical and physical methods for EPS and biofilm characterisation (partly adapted from [86]). The underlined methods were applied for this thesis.

Characterisation technique	Type of information
Spectrometric methods	
Fluorescence microscopy	Biomass quantification; microbial activity.
Photospectrometric/colorimetric	Total polysaccharide and protein content quantification; method determination of enzyme activities.
UV-Visible spectrometry	Determination of conjugated compounds in EPS such as aromatic humic acids and proteins.
Fluorescence excitation-emission matrix spectroscopy	Chemical composition of EPS.
Chromatographic and electrophoretic methods	
HPLC techniques. E.g. HPLC-MS,	Monomer composition of EPS polysaccharides (neutral and HPAEC acidic sugars) and proteins.
LC-OCD-OND	Qualitative and quantitative fractionation of EPS into biopolymers, humic acids, building blocks and low molecular weight substances; determination of dissolved organic carbon and organic nitrogen in each EPS fraction.
LC-OCD; SEC; GPC	Molecular weight (distribution) of EPS.
GC; GC-MS; GC-MS-MS	Monomer composition of EPS polysaccharides and fatty acids.
Capillary electrophoresis (CE); CE-MS	Qualitative and quantitative characterisation of carbohydrates and glycolipids.
2D gel electrophoresis	Protein separation.
Electrophoretic light scattering	Electrophoretic mobility and zeta potential measurements.
Other separation techniques	
Field-flow fractionation	Determination of particle size distribution; characterisation of (natural) colloids and particles.
Surface and interface characterisation techniques	
Scanning electron microscopy	Biofilm structure, morphology and thickness.
Confocal laser scanning microscopy	*In situ* monitoring of biofilm structure; mapping of the distribution of macromolecules in biofilms; EPS quantification by measuring the total cell volume.
Atomic force microscopy	Topographical information of biofilms.

Table A1 (*continued*).

Characterisation technique	Type of information
Optical Coherence Tomography	Biofilm quantification, morphology and thickness.
Fourier transform infrared spectroscopy	Functional groups of EPS.
Nuclear magnetic resonance	Chemical structure determination; metabolic pathways.
Optical reflectometry	*In situ* monitoring of EPS adsorption on surfaces; determination of an adsorbed amount of EPS on a layer.
Quartz crystal microbalance dissipation	Determination of EPS adsorption on surfaces and thickness with of an adsorbed EPS layer.
Ellipsometry	Determination of thickness and refractive index of an adsorbed EPS layer.
Other techniques	
Particle charge detection	Determination of EPS charge density.
Dynamic light scattering	Determination of size distribution profile of EPS in solution.

A2. EPS cationisation protocol

30 mg of harvested and dried soluble EPS (produced from the experiment in Chapter 5) was dissolved in 7.5 mL of Milli-Q water, after which 60 mg of NaOH was added in the form of pellets. The mixture was vortexed for 15 min on a vortex shaker. 6 mL glycidyltrimethylammonium chloride (GTMAC) was added to the mixture while stirring and the reaction was performed at a temperature of 50 ^{o}C. Experiments were carried out for 9, 18 and 24 h. After each experiment, the products were precipitated in 400 mL cold absolute ethanol and centrifuged at 3750 rpm for 15 min. The supernatant after centrifugation was removed and the pellet was air-dried at room temperature (21 ± 1 ^{o}C).

Charge density determination

The charge density values of the anionic and cationised EPS (solution pH 7) were determined as described in Chapter 2 of this thesis. While pDADMAC was used as the titrant against the anionic EPS solution, polyethylenesulfonate (PES) was used as the titrant against the cationised EPS solution. Each charge density analysis was carried out in duplicates.

Table A2. Charge density values of anionic and cationised EPS.

EPS	Reaction time for cationised EPS (h)	Charge density (meg/g)
Anionic EPS	Not applicable	- 5.1
Cationised EPS	9	+ 0.4
	18	+ 0.5
	24	+ 0.5

References

[1] T.T. More, J.S.S. Yadav, S. Yan, R.D. Tyagi, R.Y. Surampalli, Extracellular polymeric substances of bacteria and their potential environmental applications, J. Environ. Manage. 144 (2014) 1–25. doi:10.1016/j.jenvman.2014.05.010.

[2] F. Freitas, V.D. Alves, M.A.M. Reis, Advances in bacterial exopolysaccharides: From production to biotechnological applications, Trends Biotechnol. 29 (2011) 388–398. doi:10.1016/j.tibtech.2011.03.008.

[3] G.P. da Silva, M. Mack, J. Contiero, Glycerol: A promising and abundant carbon source for industrial microbiology, Biotechnol. Adv. 27 (2009) 30–39. doi:10.1016/j.biotechadv.2008.07.006.

[4] J.B. Russell, The energy spilling reactions of bacteria and other organisms, J. Mol. Microbiol. Biotechnol. 13 (2007) 1–11. doi:10.1159/000103591.

[5] T.R. Jarman, G.W. Pace, Energy requirements for microbial exopolysaccharide synthesis, Arch. Microbiol. 137 (1984) 231–235. doi:10.1007/BF00414549.

[6] T.P. Pirog, M.A. Kovalenko, Y. V. Kuz'minskaya, Intensification of exopolysaccharide synthesis by *Acinetobacter* sp. on an ethanol-glucose mixture: Aspects related to biochemistry and bioenergetics, Microbiology. 72 (2003) 305–312. doi:10.1023/A:1024247915758.

[7] W. Babel, R.H. Muller, Mixed Substrate Utilization in Micro-organisms: Biochemical Aspects and Energetics, Microbiology. 131 (1985) 39–45. doi:10.1099/00221287-131-1-39.

[8] L. De Temmerman, T. Maere, H. Temmink, A. Zwijnenburg, I. Nopens, Salt stress in a membrane bioreactor: Dynamics of sludge properties, membrane fouling and remediation through powdered activated carbon dosing, Water Res. 63 (2014) 112–124. doi:10.1016/j.watres.2014.06.017.

[9] D.W. Tempest, O.M. Neijssel, Eco-Physiological Aspects of Microbial Growth in Aerobic Nutrient-Limited Environments, (1978) 105–153. doi:10.1007/978-1-4615-8222-9_3.

[10] R. Bura, M. Cheung, B. Liao, J. Finlayson, B.C. Lee, I.G. Droppo, G.G. Leppard, S.N. Liss,

Composition of extracellular polymeric substances in the activated sludge floc matrix, Water Sci. Technol. 37 (1998) 325–333.

[11] S.P. Buthelezi, A.O. Olaniran, B. Eillay, Production and characterization of bioflocculants from bacteria isolated from wastewater treatment plant in South Africa, Biotechnol. Bioprocess Eng. 15 (2010) 874–881. doi:10.1007/s12257-009-3002-7.

[12] I. Akanyeti, H. Temmink, M. Remy, A. Zwijnenburg, Feasibility of bioflocculation in a high-loaded membrane bioreactor for improved energy recovery from sewage, Water Sci. Technol. 61 (2010) 1433–1439. doi:10.2166/wst.2010.032.

[13] K. van 't Riet, J. Tramper, Basic bioreactor design., CRC Press, 99, Sectie Proceskunde, , 1991. https://edepot.wur.nl/478053.

[14] J. Tamis, Resource recovery from organic waste streams by microbial enrichment cultures, 2015. doi:10.1016/j.trsl.2015.06.006.

[15] O. Lefebvre, R. Moletta, Treatment of organic pollution in industrial saline wastewater: A literature review, Water Res. 40 (2006) 3671–3682. doi:10.1016/j.watres.2006.08.027.

[16] S. Pallipad, S. Velmurugan, Pneumatically Agitated High-Density Polyethylene Mesh-Based Bioreactor Developed for Wastewater Treatment, J. Environ. Eng. (United States). 144 (2018) 1–9. doi:10.1061/(ASCE)EE.1943-7870.0001348.

[17] M.E. Ersahin, H. Ozgun, Y. Tao, J.B. van Lier, Applicability of dynamic membrane technology in anaerobic membrane bioreactors, Water Res. 48 (2014) 420–429. doi:10.1016/j.watres.2013.09.054.

[18] G. Kooijman, W. Lopes, Z. Zhou, H. Guo, M. de Kreuk, H. Spanjers, J. van Lier, Impact of coagulant and flocculant addition to an anaerobic dynamic membrane bioreactor (AnDMBR) treating waste-activated sludge, Membranes (Basel). 7 (2017). doi:10.3390/membranes7020018.

[19] H. Chu, Y. Zhang, X. Zhou, Y. Zhao, B. Dong, H. Zhang, Dynamic membrane bioreactor for wastewater treatment: Operation, critical flux, and dynamic membrane structure, J. Memb. Sci. 450 (2014) 265–271. doi:10.1016/j.memsci.2013.08.045.

[20] F. Meng, S.R. Chae, A. Drews, M. Kraume, H.S. Shin, F. Yang, Recent advances in membrane bioreactors (MBRs): Membrane fouling and membrane material, Water Res. 43 (2009) 1489–1512. doi:10.1016/j.watres.2008.12.044.

[21] L. Faust, H. Temmink, A. Zwijnenburg, A.J.B. Kemperman, H.H.M. Rijnaarts, High loaded MBRs for organic matter recovery from sewage: effect of solids retention time on bioflocculation and on the role of extracellular polymers., Water Res. 56 (2014) 258–66. doi:10.1016/j.watres.2014.03.006.

[22] L. Faust, M. Szendy, C.M. Plugge, P.F.H. van den Brink, H. Temmink, H.H.M. Rijnaarts,

Characterization of the bacterial community involved in the bioflocculation process of wastewater organic matter in high-loaded MBRs, Appl. Microbiol. Biotechnol. 99 (2015) 5327–5337. doi:10.1007/s00253-015-6402-y.

[23] T. Seviour, N. Derlon, M.S. Dueholm, H.C. Flemming, E. Girbal-Neuhauser, H. Horn, S. Kjelleberg, M.C.M. van Loosdrecht, T. Lotti, M.F. Malpei, R. Nerenberg, T.R. Neu, E. Paul, H. Yu, Y. Lin, Extracellular polymeric substances of biofilms: Suffering from an identity crisis, Water Res. 151 (2019) 1–7. doi:10.1016/j.watres.2018.11.020.

[24] B. Frølund, R. Palmgren, K. Keiding, P.H. Nielsen, Extraction of extracellular polymers from activated sludge using a cation exchange resin, Water Res. 30 (1996) 1749–1758. doi:10.1016/0043-1354(95)00323-1.

[25] H. Liu, H.H.P. Fang, Extraction of extracellular polymeric substances (EPS) of sludges, J. Biotechnol. 95 (2002) 249–256. doi:10.1016/S0168-1656(02)00025-1.

[26] T. Rudd, R.M. Sterritt, J.N. Lester, Complexation of Heavy Metals by Extracellular Polymers in the Activated Sludge Process, Water Pollut. Control Fed. 56 (1984) 1260–1268.

[27] B. Durmaz, F.D. Sanin, Effect of carbon to nitrogen ratio on the physical and chemical properties of activated sludge, Environ. Technol. 24 (2003) 1331–1340. doi:10.1080/09593330309385677.

[28] L. Hao, S.N. Liss, B.Q. Liao, Influence of COD:N ratio on sludge properties and their role in membrane fouling of a submerged membrane bioreactor, Water Res. 89 (2015) 132–141. doi:10.1016/j.watres.2015.11.052.

[29] F. Ye, Y. Ye, Y. Li, Effect of C/N ratio on extracellular polymeric substances (EPS) and physicochemical properties of activated sludge flocs, J. Hazard. Mater. 188 (2011) 37–43. doi:10.1016/j.jhazmat.2011.01.043.

[30] H.-C. Flemming, J. Wingender, The biofilm matrix, Nat. Publ. Gr. 8 (2010) 623–633. doi:10.1038/nrmicro2415.

[31] M.A. Redmile-Gordon, R.P. Evershed, P.R. Hirsch, R.P. White, K.W.T. Goulding, Soil organic matter and the extracellular microbial matrix show contrasting responses to C and N availability, Soil Biol. Biochem. 88 (2015) 257–267. doi:10.1016/j.soilbio.2015.05.025.

[32] J. Wang, H.Q. Yu, Biosynthesis of polyhydroxybutyrate (PHB) and extracellular polymeric substances (EPS) by *Ralstonia eutropha* ATCC 17699 in batch cultures, Appl. Microbiol. Biotechnol. 75 (2007) 871–878. doi:10.1007/s00253-007-0870-7.

[33] D.R. Smith, M.R. Chapman, Economical evolution: Microbes reduce the synthetic cost of extracellular proteins, MBio. 1 (2010) 28–32. doi:10.1128/mBio.00131-10.

[34] U. Remminghorst, B.H.A. Rehm, Bacterial alginates: From biosynthesis to applications, Biotechnol. Lett. 28 (2006) 1701–1712. doi:10.1007/s10529-006-9156-x.

[35] S.N. Pawar, K.J. Edgar, Alginate derivatization: A review of chemistry, properties and applications, Biomaterials. 33 (2012) 3279–3305. doi:10.1016/j.biomaterials.2012.01.007.

[36] B. Bin Wang, X.T. Liu, J.M. Chen, D.C. Peng, F. He, Composition and functional group characterization of extracellular polymeric substances (EPS) in activated sludge: the impacts of polymerization degree of proteinaceous substrates, Water Res. 129 (2018) 133–142. doi:10.1016/j.watres.2017.11.008.

[37] M. Ras, D. Lefebvre, N. Derlon, E. Paul, E. Girbal-Neuhauser, Extracellular polymeric substances diversity of biofilms grown under contrasted environmental conditions, Water Res. 45 (2011) 1529–1538. doi:10.1016/j.watres.2010.11.021.

[38] P. Lembre, C. Lorentz, P. Di, Exopolysaccharides of the Biofilm Matrix: A Complex Biophysical World, in: The Complex World of Polysaccharides, 2012. doi:10.5772/51213.

[39] T.J. Stewart, J. Traber, A. Kroll, R. Behra, L. Sigg, Characterization of extracellular polymeric substances (EPS) from periphyton using liquid chromatography-organic carbon detection-organic nitrogen detection (LC-OCD-OND), Environ. Sci. Pollut. Res. 20 (2013) 3214–3223. doi:10.1007/s11356-012-1228-y.

[40] I. Bourven, S. Simon, D. Bhatia, E.D. van Hullebusch, G. Guibaud, Effect of various size exclusion chromatography (SEC) columns on the fingerprints of extracellular polymeric substances (EPS) extracted from biological sludge, J. Taiwan Inst. Chem. Eng. 49 (2015) 148–155. doi:10.1016/j.jtice.2014.11.025.

[41] C. Garnier, T. Görner, B.S. Lartiges, S. Abdelouhab, P. De Donato, Characterization of activated sludge exopolymers from various origins: A combined size-exclusion chromatography and infrared microscopy study, Water Res. 39 (2005) 3044–3054. doi:10.1016/j.watres.2005.05.007.

[42] L. Wei, Y. Li, D.R. Noguera, N. Zhao, Y. Song, J. Ding, Q. Zhao, F. Cui, Adsorption of Cu^{2+} and Zn^{2+} by extracellular polymeric substances (EPS) in different sludges: Effect of EPS fractional polarity on binding mechanism, J. Hazard. Mater. 321 (2017) 473–483. doi:10.1016/j.jhazmat.2016.05.016.

[43] Z. Hong, W. Chen, X. Rong, P. Cai, K. Dai, Q. Huang, The effect of extracellular polymeric substances on the adhesion of bacteria to clay minerals and goethite, Chem. Geol. 360–361 (2013) 118–125. doi:10.1016/j.chemgeo.2013.10.014.

[44] H. Lin, M. Zhang, F. Wang, F. Meng, B.Q. Liao, H. Hong, J. Chen, W. Gao, A critical review of extracellular polymeric substances (EPSs) in membrane bioreactors: Characteristics, roles in membrane fouling and control strategies, J. Memb. Sci. 460 (2014) 110–125. doi:10.1016/j.memsci.2014.02.034.

[45] L. Fang, Y. Cao, Q. Huang, S.L. Walker, P. Cai, Reactions between bacterial exopolymers and goethite: A combined macroscopic and spectroscopic investigation, Water Res. 46 (2012)

5613–5620. doi:10.1016/j.watres.2012.07.046.

[46] L.H. Mikkelsen, Applications and limitations of the colloid titration method for measuring activated sludge surface charges, Water Res. 37 (2003) 2458–2466. doi:10.1016/S0043-1354(03)00021-6.

[47] J.W. Morgan, C.F. Forster, L. Evison, A comparative study of the nature of biopolymers extracted from anaerobic and activated sludges, Water Res. 24 (1990) 743–750.

[48] S.M. Boyette, J.M. Lovett, W.G. Gaboda, J.A. Soares, Cell surface and exopolymer characterization of laboratory stabilized activated sludge from a beverage bottling plant, Water Sci. Technol. 43 (2001) 175–184. doi:10.2166/wst.2001.0369.

[49] H.H.M. Rijnaarts, W. Norde, J. Lyklema, A.J.B. Zehnder, DLVO and steric contributions to bacterial deposition in media of different ionic strengths, Colloids Surfaces B Biointerfaces. 14 (1999) 179–195. doi:10.1016/S0927-7765(99)00035-1.

[50] M.R. Bohmer, O.A. Evers, J.M.H.M. Scheutjens, Weak Polyelectrolytes between Two Surfaces: Adsorption and Stabilization, Macromolecules. 23 (1990) 2288–2301.

[51] B. Bolto, J. Gregory, Organic polyelectrolytes in water treatment, Water Res. 41 (2007) 2301–2324. doi:10.1016/j.watres.2007.03.012.

[52] D.C. Sobeck, M.J. Higgins, Examination of three theories for mechanisms of cation-induced bioflocculation, Water Res. 36 (2002) 527–538. doi:10.1016/S0043-1354(01)00254-8.

[53] J. He, J. Chu, S.K. Tan, T.T. Vu, K.P. Lam, Sedimentation behavior of flocculant-treated soil slurry, Mar. Georesources Geotechnol. 35 (2017) 593–602. doi:10.1080/1064119X.2016.1177625.

[54] S.M.R. Shaikh, M.S. Nasser, I. Hussein, A. Benamor, S.A. Onaizi, H. Qiblawey, Influence of polyelectrolytes and other polymer complexes on the flocculation and rheological behaviors of clay minerals: A comprehensive review, Sep. Purif. Technol. 187 (2017) 137–161. doi:10.1016/j.seppur.2017.06.050.

[55] J. Zou, H. Zhu, F. Wang, H. Sui, J. Fan, Preparation of a new inorganic-organic composite flocculant used in solid-liquid separation for waste drilling fluid, Chem. Eng. J. 171 (2011) 350–356. doi:10.1016/j.cej.2011.03.100.

[56] A. Borthakur, S.R. Dutta Choudhury, P. Sengupta, K. V. Rao, M.C. Nihalani, Synthesis and evaluation of partially hydrolysed polyacrylamide (PHPA) as viscosifier in water based drilling fluids, Indian J. Chem. Technol. 4 (1997) 83–88.

[57] E. Pensini, B.M. Rodriguez, A.G. Marangoni, C.M. Collier, A. Elsayed, A. Siwik, Shear rheological properties of composite fluids and stability of particle suspensions: Potential implications for fracturing and environmental fluids, Can. J. Chem. Eng. 97 (2019) 2395–2407. doi:10.1002/cjce.23486.

[58] S. Emeish, M.K. Abu-Arabi, B.I. Hudaib, Removal of phosphate from Eshidiya industrial wastewater by sedimentation and enhanced sedimentation, Desalin. Water Treat. 51 (2013) 1629–1633. doi:10.1080/19443994.2012.704698.

[59] E. Sabah, Z.E. Erkan, Interaction mechanism of flocculants with coal waste slurry, Fuel. 85 (2006) 350–359. doi:10.1016/j.fuel.2005.06.005.

[60] A. Rabiee, Acrylamide-Based Anionic Polyelectrolytes and Their Applications: A Survey, J Vinyl Addit. Technol. 21 (2010) 111–119. doi:10.1002/vnl.

[61] B.J. Lee, M.A. Schlautman, E. Toorman, M. Fettweis, Competition between kaolinite flocculation and stabilization in divalent cation solutions dosed with anionic polyacrylamides, Water Res. 46 (2012) 5696–5706. doi:10.1016/j.watres.2012.07.056.

[62] M. Lapointe, B. Barbeau, Understanding the roles and characterizing the intrinsic properties of synthetic vs. natural polymers to improve clarification through interparticle Bridging: A review, Sep. Purif. Technol. 231 (2020). doi:10.1016/j.seppur.2019.115893.

[63] O. Ates, Systems Biology of Microbial Exopolysaccharides Production, Front. Bioeng. Biotechnol. 3 (2015) 1–16. doi:10.3389/fbioe.2015.00200.

[64] L. Van Haver, S. Nayar, Polyelectrolyte flocculants in harvesting microalgal biomass for food and feed applications, Algal Res. 24 (2017) 167–180. doi:10.1016/j.algal.2017.03.022.

[65] H. Wei, B. Gao, J. Ren, A. Li, H. Yang, Coagulation/flocculation in dewatering of sludge: A review, Water Res. 143 (2018) 608–631. doi:10.1016/j.watres.2018.07.029.

[66] G.P. ’t Lam, M.H. Vermuë, G. Olivieri, L.A.M. van den Broek, M.J. Barbosa, M.H.M. Eppink, R.H. Wijffels, D.M.M. Kleinegris, Cationic polymers for successful flocculation of marine microalgae, Bioresour. Technol. 169 (2014) 804–807. doi:10.1016/j.biortech.2014.07.070.

[67] U. Rajak, P. Nashine, T.N. Verma, A. Pugazhendhi, Performance and emission analysis of a diesel engine using hydrogen enriched n-butanol, diethyl ester and Spirulina microalgae biodiesel, Fuel. 271 (2020) 117645. doi:10.1016/j.fuel.2020.117645.

[68] S. Matassa, W. Verstraete, I. Pikaar, N. Boon, Autotrophic nitrogen assimilation and carbon capture for microbial protein production by a novel enrichment of hydrogen-oxidizing bacteria, Water Res. 101 (2016) 137–146. doi:10.1016/j.watres.2016.05.077.

[69] M.R. Granados, F.G. Acién, C. Gómez, J.M. Fernández-Sevilla, E. Molina Grima, Evaluation of flocculants for the recovery of freshwater microalgae, Bioresour. Technol. 118 (2012) 102–110. doi:10.1016/j.biortech.2012.05.018.

[70] Y. González-García, A. Heredia, J.C. Meza-Contreras, F.M.E. Escalante, R.M. Camacho-Ruiz, J. Córdova, Biosynthesis of Extracellular Polymeric Substances by the Marine Bacterium *Saccharophagus degradans* under Different Nutritional Conditions, Int. J. Polym. Sci. 2015 (2015) 1–7. doi:10.1155/2015/526819.

[71] S. Pal, A. Manna, A.K. Paul, Production of poly(β-hydroxybutyric acid) and exopolysaccharide by Azotobacter beijerinckii WDN-01, World J. Microbiol. Biotechnol. 15 (1999) 15–21. doi:10.1023/A:1008825009825.

[72] L.L. Wong, G. Natarajan, M. Boleij, S.S. Thi, F.R. Winnerdy, S. Mugunthan, Y. Lu, J.M. Lee, Y. Lin, M. van Loosdrecht, Y. Law, S. Kjelleberg, T. Seviour, Extracellular protein isolation from the matrix of anammox biofilm using ionic liquid extraction, Appl. Microbiol. Biotechnol. 104 (2020) 3643–3654. doi:10.1007/s00253-020-10465-7.

[73] M.G. Freire, A.F.M. Cláudio, J.M.M. Araújo, J.A.P. Coutinho, I.M. Marrucho, J.N.C. Lopes, L.P.N. Rebelo, Aqueous biphasic systems: A boost brought about by using ionic liquids, Chem. Soc. Rev. 41 (2012) 4966–4995. doi:10.1039/c2cs35151j.

[74] T. Seviour, P. Weerachanchai, J. Hinks, D. Roizman, S.A. Rice, L. Bai, J.M. Lee, S. Kjelleberg, Solvent optimization for bacterial extracellular matrices: A solution for the insoluble, RSC Adv. 5 (2015) 7469–7478. doi:10.1039/c4ra10930a.

[75] K. Chauhan, R. Kumar, M. Kumar, P. Sharma, G.S. Chauhan, Modified pectin-based polymers as green antiscalants for calcium sulfate scale inhibition, Desalination. 305 (2012) 31–37. doi:10.1016/j.desal.2012.07.042.

[76] Z. Amjad, Iron oxide dispersants for industrial water systems: Types, performance, and selection criteria, Int. J. Corros. Scale Inhib. 6 (2017) 162–179. doi:10.17675/2305-6894-2017-6-2-6.

[77] M.I. Aguilar, J. Sáez, M. Lloréns, A. Soler, J.F. Ortuño, V. Meseguer, A. Fuentes, Improvement of coagulation-flocculation process using anionic polyacrylamide as coagulant aid, Chemosphere. 58 (2005) 47–56. doi:10.1016/j.chemosphere.2004.09.008.

[78] J. Gregory, S. Barany, Adsorption and flocculation by polymers and polymer mixtures, Adv. Colloid Interface Sci. 169 (2011) 1–12. doi:10.1016/j.cis.2011.06.004.

[79] H.M. Ahmad, M.S. Kamal, M.A. Al-Harthi, High molecular weight copolymers as rheology modifier and fluid loss additive for water-based drilling fluids, J. Mol. Liq. 252 (2018) 133–143. doi:10.1016/j.molliq.2017.12.135.

[80] A.P. Abbott, T.J. Bell, S. Handa, B. Stoddart, Cationic functionalisation of cellulose using a choline based ionic liquid analogue, Green Chem. 8 (2006) 784–786. doi:10.1039/b605258d.

[81] A.P. Abbott, G. Capper, D.L. Davies, R.K. Rasheed, V. Tambyrajah, Novel solvent properties of choline chloride/urea mixtures, Chem. Commun. 9 (2003) 70–71. doi:10.1039/b210714g.

[82] STOWA, “Groen” poly-elektrolyt, 2016.

[83] A.A. Swelam, A.M.A. Salem, A.A. Ayman, Copper (II) Removal using Three Cation Exchange Resins : Ion Exchange Equilibrium and Kinetics, Middle East J. Appl. Sci. 5 (2015) 1017–1027. http://www.curresweb.com/mejas/mejas/2015/1017-1027.pdf (accessed June 17, 2019).

[84] E. Pehlivan, T. Altun, Ion-exchange of Pb^{2+}, Cu^{2+}, Zn^{2+}, $Cd^{2+,}$ and Ni^{2+} ions from aqueous solution by Lewatit CNP 80, J. Hazard. Mater. 140 (2007) 299–307. doi:10.1016/j.jhazmat.2006.09.011.

[85] E.L. Cochrane, S. Lu, S.W. Gibb, I. Villaescusa, A comparison of low-cost biosorbents and commercial sorbents for the removal of copper from aqueous media, J. Hazard. Mater. 137 (2006) 198–206. doi:10.1016/j.jhazmat.2006.01.054.

[86] E. Denkhaus, S. Meisen, U. Telgheder, J. Wingender, Chemical and physical methods for characterisation of biofilms, Microchim. Acta. 158 (2007) 1–27. doi:10.1007/s00604-006-0688-5.

Summary

Fields such as water and wastewater treatment, dredging, mining, food processing, textile and paper making, petroleum and chemical industries face the challenge of particle removal from (waste) water. The removal of solids from these water streams is generally achieved via the coagulation/flocculation process, which is a simple and effective way to destabilise, agglomerate and remove particles from water and wastewater. Currently, this process is widely accomplished with the use of inorganic coagulants and fossil-based organic flocculants. Flocculants are particularly important because they are efficient at low dosages and able to form strong flocs. However, most synthetic flocculants biodegrade poorly and some of the degradation products/monomer residues are toxic, with acrylamide from polyacrylamide as a well-known example to have carcinogenic and neurotoxic effects. Besides, unreacted toxic chemicals used to synthesise the monomer units, such as formaldehyde, epichlorohydrin, and dimethylamine, have been found as sources of contaminants in treated water. Hence, the use of synthetic flocculants can hardly be considered a sustainable (waste) water treatment approach, especially in open systems such as in surface water treatment, dredging and mining.

As an alternative, bioflocculants have gained increasing attention for water treatment since they are generally safe, biodegradable, and can effectively flocculate particles with performances sometimes comparable with synthetic flocculants. However, a class of promising bioflocculants yet to be fully explored are microbial extracellular polymeric substances (EPS). EPS are products of microbial biochemical secretions, comprising different macromolecules such as polysaccharides, proteins, lipids and humic substances. The high molecular weight of EPS coupled with their net negative charge make them anionic polyelectrolytes that can be applied in several fields such as for particle flocculation and heavy metal adsorption. Although EPS are already being produced from pure microbial strains (commercial exopolysaccharides such as alginate and xanthan gum), their high cost, due to the need for sterile conditions and expensive substrates such as glucose, limit their use to speciality applications such as food, feed, medicine and cosmetics.

To produce cost-effective EPS that can be applied as flocculants, we established a mixed-culture approach that requires non-sterile cultures and feedstocks by using (industrial) wastewater as both carbon and nutrient source. Here, one uses the potential of cooperative growth and symbiotic relationships in mixed cultures of EPS-producing and non-EPS–producing bacterial strains as found in wastewater sludge. Moreover, this approach allows the combination of biological organic pollutant removal from wastewater with the production of EPS as a useful product. By converting most of the organics that would have been mineralised to EPS, wastewater treatment plants (WWTPs) can benefit from a reduced quantity of produced sludge, which is expensive to dispose of, and can also lower their CO_2 footprint.

In **Chapter 2**, we demonstrated the possibility to combine fresh and saline (30 g/L NaCl) wastewater treatment (using a submerged membrane bioreactor) with the production of EPS as flocculants. Here, a mixture of glycerol and ethanol was used as substrate, simulating wastewater from the biodiesel and liquor industries. These substrates also make up more than 50% of the saline wastewater COD of the WWTP in Delfzijl (Netherlands), where the inoculum of the saline bioreactors was obtained.

EPS (both the soluble and bound fractions) produced from the freshwater and saline bioreactors possessed similar functional groups (namely carboxyl, hydroxyl and amine groups) and were both composed of polysaccharides and proteins, the latter in higher concentrations than the former. The higher concentration of proteins compared to polysaccharides was related to both the COD/N ratio of the feed (in this study, COD/N 16 – excess nitrogen) and the relatively long SRT of the reactor.

Furthermore, both the fresh and saline EPS, irrespective of whether soluble or bound, had a broad MW distribution (≥2000 kDa – <10 kDa), with the fresh and the saline soluble-EPS showing a similar trend; ditto for the bound-EPS produced from the fresh and saline bioreactors. These findings indicate that under comparable reactor conditions, salinity does not influence the MW distribution of wastewater-derived EPS. However, the charge density value of each EPS fraction (slightly) differed, implying that the monomer composition and content of these fractions were not the same.

The four EPS fractions (Fig. 1) showed good flocculation of kaolin clay particles (used as model particles) in both saline and non-saline environments (up to 97 and 89 % turbidity removal, respectively), with the bound EPS fractions showing comparable efficiencies with a commercial anionic polyacrylamide, albeit at a higher dosage.

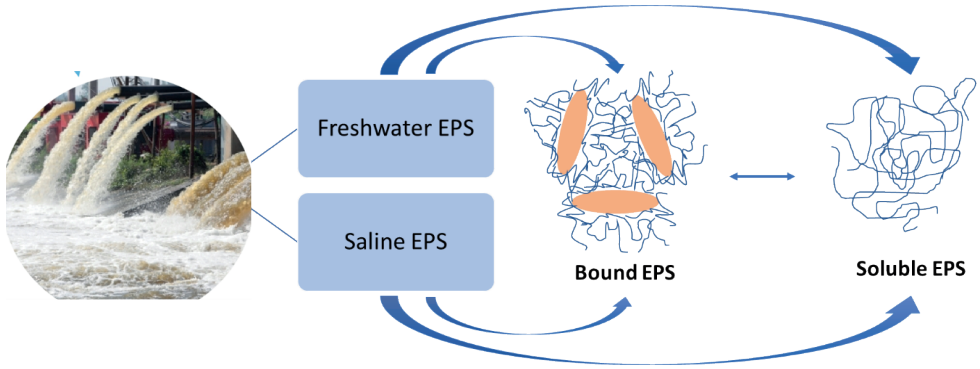

Fig. 1. Soluble and bound EPS production from fresh and saline wastewater.

Although the study in Chapter 2 yielded promising results with respect to the possibility to combine wastewater treatment with the production of effective flocculants, one major drawback was the low EPS recovery (fraction of wastewater-COD converted to EPS-COD), which was about 6 - 8%. Investigations in **Chapter 3** were designed to increase the EPS recovery to at least 30%. To achieve this, two strategies were employed. First, the SRT of the reactors was reduced from 15 days (used in the first study) to 3 days to minimise COD loss via oxidation and possible hydrolysis of EPS at long SRTs. The second strategy was to investigate the effect of excess and limited nitrogen on EPS recovery. The results in this Chapter revealed that under a limited nitrogen condition, up to 54 and 36 % EPS recoveries (at an influent COD/N ratio of 100) were possible from fresh and saline wastewater, respectively. Moreover, EPS produced under limited nitrogen had a higher molecular

weight, a higher polysaccharide content and, consequently, a better flocculation performance than the corresponding EPS produced from excess nitrogen. This chapter unambiguously showed that nitrogen limitation is crucial for high EPS recovery (at least from glycerol/ethanol-rich wastewaters), while excellent organic removal (> 94% wastewater-COD removal) remained possible.

Having established two key parameters as imperative for high EPS recovery, **Chapter 4** sheds more light on other suitable industrial wastewaters that can be valorised to EPS. Glycerol, glycerol/ethanol mixture, glucose and glucose/ethanol mixture proved to be suitable substrates to produce EPS under nitrogen-limited conditions, with recoveries between 25 - 45 % in the order glycerol > glycerol/ethanol > glucose > glucose/ethanol. With acetate and acetate/ethanol as substrate (using as inoculum, the aerobic sludge from the WWTP), EPS recovery was low (3 - 11 %) and possibly hampered by PHA production in the bacterial cells, which was visualised by microscopy. However, when acetate and acetate/ethanol substrates were fed on an EPS-rich sludge, the recovery was as high as 69% for the acetate/ethanol mixture. This suggests that the use of an EPS-rich sludge may be a good strategy to intensify EPS production, although further research is still needed to substantiate this hypothesis.

Regardless of the fed carbon source, the produced EPS were complex in composition, comprising different monosaccharides (neutral and acidic), proteins and other substances (neutral and acidic low molecular weight compounds). A further characterisation of the EPS-polysaccharides revealed their compositional heterogeneity – composed of sugars such as rhamnose, fucose, arabinose, xylose, mannose, glucose and uronic acids, and the amount of each sugar type depended on the type of substrate fed to the reactor.

In **Chapter 5**, we investigated the flocculation mechanism of wastewater-produced EPS, which are generally heterodispersed, and the influence of size dispersity on the flocculation of clay mixtures. The harvested EPS (produced from nitrogen-limited wastewater, as reported in Chapter 3) were fractionated to three molecular weights (MWs) via membrane filtration, yielding, high (HMW: 1.99 MDa), medium (MMW: 0.78 MDa) and low (LMW: 0.13 MDa) MW EPS fractions. The produced EPS and its fractions were mainly composed of polysaccharides and proteins and their ratios increased with increasing MW.

Flocculation tests using kaolinite and montmorillonite clays as model particles revealed that the harvested unfractionated EPS and the HMW-EPS fraction showed similar and excellent flocculation of kaolinite (93% turbidity removal at a dosage of 0.1 mg/g kaolinite) and montmorillonite (98 - 99% at 0.5 mg/g) in single clay systems. This showed that the presence of LMW-EPS in the harvested EPS did not hinder its flocculation performance. However, the sole use of the LMW-EPS fraction poorly flocculated any of the clay particles. In the dual clay system (a 1:1 mass ratio of kaolinite to montmorillonite), the harvested mixed EPS proved to be more efficient than the HMW-EPS fraction. By using optical reflectometry, we monitored the adsorption of each EPS fraction on a silica surface, and this revealed site-blocking effects in mixed EPS: the LMW and MMW EPS first adsorbed to the surface due to higher diffusivities and faster mass transfer to the interface, while the HMW-EPS were slowly transported but were attached to the surface irreversibly and stronger than the

LMW/MMW-EPS. We proposed from this chapter, a mixed EPS adsorption mechanism: extended anionic polymer tails in solution, thereby enhancing particle flocculation.

In **Chapter 6**, the soluble EPS fraction was immobilised on a column to adsorb and recover heavy metals (Cu^{2+}, Pb^{2+} and Au^{3+}). The immobilisation was done with the aid of silica gel (as the support material) coated with polyethyleneimine, to which EPS were irreversibly attached as shown by optical reflectometry. The fixed EPS excellently adsorbed Cu^{2+} and Pb^{2+}, with 99.9% of influent metal adsorbed before the breakthrough points. More interestingly, EPS showed very high adsorption capacities for both metal ions: as high as 780 mg Cu^{2+}/g EPS and 1200 mg Pb^{2+}/g EPS. Metal desorption was achieved with 0.1 M HCl, with an average recovery of 86% for Cu^{2+} and 90% recovery for Pb^{2+} in a 10-time concentrated metal ion solution. Furthermore, we successfully showed the possibility to regenerate and reuse the immobilised EPS for five adsorption-desorption cycles (using Cu^{2+} as an example) with no reduction in the adsorbed amount at the breakthrough point (q_{bp}). Based on the mass balance of the associated metal ions participating in the adsorption process, ion exchange was identified as the major mechanism responsible for Cu^{2+} and Pb^{2+} adsorption by EPS. The results demonstrated the potential of wastewater-produced EPS as an attractive and possibly, cost-effective biosorbent for heavy metal removal (to trace effluent concentrations) and recovery.

Finally, in **Chapter 7**, the results of this research are discussed in a broader context of the production, characteristics and application of wastewater-produced EPS. The advantages, limitations and potential markets of this promising bioflocculant were highlighted, and the possibility to cationise EPS for applications unfeasible with anionic polyelectrolytes was discussed. Lastly, future research directions and recommendations are proposed.

Author's publications and patent

V. Ajao, H. Bruning, H. Rijnaarts, H. Temmink, Natural flocculants from fresh and saline wastewater: Comparative properties and flocculation performances, Chem. Eng. J. 349 (2018) 622–632. doi:10.1016/j.cej.2018.05.123.

V. Ajao, S. Millah, M.C. Gagliano, H. Bruning, H. Rijnaarts, H. Temmink, Valorization of glycerol/ethanol-rich wastewater to bioflocculants: recovery, properties, and performance, J. Hazard. Mater. 375 (2019) 273–280. doi:10.1016/j.jhazmat.2019.05.009.

V. Ajao, K. Nam, P. Chatzopoulos, E. Spruijt, H. Bruning, H. Rijnaarts, H. Temmink, Regeneration and reuse of microbial extracellular polymers immobilised on a bed column for heavy metal recovery, Water Res. 171 (2020) 115472. doi:10.1016/j.watres.2020.115472.

V. Ajao, R. Fokkink, F. Leermakers, H. Bruning, H. Rijnaarts, H. Temmink, Bioflocculants from wastewater: insights into adsorption affinity, flocculation mechanisms and mixed particle flocculation based on biopolymer size-fractionation, J. Colloid Interface Sci. 581 (2020) 533–544. doi:10.1016/j.jcis.2020.07.146.

V. Ajao, M.C. Gagliano, M. Rogowska, P. van Veelen, M.A. Kabel, P. de Gijsel, H. Bruning, H.H.M. Rijnaarts, H. Temmink, Microbial extracellular polymer production from various substrates mimicking industrial wastewaters: polymer properties and microbial community. (*In submission*).

H. Temmink, V. Ajao, Method and system for production of natural polyelectrolytes such as microbial extracellular polymeric substances, (2019). Patent number NL2019171B1.

Acknowledgements

As the African proverb says, 'it takes a village to raise a child'. My PhD journey would have been practically impossible without the support, care, collaboration, and encouragement of a lot of people, whom I am whole-heartedly grateful to.

Wetsus has been the heart of my PhD experience. Thank you *Cees* and *Johannes* for the great vision of Wetsus, and indeed, I must say I enjoyed every bit of being at Wetsus. You have created a world-class institute dedicated to scientific innovation in water technology. Thank you for all your hard work to ensure the highest possible scientific standards.

My deepest gratitude goes to my supervisors – *Hardy*, *Harry* and *Huub*. Thank you for believing in me to carry out this project (and by the way, I hope I measured up to your expectations for the project). These four years will always be remembered for good because you made it so. Thank you sirs! *Hardy*, I must say I am indebted to you for your help and support throughout this project. Thank you for your very constructive and helpful comments. Through it all, I saw your undying passion for the project: you immersed yourself into the topic, open doors of collaboration, never got tired of the several rounds of manuscript reviews and even offered to write. Of course, I will also not forget your kind invitation to your home (many thanks to *Miriam* too!). Thanks a million *Harry* for those valuable comments during manuscripts review. You nicely brought out those seemingly small but very important details that were overlooked. My special regards to *Huub*; you've just got this nice father-figure that calms fears. I sincerely appreciate your suggestions during the project, the frequent meetings, and your willingness to help even in my personal life.

My special gratitude to all the academics we collaborated with. Your assistance was indeed crucial to the completion of this project. From *Evan*, a physical organic Chemist to *Frans* and *Remco* (Polymer and Colloid science experts), *Cristina* (a Microbiologist), and *Mirjam* and *Peter* (Food Chemist), you all made it possible to explore the various aspects of this wonderful, slimy, sticky stuff called EPS. *Evan*, it was a real pleasure meeting you and seeing how passionate you were to bring in your expertise into a quite different field, and indeed, it was a successful collaboration. *Frans*, we could talk about adsorption and flocculation mechanisms for hours without realising it was lunch time or time for other appointments. Your passion and enthusiasm for polyelectrolytes is incredible. Thank you very much for those experimental suggestions and your constructive feedback. The outcome of our collaboration turned out to be one of my favourite chapters. *Remco*, you were a wonderful engine in the collaboration with Frans. Your practical assistance in setting up the reflectometry and helping with the ellipsometry and DLS measurements are highly appreciated. Thank you very much *Cristina* for making the microbiology part of this thesis possible. The bugs are indeed the machinery of the thesis, and you made it achievable to explore this part. A big thank you to *Pieter* too for the microbial analysis. *Mirjam*, thank you for your warm hand of welcome into the world of sugar analysis and for the manuscript review. *Peter*, you indeed put me through in this world of sugars. I am grateful for your practical support. *Dainis*, I will not forget your help with the sugar analysis of my first samples. You opened the door and I could walk in. Thank you for the kind gesture and I appreciate those discussions we had on EPS.

At the very foundation of some of the results of this thesis is the hard work of the enthusiastic students that have worked with me during this project. My wholehearted appreciation to *Siti*, *Paraschos*, *Geert-Jan*, *Daniel*, *Kang*, *Magda*, *Andre*, *Chufeng* and *Ema*. You all brought your motivation and intelligence into this thesis and I really enjoyed supervising your thesis/internships. It was also nice to get to know each one of you a little better during the period, and I hope you keep up the good work wherever you are. Also, at the core of this work is the *Analytical team* at Wetsus. Thank you all for those timely and accurate analyses. I must say it made the PhD ride a pretty smooth one. Most times, we did not know who did what, but the synergy in the team made the process even smoother. Special thanks to *Mieke* (I always have to check the spelling if 'i' comes before 'e' or vice versa 😊). Although it took almost a year before getting the molecular weight method developed, you did not give up and you made it possible. You may not know, but the developed method has been a crucial part of all the chapters of this thesis. By the way, I know you will miss my nice LC-OCD samples 😊. *Tom*, the last weeks before your retirement were profitable for the project. Thank you very much for the amino acid method development. *Agnieszka* and *Bianca*, I am very grateful for your help with the microbial analysis.

Still on the scientific part of this thesis, worthy of mention are the members of the 'Natural Flocculant' theme at Wetsus (*Pentair*, *Paques*, *Evides*). Thank you for the fruitful discussions and funding. *Leo* and *Remon*, it was nice collaborating with you on the application of EPS to your system, and for your prompt approvals regarding my manuscripts and presentations. To the internal (bio)fouling group members (*Natascha*, *Rik*, *Emanuel*, *Diego*, *Paulina*, *Ettore*, *Xiaoxia*, *Rose*, *Barbara*, *Evelyn*, *Olga*, *Cristina*, *Michel*, *Antoine Kemperman* and *Caroline*), what a nice thing to have such a platform to discuss and share on different aspects of fouling! Thank you *Paula*, *Caroline* and *Antoine Kemperman* for chairing the meetings and keeping the spirit alive. I enjoyed the discussions we had. Special thanks to *Caroline* for your interest in my project and willingness to help. I appreciate the talks we had and will not forget the door of collaboration you opened with the NMR Centre at WUR. *Aldrik*, although circumstances made it impossible to see the fruition of our collaboration on labelled substrate tracing using NMR, I do appreciate your willingness to help despite your very busy schedule. I hope something great will come forth from the NMR results. *Alan*, as I wrote in my last mail to you, I wish we had more discussions on PHA *vs* EPS production from microbes, but I must say I appreciate the few we had and your contributions to one of my thesis chapters. *Claire Chassagne*, I appreciate those helpful discussions on adsorption and flocculation. Thank you once again for the opportunity to carry out zeta potential measurements in your lab.

Special thanks to *Leon* and *Prashanth* for having me in the George Barley Prize team. I am very grateful for the privilege. *Michele*, *Adam* and *Olivier*, you even took the media part of the challenge farther than we expected. I will not quickly forget my dubbed voice. I still listen to it and get amused. That was so creative and ultimately, the prize was brought home. *Bert H.*, thank you very much for your comments after my second lunch presentation. They were extremely useful and pivotal to the oral presentation award I got in Ghent.

Without an enabling environment, the scientific part of this work would at its best crawl. I appreciate the invaluable assistance of the *technical team* at Wetsus. *Harrie* (although no longer at Wetsus),

you were my first technical support and you made it possible to start experiments in a very short time. You may not know how appreciative I am of that, but I really am… Thank you very much *Jan Jurjen* (*JJ*) for taking over when Harrie left. You worked with so much zest and were prompt in taking actions when something needed to be done. Thank you for thinking along and for your willingness to make the set-up better and updated. *Piet*, those smiles of yours I miss. In a short time, you designed and constructed the Pilot-scale reactor. Thank you very much. My special regards to the Secretarial office at Wetsus and ETE. *Liesbeth*, perhaps I have only seen you twice, but you have been such a pillar on all organisational and practical questions. I must say I appreciate your prompt response to emails. To the *Secretarial office* at Wetsus, you are highly appreciated for your kind gesture and for being the grease that makes Wetsus run smoothly. *Nynke* and *Anke*, thank you for being gracious to me. Twice, you helped extend the contract of one of my students. You may not know, but the 2nd extension period was actually the most profitable time of his internship, and the outcome led to one of the publications of this thesis. *Jannie*, *Trienke* and *Willy*, I can't count the number of times I had to send samples by post and you made it all easy. I am very grateful for all your acts of kindness. *Riet*, those smiles of yours can soften the hardest heart. *Gerben*, you love what you do and we love you for it. Thank you for being that calm person you are and sharing your good energy. *Catharina*, you are a great plus to the Canteen team. You sort of love me as your son, and I must say that means a lot to me. Of course, this is also a good medium to congratulate you on being a grandma 😊. Will definitely miss you. *Gerrit*, my fellow brother. I cannot appreciate you enough for your help with chemical purchasing and follow-up calls. *Rienk*, you are always a call away to help solve one IT problem or the other. Thank you.

To my lovely office mates (the kingdom 1.18C), from the retired Kings (Philipp, Andrew, Gerwin, Patrick) and Queen Terica to the present dynasty, it has been amazing – from the office decorations to the dinners, to the office end of the year gift sharing, to the gift sent to Tomisin when he was born, etc. You all made our office distinct and unique. *Philipp*, the boss, your aura to me was that of calmness and brilliance. Thank you for my first trip to the WWTP – the experiments got started from there – the inoculum. *Andrew*, my Zimbabwean-German friend, discussing with you is always nice. I hope we get to meet for at least a cup of coffee. *Terica*, although may look tough on the outside but you are really sweet on the inside, thank you for making our office lively and cool. Your initiative of decorating our office during the Yuletide season has come to stay and has become enviable by other offices. *Gerwin*, my first office neighbour, thank you for being a nice and cool dude. *Patrick*, our meeting time was short but you cannot be quickly forgotten. *Wiecher*, I must say it is really a pleasure meeting you. Thank you for driving miles to come join our office dinners. We hope we can also have one at your place after this Coronavirus pandemic. *Goncalo*, aside Wetsus, you know you hold a special place in my family. Tomisin will not forget your kind gestures prior to and after his delivery. I really appreciate your selflessness (by the way, regards to *Patricia* too). *Thomas*, what's up man? I hope you get the right answer to this popular Victor's way of greeting before the end of your PhD 😊. *Shuyana*, thank you for being a vibrant Queen of the office too. It was nice meeting your mum and brother when they came visiting. *Catarina*, I write on behalf of Tomisin for those times you pleasantly took care of him in the office and outside the office. It is always a busy time as PhDs but you cared so much to take care of Tomi all the time he came visiting. *Rhuzie*, I will not

forget so quickly the potluck at your place and for introducing it to the office. Thank you also for those TGA analyses. *Swarupa*, although it was quite a short time together in the office, it was good having you as a neighbour.

To my other friends at Wetsus that made my stay memorable: *Hakan* (dostum), I wish I can be as calm as you are, my man. With your cup of tea lifted at an angle of 90 °C to your shoulders, walking slowly on the corridor like a man having all under control 😊. Thank you for those Turkish lessons, and I will not also forget those excel tricks you taught me. *Nimmy*, good to find a sister in you. Gentle yet jovial in a lovely way. *Emanuel*, it was nice discussing EPS together. Thank you for your willingness to co-supervise the Honours programme. You were always available when I needed help and I am very grateful for that. *Evelyn*, good to also have you in the EPS community. I cherish the discussions we had and wish you the very best in your thesis. *Raquel*, such a lovely person you are. Those biomasses you gave me are well appreciated. *Sebastian*, you are always eager to be of help. Thank you for going all out to prepare those cyanobacteria cultures for me. *Mark* and *Mariana*, beyond Wetsus, parenthood even got us closer. Always a great time at Elias' birthday celebration and we are thankful for the invitations. *Lucia*, those cheesecakes at your kids' birthday celebration…, you know what I mean 😊. Thank you for the invites and for always using your nice cakes as a bait 😊. *Angel*, can't lay my hands on it, but there is something lovely about you. Thank you for the TGA measurements and for giving Bukola's thesis a good push. Mr *Belloni* my friend, the aura around you is always bright and breezy. *Ricardo*, *Casper* and *Steffen*, it was nice working together on the Wetsus BWT practicals. *Maarten* (the Pianist, the vortex shaker), thanks for the nice evening notes. *Mariana Rodrigues*, that tries to 'bully' a Nigerian dude 😊, quite a dead-end my friend. But it was nice chatting with you and having you in our office. *Chris*, my German dude, I will not forget the TSS/VSS analysis you put me through back then (2016) when you were a student. Thanks man! *Paulina*, (*Pawpaw*), a soft but strong lady you are. Nice to have you as a late lunch-mate and as a dear friend. *Yang Lei* (as I fondly call), a pragmatic researcher, nice conversations we had, and I wish you the very best in your career. *Natascha*, thank you for those nice pastries you brought. You also introduced me to the world of alginate and ALE; well appreciated. *Antoine* (*Karengera*), we've come a pretty long way together. Thank you for your warm hand of love to my family. *Roel*, I will not forget your help during the patent application. Thank you very much and I hope we get to collaborate in the future on other projects. *Jan* (*de Groot*), thank you for your willingness to help on the financial matters, and equally important, for organising the football sessions. *Marco* (*de Graaf*), you are such a nice guy. I love what you do with the Talent programme; your passion and determination to see kids love water science and technology is terrific. And to *Eliane* and *Gerjanne*, it was really my pleasure supervising you for the Honours programme. Keep up the good work and stay motivated in science.

To my paranymphs, *Gerben* and *Prashanth*, thank you for not just saying 'Yes' to my request but also being very willing to stay with me during those demanding 45 minutes of thesis defense. *Sope Adebowale*, a friend and a brother, you are heartily appreciated for the cover design layout of this book and for the other collaborations we have had during these four years. *Marissa*, it is great

working with you at SusPhos. Thanks a million for the time you gave me to complete my thesis while already working for SusPhos.

To the reading committee of my thesis (*Prof. Stams*, *Prof. Euverink*, *Dr Kleerebezem*, *Dr Chassagne*), you are highly appreciated for your time and efforts to read my thesis and make it for my defense.

Finally, my family! Thank you *Ifemi* for all your support during this period. The ride was a smooth one because you cared and helped relentlessly. Thank you indeed for all you sacrificed and for even proof-reading my manuscript for English language errors. You are an amazing wife and partner. I love you! *Tomisin*, your coming to this world during my PhD brought light and love afresh. Thank you for welcoming me back home with smiles after the day's rigorous work. With you, there was no delay in my work at all; rather, your coming helped me manage my time judiciously. And of course, we cannot wait for *Toluwanimi* to come and join this lovely and joyful family. To my step mum, parents-in-law and siblings (*Segun*, *Biodun*, *Damilola*, *Pelumi*, *Damilare*, *Dimeji*), thank you for all your support during this period and for being there. To my *dad (Baba oooo,* in Tomi's voice*)*, hmmm, I'm short of words at this juncture; words indeed cannot fully express how grateful I am for always being by my side and being my number 1 fan for years. And to the loveliest *mum* that longed for this time but unfortunately could not because she passed away on 22nd December 2012. Although you had little, you still sacrificed the little you had to see your children succeed. Thank you ma'am, and to you I dedicate this thesis!

About the Author

Victor O. Ajao was born in Lagos, Nigeria on the 22nd of September 1990. He grew up in the same city for 16 years before moving to the city of Ibadan to study Industrial Chemistry at Nigeria's premier University, the University of Ibadan, where he obtained his bachelor's degree. In 2013, he was awarded the Erasmus Mundus scholarship to pursue a master's degree in Chemical Innovation and Regulation. This programme allowed him to study at the University of Algarve (Portugal) and University of Bologna (Italy). In September 2015, Victor obtained his MSc. degree and graduated *cum laude* with a thesis focused on the *production of microbial polyhydroxyalkanoates (bioplastics) from paper wastes*. He continued as a Researcher in the same research group on the *pertraction of volatile fatty acids through biodiesel-based liquid membranes*. In March 2016, Victor moved to Leeuwarden to start a new journey as a PhD candidate at Wetsus in collaboration with the Environmental Technology department of Wageningen University. His PhD research focused on the *production, characterisation and applications of microbial extracellular polymeric substances (EPS) from wastewater*. During his PhD, he was part of the Wetsus team that participated in the George Barley Water Prize, a contest aimed to solve the phosphorus pollution in the Everglades, Florida. Victor was also involved in working with students from the Wetsus Honours programme that later won the WaterCampus science fair competition in 2019. In 2018, he was co-awarded the Marcel Mulder prize for his research work.

Victor could say that he enjoyed every bit of the PhD journey and is so excited to share with you the outcomes of the four productive years.

Netherlands Research School for the
Socio-Economic and Natural Sciences of the Environment

D I P L O M A

for specialised PhD training

The Netherlands research school for the
Socio-Economic and Natural Sciences of the Environment
(SENSE) declares that

Victor Olusola Ajao

born on 22 September 1990 in Lagos, Nigeria

has successfully fulfilled all requirements of the
educational PhD programme of SENSE.

Leeuwarden, 11 September 2020

Chair of the SENSE board

Prof. dr. Martin Wassen

The SENSE Director

Prof. Philipp Pattberg

The SENSE Research School has been accredited by the Royal Netherlands Academy of Arts and Sciences (KNAW)

KONINKLIJKE NEDERLANDSE
AKADEMIE VAN WETENSCHAPPEN

The SENSE Research School declares that **Victor Olusola Ajao** has successfully fulfilled all requirements of the educational PhD programme of SENSE with a work load of 44.2 EC, including the following activities:

SENSE PhD Courses

- Environmental research in context (2016)
- Research in context activity: 'Wetsus Honours Programme supervision (2018-2019)'

Other PhD and Advanced MSc Courses

- Research Methodology: From topic to proposal, Wageningen School of Social Sciences (2016)
- Student supervision course, Wetsus (2016)
- Presentation course, Wetsus (2016)
- Image processing course, Wetsus (2016)
- Data management planning, (2016)
- Design of experiments, Wetsus (2017)
- Scientific writing, Wageningen Graduate Schools (2019)

Management and Didactic Skills Training

- Supervising 8 MSc students with thesis (2017-2020)
- Supervising one BSc student with thesis (2018-2019)
- Assisting and co-organising the lab practicals of the MSc course 'Biological Processes for Resource Recovery course' (2017-2019)
- Co-organising the Wetsus WaterSEED Recruitment Challenge (2016- 2017)
- Supervising 5 students for the Wetsus Honours Programme (2016-2020)

Selection of Oral Presentations

- **Best presentation award***: Natural flocculants from fresh and saline wastewaters*. Young Water Professionals IWA conference, 5 – 7 July 2017, Ghent, Belgium
- N*atural polyelectrolytes from fresh and saline industrial wastewater*. Green and Sustainable Chemistry conference, 14 – 16 May 2018, Berlin, Germany
- *Fresh and saline wastewater valorisation to natural flocculants*. Sludge Management in Circular Economy conference, 23 – 25 May 2018, Rome, Italy
- *Combined wastewater treatment and bioflocculant recovery*. Resource Recovery conference, 8 – 12 September 2019, Venice, Italy

SENSE coordinator PhD education

Dr. ir. Peter Vermeulen

This work was performed in the cooperation framework of Wetsus, European Centre of Excellence for Sustainable Water Technology (www.wetsus.nl). Wetsus is co-funded by the Dutch Ministry of Economic Affairs and Ministry of Infrastructure and Environment, the European Union Regional Development Fund, the Province of Fryslân and the Northern Netherlands Provinces. This work has also received funding from the European Union's Horizon 2020 research and innovation programme under the Marie Skłodowska-Curie [grant agreement No. 665874]. The author thanks the participants of the research theme 'Natural flocculants' for the fruitful discussions and financial support.

Financial support from both Wageningen University and Wetsus for printing this thesis is gratefully acknowledged.

Cover design concept by Victor O. Ajao

Cover layout by Mosope Adebowale

Printed by Proefschriftenprinten.nl on FSC-certified paper